Synthesis and characterization of chitosan bead/flakes for the removal of arsenic and vanadium oxyanions from aqueous solutions

Synthesis and Characterization of Chitosan beads/flakes for the Removal of Arsenic and Vanadium Oxyanions from Aqueous Solutions

by

Abigail Padilla-Rodríguez

A dissertation submitted in partial fulfillment of the requirements for the degree of

Doctor in Philosophy

in

APPLIED CHEMISTRY

UNIVERSITY OF PUERTO RICO

MAYAGÜEZ CAMPUS

2014

Approved by:

Nilka M. Rivera, PhD Member, Graduate Committee	Date
Ricky Valentín, PhD Member, Graduate Committee	Date
Enrique Meléndez, PhD Member, Graduate Committee	Date
Oscar Perales-Pérez, PhD Co-President, Graduate Committee	Date
Félix R. Román, PhD President, Graduate Committee	Date
Carlos Velázquez , PhD Representative of Graduate Studies	Date
Aidalu Joubert, PhD Chairperson of the Chemistry Department	Date

ABSTRACT

Arsenic and vanadium oxyanions are contaminants that are toxic to humans, the environment and other living organisms from natural and anthropogenic sources. The Environmental Protection Agency (EPA) regulated a maximum arsenic level in drinking water of 0.010 mg/L, and vanadium is registered as a contaminant candidate list (CCL). Both contaminants have been removed using diverse techniques such as ion exchange, filtration, precipitation, electrochemicals and others. However, these techniques are expensive and their optimum conditions are not efficient for the removal of these oxyanions. Based on this, adsorption is considered as a removal technique for these contaminants at trace levels from aqueous solutions. The adsorbent used in our studies was chitosan, which is a natural, non-toxic, inexpensive, and effective material.

This study uses diverse beads/flakes consisting of chitosan for the removal of V(III), V(IV), V(V), As(III) and As(V) oxyanions from aqueous solutions at trace levels. PCF removed a 99-100% for vanadium oxyanions, and 97% for As(V) oxyanion during the first two hours of contact when using 5 g/L of the adsorbent and an initial contaminant concentration of 0.500 mg/L at pH 6.0. On the other hand, Fe(III)-CB removed a 95 and 99% of As(III) and As(V) oxyanions respectively under the same conditions. These oxyanions were removed efficiently in presence of co-existing anions, such as chloride, carbonate, sulfate and phosphate. The adsorption of vanadium and arsenic species were fitted by Freundlich and Langmuir models, with Langmuir isotherm as the best fit. The maximum adsorption capacity (Q^0) of the PCF were 12.22, 6.50, 2.58 and 5.43 mg/g for V(III), V(IV), V(V) and As(V), respectively. The protonation of the amine group in chitosan is responsible for the adsorption due to the occurring electrostatic attraction between the negative charge of the oxyanion and the positive charge of

the adsorbent. The Q^0 Langmuir parameters using Fe(III)-CB as adsorbent for As(III) and As(V) were 1.48 and 2.72 mg/g. The As(V) oxyanion adsorption is due to the formation of an inner and outer-sphere complex via ligand exchange and electrostatic attraction. On the other hand, As(III) oxyanion adsorption is due to the formation of an inner-sphere complex via ligand exchange. However, the adsorption of both arsenic species is principally for the immobilization of the ferric hydroxide onto the chitosan beads surface. Our results confirmed that PCF and Fe(III)-CB are simple, non-toxic, efficient, environmentally-friendly, reusable and cost effective adsorbents for vanadium and arsenic oxyanion removal at trace levels from aqueous solutions.

RESUMEN

Oxianiones de arsénico y vanadio son contaminantes tóxicos a humanos, al ambiente y a otros organismos vivientes provenientes de fuentes naturales y antropogénicas. La Agencia de Protección Ambiental (EPA) reguló un nivel máximo de arsénico en aguas potables de 0.010 mg/L, y vanadio está registrado en la Lista de Contaminantes Candidatos a ser regulados por la EPA. Ambos contaminantes han sido removidos por diversas técnicas tales como intercambio de iones, filtración, precipitación, electroquímica y otros. Sin embargo, estas técnicas son caras y sus condiciones óptimas no son eficientes para la remoción de estos oxianiones. Basado en esto, consideramos adsorción como técnica de remoción de estos contaminantes a niveles traza de soluciones acuosas. El adsorbente usado en nuestro estudio fue quitina, cual es un material natural, económico y efectivo.

En este estudio usamos diversos cuencas/hojuelas de quitina para la remoción de los oxianiones de V(III), V(IV), V(V), As(III) y As(V) de soluciones acuosas a niveles traza. PCF removió un 99-100% para los oxianiones de vanadio durante las primeras 2 horas de contacto cuando usamos 5 g/L del adsorbente y una concentración inicial del contaminante de 0.500 mg/L en pH 6.0. Por otro lado, Fe(III)-CB removió un 95 y 99% de los oxianiones de As(III) y As(V), respectivamente bajo las mismas condiciones. Estos oxianiones fueron removidos eficientemente en presencia de aniones comunes, tales como cloruro, carbonato, sulfato y fosfato. La adsorción de las especies de vanadio y arsénico fueron ajustadas por los modelos de isotermas de Freundlich y Langmuir, logrando el mejor ajuste la isoterma de Langmuir. La capacidades máximas de adsorción (Q^0) del PCF fueron 12.22, 6.50, 2.58 y 5.43 mg/g para V(III), V(IV), V(V) and As(V), respectivamente. La protonación del grupo amino en quitina es responsable de la adsorción debido a las atracciones electróstaticas entre la carga negativa de el

oxianión y la carga positiva del adsorbente. Los parámetros de Langmuir usando Fe(III)-CB como adsorbente para As(III) y As(V) fueron 1.48 y 2.72 mg/g. La adsorción del oxianión de As(V) es debido a la formación de un complejo de esfera interna y externa a través de intercambio de ligando y atracciones electrostáticas. En cambio, la adsorción del oxianión de As(III) es debido a la formación de un complejo de esfera interna a través de intercambio de ligandos. Pero, la adsorción de ambas especies de arsénico es principalmente por la inmobilización del hidróxido férrico en la superficie de las cuencas de quitina. Nuestros resultados confirman que PCF y Fe(III)-CB son adsorbentes simples, no-tóxicos, eficientes, amigables al ambiente, reusables y costo efectivos para la remoción de los oxianiones de vanadio y arsénico de soluciones acuosas.

Dedicated:

To God

To my children Angelis & Bryan

To my parents Alba & Jorge

To my husband Hector Varela

To my brother Samuel

To my family

To my friends

Thank you for all your support and love…

ACKNOWLEDGEMENTS

My graduate studies at the University of Puerto Rico have been possible thanks to the support, collaboration, and advice of various people, organizations and institutions. This section is dedicated to expressing my gratitude towards them.

First, I thank God for being my guide and giving me strength, support, and faith throughout my career.

I want to thank my advisor, Dr. Felix R. Román Velázquez, for his support, motivation, guidance, and confidence throughout these years of study and research.

Furthermore, I want to thank my co-advisor, Dr. Oscar Perales Pérez, for all his guidance, support, and assistance in conducting this research.

I also want to express my gratitude to my graduate committee, composed Dr. Nilka Rivera, Dr. Ricky Valentín and Dr. Enrique Meléndez, for all their help.

Moreover, I want to thank the personnel and use of characterization facilities:

Dr. Oscar Perales, Dr. Yarilin Cedeño and Mr. Boris Rentería from The Nanomaterials Processing Laboratory for their help in FT-IR and TGA lectures.

Dr. Arturo Hernández and Krisiam Ortíz for the BET analysis.

Dr. Nelson Cardona and David A. Mota for their help in SEM photos.

Mr. Jose Figueroa for his assistance with ISP photos.

The Department of Chemistry at the University of Texas El Paso, especially Dr. Jorge Gardea, Dr. José Peralta, for their support and giving me the opportunity to do part of my internship in their facilities. I also wish to thank Dr. José A. Hernández, Dr. Marta L. López and other classmates for their help in the LA-ICP-MS and XRF measurements.

I also would like to express my gratitude to the Aqueduct and Sewer Authority (AAA) in Aguada for allowing me to conduct part of my internship in their facilities. My special thanks to Ing. Joel Lugo, Mr. Agustin Collazo, Mr. Gino Giovannetti, operators and personnel.

United States Department of Agriculture, especially Dr. Eton Codling, for giving me the opportunity to participate in an internship in their laboratory in Beltsville Agricultural Research Center in Maryland, USA.

I want to thank the following organizations for their financial support for research: Alfred P. Sloan Foundation Graduate Scholarship Program, the Department of Education, the Department of Defense Research Scholarship (DoESR), the United States Department of Agriculture Grants (# 2008-02146, # 2011-38422-30835, PRE-2011-02986), the Puerto Rico Solid Waste Management Authority (ADS), and the Puerto Rico Water and Research Institute (PRWERI).

I would also like to thank my family, especially my parents Alba I. Rodríguez and Jorge L. Padilla, my brother Samuel Padilla, my children Angelis Varela and Bryan Y. Varela, and my husband Hector Varela for your support, understanding, help, and love. Also, to my nieces (Betzaliz, Anisha and Yoaneliz), my nephews (Youscar and John), Heydi Varela and Carla Avilés.

Lastly, I want to thank my laboratory partners and friends: Diana Sánchez, Sonia Bailon, Luis Alamo, Jose López, Victor Fernández, Maria Ortíz, Angel Vega, Tatiana Luna, Myrna Blas, Tamara Félix, Mario Ortega, Jenny Vargas, Misael Viruet, Francis Barrios, Eileen Rodríguez and others. My special thanks to Dr. Diana Sánchez for all her help with the research.

TABLE OF CONTENTS

LIST OF ABBREVIATIONS AND SYMBOLS

Environmental Protection Agency	EPA
Contaminant Candidate List	CCL
Maximum Contaminant Level	MCL
World Health Organization	WHO
National Toxicology Program	NTP
Agency for Toxic Substances & Disease Registry	ATSDR
International Agency Research Cancer	IARC
Occupational Safety and Health Administration	OSHA
National Institute for Occupational Safety and Health	NIOSH
Vanadium	V
Vanadium(IIII)	V(III)
Vanadium(IV)	V(IV)
Vanadium(V)	V(V)
Arsenic	As
Arsenic(III)	As(III)
Arsenic(V)	As(V)
Protonated Chitosan Flakes	PCF
Iron hydroxide Chitosan Beads	Fe(III)-CB
Chitosan Beads	CB
Chitosan Flakes-N-acetyl-L-cysteine	CF-NAC
Chitosan Beads-Dimercapto succinic acid	CB-DMSA

Chitosan Beads-Gluteraldehyde	CB-GLA
Inductively Coupled Plasma- Mass Spectrometry	ICP-MS
Scanning Electron Microscopy	SEM
Laser Ablation Inductively Coupled Plasma Mass Spectrometry	LA-ICP-MS
X-ray Fluorescence Spectrometer	XRF
Fourier Transform – Infrared Spectroscopy	FT-IR
Image Stacking Photography	ISP
Thermogravimetric analyzer	TGA
Brunauer, Emmet and Teller	BET
Point of zero charge	pH_{pzc}
Degradation temperature	T_{deg}
Revolution per minute	rpm
Maximum adsorption capacity	Q^0
Dimensionless constant	R_L
Co-existing anions	CA
Gluteraldehyde	GLA
N-acetyl-L-cysteine	NAC
Dimercapto succinic acid	DMSA
Acetic acid	CH_3COOH
Nitric acid	HNO_3
Hydrochloric acid	HCl
Sulfuric acid	H_2SO_4

Sodium hydroxide	$NaOH$
Sodium chloride	$NaCl$
Chloride	Cl^{-}
Carbonate	Co_3^{-2}
Sulfate	SO_4^{-3}
Phosphate	PO_4^{-3}

LIST OF TABLES

LIST OF FIGURES

1 INTRODUCTION

1.1 Motivation

Oxyanions released in the environment introduce various harmful metals and metalloids and have attracted worldwide attention because of their toxicity to humans and wildlife. Furthermore, they are strongly dependent on aqueous solutions and redox potential (Goh et al., 2008; Mahmudov and Pau, 2011). Oxyanions of major environmental concern are arsenic and vanadium. Arsenic is one of the most toxic and carcinogenic metalloids that is released into the environment through natural and anthropogenic sources, which can be dispersed widely and plays an important role in the contamination of soils, water and air (Codling and Ritchie, 2005; Ansari and Sadaegh 2007; Rahmani et al., 2011). Both organic and inorganic arsenic have been found in water as contaminants, and the inorganic species are generally more toxic than the organic. The maximum contaminant level (MCL) in drinking water regulated by the Environmental Protection Agency (EPA) and World Health Organization (WHO) is 0.010 mg/L (WHO, 2001; Guo et al., 2007; EPA, 2007). Another contaminant of interest is vanadium, which can have a toxic effect to humans and the environment after prolonged exposure. The most common oxidation states of vanadium are V, IV and III, where V is most toxic (Bhatnagar et al., 2008; Langmuir et al., 2003; ATSDR, 2012; Parks and Edwards, 2006). Vanadium is presently registered on the contaminant candidate list (CCL) by the EPA, with the possibility of being listed as a regulated contaminant in the future (Naeem et al., 2007; NTP, 2008; Parks and Edwards, 2006; Prathap and Namasivayam 2009; EPA, 2009). Both contaminants cause major health effects, such as

damage to the respiratory, cardiovascular, neurological and reproductive systems, skin and cancer (WHO, 2001; IARC, 2006; NTP, 2008).

New and innovative methods are needed to remove trace levels of arsenic and vanadium from natural and contaminated waters. The purification methods for the proposed species have to avoid generation of secondary waste and involve materials that can be recycled and easily used at industrial scales. The adsorption process, which uses cheap and nonpolluting adsorbent materials, may be a suitable technology to remove contaminants from polluted waters. Conventional water cleaning processes such as chemical precipitation, ion exchange, solvent extraction, filtration, electro-dialysis and activated carbon have been used for the removal of the above mentioned species from contaminated waters (EPA, 2000; Namasivayam and Sangeetha, 2006; Yeom et al., 2009; Zeng et al., 2009; Sasaki et al., 2009; Balasubramanian et al., 2009; Nguyen et al., 2009; Martinson and Reddy, 2011; Shinde et al., 2013; Shang et al., 2014); however, using these options for the treatment of large volumes of wastewater or industrial effluents having extremely low content of contaminants has become ineffective and expensive. On this basis, the possibility of using a novel adsorbent based on beads or flakes with a customized surface to interact with As or V species in water would result in an environmentally friendly, simple, rapid, and cost-effective solution to this problem. In this context, the use of beads or flakes of chitosan is convenient since they are non-toxic, natural, biodegradable materials that have the suitable mechanical strength to assure their reusability after contaminant adsorption/desorption cycles.

1.2 Literature Review

1.2.1 Arsenic Removal

Sivaraman (2004) evaluated the removal of inorganic arsenic from aqueous solutions using chitosan beads. In this experiment, chitosan beads were functionalized with expensive compounds such as dimercapto succinic acid (DMSA), cysteine, and penicillamine, and the thiol groups, which have an affinity for As. In this study 50 g/L of adsorbent were used, with a time equilibrium of 72 hours at pH 7. The maximum removal obtained was using chitosan-DMSA beads with a 63% removal of As(V) in an initial concentration of 4.6 mg/L, and a 65% removal of As(III) with an initial concentration of 1.6 mg/L.

Shevade and Ford (2004) investigated the removal of As(V) using zeolites as an adsorbent. They were using 100 g/L of adsorbent, and the equilibrium time was reached after 24 hours at pH 10 and an initial concentration of 50 mg/L. The results obtained were a 90% for As(V) while As(III) had negligible results.

Pokhrel and Viraraghavan (2006) showed the arsenic removal from aqueous solution by a modified fungal biomass. They worked with high temperatures, an equilibrium time of 6 days, and multiple steps for the synthesis of the adsorbent. This study obtained a removal for As(V) of 95% and 75% for As(III) in an initial concentration of 0.100 mg/L at pH 6 and 7, respectively.

Ansari and Sadegh (2007) studied the removal of arsenic using activated carbon as an adsorbent. The experimental conditions were: 100 g/L of adsorbent, equilibrium time of 1 hour at pH 12 for As(III) and pH 3 for As(V). They found a removal of 84% for As(V) and 95% for

As(III) at initial concentration of 10 mg/L. To achieve the removal of As(III) they had to pre-oxidize the As(III) to As(V).

Chen et al. (2008) investigated the removal of arsenic species using molybdate-impregnated chitosan beads (MICB). The experimental conditions were 5 g/L adsorbent, an equilibrium time of 24 hours, and a low temperature (20˚C) at pH 5. The results showed a maximum removal of 99.5% for As(V) and 99% for As(III) at an initial concentration of 10 mg/L. Also, they found that the presence of common anions did not interfere in the arsenic adsorption.

Gang et al. (2010) studied the removal of As(III) using an iron-impregnated chitosan adsorbent. The removal of As(III) was achieved by converting it to arsenic hydride with hydrochloric acid, using 0.2 g/L of adsorbent, and 6 hours were required to reach an adsorption equilibrium at pH 8. The Langmuir maximum adsorption capacity was 6.48 mg/g for an initial concentration of 1.007 mg/L.

Sánchez et al. (2012) evaluated the removal of As(V) and As(III) using Ca-Fe(III) alginate beads as an adsorbent. The experimental conditions used were 5 g/L of adsorbent, 24 hours of equilibrium time, a range concentration of 0.100 to 2 mg/L at pH 6.0. The results showed a most fits using Langmuir model with a maximum adsorption capacity (Q_{max}) of 0.117 mg/g for As(III) and 0.364 mg/g for As(V).

1.2.2. Vanadium Removal

Qian et al. (2004) investigated the removal of Vanadium(V) from aqueous solutions by adsorption crosslinking chitosan-epichlorohydrin. The adsorbent concentration was 0.2 g/L with an equilibrium time of 1 hour at pH 4. The results showed a 97% removal for an initial concentration of 0.300 mg/L.

Manohar et al. (2005) studied the adsorption of Vanadium(IV) using aluminum-pillared bentonite (Al-PILC). The adsorption experimental conditions were: adsorbent dosage (4.2 g/L), equilibrium time (24 hours), pH (5.0) and temperature (30˚C). They found a most fit using Langmuir adsorption and their maximum adsorption capacity (Q_{max}) was 24.16 mg/g for a range concentration of 5- 400 mg/L.

Namasivayam and Sangeetha (2006) worked in the adsorption of Vanadium(V) using $ZnCl_2$ - activated carbon. They were using 4 g/L as the adsorbent dosage, reached an equilibrium in 40 min, had a pH range of 4-9, a temperature of 35˚C, and a range concentration of 0.020 to 0.100 mg/L. The Langmuir adsorption capacity (Q_{max}) was 24.9 mg/g. They showed that the addition of common anions such as nitrate, selenite, molybdate, phosphate, sulphate, chloride and perchlorate using concentrations between 20 to 100 mg/L decreased the vanadium adsorption.

Bhatnagar et al. (2008) studied the Vanadium(V) removal in water using waste metal sludge and a post treatment of cement immobilization. They obtained a Langmuir adsorption capacity for vanadate of 24.8 mg/g, once reached equilibrium of 10 hours at 25˚C, and had an initial concentration of 1.5×10^{-4} to 9.5×10^{-4} M (10-50 mg/L). The preparation of waste metal sludge and the post treatment with cement entails multiple steps.

Sánchez (2013) evaluated the removal of Vanadium(V) and Vanadium(IV) using CA-Fe(III) alginate beads and dried sludge as an adsorbent. This study used 5 g/L (CA-Fe(III) alginate beads) and 10 g/L (dried sludge) of adsorbents, 24 hours equilibrium time at pH 6.0, and a range concentration of 0.600 to 2 mg/L. The maximum adsorption capacity were 0.026 mg/g for V(IV) and 0.365 mg/g for V(V) using dried sludge as an adsorbent. When Ca-Fe(III) alginate beads were used a maximum adsorption capacity of 6.77 mg/g for V(IV) and 0.799 mg/g for V(V) were obtained.

The previous works mentioned above used for the removal of inorganic arsenic and vanadium contaminants from aqueous solutions have several disadvantages. Several methods did not present isotherm adsorptions (Sivaraman, 2004; Shevade and Ford, 2004; Pokhrel and Viraraghavan, 2006; Ansari and Sadegh, 2007; Chen et al., 2008; Gang et al., 2010; Qian, 2008), which are very important in the development of scale up procedure or had multiple steps (Sivaraman, 2004; Shevade and Ford, 2004; Pokhrel and Viraraghavan, 2006; Ansari and Sadegh, 2007; Gang et al., 2010; Qian, 2008; Manohar, 2005; Namasivayan and Sangeetha, 2006; Bhatnagar et al., 2008), which is not cost-effective in the application of real scenarios due to the consumption of energy and high costs. Moreover, some adsorbents are highly toxic (Ansari and Sadegh, 2007; Manohar, 2005; Namasivayan and Sangeetha, 2006), require high doses (Sivaraman, 2004; Shevade and Ford, 2004; Ansari and Sadegh, 2007), operate at acidic or alkaline pH (Shevade and Ford, 2004; Ansari and Sadegh, 2007; Chen et al., 2008; Gang et al., 2010; Qian, 2008; Manohar, 2005; Namasivayan and Sangeetha, 2006), work in high or low temperature (Pokhrel and Viraraghavan, 2006; Chen et al., 2008; Namasivayan and Sangeetha, 2006), need to be modified or functionalized (Sivaraman, 2004; Pokhrel and Viraraghavan, 2006; Chen et al., 2008; Gang et al., 2010; Qian, 2008; Manohar, 2005; Namasivayan and

Sangeetha, 2006; Bhatnagar et al., 2008), reach a slow equilibrium adsorption (Sivaraman, 2004; Pokhrel and Viraraghavan, 2006), and do not remove the contaminants at trace levels (Shevade and Ford, 2004; Ansari and Sadegh, 2007; Chen et al., 2008; Manohar, 2005). Therefore, the adsorption method is an easy, effective alternative for the removal of arsenic and vanadium oxyanions from aqueous solutions at trace levels. For this reason chitosan was used as part of this research, since it can be considered an efficient, scalable, non-toxic and cost-effective adsorbent for the removal of As and V species.

1.3 Objectives

1.3.1 Main Objectives

- Many studies showed that chitosan beads are used for adsorption of inorganic and organic compounds of environmental interest. However some of the published results involving the use of chitosan have the following limitations such as lack isotherms adsorptions, have multiple steps, have high energy needs, are highly toxic, require high doses, operate at acidic or alkaline pH, work at high or low temperatures, need to be modified or functionalized, reach a slow equilibrium adsorption, or do not remove the contaminants at trace levels. The main objective of this research project is to develop novel, simple, efficient, reusable, low cost and environmentally friendly adsorbent based on chitosan polymeric beads or flakes for the removal of trace levels of As and V species in aqueous solutions at pH near those found in natural waters.

1.3.2 Specific Objectives

- Determine optimum conditions for the synthesis of chitosan beads/flakes.
- Determine structural, morphological and analysis elemental characterization of chitosan beads/flakes.
- Determine optimum conditions for the efficient removal of As(III and V) and V(III, IV and V) oxyanions from aqueous solutions.
- Propose or provide insights of the adsorption mechanism of As(III and V) and V(III, IV and V) oxyanions.
- Evaluate the reversibility of the adsorption in order to evaluate the re-use of the adsorbent.

2 THEORETICAL BACKGROUND

2.1 Oxyanions and adsorbent

2.1.1 Arsenic

Arsenic (As) is a metalloid with an atomic number 33 and atomic weight of 74.92. It is the 20th element found on the earth's crust and is a component of more than 200 minerals, such as arseno-pyrite (FeAsS), arsenolite (As_2O_3), cobaltite (CoAsS), realgar (AsS) and others (Sánchez et al., 2013; Vasireddy, 2005; Sivaraman, 2004). In the environment, arsenic exists in organic and inorganic forms. The more common organic forms are: monomethyl arsenic acid (MMAA), dimethyl arsenic acid (DMAA), and arseno-sugars (Vasireddy, 2005; Sharma and Sogn, 2009). The most common oxidation states are: -3, 0, +3, +5 (Guo et al., 2007; Boyaci et al., 2010; Gerente et al., 2010; Wällstedt et al., 2010). The more stable forms in natural and potable water are trivalent (As(III)) and pentavalent (As(V)) (Ansari and Sadegh, 2007; Boddu et al., 2008). The chemical speciation depends on the redox potential (Eh) and pH value, where arsenite exists as H_3AsO_3 and $H_2AsO_3^-$, and arsenate as $H_2AsO_4^-$, $HAsO_4^{-2}$ and AsO_4^{-3} (Boddu et al., 2008; Boyaci et al., 2010; Couture and Capellen, 2011). Arsenite predominates in anaerobic conditions whereas arsenate predominates in aerobic conditions. Arsenite is more toxic than arsenate in the environment (Guo et al., 2007; Gerente et al., 2010; Duo et al., 2014). The figure 1 shows the As(III) and As(V) oxyanions.

Arsenic acid, As(V) Arsenious acid, As(III)

Figure 1: As(V) and As(III) oxyanions in the environment.

Arsenic is one of the most toxic and carcinogenic oxyanions distributed in the water, soil, air, sediments, food and living organisms as a result of natural and anthropogenic activities (Rahmani, 2011; Ansari and Sadegh, 2007; Liu et al., 2011; Pontoni and Fabbricino, 2012). Arsenite and arsenate are generated from the dissolution of specific As-bearing minerals and rocks, such as components in wood preservatives, volcanic ash, ores, crop desiccants, pigments, insecticides, herbicides, pesticides, burning fossil fuels, metallurgical, semiconductor, ceramic and electronics devices, among others (Codling and Ritchie, 2005; Boyaci et al., 2010; Gerente et al., 2010; Sánchez et al., 2012; Xia et al., 2014; Padilla et al., 2014, 2015b). Arsenic is released to the atmosphere as particles and removed through wet and dry precipitation (Sivaraman, 2004). Lately, it has been found in rice, seafood, apple and grape juices, grown chicken, among others (Codling, 2009; Rintala et al., 2014; Shraim, 2014; Xia et al., 2014; Codling et al., 2014). In a near future, the World Health Organization (WHO) will have a maximum allowed concentration in rice of 200-300 µg/L (Consumer reports magazine).

The United States Environmental Protection Agency (EPA) and the World Health Organization (WHO) have set regulations that established a maximum contaminant level in the drinking water at 0.010 mg/L (WHO 2001; EPA 2007; Boyaci et al., 2010; Gerente et al., 2010; Wällstedt et al., 2010; Mondal et al., 2012).

The arsenic contamination of groundwater has been documented in many countries, such as Argentina, Asia, Australia, Canada, Chile, China, El Salvador, Spain, Japan, Mexico, Nepal, Pakistan, Peru, Taiwan, Thailand, United States, and Vietnam (Dambies et al., 2002; Chen and Chung 2006; Pokhrel and Viraraghavan, 2006; Lakshmipathiraj 2010; among others). The terrible consequences of arsenic contamination are especially seen in Bangladesh, where millions have been diagnosed with arsenic poisoning. For example, concentrations of 10-1000 µg/L have

been reported in Bangladesh; in Argentina, concentrations higher than 1000 µg/L; in Chile, concentrations higher than 50 µg/L; and in China, concentrations higher than 800 µg/L (Sánchez 2013; Bocanegra et al., 2002; Nicolli et al., 2012; Ferreccio et al., 2006; Rodriguez et al., 2013). Nine mg/L of arsenic in soil have been found in some parts of the U.S.A. (Langmuir et al., 2003; Codling, 2009). In these countries the maximum contaminant list have been exceeded, which has promoted the dissemination of diseases like anemia, abdominal pains, nausea, cirrhosis, gangrene, dermatitis, keratosis, respiratory problems, cardiovascular problems, nervous and neurological conditions, reproductive and hematopoietic problems, and an increase in the risk of cancer in the kidneys, liver, lung, bladder and skin, or even terminal cancer (WHO, 2001; Shevade and Ford, 2004; Pokhrel and Viraraghavan, 2006; Rahmani et al., 2011; Roy et al., 2014, and among others). The most common routes for the adsorption of arsenic are through the gastrointestinal tract, skin and lungs.

Arsenic has a high affinity for thiol groups, in compounds such as cysteine, glutathione and DMSA (Sivaraman, 2004; Manahan, 2000). These form complexes with enzymes and act as coagulating protein (Manahan, 2003). Another important factor of arsenic toxicity is that it biochemically inhibits the formation of adenosine triphosphate (ATP) due to the fact that it has similar properties to the phosphorus compounds. ATP is an essential substance in the body's metabolism to release energy. In figure 2 we can see how As(III) takes the place of phosphate and adheres to the compound (Gliceraldehyde 3-phosphate), thus giving the formation of a spontaneous hydrolysis and preventing the formation of ATP in the citric acid cycle (Manahan, 2003).

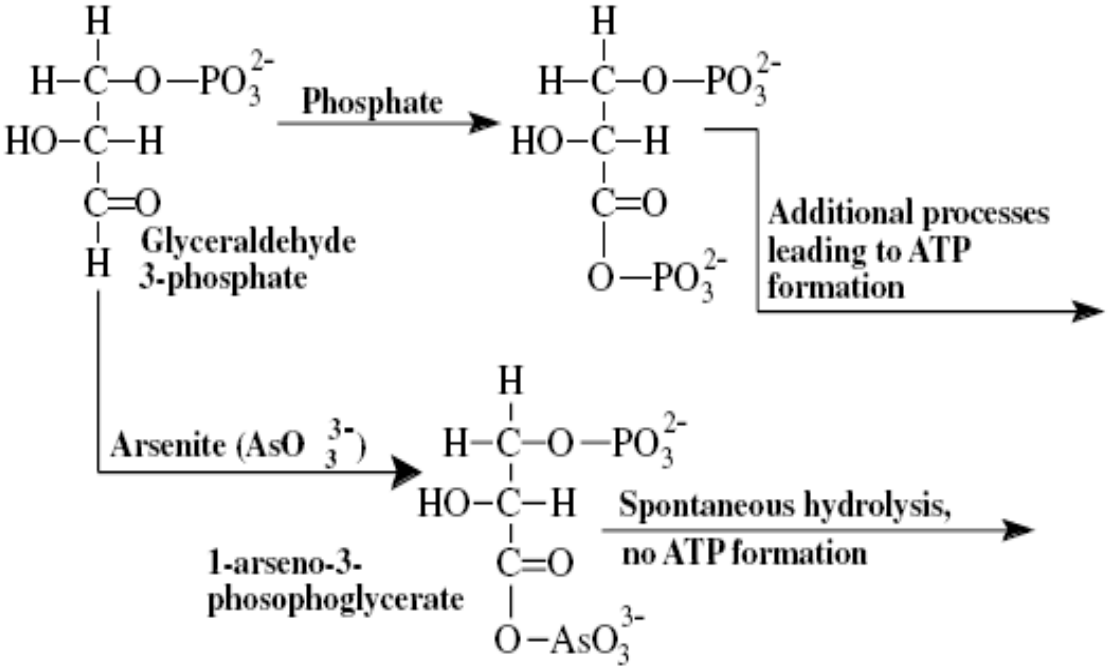

Figure 2: Inhibition of the formation of ATP by arsenite in a citric acid cycle.

(Stanley E. Manahan, Toxicological Chemistry and Biochemistry, 2003, 3rd ed, p 241)

2.1.2 Vanadium

Vanadium(V) is a transition metal with atomic number and atomic weigh of 23 and 50.94, respectively. As with arsenic and others metals, vanadium is distributed into the environment as a potentially dangerous contaminant. Vanadium is registered in the Contaminant Candidate List (CCL) (Naeem *et al*., 2007; NTP, 2008; Parks and Edwards, 2006; Prathap and Namasivayam, 2009; EPA 2009; Padilla et al., 2015a). This element has the possibility of being included as a regulated contaminant in the near future by the United States Environmental Protection Agency (EPA). The Occupational Safety and Health Administration (OSHA) have determined that the exposure limit to vanadium pentoxide dust is 0.5 mg/m^3 and for vanadium

fumes is 0.1 mg/m^3 during an 8-hour work day (IARC, 2006; NTP, 2008; ATSDR, 2012). The National Institute for Occupational Safety and Health (NIOSH) recommends that the exposure limit to vanadium dust or fumes be 0.05 mg/m^3 for a maximum of 15 minutes (IARC 2006; NTP, 2008; ATSDR, 2012).

In aqueous solutions, the most common oxidation states of vanadium are III, IV and V, where Vanadium(V) is the most toxic (Bhatnagar et al., 2008; Langmuir et al., 2003; Parks and Edwards, 2006; Filik and Yanaz, 2009; Liu et al., 2012). V(V) is most common in oxidizing conditions, and V(IV) and V(III) in reducing conditions (NTP, 2008; Gorzsás, 2005; Sánchez, 2013). Twelve species can exist in a solution , such as cationic, neutral and anionic forms, for example, VO_2^+, $VO(OH)_3$, $V_{10}O_{26}(OH)_2^{4-}$,VO_4^{3-} (Guzmán et al., 2002; Naeem et al., 2007; Bhatnagar et al., 2008). The vanadium species are oxidized in the water and air rapidly, going from an oxidation state of III and IV to state V. Therefore, every vanadium species behaves as a vanadate at neutral pH (NTP, 2008; Gorzsás, 2005; WHO, 2001; Padilla et al., 2015a). Figure 3 shows the Vanadium(V, IV and III) species in the environment.

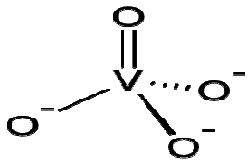

Vanadate, V(V)

Vanadyl, V(IV)

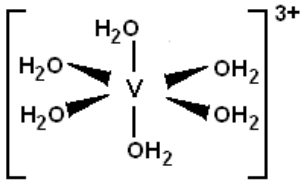

V(III)

Figure 3: V(V), V(IV) and V(III) species in the environment.

Vanadium is the result of natural and industrial sources. It is found in approximately 80 minerals in the earth's crust, and can be frequently found in fuel oil, fly ash, coal combustion, mineral ores, volcanic emissions, phosphorous ores and foods (Guidroz and Sneddon, 2002;

Garcia et al., 2004; Miyazaki et al., 2005; Naeem et al., 2007; Prathap and Namasivayam, 2009; Zeng et al., 2009; Aydin et al., 2013; Tian et al., 2014; Ritcher et al., 2014). The major anthropogenic sources are petroleum, combustion, and metallurgic and electronic refining (IARC, 2006). Vanadium is a component in the production of stainless steel, catalysts, jet engines, glass, paint, insecticide and ceramics (Pourret et al., 2012; Yeom et al., 2009; Filix and Yanaz, 2009; Chio et al., 2014; Hu et al., 2014; Hu et al., 2014; and among others). It is also used in the catalyst of sulfuric acid, where it oxidized the sulfur dioxide (IARC, 2006; Rout and Sarangi, 2014). In many countries, vanadium contamination in the environment has been documented with concentrations higher than 100 µg/L (IARC, 2006). Vanadium is an essential element in trace concentrations for the fixation of nitrogen in plants, mammalian nutrition, inhibition of enzymes, and in the insulin for diabetes treatment (Leonard and Gerber, 1994; Fan et al., 2005; IARC 2006; Erdem et al., 2011; Tian et al., 2014; Xie et al., 2014). High concentrations and prolonged exposure to vanadium damage the integumentary, respiratory, pulmonary, circulatory, skin, central nervous, gastrointestinal and digestive systems, as well as increase the risk of lung cancer and bronchial pneumonia (Vega et al., 2003; Mukherjee et al., 2004; IARC, 2006; NTP, 2008; ATSDR, 2012; Fortoul et al., 2014).

2.1.3 Chitosan

Chitosan is a natural polysaccharide obtained by the deacetylation of chitin, which is the second natural biopolymer most abundant after cellulose (show in Figure 4) (Jansson-Charrier et al., 1996; Gotoh et al., 2004; Kartal and Imamura 2005; Viswanathan et al., 2009; Aranaz et al., 2009; Vincentini et al., 2014). This natural polymer contains β (1→4)-2-acetamido-2-deoxy-β-

D-glucopyranose and 2-amino-2-deoxy-β-D-glucopyranose residues (Merrifield et al., 2004; Bhatnagar and Sillanpää, 2009; Dash et al., 2011; AbdElhady et al., 2012; Lertsutthiwang et al., 2013). The chitosan has a pKa of 6.2 to 7, is a cationic polymer and has a low specific area between 2 and 30 m^2/g (Boddu et al., 2008). Removing the acetyl groups makes it partially soluble in dilute mineral acids, such as hydrochloric, nitric, and phosphoric acid (Boduu *et al*., 2008; Crini, 2005; Guibal, 2004). The various chitosan molecular weights are: low molecular weight (less than 50,000 Daltons), medium molecular weight (50,000 to 150,000 Daltons), and high molecular weight (greater than 150,000 Daltons) (Blagg, 2012). It is a poly-N-acetylglusosamine extracted from the exoskeleton of crustacean shells, algae, fungal biomass, lobsters, insects and marine arthropods (Lu et al., 2000; Chen and Chung, 2006). Example of an exoskeleton of crustacean shells is shown in the figure 5.

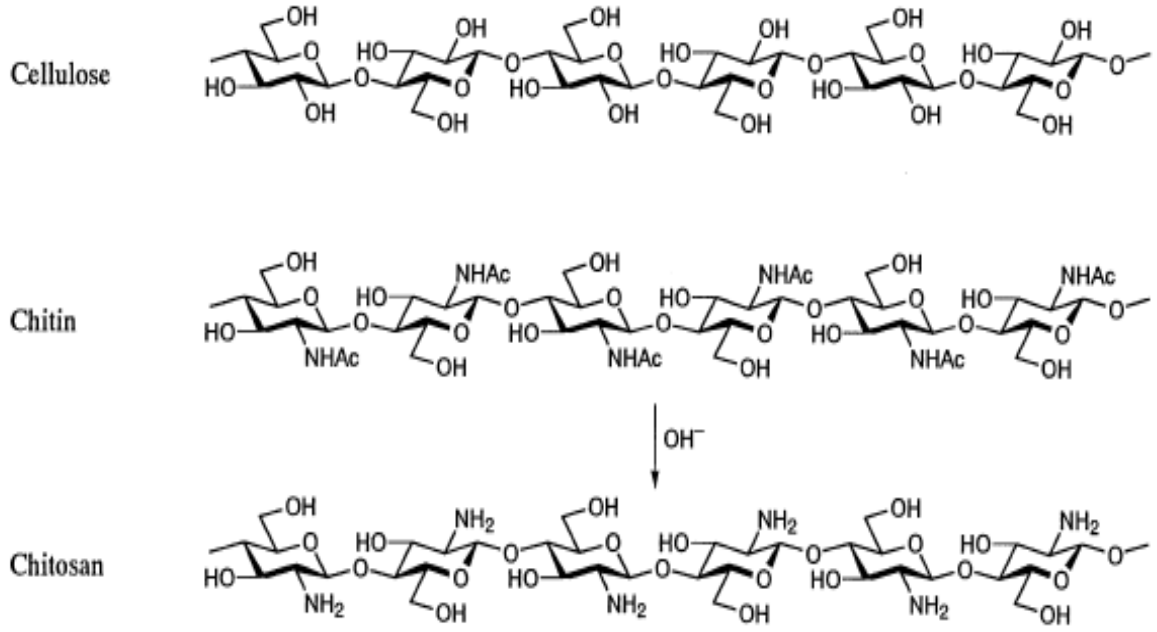

Figure 4: Cellulose, Chitin and Chitosan structure (Kurita, K. Controlled functionalization of the polysaccharide Chitin. Prog-Polym. Sci 2001, 26, 1921-1971).

Figure 5: Exoskeleton of crustacean shells for the preparation of chitosan.

Chitosan is a green adsorbent that has suitable characteristics such as non-toxicity, a high affinity for heavy metals and proteins, biodegradability, high availability, and metal ion chelation. It is also antibacterial, forming gel, has flexible structure on its polymeric chains, it is biocompatible and cost-effective (Babiker 2002; Gotoh et al., 2004; Kartal and Imamura, 2005; Yang and Hon, 2009; Liu et al., 2010; Xie et al., 2010; Zhang et al., 2011; Balan and Veristiuc, 2014, among others). This biopolymer presents a high adsorption capacity due to the presence of the amino ($-NH_2$) and hydroxyl (-OH) groups that can be chemically modified (Qian et al., 2004; Ngah and Fatinathan, 2008, 2010; Azlan et al., 2009; Xie et al., 2010; Lv et al., 2014) to interact with other species.

The specific applications for chitosan are focused in the areas of biotechnology, biomedical research, pharmaceutical research, drug delivery methods, dietetic research, agriculture, residual waters, cosmetics, textile and food industry (Albartogui et al., 2000; Adriano et al., 2005; Silva et al., 2006; Tikhonov et al., 2006; Liu et al., 2010; Cruz-Romero et al., 2013). The mechanical properties of chitosan can be increased using a crosslinking agent, such as gluteraldehyde (GLA), 1-(3-Dimethylaminopropyl)-3-ethylcarbodiimide (EDAC),

epichlorhydrin (ECH), thiols compounds, ethylene glycol diglycidyl ether (EGDE) and alginate (Sivaraman, 2004; Gotoh et al., 2004; Kolodyńska, 2012; Viswanathan et al., 2009; Ngah and Fatinathan, 2008; among others).

Chitosan has increasingly been studied for the adsorption of inorganic and organic dyes and anionic compounds, such as fluoride (Viswanathan et al., 2009), perchlorate (Xie et al., 2010; Lv et al., 2014), chromium (Liu et al., 2010; Kartal and Imamura, 2005), Copper(II) (Gotoh et al., 2004; Kolodyńska 2012; Kartal and Imamura, 2005; Ngah and Fatinathan, 2008), Cadmium(II) (Gotoh et al., 2004; Kolodyńska 2012), Cobalt(II) (Gotoh et al., 2004), Lead(II) (Kolodyńska, 2012; Nagh and Fatinathan, 2010), arsenic (Boduu et al., 2008; Kartal and Imamura, 2005), nitrate (Chatterjee et al., 2009), molybdate (Guibal et al., 1998), mercury (Merrifield et al., 2004), tungsten (Qian et al., 2004), amoxilin (Adriano et al., 2005) and others (Bhatnagar and Sillanpää, 2009; Guibal, 2004) from diluted solutions or wastewater due to interactions with its functional groups (-NH_2 and –OH).

2.2 Conventional Technologies

Conventional technologies have been used for the removal of arsenic and vanadium oxyanions in natural and drinking water, but some have not been sufficiently effective. Some of these techniques are: ion exchange, filtration process, chemical precipitation, electrochemical process, nanoparticles remediation, and adsorption. These are discussed below.

Ion exchange

Ion exchange is a physical/chemical process that involves an exchange of ions between the solid and liquid phase. This solid phase typically consists of resins that adsorb contaminants present in the water. There are three types of exchange: cationic (positive ion exchange), anionic (negative ion exchange) and amphoteric (simultaneous exchange of cations and anions). In this process the liquid phase is maintained in continuous contact with the solid phase until the ion exchange is achieved. Common ions used in this process are: hydroxide, chloride, hydrogen, and sodium, among others (Fu and Wang, 2011; Awual et al., 2012). This is a reversible process in which resin can be regenerated by washing it with a suitable regenerant. This process depends on various parameters such as pH, type of resin, ion competition, affinity and concentration of the contaminant (Shevade and Ford, 2004; Oehmen et al., 2006; Yeom et al., 2009; Hu et al., 2009; An et al., 2011; Awual et al., 2011).

Filtration process

In the filtration process, the membranes allow some components of interest through while blocking others to separate them from the water. Several of these membranes are classified by

the size of the pore; these are: microfiltration (MF), ultrafiltration (UF), nanofiltration (NF) and reverse osmosis (RO). The membranes pore sizes are 0.1-10 µm (MF), 0.01-0.1 µm (UF), 0.001-0.01 µm (NF) and 0.0001-0.001 µm (RO). MF and UF need low pressure, and NF and RO need high pressure, which tends to remove more constituents. The common materials used in the membrane include sand, cellulose, and polyamide, among others. These techniques depend on the driving force, including pressure, electrical potential, concentration and temperature. The different types of filtration processes have been applied in the removal of heavy metals from aqueous solutions (Ning, 2002; Gecol et al., 2004; Ergican et al., 2005; Saitúa et al., 2005; Fu and Wang, 2011; Yu et al., 2013; Kiani and Mousavi, 2013; Shang et al., 2014; Reddy et al., 2014).

Chemical Precipitation

Chemical precipitation is the process that occurs through the addition of a chemical reagent to the solution to form an insoluble compound. Common chemical reagents are: lime, sodium carbonate, sodium hydroxide, aluminum and iron hydroxides, among others (Richmond et al., 2004; Parks and Edwards, 2006; Sasaki et al., 2009; Park et al., 210; Donmez and Akbal, 2011). This is a three-step process: coagulation, flocculation and sedimentation. In coagulation, the contaminant particles are destabilized through fast agitation that promotes the agglomeration of particles. Examples of coagulants include sodium hydroxide, ferric sulfate, iron sulfide, sodium sulfide, and ferric chloride, among others. Flocculation is the formation of larger flocs that occurs by a softer agitation. Finally, in sedimentation, the flocs are completely separated from the liquid, thereby forming two layers in the solution which can be separated easily. The

disadvantages of this process are: pH dependence, solubility, high coagulant quantity, dependence on concentration of the analyte, species, low removal efficiency, and high cost.

Electrochemical process

An electrochemical process is a chemical reaction where ions are transferred through membranes by the movement of electrical currents. This involves the electron transfer between the electrode and the species in a solution, a type of oxidation-reduction reaction. Most of the studies used electrochemical cells for the removal of heavy metals and oxyanions (Anbari et al., 2008; Balasubranian et al., 2009; Lakshmipathiraj et al., 2010). Some disadvantages are: routine maintenance, instrument calibration, membrane replacement, and high cost.

Nanoparticles remediation

The remediation with nanoparticles has been of great interest in the removal of contaminants in water in recent years. Nanoparticles are particles with a size between 1 and 100 nm. These have large surface areas, and atomic and molecular properties, which are dependent on the size of the particles. In previous works, nanoparticles have been used for the removal of arsenic (Kanel et al., 2005; Rahmani et al., 2011; Martinson and Reddy, 2009). Although they have had very good adsorption capacity, their disadvantages are the syntheses are complex, they need high purity reagents, the materials are expensive, and they are not feasible for water treatment applications (Ge et al., 2012). Also, they might be toxic to the environment and humans (Mnyusiwalla et al., 2003).

Adsorption process

Adsorption is a chemical process where the pollutant adhered onto the surface of an adsorbent. In general, the adsorbent is a solid, and the adsorbate is in liquid or gas phase. Adsorption involves chemical forces (covalent bonding, hydrogen bonding, ligand exchange) and physic forces (Van der Waals and electrostatic attractions). The adsorbent most common is activated carbon (Namasivayam and Sangeetha, 2006; Ansari and Sadegh, 2007; Chen et al., 2007; Israt Jahan et al., 2008; Asadullah et al., 2013).

Adsorbents that have been used for the removal of vanadium and arsenic are: natural siderite and hematite (Guo et al., 2007), biomass (Pokhrel and Viraraghavan , 2006; Haque et al., 2009; Pennesi et al., 2013), iron coated materials (Katsoyiannis and Zouboulis, 2002; Li et al., 2009; Mak et al., 2009; Zhao et al., 2009; Santos et al., 2012; Tang et al., 2013), polypirrole (Eisazadeh 2008), waste rice husk (Ahim et al., 2006), sodium silicate (Boyaci et al., 2010), nZVI (Kanel et al., 2005; Tanboonchuy et al., 2010), aluminum based in water treatment residual (Makris et al., 2009), waste metal sludge (Bhatnagar et al., 2008), calcium hydroxyapatite (CAP) adsorption (Vega et al., 2003), Fe(III)/Cr(III) hydroxide waste (Prathap and Namasivayam, 2009), aluminum-pillared bentonite (Manohar et al., 2005), silica gel (Fan et al., 2011), zeoiltes (Xu et al., 2002), bauxite (Bhakat et al., 2006), among others (Mohan and Pittman, 2007; Martinson and Reddy 2009; Kumar et al., 2011; Meng et al., 2012; Alagumuthu and Sumathi, 2012; Sánchez et al., 2012; Sánchez et al., 2013; Cui et al., 2013; Pan et al., 2014). Also, chitosan derivates have been used in the removal of these oxyanions (Dambies et al., 2002; Sivaraman 2004; Chen and Chung 2006; Boddu et al., 2008; Chen et al., 2008; Rana et al., 2009; Gupta et al.; 2009, Boyaci et al., 2010; Gerente et al., 2010; Miller et al., 2011; Guibal et al., 1998; Jansoon-Charrier et al., 1996; Qian et al., 2004; Xia et al., 2014; Du et al., 2014).

These technologies or methods have several disadvantages, such as a high cost, the consumption of high amounts of energy, the necessity for a high adsorbent dosage, acidic or basic pH and high temperatures, and a slow equilibrium process. With respect to the adsorbent presenting high toxicity, most need to be modified and represents a high cost. Among these, chitosan, as an adsorbent, can be considered an efficient, simple, cost-effective alternative for the removal of arsenic and vanadium oxyanions at trace levels from aqueous solutions.

2.3 Isotherms

The adsorption isotherms models describe the equilibrium and adsorption capacity of a material on the surface of the adsorbent. Once the adsorbate concentration does not change with time in the adsorption process, equilibrium is obtained. To describe the equilibrium of the adsorbent with the adsorbate, the two isotherm models most commonly used in the adsorption process are Langmuir and Freundlich.

2.3.1 Langmuir isotherm

The Langmuir isotherm model assumes that every adsorption site of the adsorbent is equivalent in energy and forms a saturated monolayer on the surface of the adsorbent (Padilla et al., 2014; Sánchez et al., 2012; Kannan and Singanan, 2014; Saravanan et al. 2013; Murugan and Ganapathy, 2012). The Langmuir equation was calculated from the linear form shown below:

$$\frac{C_{eq}}{q_e} = \frac{1}{Q^o\, b} + \frac{C_{eq}}{Q^o} \qquad (1)$$

Where,

C_{eq} = the concentration of adsorbate in solution at equilibrium (mg/L)

q_e = the adsorption capacity of the adsorbent at equilibrium (mg/g);

Q^o = the maximum adsorption capacity for a monolayer until saturation (mg/g)

b = the affinity of the solute for the adsorbent (L/mg).

These parameters were calculated using the slope and intercept of the plot C_{eq}/q_e *vs.* C_{eq}.

The Langmuir isotherm can determine the favorability of the adsorption process, which was expressed by the dimensionless constant R_L, and calculated from the following equation (Boddu et al., 2008; Saravanan et al., 2013; Padilla et al., 2014, 2015a, 2015b):

$$R_L = \frac{1}{1+bC_0} \quad (2)$$

Where,

C_o = the initial concentration of the adsorbate (mg/L)

b = the Langmuir constant (mg/g)

The $1>R_L>0$ value indicates that the adsorption is favorable; the $R_L> 1$ value indicates that it is unfavorable; the $R_L=1$ value indicates that it is linear; the $R_L=0$ value indicates that it is irreversible.

2.3.2 Freundlich Isotherm

The Freundlich isotherm model assumes that the adsorption sites are heterogeneous in energy and form a multilayer on the surface of the adsorbent (López et al., 2012; Boyaci et al., 2010; Saravanan et al., 2013). The linear Freundlich equation is expressed as follows:

$$logq_e = logK_F + \left(\frac{1}{n}\right) logC_{eq} \quad (3)$$

Where,

q_e = the adsorption capacity of the adsorbent at equilibrium (mg/g)

C_{eq} = the equilibrium concentration of the solute (mg/L)

1/n = the adsorption intensity

K_F = a measurement of relative adsorption capacity ((mg/g)(L/mg)^n)

The n value yields information of the adsorption process, which is favorable at low concentration (n>1), independent of the concentration (n=1) and favorable at high concentration (n<1). The inverse of n (1/n) indicates how strongly the adsorbate is attached to the surface; a value between 0 and 1 indicates that the adsorption was a favorable process. These were calculated from the slope and the intercept of the plot *log* q_e *vs. log* C_{eq}.

2.4 Instrumentation

2.4.1 Inductively Coupled Plasma- Mass Spectrometry (ICP-MS)

This is the principal technique used in our studies. Figure 6 shows the ICP-MS instrument used in our experiments. Inductively coupled plasma - mass spectrometry (ICP-MS) is a technique for elemental analysis that is rapid, highly sensitive, simple, robust and multi-elemental. It is used in various fields such as environment, chemical, food, clinical, forensic, metallurgy, physics, geology, and pharmaceuticals, among others. This technique has detection limits for the analysis of trace elements at ppb to ppt levels. The sample is ionized by the high temperatures present in the argon plasma. These ions will be separated by their mass/charge ratio in a mass spectrometer and then guided to a detector. The parts of the equipment are: sample introduction (nebulizer and spray chambers), ionization source (torch), interface extraction (cone sampler and cone skimmer), collision cell/reaction (octapole), ion lenses, mass spectrometer (Quadrupole) and detector (electron multiplier).

Sample introduction: The liquid samples are injected into a nebulizer by means of a peristaltic pump in aerosol form. Then, the spray chamber separates the large droplets (greater than 10 µm in diameter) that have been formed and discard them. Only small droplets are transported to the plasma.

Ion Source: The torch is made of concentric quartz tubes and surrounded by coils 2-4 turns, which transmits argon current, and generates a radio frequency and electromagnetic field. Here the plasma is generated and the ionization of the sample occurs.

Plasma: Plasma consists of ionized argon gaseous atoms in the high temperature zones and coexists in a mixture of ions, electrons, neutral atoms and excited atoms. This is caused due a

high voltage spark as a result of Ar^{+} ions and e- in the walls of the outer tube of the torch. A good temperature for argon discharge is about 6,000 to 10,000 K, and the ions formed are positive.

Vacuum System: Mass spectrometers operate at low pressure (high vacuum). There are three systems of vacuum pumps (the interface area, the pre- parser, and analyzer area).

Plasma Interface/Empty: The function of the interface is to extract the gas plasma that was added to the original sample to avoid collisions of the ions with the constituent molecules of air. The interface has two metal cones (Ni or Pt) with a small central hole through by which the analyte ions are extracted into the mass spectrometer through an increasing level of vacuum. The first cone is called a "sampler" (sampling cone) and the second a "skimmer" (cone separation). The sampler cone leads to a chamber with a vacuum of 10 mbar and a rapid expansion of the gas, which causes cooling. The skimmer cone reaches a pressure of 10^{-3} mbar. There the gas is separated from the positive ions and pumped out. The cations are focused on the mass spectrometer through ion lenses.

Ionic lenses: The ionic lenses are electrostatic plates transporting the ion beam coming from the skimmer to the mass spectrometer. They are also responsible for separating the ions and neutral species of the photons through the electrostatic fields created.

Reaction collision cell: The cell collision involves an Octopole Reaction System (ORS) in which are eliminated the polyatomic interferences due to the collisions effect of hydrogen (reactive gas used to interact with some of the interferences) or by collisions with helium (inert gas that collides with interferences). The hydrogen gas is specific for eliminating interference polyatomic argon. Helium gas eliminates multiple interferences; it does not react with the matrix of the

sample, whereby no new interference is not produced. During normal use the ORS in not active and operates without gas and only acts as a guide of the ion beam.

Mass analyzer: The principal is the quadrupole, which are four metal bars that are parallel and equidistant. These work under a continuous current potential and a radio frequency source. This separates the ions based on their mass to charge (m/z) ratio and then guide the selected mass to the detector.

Detector: The main detector is the electron multiplier, which generates an electrical signal. This is generated by the change in potential when the ions collide with the surface, secondary electrons are moved to other regions where they collide and originate a cascade of electrons.

Figure 6: ICP-MS Agilent 7500ce used in our studies.

2.4.2 Laser Ablation Inductively Coupled Plasma Mass Spectrometry (LA-ICP-MS)

In Laser ablation inductively coupled plasma mass spectrometry, the solid sample is directly analyzed by ablation with a pulsed laser beam. The created aerosols are transported into the core of ICP, which generates high temperatures. The plasma in ICP-MS is used to generate ions that are then introduced to the MS, where they are separated and collected according to their m/z ratios. The selected elements of an unknown sample can be identified and measured. There are no sample size requirements and no sample preparation procedures.

LA-ICP-MS can determine minor, major, and trace elements as well as isotope-ratio measurements, which offers superior technology for direct solid sampling in analytical, forensic, trace mineral, geology, fossil, metals, semiconductors and environmental chemistry analyses. The advantages of LA-ICP-MS include direct analysis of solids, no chemical dissolution, analysis of small sample mass, reduced risk of contamination, and determination of spatial distributions of elemental compositions (Trejos et al., 2006; Mokgalaka and Gardea-Torresday, 2006; D'Oriano et al., 2008; Jackson, 2008). The disadvantage of LA-ICP-MS is that the required optimization of laser parameters changes depending on the matrix sample (Trejos et al., 2006; Mokgalaka and Gardea-Torresday, 2006; D'Oriano et al., 2008) and the lack of availability of standars for the different matrices. Several parameters were optimized, such as depth/pass, rep rate, light, output and spot size of the laser beam passes over the sample. The equipment used in our experiments consists of a high performance Nd:YAG deep UV 213nm (UP213 Universal Platform) laser ablation system and the software is ELAN DRC II- ICP-MS (Figure 7).

Figure 7: Laser ablation (UP-213) used in our studies.

2.4.3 X-ray Fluorescence Spectrometer (XRF)

X-ray fluorescence (XRF) is an instrument consisting of a conventional X-ray tube, a focussing LiF monochromator, a rotating stage holding the sample on a petrographic microscope, and a solid-state X-ray detector (Engi et al., 2002). A primary X-ray beam illuminates the sample, emits X-rays along a spectrum of wavelength characteristics of the types of atoms present in the sample. The atoms in the sample absorb X-ray energy by ionizing and ejecting electrons from the lower energy levels. The ejected electrons are replaced by electrons from the higher energy orbital. This energy releases in the form of X-rays which is unique to the type of atom present. It is used for relatively non-destructive chemical analyses of rocks, cements, minerals, soils, metals, ceramic, glass, petroleum and environmental studies. The XRF is comparatively inexpensive, simple to operate, no sample preparation, no chemical procedures, non-destructive and reduces risks of analyte loss or cross contaminations, and independent of

sample geometry (Engi et al., 2002). Their limitations are: standard is required for similar composition, relatively large samples (typically > 1 gram powder), limited in precision and accuracy measurements; the abundances of elements with Z<11, cannot distinguish variations among isotopes of an element or ions of the same element in different valence states. Optimizing of several parameters including: XRF primary filter, collimator, voltage and base. The instrument used in this study is a FISHERSCOPE X-RAY XDAL spectrometer (Figure 8).

Figure 8: X-Ray Fluorescence used in our studies.

2.4.4 Mars Express Microwave

The microwave oven is a technique used mostly for digesting organic, inorganic and volatile samples. Microwaves are electromagnetic waves generated by a device of high potential called a magnetron. To digest the samples, a suitable solvent is used, in most cases acids. Several advantages of using this technique are: fast, does not break chemical bonds, is not ionizing radiation, and can be subjected to high temperatures and pressures. These are carried out in closed vessels made of polymers (usually Teflon) that resist high temperatures and pressures, do not react with analyte, and allow no contamination or volatilization of the sample. All samples are subjected to controlled and similar conditions, which contributes to the precise analysis. Figure 9 shows the Mars Express Microwave used in our experiments.

Figure 9: Microwave Mars Xpress used in our studies.

2.4.5 Scanning Electron Microscopy (SEM)

The SEM is an instrument that produces a largely magnified image of a sample surface by using electrons to form an image. A beam of electrons is produced at the top of the microscope by an electron gun, which follows a vertical path through the microscope in vacuum. The beam travels through electromagnetic fields and lenses, once the beam hits the sample, electrons and X-rays are ejected from the sample and convert them into a signal image.

For sample preparation, all the water must be removed from the samples and it needs to be conductive, therefore are covered with a thin layer of conductive material. This is done by a device called a sputter coater, which uses an electric field and argon gas, where the sample is placed in a small chamber that is under vacuum (10^{-4} to 10^{-6} torr). Argon ions are attracted to a negatively charged gold foil. These gold atoms fall and settle onto the surface of the sample producing a thin gold coating.

The technique is applied in many disciplines of the science and is used as a research tool, where is analyzed the state of the surface and the estimation of morphology. The SEM permits the observation and characterization of heterogeneous organic and inorganic materials on a nanometer (nm) to micrometer (μm) scale (Kowalewska and Szwedo, 2009). Its a relatively simple to use, inexpensive equipment, has a large depth of field and high resolution for clear images (Wang et al., 2011).

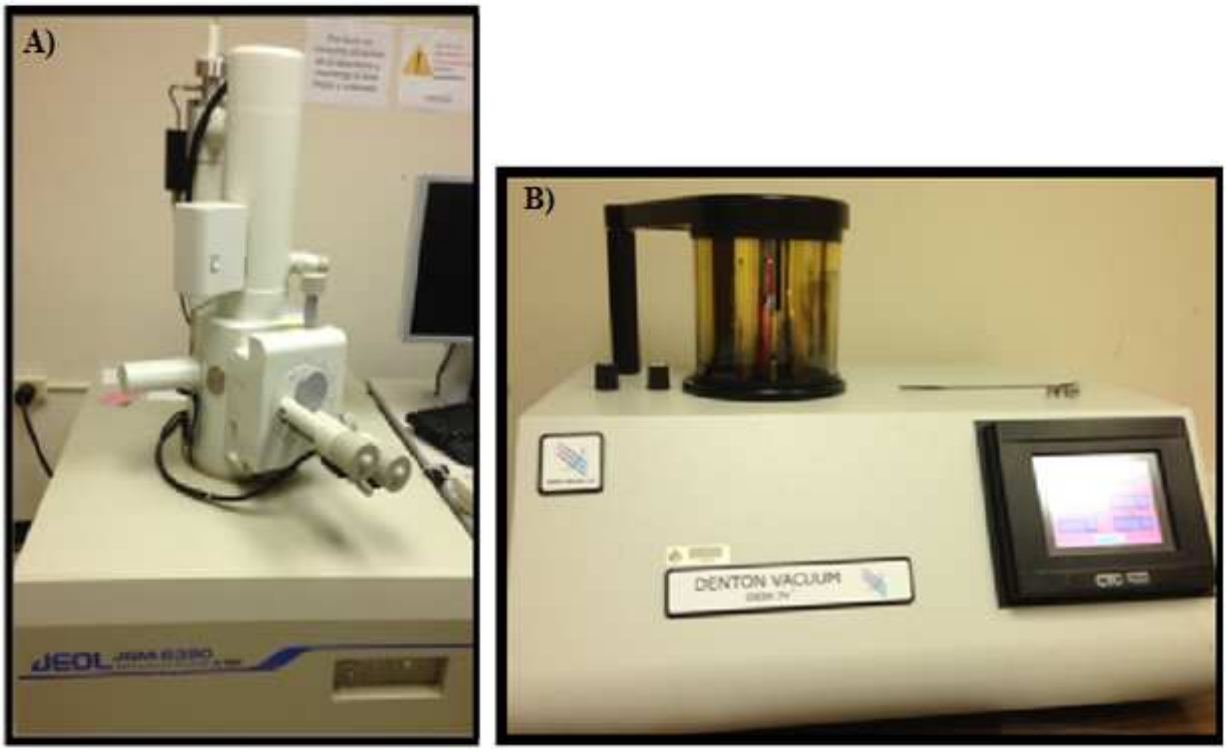

Figure 10: A) SEM Model JEOL JSM-6390 and B) Sputter coater Denton Vacuum Desk IV.

2.4.6 Fourier Transform – Infrared Spectroscopy (FT-IR)

FT-IR is a spectroscopic technique used to identify functional groups in molecules or organic compounds. The FT-IR spectra are the fingerprint of each compound, corresponding to the vibrational modes of the absorption or transmittance of electromagnetic radiation by the organic molecules. The frequencies at which the functional groups absorb the electromagnetic radiation are at a wavelength in the range of 400 to 10,000 cm^{-1}. The Fourier Transform converts the molecular motions into a computarized signal, which is represented in a graph called spectrum. This allows the analysis of solids, liquids or gaseous samples, either as a pure liquid or gas, liquid solution, powder, or as potassium bromide tablets or oil mulls. Advantages of using

this technique are that it is fast, easy to use and provide accurate results. Figure 11 shows the ATR-FT-IR used in our studies.

Figure 11: ATR-FT-IR Model IR Affinity-1 used in our studies.

2.4.7 Image Stacking Photography (ISP)

The stacking technique takes pictures focusing on different planes of the sample and a digital image is obtained with a greater depth of field. This is done using dedicated software for stacking. The ISP gives us information on the morphology of the sample and generates a digital image. The fields that apply the ISP technique are chemistry, physics, geology and biology. Figure 12 shows the ISP used in our studies.

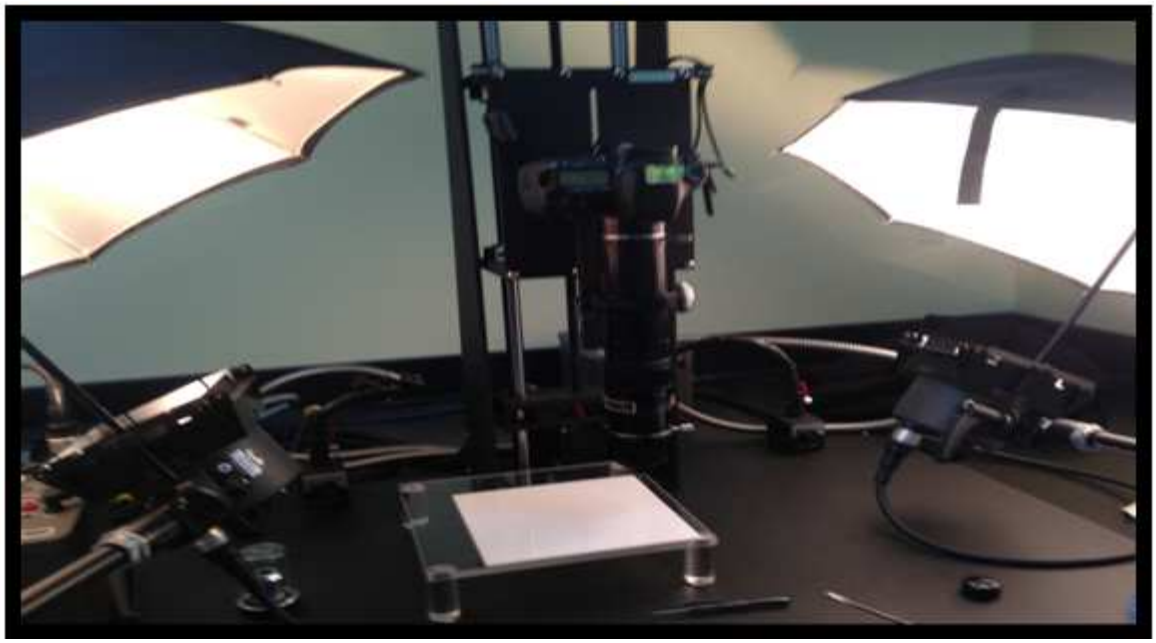

Figure 12: Image Stacking Photography used in our studies.

2.4.8 Thermogravimetric Analyzer (TGA)

Thermogravimetry analyzer (TGA) is based on a method of thermal analysis, which measures the change in mass of a sample when subjected to a temperature change in a controlled atmosphere. The loss or gain of mass will give us information about whether the sample decomposes or reacts with other components as a function of the increase in temperature or time. With this technique it can be determined degradation temperature, reaction rate, sample identification, among others. TGA could be used in conjunction with other techniques such as IR, allowing one to obtain additional information on the thermal behavior of a sample. Figure 13 shows the equipment used in our studies.

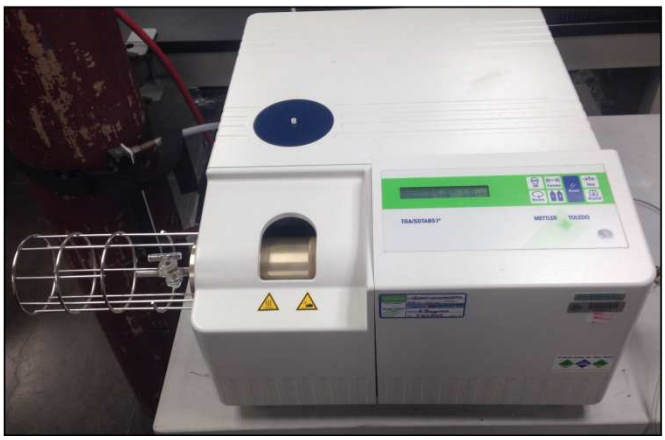

Figure 13: TGA instrument used in our studies.

2.4.9 Brunauer, Emmet and Teller (BET)

Brunauer, Emmet, and Teller (BET) and Langmuir equation are methods to measure the surface area of a material. BET is characteristic of solids on which the superior layer is in equilibrium with the gaseous molecules. It is determined by the physical adsorption of gas molecules on a solid surface. Langmuir method assumes that the adsorption is limited to one monolayer.

3 METHODOLOGY

In this chapter the methodology is summarized by reagents, materials and instrumentation; synthesis of adsorbents; characterization of adsorbents; adsorption test; desorption tests; and adsorption/desorption test.

3.1 Reagents, materials and instrumentation

3.1.1 Reagents

Only high purity and certified analytical chemicals were used in all the experiments.

- Sodium hydrogen arsenate heptahydrate ($Na_2HAsO_4.7H_2O$) (Alfa Aesar CO., ACS grade)*
- Sodium arsenite ($NaAsO_2$) (Ricca Chemical Co., Reagent grade)*
- Ammoniun metavanadate (NH_4VO_3) (Sigma Aldrich Chemical Co.)*
- Vanadium(IV) oxide sulfate hydrate ($VOSO_4.5H_2O$) (Sigma Aldrich Chemical Co.)*
- Vanadium(III) chloride (VCl_3) (Sigma Aldrich Chemical Co.)*
- ICP-MS standard solutions (Sigma Aldrich Chemical Co.)*

  *These were used for solutions preparation for adsorption process, and standards solutions for the construction of calibration curves.

- Nitric acid (HNO_3) (Fisher Co. Optima grade) was used to adjust pH, desorption experiments and solid samples digestion. Also, it was used for the cleaning of glassware and plastics, and in the preparation of the blanks and calibration curves for standard solutions for ICP-MS analysis.

- Sodium hydroxide (NaOH) (Fisher CO., ACS grade) was used to adjust pH, and desorption experiments. Also, it was used for the chitosan beads preparation.
- Hydrochloric acid (HCl) (Fisher Co., trace metal grade) was used for the desorption experiments. Also, it was used to rinse the chitosan beads.
- Sulfuric acid (H_2SO_4) (VWR Co., Reagent ACS) was used for the desorption experiments.
- Glacial acetic acid (CH_3COOH) (Fisher Co., Certified ACS) was used for the dissolution of chitosan and chitosan solutions preparations.
- Sodium chloride (NaCl) (Fisher Co., ACS grade), sodium carbonate monohydrate (Na_2CO_3. H_2O) (Alfa Aesar Co., 99.5% purity), sodium sulfate (Na_2SO_4) (Fisher Co., 99.5% purity), sodium phosphate monobasic ($NaH_2PO_4.H_2O$) (Fisher Co., ACS grade) were used as co-existing anions for adsorption process.
- Chitosan Medium molecular weight degree of deacetylation 75-85% (Sigma Aldrich Co.) was used for the synthesis of chitosan beads or flakes.
- Meso-2,3-dimercapto succinic acid 98% (DMSA) (Fisher CO.), N-acetyl-L-cysteine (NAC) (Fisher Co.) and gluteraldehyde solution Grade I, 50% (GLA) (Sigma Aldrich Co.) were used for the functionalization of chitosan beads.
- Sodium molybdate (Na_2MoO_4) (Sigma Aldrich Co.) was used for the preparation of DMSA and NAC solution.
- Ferric chloride hexahydrate ($FeCl_3.6H_2O$) (Ricca Chemical Co.) was used for the preparation of Fe(III)-CB.
- Deionized water 18.2 MΩ and destilled water was used for all the studies.
- Argon high purity gas (99.9%) was used for ICP-MS analysis.

3.1.2 Materials and equipment

- Peristaltic Pump
- Thermostated shaker bath
- pH meter (Oakton pH 510 Series)
- Filtration system
- Analytical balance
- Polyethylene bottles
- Centrifuge tubes
- Filters papers (Whatman #1, 90 mm)
- Magnetic stirrers
- Beakers
- Volumetric flasks
- Plastic flasks
- Volumetric pipettes
- Micropipettes
- Funnels
- Watch glasses
- Paper and plates weight

3.1.3 Instrumentation

- Inductively Coupled Plasma- Mass Spectrometry (ICP-MS)
- Mars Express Microwave
- Scanning Electron Microscopy (SEM)
- Laser Ablation Inductively Coupled Plasma Mass Spectrometry (LA-ICP-MS)
- X-ray Fluorescence Spectrometer (XRF)
- Fourier Transform – Infrared Spectroscopy (FT-IR)
- Image Stacking Photography (ISP)
- Thermogravimetric analyzer (TGA)
- Surface area analyzer (BET and Langmuir methods)

3.2 Synthesis of adsorbents

In this session, the preparation of the various modifications or functionalizations of chitosan beads are summarized.

3.2.1 Chitosan Beads (CB)

The chitosan beads were synthesized using chitosan powder medium molecular weight dissolved in glacial acetic acid solution (5%) to obtain a 2% w/v chitosan solution. The resulting viscous chitosan solution was added droppedwise using a peristaltic pump into a 1.0 M aqueous NaOH solution to form uniform chitosan beads. The aqueous NaOH solution was under a continuous stirring using a mechanical stirrer at 200 rpm. After gelling in 1 M NaOH solution, the beads were rinsed with deionized water to remove the excess NaOH. The content was filtrated and finally dried at room temperature or at 60 °C. Figure 14 shows the schematic for the synthesis of chitosan beads.

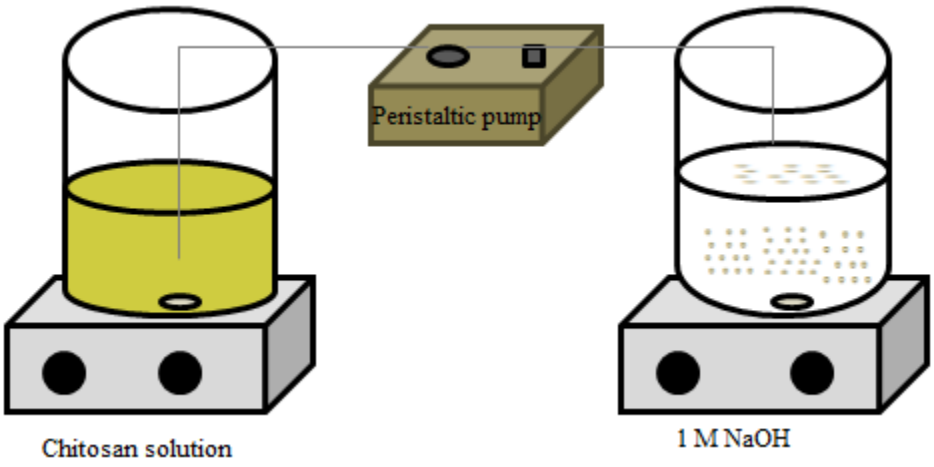

Figure 14: Schematic for the synthesis of chitosan beads.

3.2.2 Chitosan Beads-Gluteraldehyde (CB-GLA)

Once the formation of chitosan beads (CB) into 1 M NaOH solution, they were rinsed with deionized water to remove the NaOH excess. Then, the CB were placed in contact with 0.025 M GLA (shown in figure 15) solution without agitation at room temperature for 24 hours. After crosslinking, the CB-GLA were rinsed with deionized water to remove any free GLA and dried at room temperature or at 60˚C.

Figure 15: Gluteraldehyde (GLA) structure

3.2.3 Chitosan functionalized with DMSA and NAC (CB-DMSA and CF-NAC)

A similar procedure as the one described previously by Sivaraman (2004) was used for the functionalization of chitosan beads with dimercapto succinic acid (DMSA) and N-acetyl-L-cysteine (NAC). Figure 16 shows the DMSA and NAC structure. Once, the chitosan beads were in contact with 1 M NaOH and rinsed with deionized water to remove excess of NaOH, these were functionalized with NAC or DMSA solution for 48 hours without agitation at room temperature. NAC or DMSA solution were prepared by dissolving 1.2 g of DMSA or NAC powder in 200 mL of 0.094 M sodium molybdate solution., which was used to protect the thiol groups during the crosslinking process. After crosslinking, the chitosan beads were rinsed with 0.1 M HCl to release the molybdenum and expose the thiol groups. Afterwards, the beads were

rinsed with deionized water until it reached a neutral pH. Finally, the beads were dried at room temperature or at 60˚C.

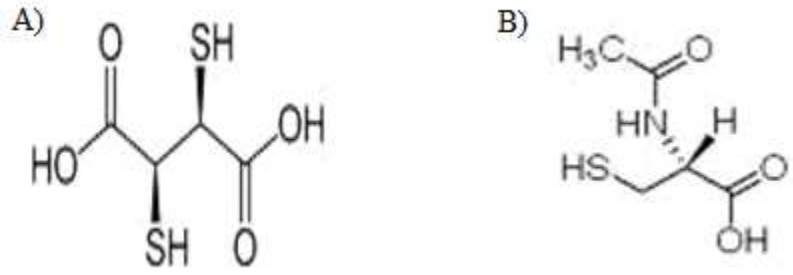

Figure 16: A) Dimercapto succinic acid (DMSA) and B) N-acetyl-L-cysteine (NAC) structure

3.2.4 Protonated Chitosan Flakes (PCF)

After the chitosan beads were formed, they were rinsed with deionized water, followed by a dilute HCl solution (0.1 M) until the adsorbent suspension solution reached a pH of 5.00 ± 0.1. The PCF was rinsed with deionized water to remove the HCl excess, and then it was filtered and dried at room temperature or at 60° C.

3.2.5 Fe(III)-Chitosan beads (Fe(III)-CB)

Once the chitosan beads were rinsed several times with deionized water to remove NaOH excess, these were placed in a beaker containing a $FeCl_3$ solution (0.01, 0.05 or 0.1 M) at a pH adjusted to 8.0 ± 0.1 and kept under stirring (200 rpm) at 25˚C for 24 hours of contact time. This contact time allows for the ferric hydroxide colloids formation and its immobilization onto the chitosan beads' surface. The resulting Fe(III)-CB were rinsed with deionized water to remove excess iron and dried at room temperature or at 60˚C.

3.3 Characterization of adsorbents

3.3.1 Image Stacking Photography

The technique of Image Stacking Photography (Visionary Digitals, BK Plus Lab System) in CF4-P1magnification was used to determine the average sizes of the beads or flakes.

3.3.2 Scanning Electron Microscope (SEM)

A scanning electron microscope (JEOL JSM-6390) was used to determine the morphology and shape of the beads or flakes at diverses magnifications (30, 1500 and 7000X). To improve the SEM image quality, all samples were coated with gold using a Gold Sputter Denton Vacuum Desk IV.

3.3.3 Fourier Transform-Infrared (FT-IR)

FT-IR spectra were conducted using an IR affinity-1 Fourier Transform Infrared Spectrophotometer (Shimadzu) with Attenuated Total Reflectance (ATR) to determine the presence of functional groups onto the beads surface. All the spectra were obtained by the accumulation of one-hundred scans, a resolution of 8 cm^{-1} and a wavenumber range of 500 - 4000 cm^{-1}. ATR was used in all the spectra because it allows the analysis of adsorbent without the need for sample preparation.

3.3.4 Inductively Coupled Plasma Mass Spectrometry (ICP-MS)

ICP-MS was used for elemental analysis of arsenic and vanadium oxyanions during the adsorption and desorption studies. Also, was used to determine the content and release of iron from Fe(III)-chitosan beads. The Fe(III)-CB (10 g/L) in contact with concentrated nitric acid were digested in duplicate using a Mars Express Microwave with an irradiation of 20 min at 150˚C. The iron content in the beads was determined using an Inductively Coupled Plasma-Mass Spectrometry (ICP-MS, Agilent 7500ce Series). In addition, the potential release of iron from the beads during adsorption tests were investigated by performing experiments varying the solution pH (2, 4, 6, 8 and 10) for 26 hours of contact time at 25˚C and 200 rpm in batch mode. The total concentration of iron was determined in accordance with the EPA method 200.8 rev.5.4 with a modification. The modification consisted in the use of the reaction cell in hydrogen mode for the analysis of iron to eliminate polyatomic interferences. Scandium was used as an internal standard. Method blank and matrix spikes were analyzed to determine possible interferences and contamination from solutions or containers.

3.3.5 Point of zero charge (pH_{pzc})

The point of zero charge (pH_{pzc}) was obtained using a batch equilibrium technique (Appel et al., 2003; Faria et al., 2004). The beads (0.15 g) were contacted with 50 mL of sodium chloride solution (0.01 M) in diverse pH range of 2 to 12 by 48 hours at 200 rpm. The pH_0 and pH_f was measured to construct the graph of pH_0 - pH_f vs. pH_0 (Faria et al., 2004; López et al., 2012; Rao et al., 2011). The pH_{pzc} was obtained by the curve intersect in the x-axis of the graph. This information shows that a pH below the pH_{pzc} indicates an electrostatic attraction and the net

surface charge is positive and will attract anions. Also, over this pH_{pzc} indicates an electrostatic repulsion with a negative net surface charge, and will attract cations (Appel et al., 2003; López et al., 2012; Manahan, 2000; Rao et al., 2011).

3.3.6 Solubility and swelling effect

Solubility and swelling studies were performed using a similar procedure described previously (Ngah and Fatinathan, 2008). The diverse chitosan beads or flakes (50 g/L) were immersed in different solutions individually in centrifuge tubes. These solutions were acetic acid 5% v/v, hydrochloric acid 0.1 M, sodium hydroxide 0.1 M and deionized water. The solubility was determined after 24 hours of agitation as is soluble, insoluble or partially soluble. The swelling effect provided important information about the nature of the adsorbent, where a high percentage indicates that the adsorbent is very fragile and inadequate for the adsorption process. The height of the solution in the centrifuge tubes was marked before and after the 24 hours of immersion at 200 rpm. The swelling percentage was calculated utilizing Equation 1,

$$\% \, Swelling = \frac{h_t - h_0}{h_0} \, x \, 100 \qquad (4)$$

where h_t is the height level (cm) after 24 hours of immersion; and h_0 is the height (cm) measured right after the beads were immersed.

3.3.7 Laser Ablation-Inductively Coupled Plasma Mass Spectrometry (LA-ICPMS)

Laser Ablation Inductively Coupled Plasma Mass Spectrometry (LA-ICP-MS) spectra were determined by a New Wave Research UP series 213 (Nd:YAG deep UV 213 nm) and an ELAN DRC II-ICP-MS software. A 100 µm spot size impacted the sample following a predetermined raster, the laser used an energy of 1.6 mJ and a repetition rate of 20 Hz. ICP-MS parameters used were as follows: plasma radiofrequency power, 1,400 W; plasma gas flow (Ar), 18 l min^{-1}; Carrier (Ar) flow rate 1.3 L min^{-1}; scanning mode peak hopping; dwell time, 35 ms; 1 sweeps, 1200 readings; and 1 replicates. The others parameters used with laser ablation were scan speed (50 µm/s), depth/pass (10 µm), output (100%), rep rate (20 Hz), and spot size (110 µm). The analysis time was 2 min per spot, including 1 min of background acquisition. The oxyanions signal onto adsorbent was determined by comparing it with the carbon signal found in the chitosan structure to obtain graphical representation of element intensity as function of time in seconds. Carbon was used as an internal standard in the biological matrix.

3.3.8 X-ray Fluorescence (XRF)

X-ray fluorescence spectra were used to determine the presence of the oxyanions traces onto the chitosan flakes using a FISHERSCOPE X-RAY XDAL. The parameters used in this study were: a collimator of 0.60 Dm, high voltage of 50 eV, a non-primary filter, and as base were used gold (Au) for vanadium oxyanions and titanium (Ti) for arsenic oxyanions.

3.3.9 Thermogravimetric analyzer (TGA)

TGA was used to determine the degradation of the sample in function of temperature. These measurements were evaluated on a Mettler Toledo TGA. The beads were analyzed in a nitrogen atmosphere with a temperature ramp of 10 °C/minute from 25 to 600 °C.

3.3.10 Surface area (BET and Langmuir Methods)

BET and Langmuir methods were used to determine the specific surface area of the beads/flakes under nitrogen atmosphere at 77 K using a Micromeritics 2020.

3.4 Adsorption tests

Adsorption experiments were conducted in batch mode using 125 mL plastic sealed bottles in a water shaker batch (Shown in Fig. 15). All experiments were carried out in duplicate and agitated at 200 rpm to reach equilibrium at room temperature (25˚C). Aqueous samples were analyzed at different contact for 26 hours. For the adsorption experiments, the oxyanions solution were individually contacted with 5 g/L of PCF or Fe(III)-CB at initial pH 6.0 ± 0.1. Adsorption isotherms were studied at initial concentration of Vanadium(III) from 3 to 8.8 mg/L, Vanadium(IV) from 1 to 6.3 mg/L, Vanadium(V) from 1 to 5.5 mg/L and Arsenic(V) from 0.075 to 5.0 mg/L using PCF as adsorbent. For the studies that used Fe(III)-CB as adsorbent, the range concentrations were of 0.1 to 5.0 mg/L for Arsenic(III) and Arsenic(V) oxyanions. Lower concentrations than those used for the isotherms obtained a 100 removal percent.

Several conditions were studied at an initial oxyanions concentration of 0.500 mg/L, such as the contact time (0-26 h), adsorbent concentration (1, 3, 5 and 10 g/L), the pH of the aqueous solution (2, 4, 6, 8 and 10), pH adsorbent suspension solution (4, 5, 6, 7, 8, 10 and 12) and the analysis of the co-existing anions. These co-existing anions were carbonate, chloride, sulfate and phosphate at concentration levels of 0.01 and 0.02 mmol which were contacted independently.

All the samples were acidified with nitric acid 2 % v/v for preservation. The pH solution was adjusted with diluted nitric acid or sodium hydroxide solutions. The total oxyanions concentration were analyzed in triplicate using an ICP-MS (Agilent ICP-MS 7500ce Series), in accordance to the EPA method 200.8 rev.5.4. The method blank and matrix spikes were analyzed to determine possible interferences and contamination from solutions or containers.

Figure 17: Shaker Bath for adsorption experiments.

3.5 Desorption tests

Desorption experiments were carried out in a water shaker batch under the same conditions of the adsorption process (200 rpm and 26 hours at room temperature). The beads coming from the adsorption tests were removed from the solution by filtration and finally dried at room temperature. Then, 5 g/L of the beads or flakes were contacted individually with 0.1 M and 1 M of hydrochloric acid, nitric acid, sulfuric acid and sodium hydroxide. Samples were taken at predetermined time intervals and diluted with nitric acid 2% v/v to analyze the oxyanions concentration using ICP-MS. To determine possible contamination or interferences from the solutions or containers, a blank of each eluent and matrix spikes were analyzed.

3.6 Adsorption/Desorption tests

This process only was performed for the removal of arsenic(V) and arsenic(III) using Fe(III)-CB as adsorbent. Five cycles of adsorption/desorption experiments were performed to evaluate the reusability of Fe(III)-CB using the conditions described in the adsorption and desorption tests sections 3.4 and 3.5. All experiments were performed in duplicate.

4 RESULTS AND DISCUSSION

4.1 Characterization and selection of the adsorbent

In this section we discuss the characterization of the diverse adsorbents containing chitosan. Also, based on the percentage of removed oxyanions, we selected the best adsorbent for the adsorption tests.

4.1.1 Characterization

4.1.1.1 Image Stacking Photography Analysis

Figures 18A-18G show images of the diverse chitosan beads/flakes analized with an Image Stacking Photography. Figure 18A is the chitosan powder and the images 18B-18G are the chitosan beads/flakes. This showed the average size of each one. The CB showed an average size of 1.87 ± 0.40 mm, the CB-GLA was 1.13 ± 0.06 mm, the CB-DMSA was 1.86 ± 0.40 mm, the CF-NAC was 2.09 ± 0.68 mm, the PCF was 1.38 ± 0.23 mm, and Fe(III)-CB was of 1.70 ± 0.30 mm. The PCF and CF-NAC showed an irregular shape, and the other beads showed a spherical shape with irregular edges.

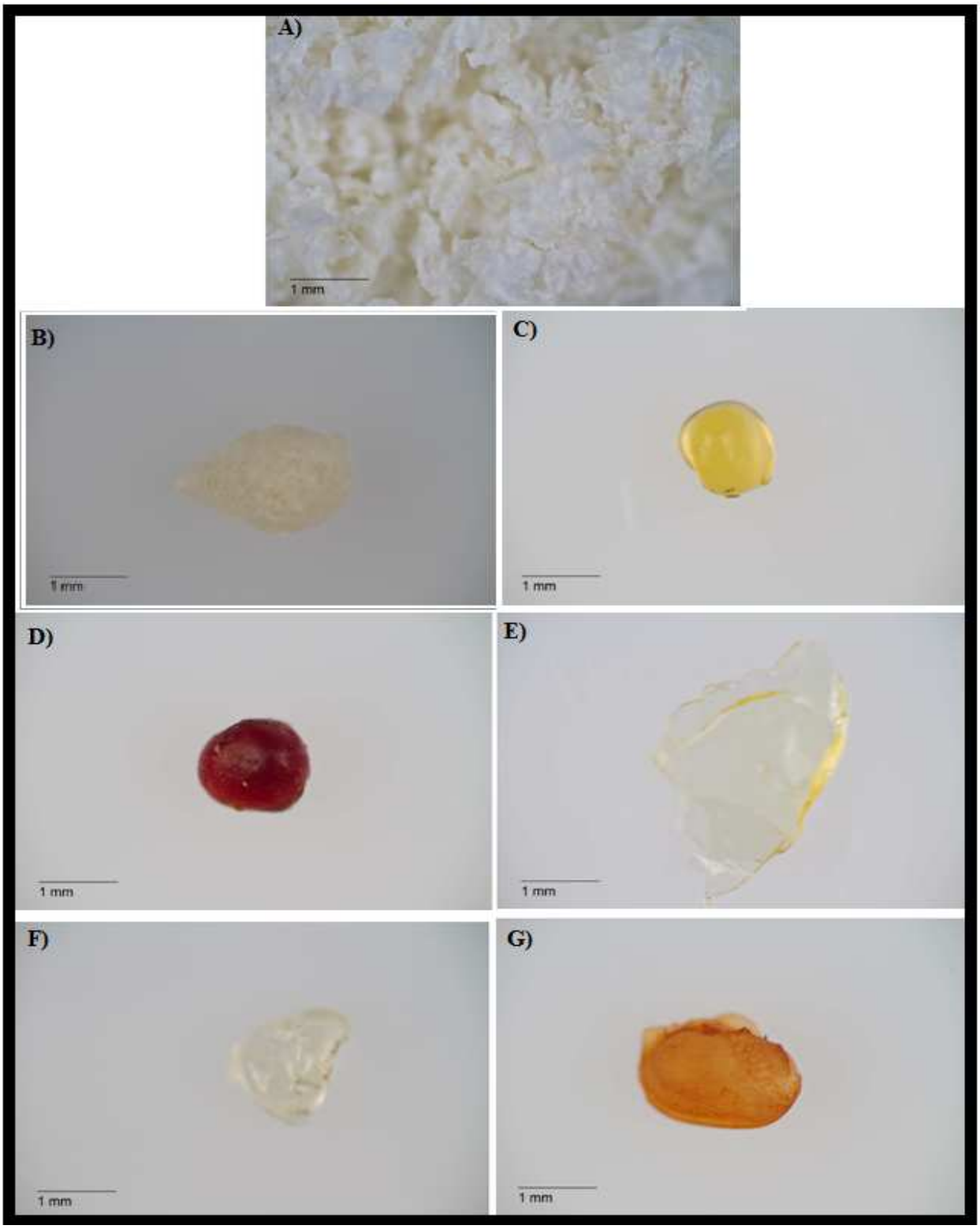

Figure 18: ISP images of (A) Chitosan powder; (B) CB; (C) CB-GLA; (D) CB-DMSA; (E) CF-NAC; (F) PCF; and (G) Fe(III)-CB.

4.1.1.2 Scanning Electron Microscopy Analysis

Figures 19-25 show the SEM micrographs of Chitosan powder, CB, CB-GLA, CB-DMSA, CF-NAC, PCF, and Fe(III)-CB at 1500X and 7000X magnifications. The PCF and CF-NAC show a non-porous surface. In addition, chitosan powder, CB, CB-GLA, CB-DMSA, and Fe(III)-CB show a rough surface.

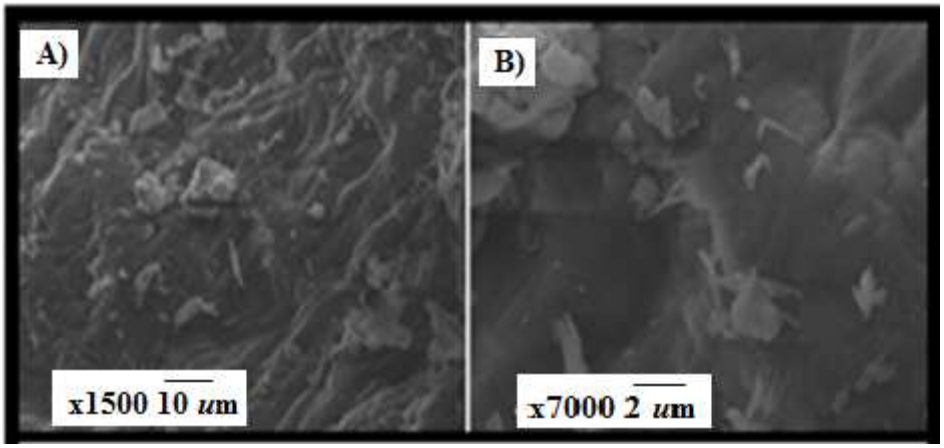

Figure 19: SEM images of Chitosan powder at magnification A) 1500X and B) 7000X.

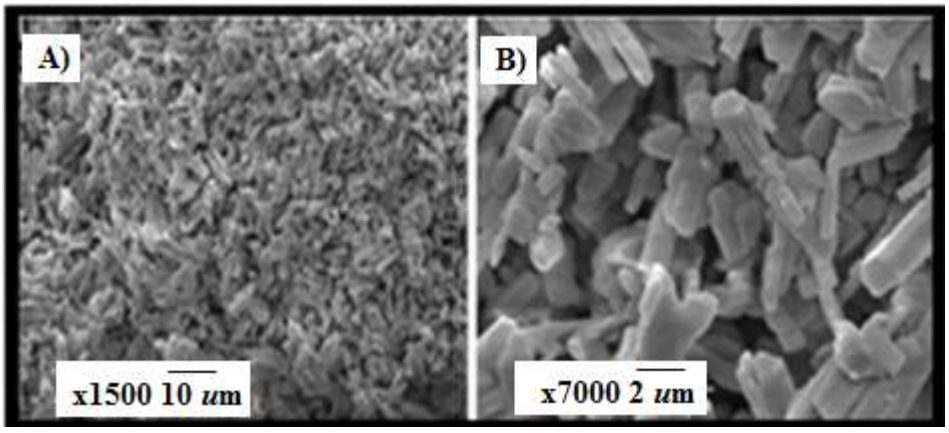

Figure 20: SEM images of CB at magnification A) 1500X and B) 7000X.

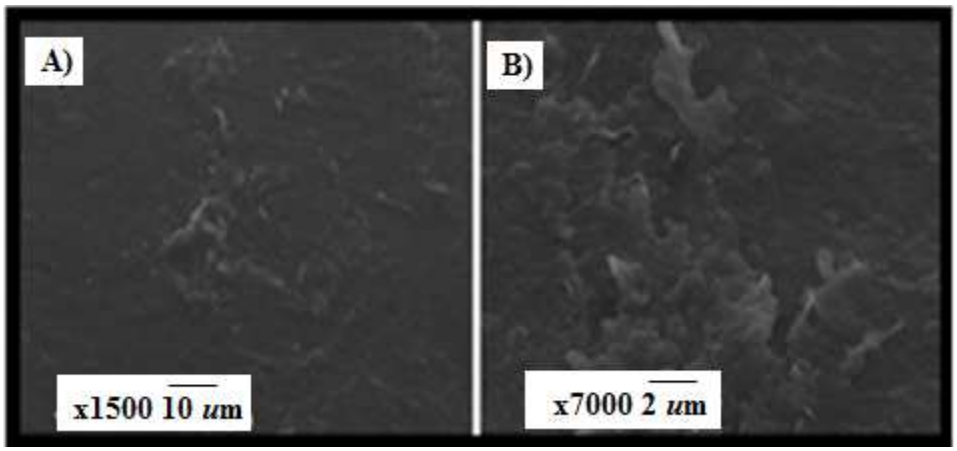

Figure 21: SEM images of CB-GLA at magnification A) 1500X and B) 7000X.

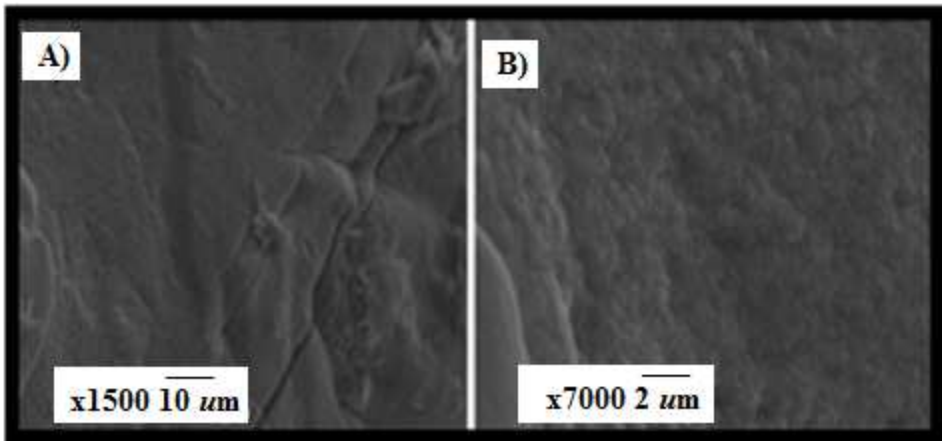

Figure 22: SEM images of CB-DMSA at magnification A) 1500X and B) 7000X.

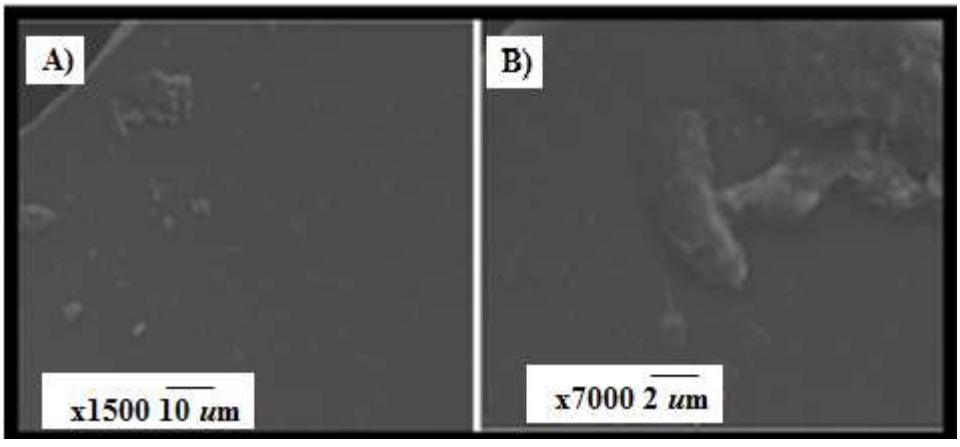

Figure 23: SEM images of CF-NAC at magnification A) 1500X and B) 7000X.

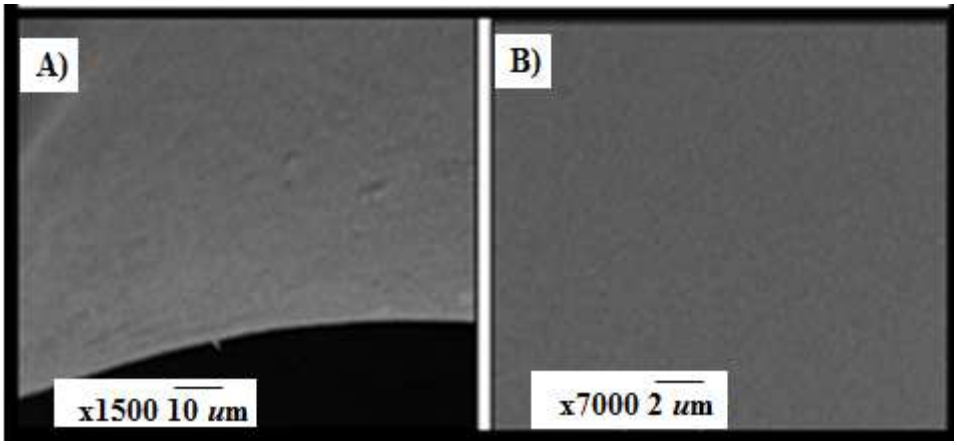

Figure 24: SEM images of PCF at magnification A) 1500X and B) 7000X.

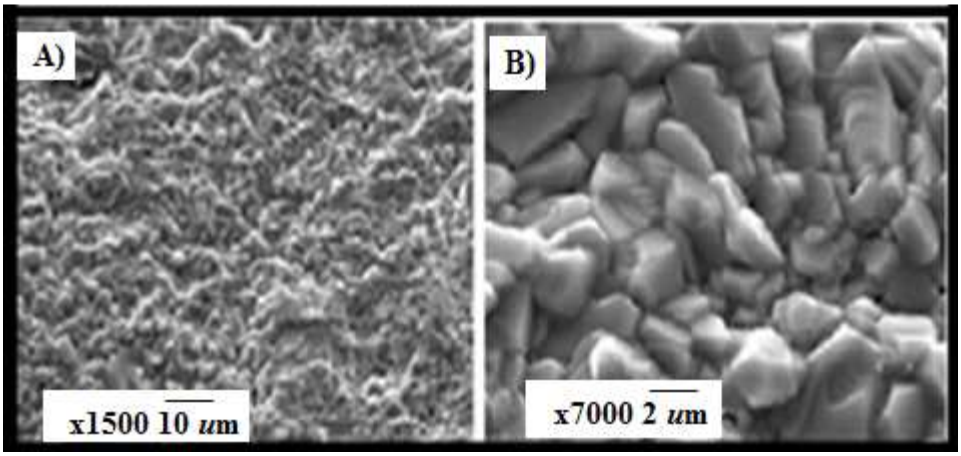

Figure 25: SEM images of Fe(III)-CB at magnification A) 1500X and B) 7000X.

4.1.1.3 FT-IR Analysis

The functional groups of chitosan beads/flakes are shown in figures 26A-26G. The FT-IR spectra showed six important bands: a broad band at 3367 cm^{-1} correspond to the stretching vibrations of the -OH and $–NH_2$ groups, a small band at 2877 cm^{-1} due to the stretching vibrations of –CH and $-CH_2$ groups, a band at 1647 cm^{-1} is attributed to the stretching vibrations of the $-NH_2$ group, 1377 cm^{-1} correspond to -CH symmetric bending vibrations in the –CHOH group, and finally 1064 cm^{-1} and 1029 cm^{-1} are assigned to -CO stretching vibration in the –COH group. The bands of $–NH_2$ and –OH stretching vibrations present an overlapping, as is reported in the literature (Viswanathan et al., 2009). All the bands are similar in every beads/flakes.

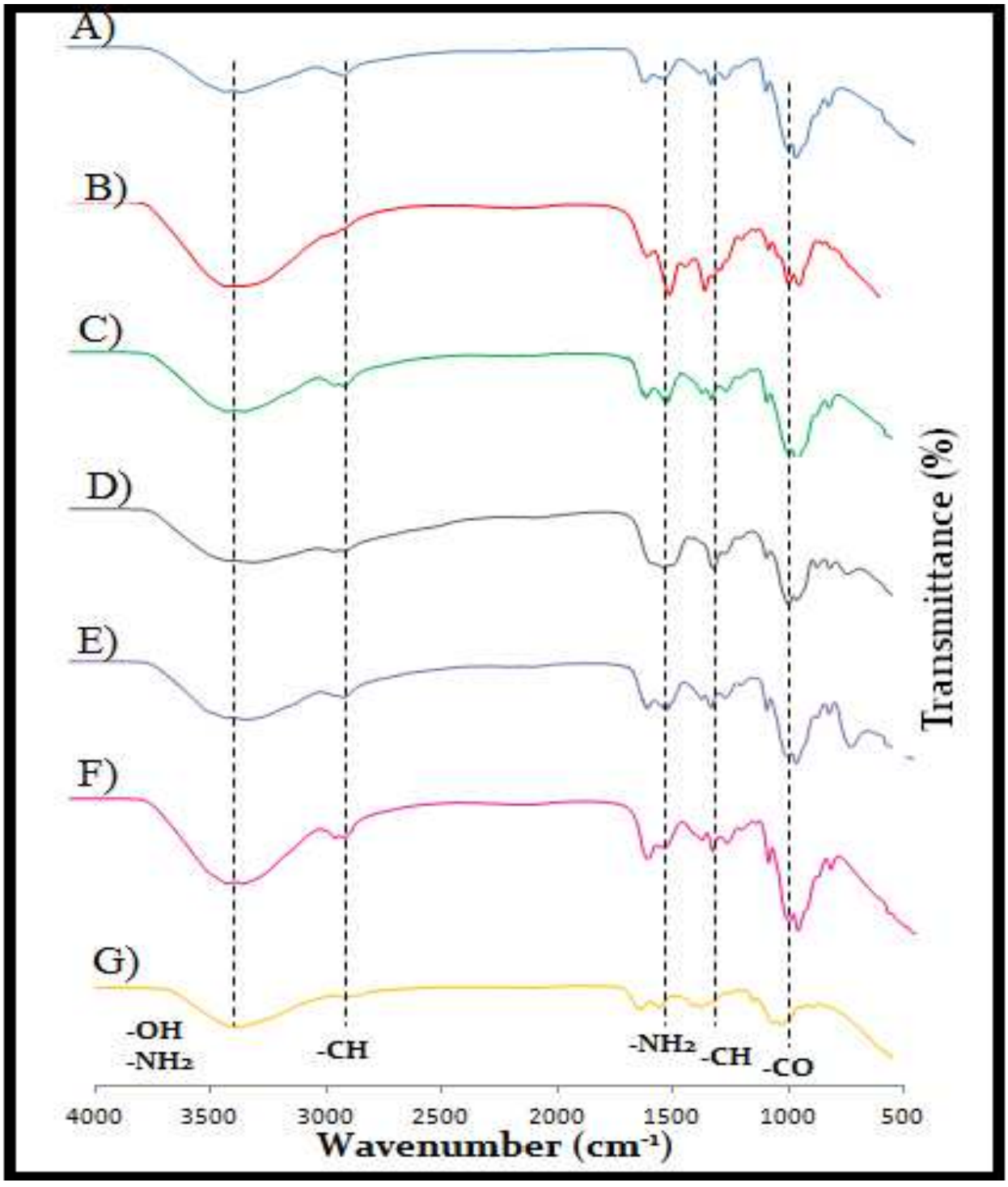

Figure 26: FT-IR spectrum of A) Chitosan powder; B) CB; C) CB-GLA; D) CB-DMSA; E) CF-NAC; F) PCF; and G) Fe(III)-CB.

4.1.1.4 Point of zero charge determination

The point of zero charge is shown in figure 27 for the diverse chitosan beads/flakes. The pH_{pzc} of chitosan powder and CB is 7.3. The beads functionalized with GLA and DMSA showed a pH_{pzc} of 7.5 and 5.4, respectively. The PCF and CF-NAC showed a pH_{pzc} of 6.3, and the Fe(III)-CB a pH_{pzc} of 8.4. Electrostatic attraction occurs below the pH_{pzc} due to the positive net charge of the surface and negatively charged ions of adsorbate. Above the pH_{pzc} is expected electrostatic repulsion between oxyanions because the surface of the adsorbent becomes negative charged.

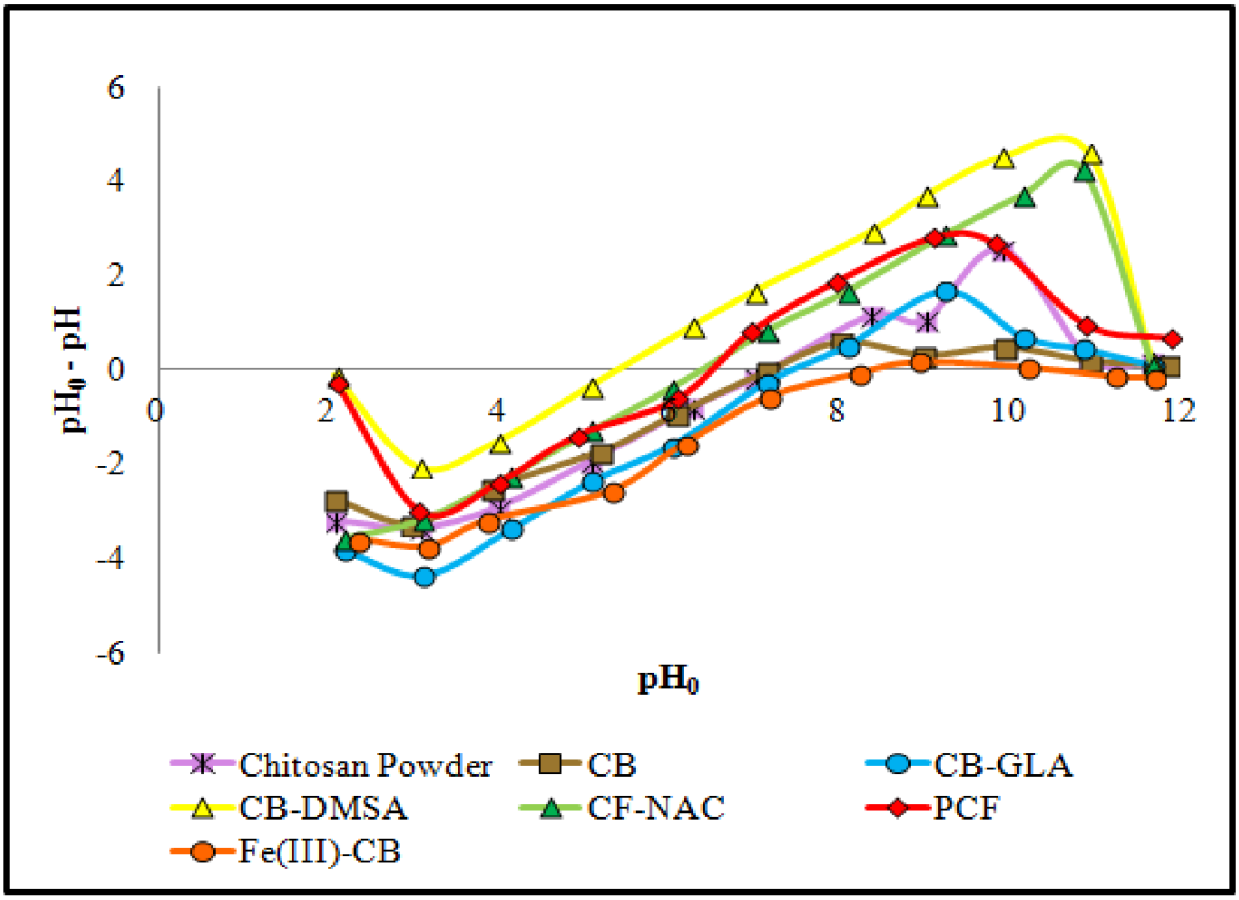

Figure 27: Point of zero charge (pH_{pzc}) of the diverses chitosan beads/flakes.

4.1.1.5 Solubility and Swelling Analysis

The effect of solubility in diverse adsorbents containing chitosan is shown in Table 1. The results showed that chitosan powder was soluble in 5% v/v acetic acid, partially soluble in 0.1 M HCl, and insoluble in deionized water and 0.1 M NaOH. The CB-GLA, CB-DMSA and CF-NAC were insoluble in all evaluated solutions. The CB, PCF and Fe(III)-CB were soluble in 5% v/v acetic acid, partially soluble in 0.1 M HCl, but insoluble in deionized water and 0.1 M NaOH solution. The dissolution is due to the fact that the chitosan is partially soluble in acidic solution (Crini, 2005).

Table 1: Solubility effect of diverse chitosan beads/flakes.

	Solubility Effect			
	Deionized water	Acetic acid 5% v/v	HCl 0.1 M	NaOH 0.1 M
Chitosan Powder	Insoluble	Soluble	Partially soluble	Insoluble
CB	Insoluble	Soluble	Partially soluble	Insoluble
CB-GLA	Insoluble	Insoluble	Insoluble	Insoluble
CB-DMSA	Insoluble	Insoluble	Insoluble	Insoluble
CF-NAC	Insoluble	Insoluble	Insoluble	Insoluble
PCF	Insoluble	Soluble	Partially soluble	Insoluble
Fe(III)-CB	Insoluble	Soluble	Partially soluble	Insoluble

The swelling effect is showed in Table 2. The results show that CB, CB-GLA and PCF have 0% swelling once exposed to acidic, alkaline and neutral media, therefore are stable and potential candidates for the adsorption test. The swelling percentage for Fe(III)-CB was 15% in all evaluated solutions. The CB-DMSA showed swelling with every solution and the CF-NAC showed swelling in deionized water and acidic solutions. The beads that showed some swelling were a few when compared to other adsorbents; therefore they were shown to be a stable adsorbent with potential application for the adsorption processes (Ngah and Fatinathan, 2008). The swelling factors in an adsorbent are affected by the pH solution, ionic strength and functionalization material (Gupta et al., 2006; Colinet et al., 2010; Ninni et al., 2014; Gao et al., 2014).

Table 2: Swelling Effect of diverse chitosan beads/flakes.

	Swelling Percentage (%)			
	Deionized water	Acetic acid 5% v/v	HCl 0.1 M	NaOH 0.1 M
Chitosan Powder	0	5	0	0
CB	0	0	0	0
CB-GLA	0	0	0	0
CB-DMSA	5	25	5	35
CF-NAC	5	25	25	0
PCF	0	0	0	0
Fe(III)-CB	15	15	15	15

4.1.1.6 TGA analysis

Figure 28 shows the thermal degradation curve of chitosan powder and the diverse chitosan beads/flakes, which degradation temperatures (T_{deg}) between 242 to 293 ˚C. Table 3 shows the T_{deg} (˚C) and weight loss (%) values of chitosan powder and the diverses chitosan beads/flakes. These values show that chitosan powder has a slightly higher degradation temperature than the others, which is more stable. These weight losses may be attributed to the loss of water and the degradation of the main chain of the polymers (Blagg, 2012; Boyaci et al., 2010).

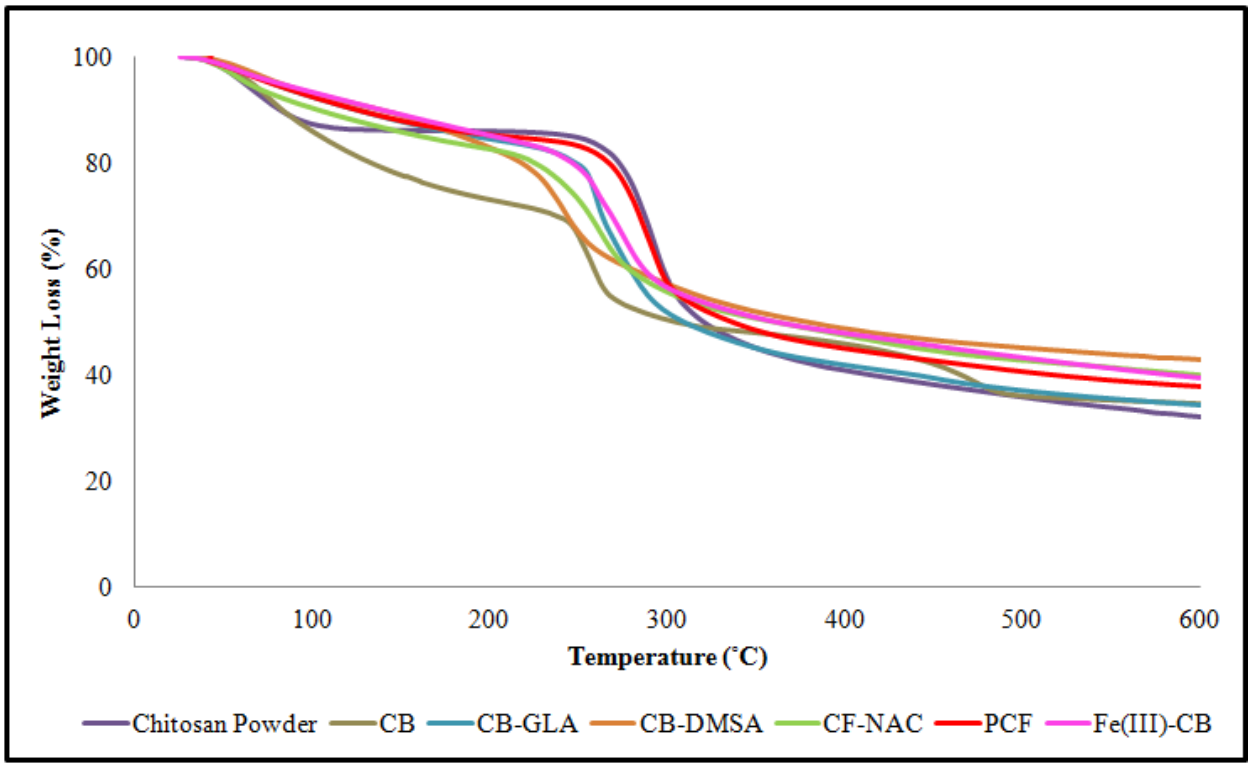

Figure 28: TGA analysis of the diverses chitosan beads/flakes

Table 3: T_{deg} (˚C) and weight loss (%) values of the diverses chitosan beads/flakes

	T_{deg} (˚C)	Weight loss (%)
Chitosan powder	293.05	29.32
CB	249.75	32.72
CB-GLA	267.67	32.61
CB-DMSA	242.08	41.27
CF-NAC	259.41	36.78
PCF	286.35	35.97
Fe(III)-CB	271.89	36.51

4.1.1.7 Surface Area Analysis

Table 4 shows the BET and Langmuir surface area values of chitosan powder, CB, CB-GLA, CB-DMSA, CF-NAC, PCF and Fe(III)-CB. CB-GLA had the higher surface area with a 2.99 m^2/g (BET) and 14.7 m^2/ g (Langmuir). CF-NAC presented 0 m^2/g for both because it did not adsorb the nitrogen molecules at 77K; Non-porous surface have limited access of nitrogen molecules in the surface (Iqbal et al., 2011). The other beads/flakes showed values between 0.27 to 1.15 m^2/g for BET method and 0.28 to 4.42 m^2/g for Langmuir method. These values are in close agreement with what is reported in the literature and could have a low porosity (Ngah and Fatinathan, 2008; Kamari et al., 2009; Feng et al., 2012).

Table 4: BET and Langmuir surface area values of the diverses chitosan beads/flakes

Sample	BET Surface Area (m^2/g)	Langmuir Surface Area (m^2/g)
Chitosan powder	0.53	1.13
CB	1.11	3.28
CB-GLA	2.99	14.7
CB-DMSA	1.15	4.42
CF-NAC*	0	0
PCF	1.13	1.58
Fe(III)-CB	0.27	0.28

* **Note:** Sample did not adsorb N2 @ 77K.

4.1.2 Selection of adsorbent for vanadium and arsenic removal

Figures 29 and 30 show the percent removal of vanadium and arsenic oxyanions onto Chitosan powder, CB, CB-GLA, CB-DMSA, CF-NAC, PCF and Fe(III)-CB. Each oxyanion was placed in contact with 5 g/L of adsorbent at pH 6.00 ± 0.1, individually. Figure 29 showed the percentages of vanadium oxyanions, which the maximum removal was 99-100% using PCF as the adsorbent. Figure 30, shows the percentage removal of arsenic oxyanions, where the maximum removal for As(V) was 97% and 99% using PCF and Fe(III)-CB as adsorbent, respectively. Also, showed an 95% for the As(III) removal using Fe(III)-CB. The protonated amine groups of PCF are responsible for higher sorption capacity than the original amine groups

of chitosan for the removal of V(III), V(IV), V(V), and As(V). The As(III) removal was achieved by the addition of ferric hydroxide into the chitosan surfaces due to complex formations. Hence, further studies were limited only to PCF for vanadium and arsenate oxyanions and Fe(III)-CB for arsenic oxyanions.

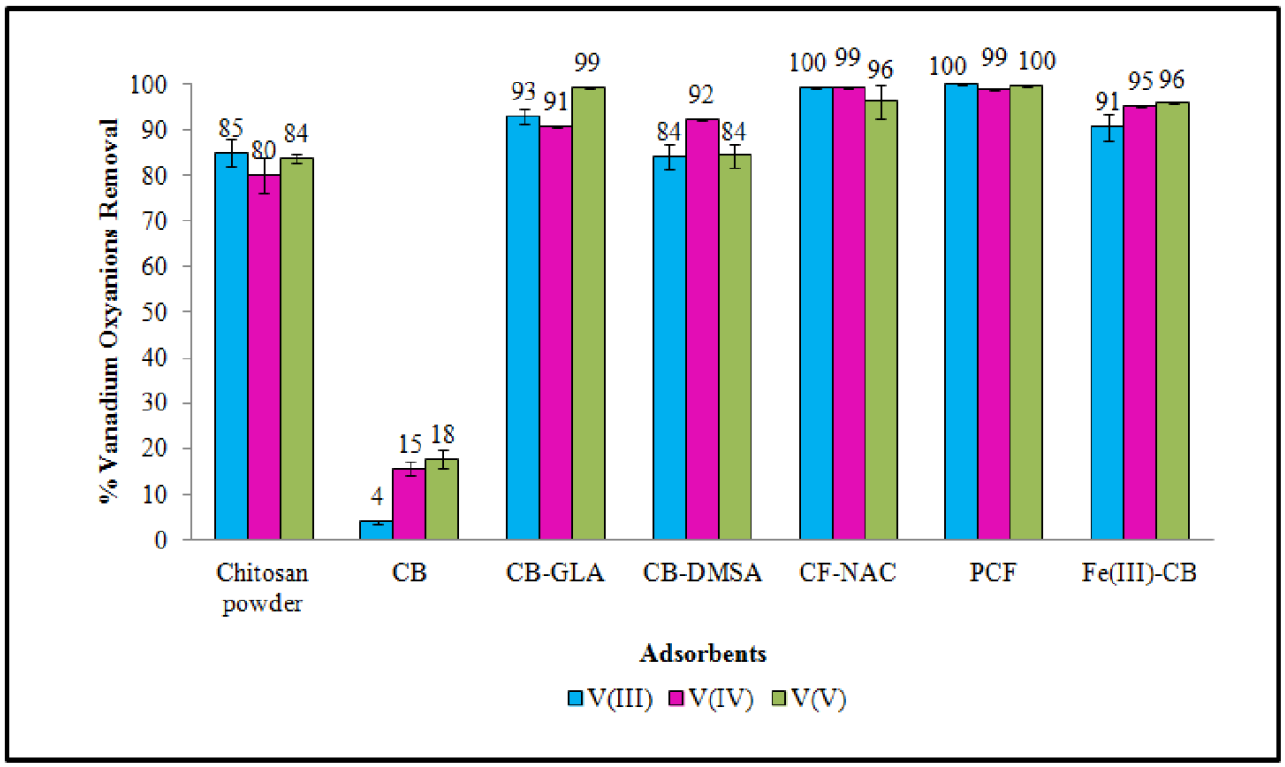

Figure 29: Removal of vanadium oxyanions using diverses chitosan beads/flakes.

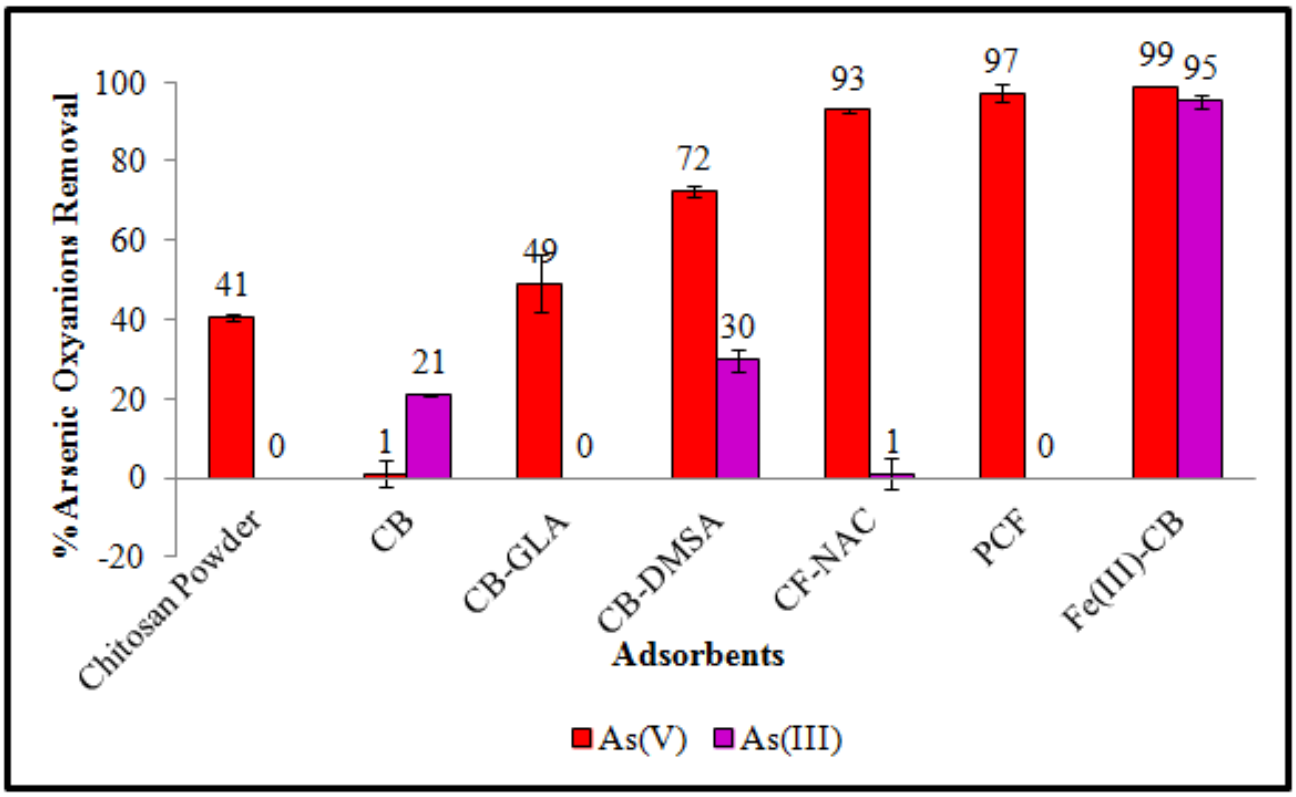

Figure 30: Removal of arsenic oxyanions using diverses chitosan beads/flakes.

4.2 Adsorption of Vanadium oxyanions using PCF Results

4.2.1 Synthesis and Characterization

4.2.1.1 Adsorbent synthesis optimization and Protonation Procedure

Figure 31 shows the pH adsorbent suspension solution for the protonation and conditioning of chitosan beads/flakes to achieve the maximum removal of vanadium oxyanions. The pHs evaluated were 4, 5, 6, 7, 8, 10 and 12 in contact with 5 g/L of adsorbent and at initial vanadium concentration of 0.500 mg/L at room temperature. The maximum vanadium oxyanions removals were of 99-100% at pH into 4.00-5.00 due to the protonation of amine group. Once the pH increases, the concentration of H^+ ions decreases because the amine group is neutral. Therefore, electrostatic repulsions may be occurring between the vanadium oxyanions and the adsorbent at high pH values and electrostatic attraction in acidic pH. In pH 4.00 the flakes start dissolving, therefore the optimum pH was 5.00.

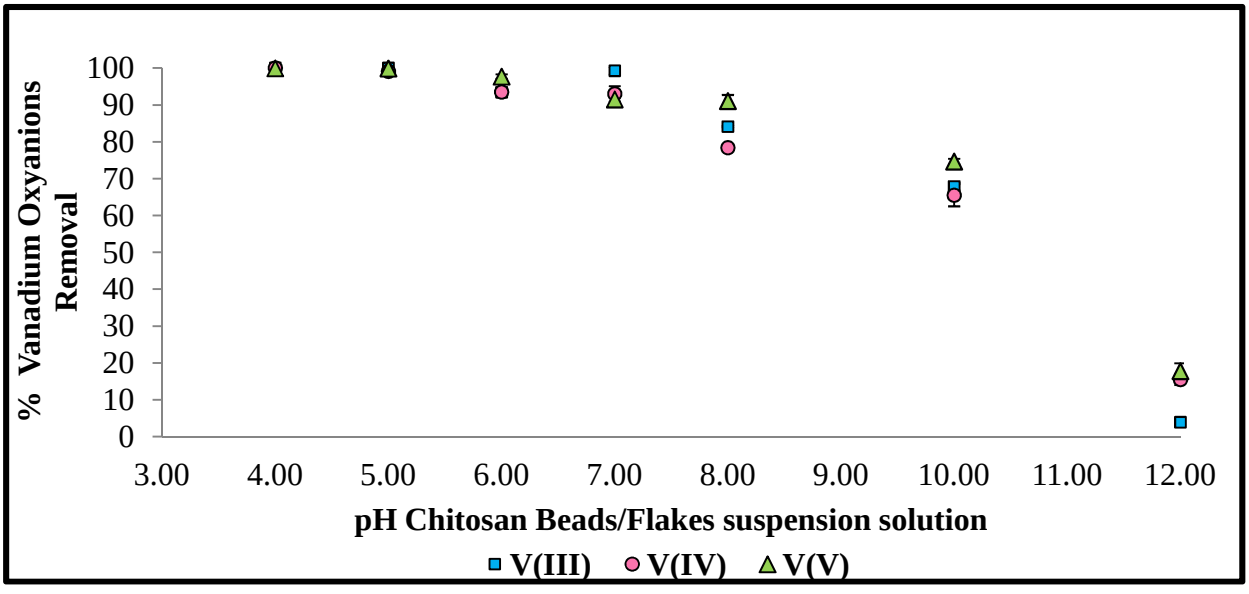

Figure 31: pH of chitosan beads/flakes suspension solution for the removal of vanadium oxyanions.

4.2.1.2 Scanning Electron Microscopy Analysis

SEM images are shown in Figure 32 to 35 at diverses magnifications, A) 30X, B) 1500X, and C) 7000X**.** The figures showed the PCF surface before and after vanadium oxyanions adsorption. The PCF show surfaces without pores in each magnification. After the vanadium oxyanions adsorption, the surface does not show a significant difference (Figure 33-35).

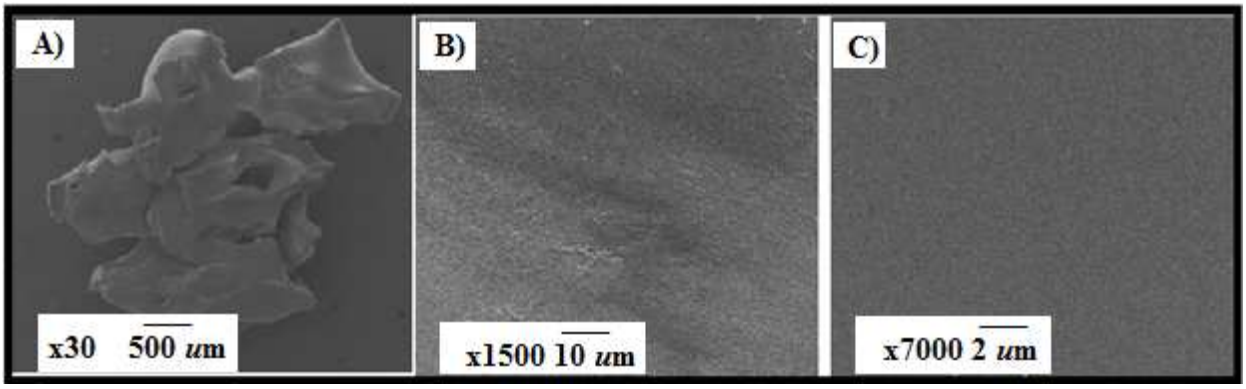

Figure 32: SEM micrograph of PCF at magnification of A) 30X, B) 1500X, and C) 7000X.

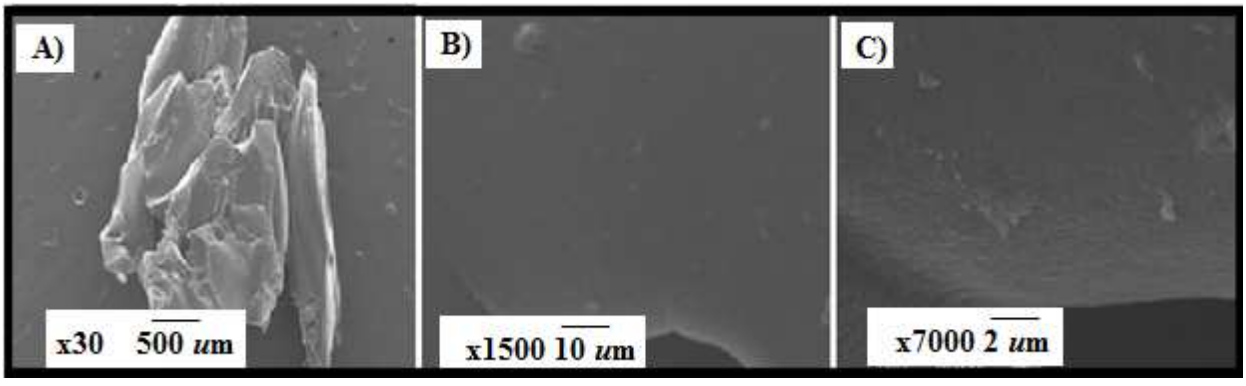

Figure 33: SEM micrograph of Vanadium(III) onto PCF at magnification of A) 30X, B) 1500X, and C) 7000X.

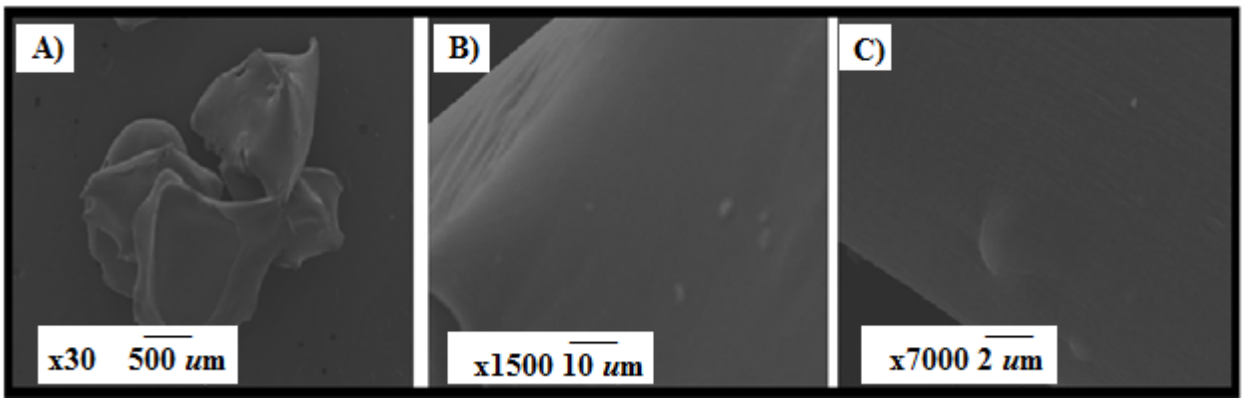

Figure 34: SEM micrograph of Vanadium(IV) onto PCF at magnification of A) 30X, B) 1500X, and C) 7000X.

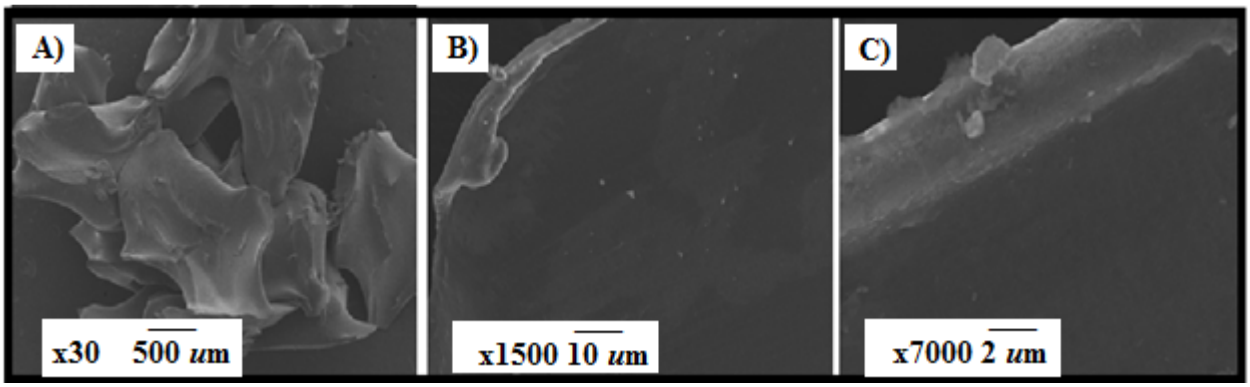

Figure 35: SEM micrograph of Vanadium(V) onto PCF at magnification of A) 30X, B) 1500X, and C) 7000X.

4.2.1.3 Infrared Spectroscopy Analysis

FT-IR spectra of PCF and the interactions of V(III), V(IV), and V(V) oxyanions onto PCF are shown in Figure 36. The functional groups of the adsorbent were discussed in section 4.1.1.3. Once the vanadium oxyanions are adsorbed by the PCF adsorbent, the different functional groups are similar to PCF bands (Figure 36A). Therefore, no significant differences are observed in the IR spectra. These results suggest no chelation effect as a consequence of the

adsorption process, which also suggest an electrostatic attraction between the PCF and the vanadium oxyanions as the dominant mechanism.

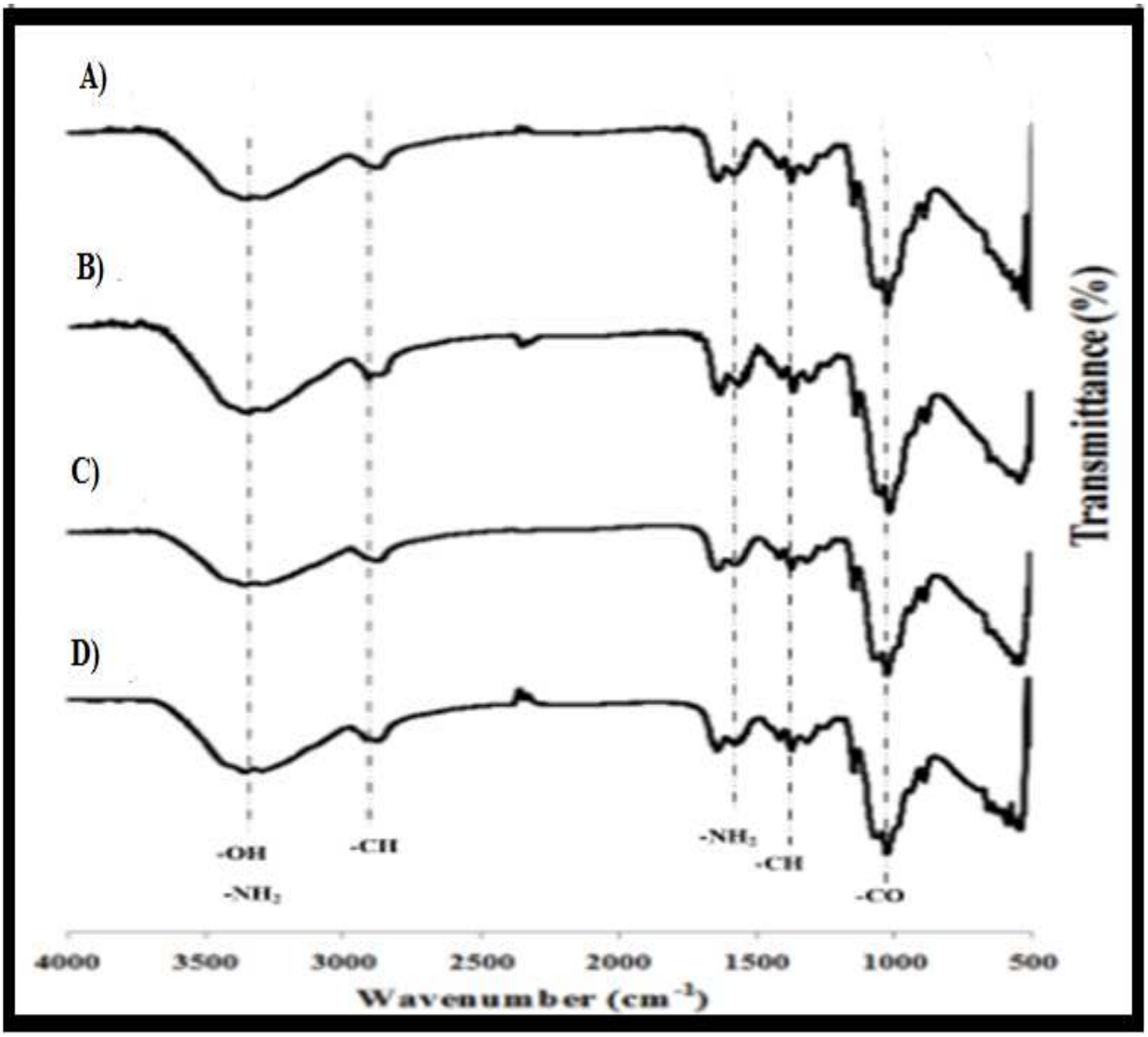

Figure 36: FT-IR spectrum of (A) PCF, and interactions of (B) Vanadium(III), (C) Vanadium(IV) and (D) Vanadium(V) oxyanions onto PCF.

4.2.1.4 LA-ICP-MS Analysis

The presence of vanadium oxyanions traces onto PCF were determined by LA-ICP-MS (figures 37-40). The vanadium peak intensity was obtained by measuring the signal intensity at the centre points of the PCF; the sample was directly analyzed by ablating with a pulsed laser beam. The signal intensity of vanadium oxyanions is proportional to the concentration of analyte (D'Oriano et al., 2008; Mokgalaka and Gardea-Torresday, 2006).

The blue line on the figures 37-40 located at the upper right of the graphs depicts where the laser passed over the PCF's surface during the analysis. Also, the blue line in the spectra represents the vanadium intensity of the chitosan flakes and the red line indicates the carbon intensity that was used as a base line due to its presence in the chitosan matrix. In this analysis, we confirmed the presence of the vanadium oxyanion on the surface of PCF after its exposition to an initial concentration of 1.5 mg/L and compared with the unexposed PCF, which showed no Vanadium signal (Figure 40).

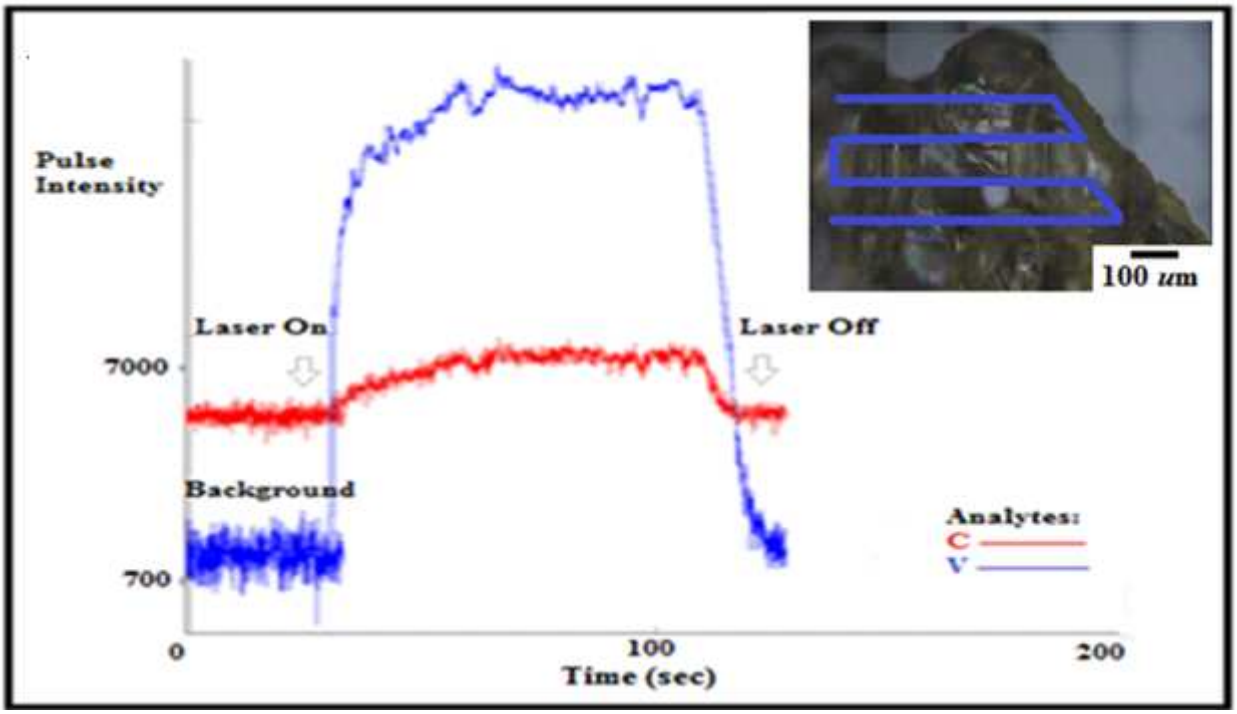

Figure 37: LA-ICP-MS spectra and image of Vanadium(III) interacting with PCF.

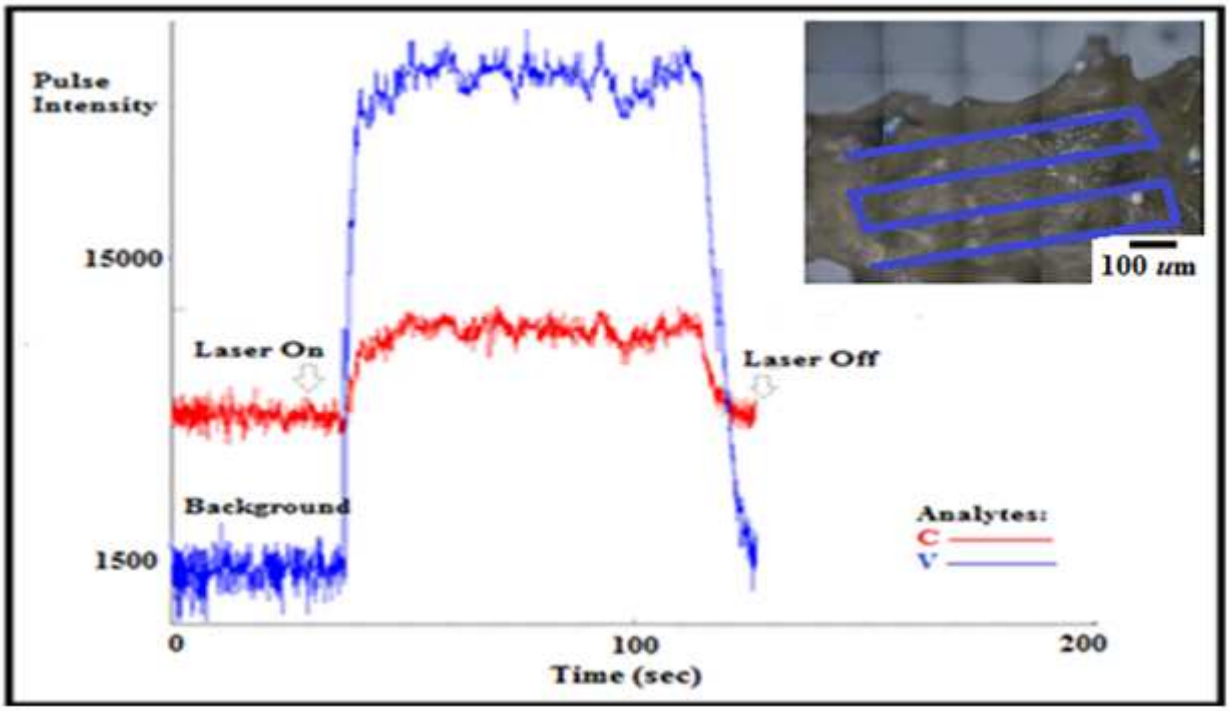

Figure 38: LA-ICP-MS spectra and image of Vanadium(IV) interacting with PCF.

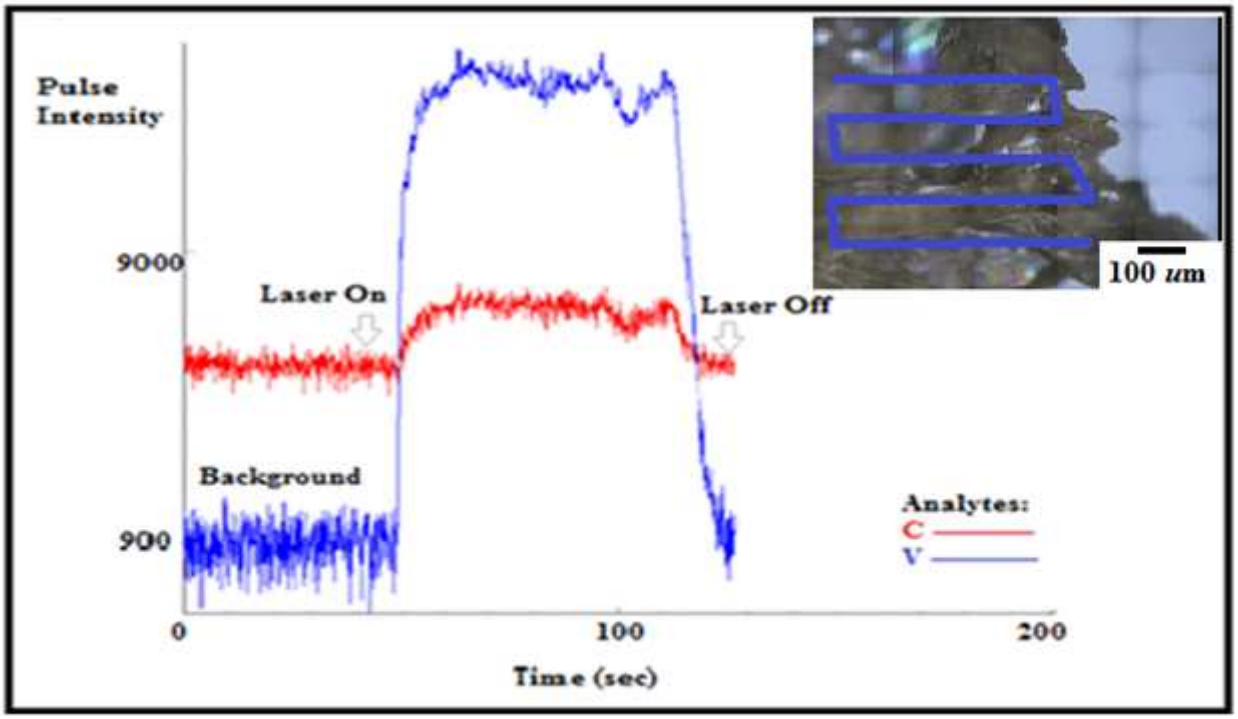

Figure 39: LA-ICP-MS spectra and image of Vanadium(V) interacting with PCF.

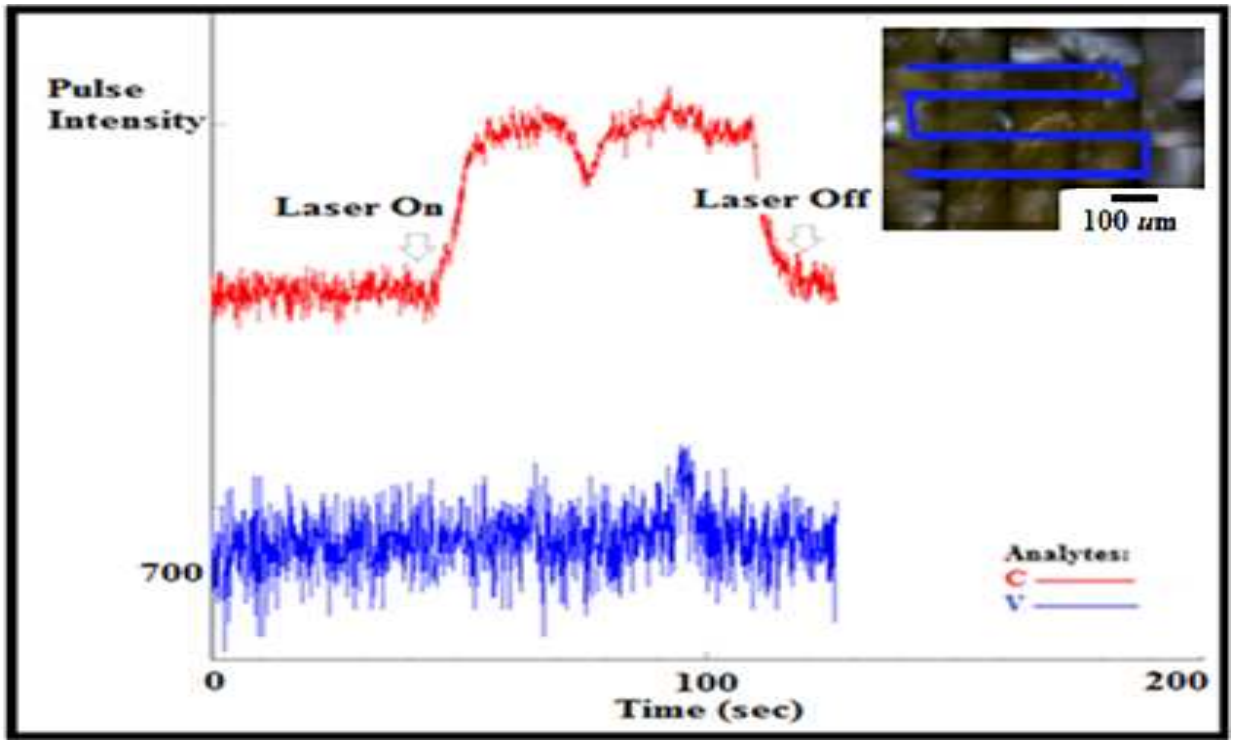

Figure 40: LA-ICP-MS spectra and image of PCF without contaminant.

4.2.1.5 XRF Analysis

The presence of Vanadium(III, IV, and V) oxyanions traces onto PCF were shown in the XRF spectra (Figure 42 to 44). Figure 41 shows the PCF without the exposition to traces of vanadium oxyanions. The circle on the image shows the X-rays incidence point on the irradiated samples. The peaks corresponding to the vanadium signal onto the PCF are those fluorescence lines of Ka_1 of 4.9 and Kb_1 of 5.4 KeV. The other peaks belong to the PCF signal and the base (Au) used in the analysis (Figure 42). The oval in red (Figures 42-44) is use to identify the vanadium signal and one in blue without vanadium (Figure 41). Its clearly seen in figure 41 the absence of the vanadium signal.

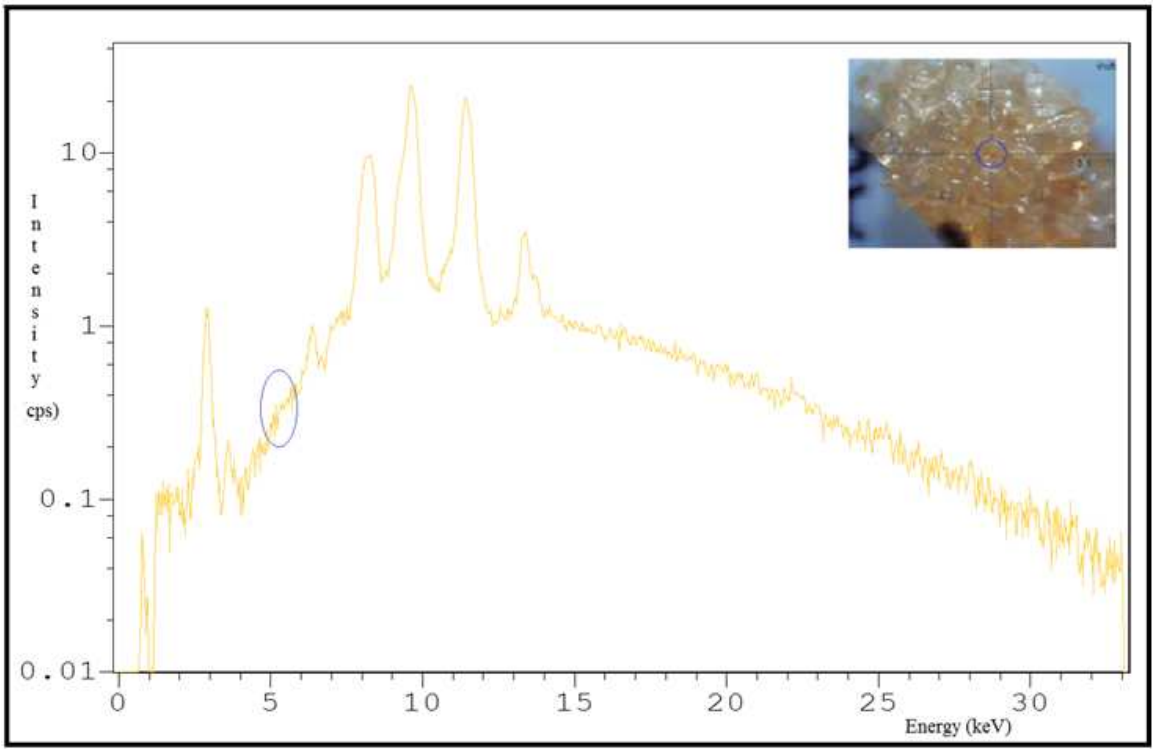

Figure 41: XRF spectra and image of PCF without the contaminant.

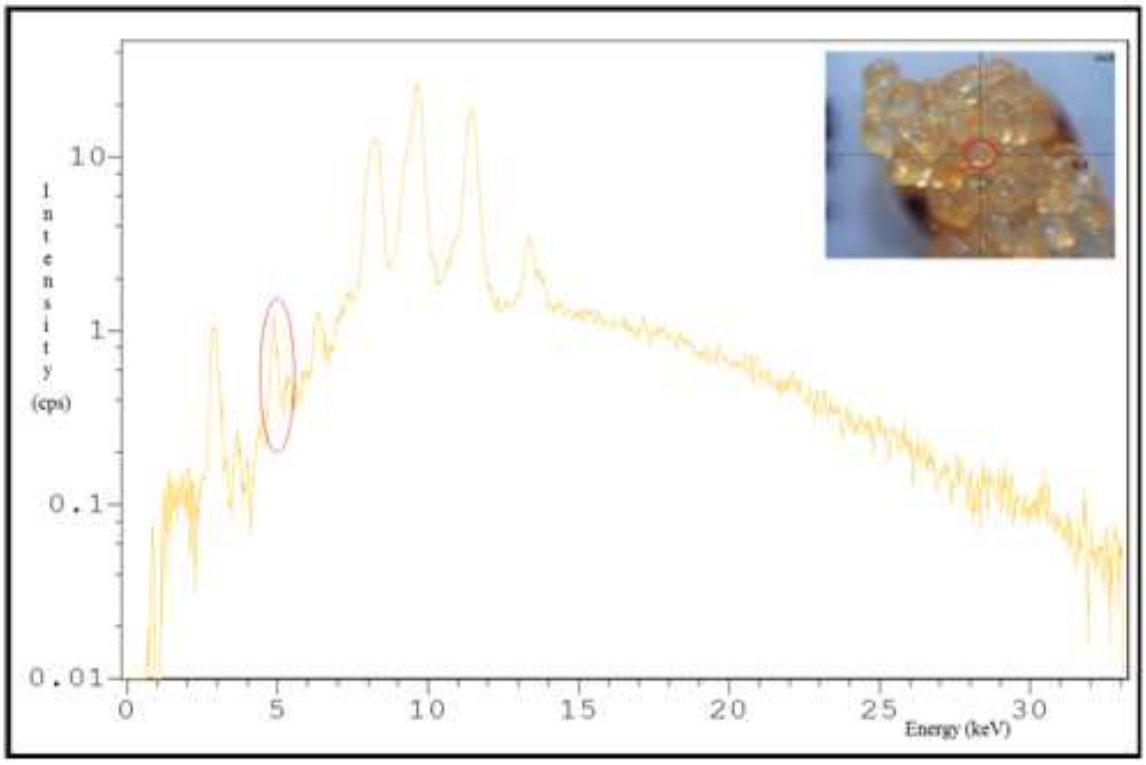

Figure 42: XRF spectra and image of Vanadium(III) interacting with PCF.

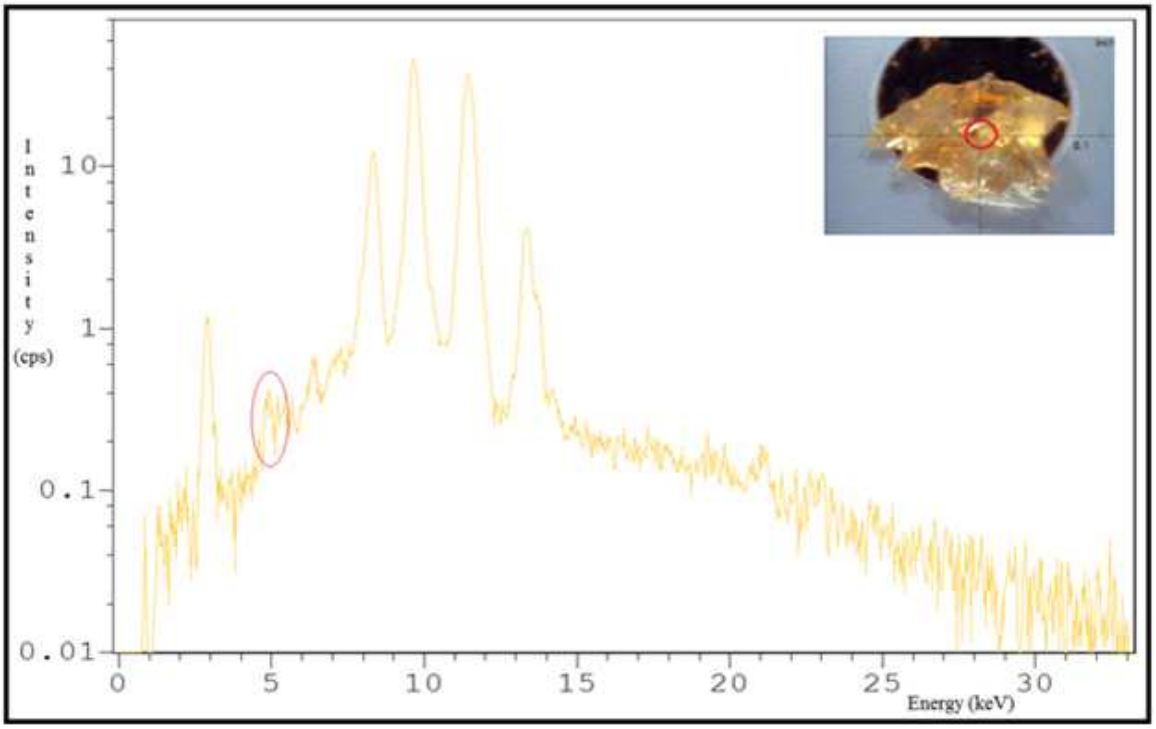

Figure 43: XRF spectra and image of Vanadium(IV) interacting with PCF.

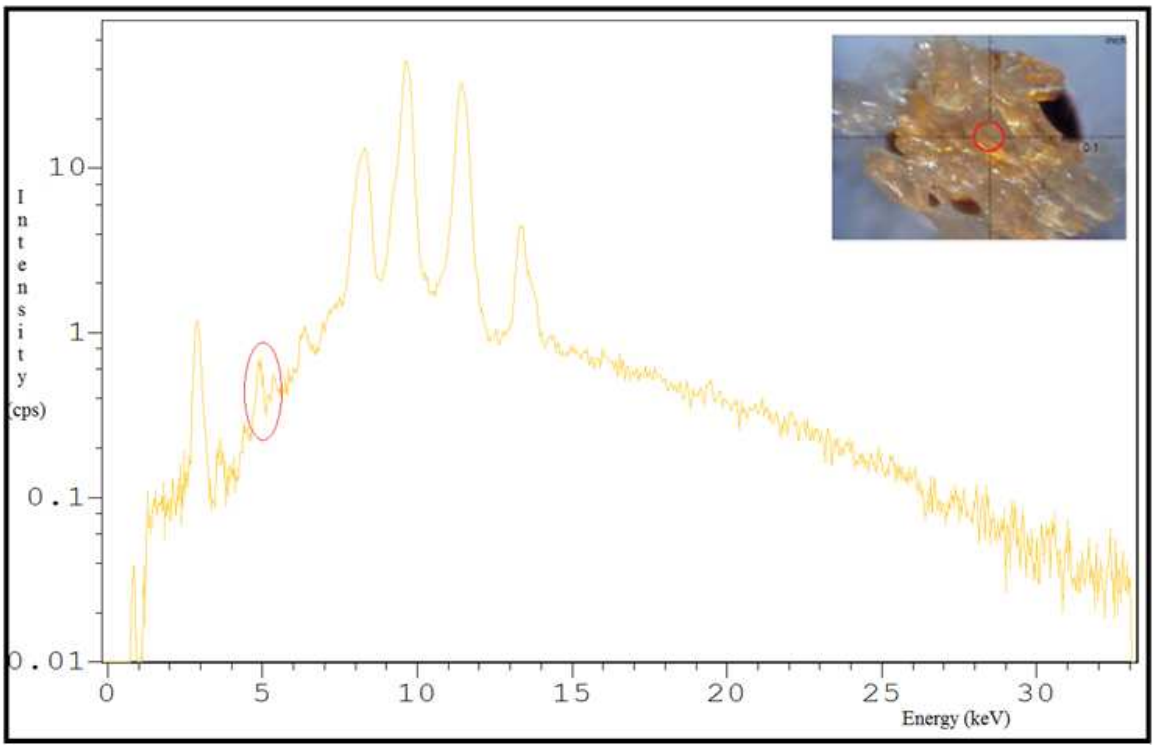

Figure 44: XRF spectra and image of Vanadium(V) interacting with PCF.

4.2.2 Adsorption Analysis

This section discusses the adsorption studies for the vanadium oxyanions removal, such as pH aqueous solution, concentration adsorbent, contact time, co-existing anions competence, and adsorption isotherms.

Effect of pH aqueous solution

The effect of pH in the aqueous solution removal of vanadium oxyanions is shown in figure 45. The different pHs studied were 2, 4, 6, 8 and 10. The maximum percentage removal for vanadium oxyanions was at pH 6, with a 100% for V(III), 99.9% for V(IV), and 99.9% for V(V). This is due to the amine group protonation in PCF, which maintained a stable pH with the vanadium oxyanions. The vanadium species was oxidized in the water rapidly from an oxidation state III and IV to state V, therefore every vanadium species behaves as $H_2VO_4^-$ at pH 6.0-8.0 as shown in figure 43 (Erdem et al.; 2011; NTP, 2008; Gorzsás ,2005; WHO, 2001; Langmuir et al., 2003). At pHs below 4, the removal of vanadium oxyanions decreases due to the formation of $VO_2^{+,}$ HVO^{+2}, V^{+3} (NTP, 2008; Langmuir et al., 2003) generating electrostatic repulsion with the positively charged chitosan matrix, however the removed percentage is attributed to an inner-sphere complex via hydrogen bonding. On the other hand, the removal at high pHs decreases due to the formation of species HVO_4^{-2} (NTP, 2008; Langmuir et al., 2003), generating repulsion by the negative charge in chitosan matrix above the pH_{pzc} of 6.3. Hence, throughout the study the optimum pH of the medium was at pH 6.0 ± 0.1, which is the pH approximate of residual waters. Therefore, once the adsorbent is protonated, it is not necessary to add acid to the aqueous solution.

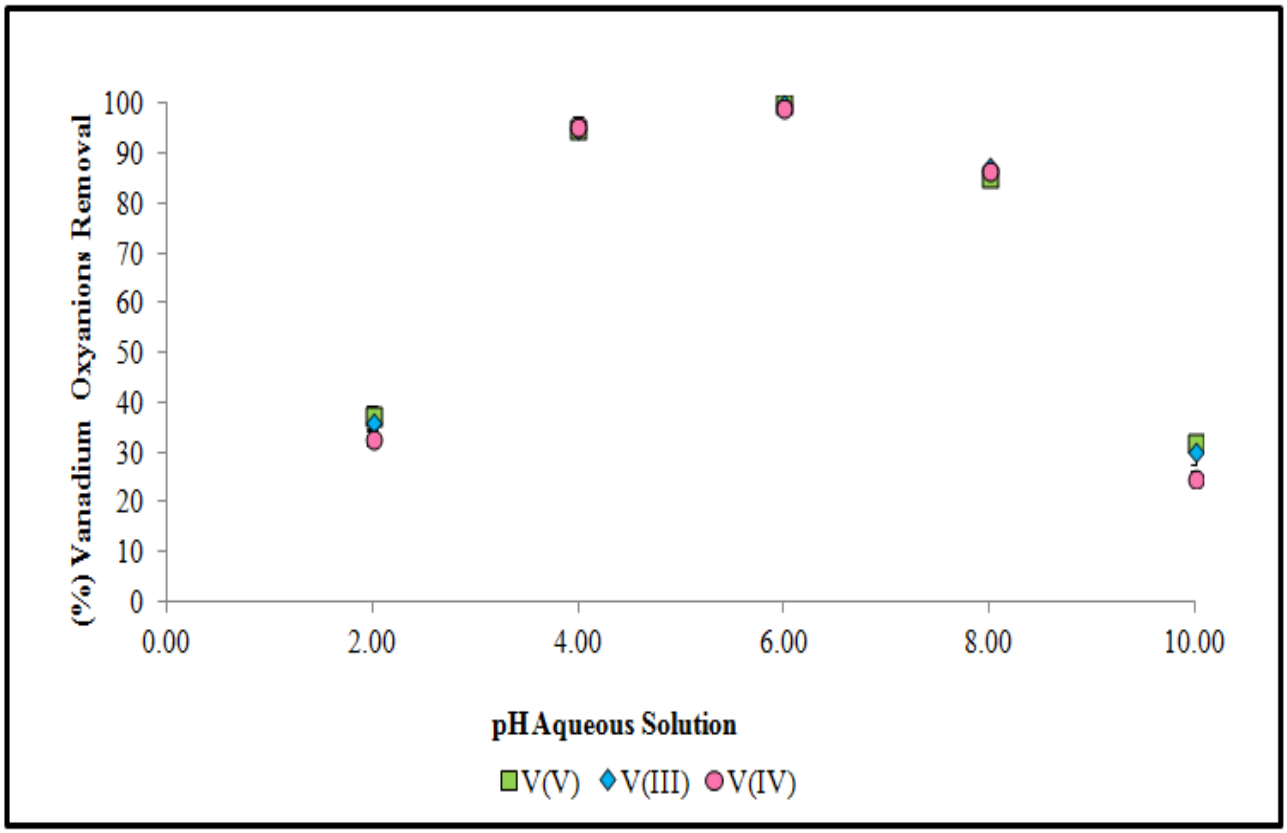

Figure 45: Effect of pH aqueous solutions on the adsorption of Vanadium(III, IV, and V) oxyanions onto PCF. Experimental conditions: initial concentration of vanadium species = 0.500 mg/L; adsorbent concentration = 5 g/L; contact time = 26 h; shaker speed = 200 rpm.

Effect of adsorbent concentration

Figure 46 shows the studies done to determine the optimum adsorbent concentration by adding 1, 3, 5 and 10 g/L of PCF to the vanadium oxyanions and verifying the maximum tolerance limit. The removal percentage of Vanadium(III) were 89% (1 g/L) and 100% (3, 5 and 10 g/L). For Vanadium(IV) were 81% (1 g/L), 99% (5 g/L) and 100% (3 and 10 g/L). Also, for Vanadium(V) were 89% (1 g/L) and 100% (3, 5 and 10 g/L). As the adsorbent concentration was higher that 1 g/L, the removal percentage was 99-100% for every vanadium oxyanions. This is due to the increase of available active sites, therefore the optimum adsorbent

concentration was 5 g/L. These results demonstrate that PCF represents an excellent alternative for the removal of vanadium species in different oxidation states from contaminated water.

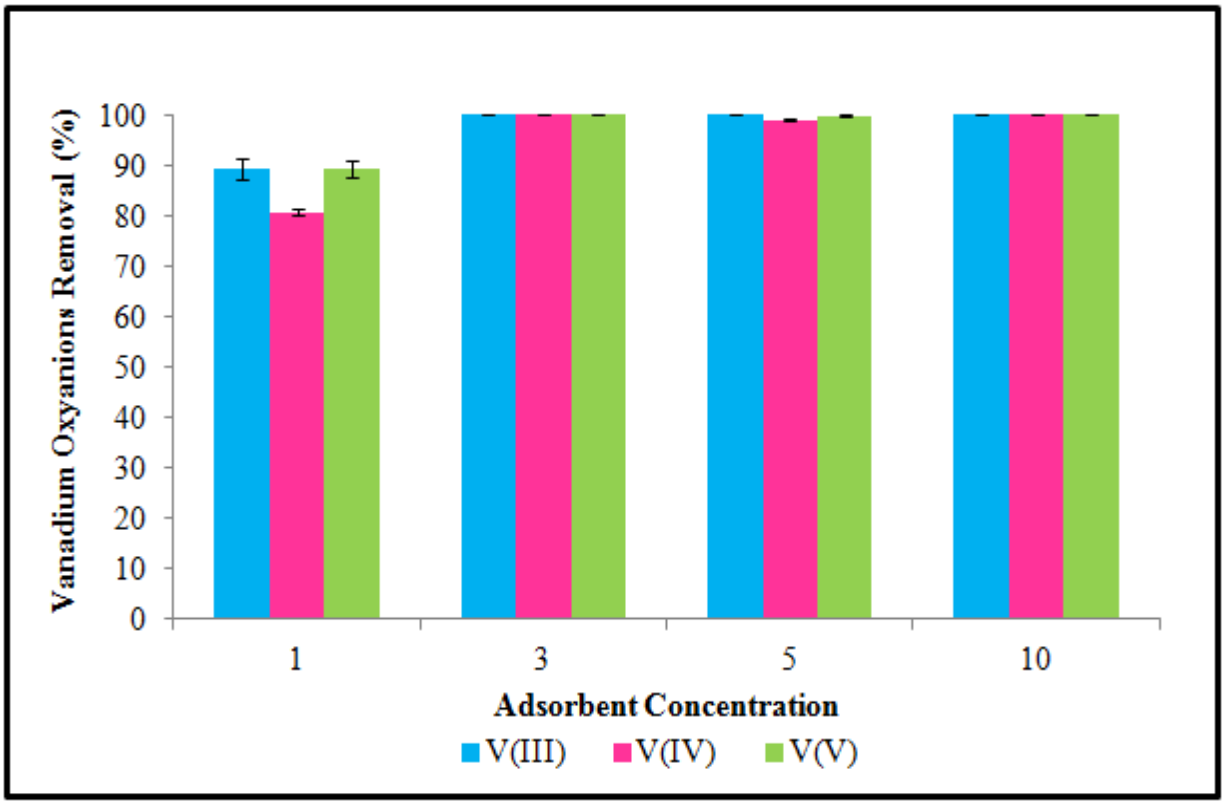

Figure 46: Effect of adsorbent concentrations on the adsorption of Vanadium(III, IV and V) oxyanions onto PCF. Experimental conditions: initial concentration of vanadium species = 0.500 mg/L; contact time = 26 h; shaker speed = 200 rpm; pH aqueous solutions = 6.0 ±0.1.

Effect of contact time

Figure 47 shows the variation of vanadium oxyanions onto PCF found by varying contact time, 0–26 hours. We can see that all the vanadium oxyanions reached equilibrium approximately after 2 hours. The final concentration in equilibrium for V(III), V(IV) and V(V)

oxyanions were 0, 0.005 and 0.001 mg/L, respectively. These obtained excellent percentage removal with a 100% for V(III), 99.1% for V(IV) and 99.9% for V(V). The higher adsorption capacity is due to the protonated amine groups of PCF, which interacts with the negative charge of the oxyanions. The optimum contact time was 26 hours in order to observe that it remained in constant equilibrium.

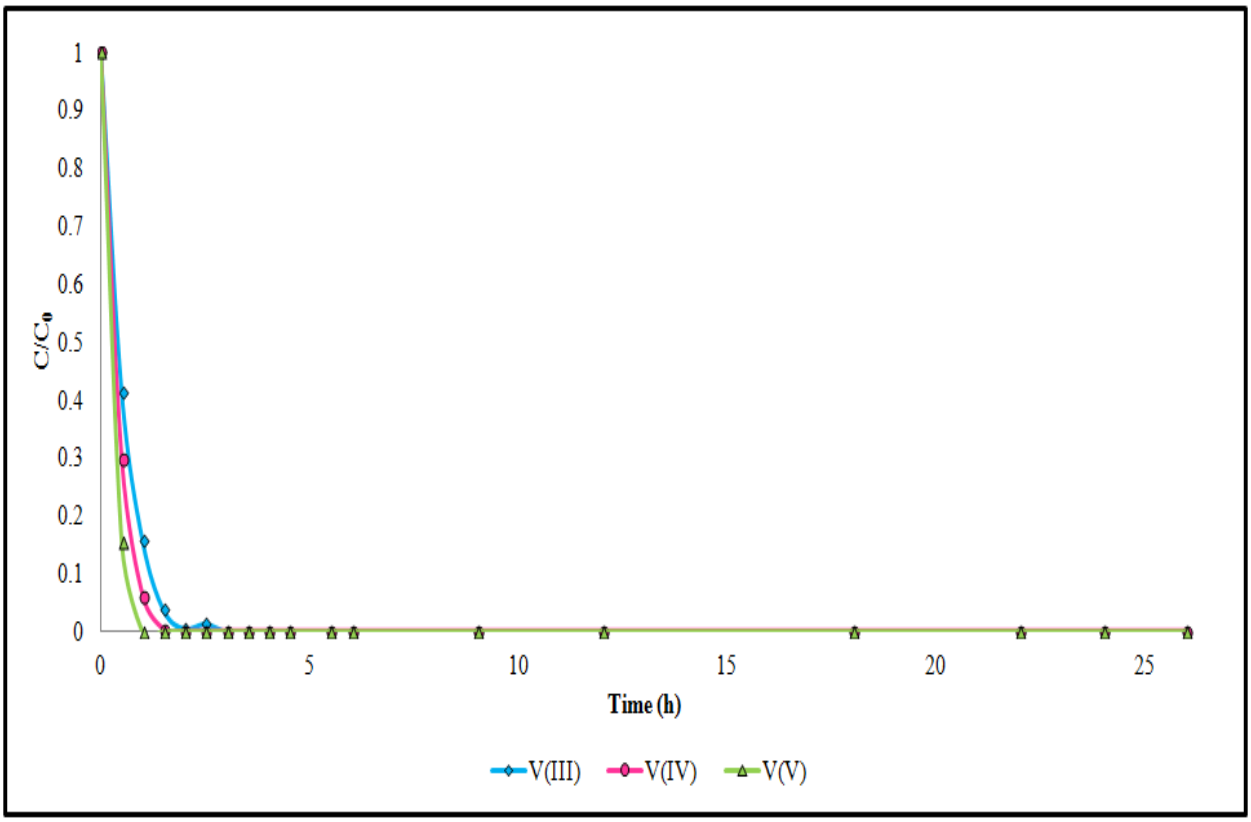

Figure 47: Effect of contact time on Vanadium(III, IV and V) oxyanions onto PCF. Experimental conditions: initial concentration of vanadium species = 0.500 mg/L; adsorbent concentration = 5 g/L; shaker speed = 200 rpm; and pH aqueous solutions = 6.0 ± 0.1.

Effect of co-existing anions competence

The effect of co-existing anions, such as chloride, sulfate, carbonate and phosphate (Cl^-, SO_4^{-2}, CO_3^{-2}, PO_4^{-3}), which are normally present in residual waters were studied. The concentration (0.01 and 0.02 mmol) of these anions were varied in a proportion 1:0, 1:10 and 1:20 (V:CA) by keeping 0.001 mmol as the initial concentration of vanadium at pH 6.0 ± 0.1 onto 5 g/L of PCF. The results do not show a considerable effect on the percentage removed of vanadium oxyanions in the presence of these commons anions (shown in Table 5). The removal efficiency of vanadium oxyanions was 93-97% in the presence of chloride oxyanions at both proportions. Also, in the presence of carbonate, sulfate and phosphate oxyanions were 95-97%, 95-98% and 91-100%, respectively. The PCF selectively removes the vanadium species even in the presence of other common anions at different ionic strenghts. These values confirm that the mechanism involved could be a combination of outer-sphere and inner-sphere complex. The results suggest that the PCF can be used to remove vanadium oxyanions in real effluents even in the presence of common co-existing anions, which are frequent in the environment.

Table 5: Adsorption studies for Vanadium(III, IV and V) oxyanions onto 5 g/L of PCF at diverse co-existing anions (CA).

		Vanadium(III)	Vanadium(IV)	Vanadium(V)
	Ratio V:CA (mol:mol)	% Removal ± SD	% Removal ± SD	% Removal ± SD
	1:0	100.0 ± 0	99.1 ± 0.2	99.9 ± 0.2
Cl^-	1:10	96.5 ± 0.2	94.5 ± 0.3	96.1 ± 0.1
	1:20	94.7 ± 0.4	93.2 ± 0.2	95.3 ± 0.5
CO_3^{-2}	1:10	94.4 ± 0.03	95.1 ± 0.6	95.3 ± 0.1
	1:20	96.3 ± 0.5	97.3 ± 0.8	97.4 ± 0.5
SO_4^{-2}	1:10	97.1 ± 0.1	97.4 ± 0.1	96.5 ± 0.7
	1:20	97.6 ± 0.9	95.3 ± 0.6	95.7 ± 0.004
PO_4^{-3}	1:10	100 ± 0	97.0 ± 2	99.9 ± 0.1
	1:20	92.1 ± 0.4	90.7 ± 0.5	98.9 ± 1

Adsorption Isotherm

Table 6 shows examples of the initial vanadium concentrations used for adsorption experiments using 5 g/L of PCF at pH 6.0. The removal percentages were efficient for vanadium oxyanions, however, the removal percentages decrease once the V(V) concentration increase. The uptake capacity for all vanadium oxyanions increased once the initial concentration increase.

Figures 48 and 49 show the Freundlich and Langmuir isotherm models for vanadium oxyanions, and table 7 shows the isotherm parameters. Adsorption isotherms were studied as the initial concentration of Vanadium(III) increased from 3 to 8.8 mg/L, Vanadium(IV) increased from 1 to 6.3 mg/L and Vanadium(V) increased from 1 to 5.5 mg/L at a pH 6.0 ± 0.1 with 5 g/L of PCF. Lower concentrations than those used for the isotherms obtained 100% removal. Langmuir isotherms model show a better correlation coefficient (R^2) than Freundlich isotherms values for vanadium with oxidation state III, IV and V, 0.9941, 0.9601 and 0.9985, respectively. The Langmuir Q^0 parameters for the mentioned vanadium species were also higher than the Freundlich parameter, which were 12.22 mg/g for Vanadium(III), 6.50 mg/g for Vanadium(IV) and 2.58 mg/g for Vanadium(V). Also, the b parameter for Vanadium(III) is 0.14 L/mg, Vanadium(IV) is 0.22 L/mg and finally Vanadium(V) is 0.11 L/mg shown that the process is favorable because it requires less energy to occur. Also, the process is more energetically favorable for the adsorption of Vanadium(IV). The R_L values for vanadium oxyanions are shown in table 8. These results suggest that the adsorption process is favorable because it lies between 0 and 1. Table 9 compared our results with other adsorbents reported in previous studies, such as activated carbon, waste metal sludge, bentonite (Manohar et al., 2005; Namasivayam and Sangeetha, 2006; Bhatnagar et al., 2008; among others). These previous works have a higher Q^o, however they do not remove vanadium in the different oxidation states, are expensive, require complex procedures and require low pH and high concentrations. Therefore, our adsorbent is inexpensive, environmentally friendly, can remove vanadium in the three oxidation states, which are more commons at trace levels in the environment.

Table 6: Adsorption results for vanadium oxyanions using 5 g/L of PCF at pH 6.0.

	V(III)		V(IV)		V(V)	
Initial concentration (mg/L)	% Removal	Uptake capacity (mg/g)	% Removal	Uptake capacity (mg/g)	% Removal	Uptake capacity (mg/g)
0.075	100	0.015	100	0.015	100	0.015
0.1	100	0.02	100	0.02	100	0.02
0.5	100	0.11	99.1	0.11	99.9	0.11
1.5	100	0.28	95.8	0.26	73.6	0.23
3	96.8	0.62	93.8	0.58	43.8	0.27
5	97	0.96	89.9	0.9	30.1	0.31

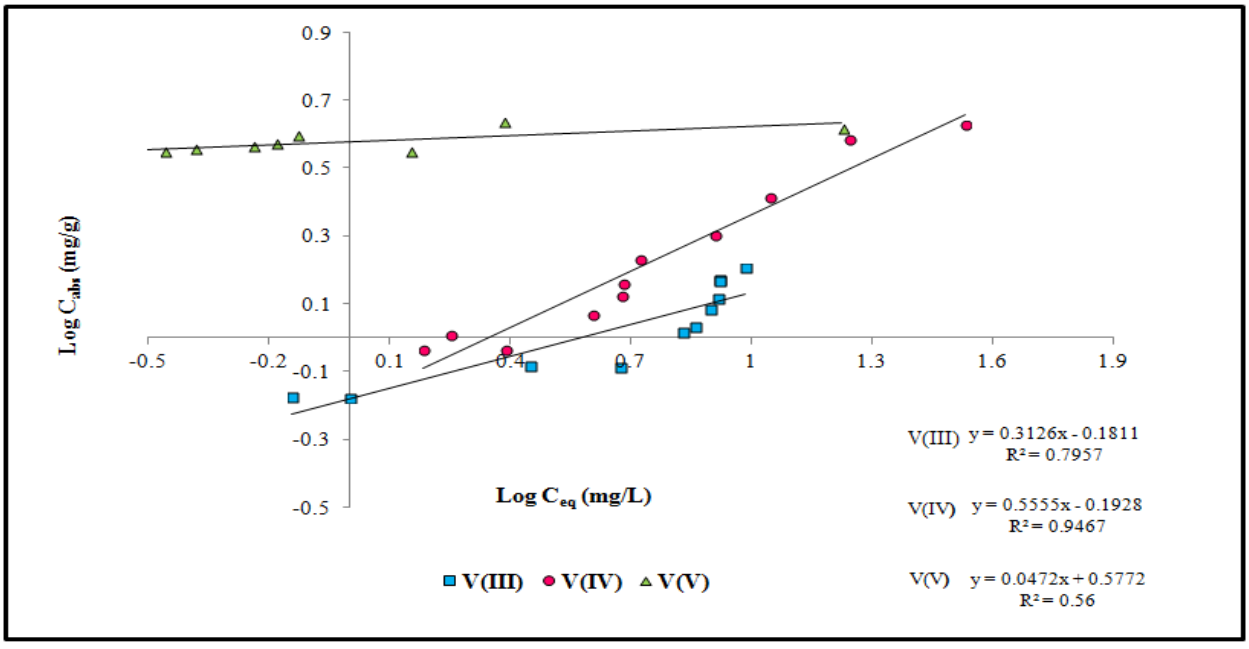

Figure 48: Freundlich isotherm model for Vanadium(III, IV and V) oxyanions using 5 g/L of PCF at pH 6.0.

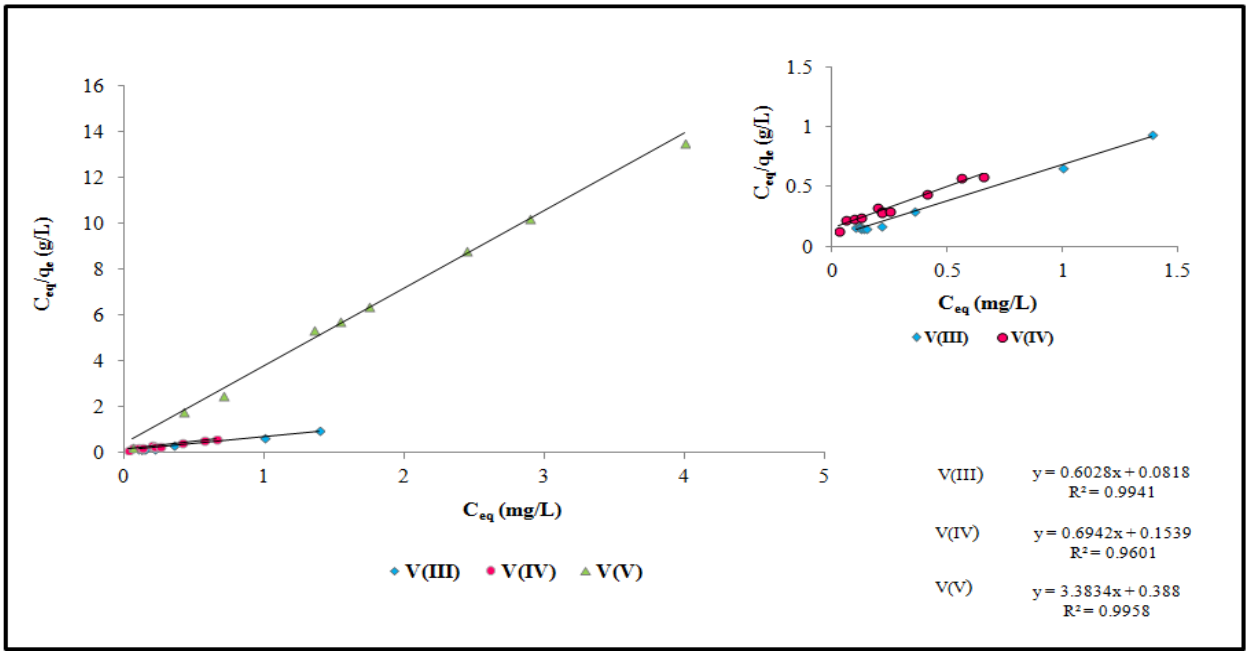

Figure 49: Langmuir isotherm model for Vanadium(III, IV and V) oxyanions using 5 g/L of PCF at pH 6.0.

Table 7: Langmuir and Freundlich parameters using 5 g/L of PCF at pH 6.0 for the removal of Vanadium(III, IV and V).

		V(III)	V(IV)	V(V)
Langmuir	R^2	0.9941	0.9601	0.9985
	Q^0 (mg/g)	12.22	6.5	2.58
	b (L/mg)	0.14	0.22	0.11
Freundlich	R^2	0.7957	0.9467	0.5600
	K_F ((mg/g)(L/mg)^n)	5.52	5.19	1.74
	N	3.2	1.8	21.18
	1/n	0.31	0.55	0.05

Table 8: R_L parameter for vanadium oxyanions using 5 g/L of PCF at pH 6.0.

Concentration (mg/L)	R_L		
	V(III)	V(IV)	V(V)
0.1	0.98	0.98	0.86
0.5	0.92	0.92	0.83
1.0	0.85	0.87	0.67
1.5	0.81	0.83	0.62
2.0	0.75	0.77	0.54
2.5	0.71	0.72	0.49
3.0	0.66	0.68	0.45
3.5	0.64	0.65	0.40
4.0	0.61	0.63	0.37
5.0	0.56	0.55	0.32

Table 9: Comparison of Q^0 Langmuir parameters with other adsorbents reported in previous studies for the removal of V(III, IV and V)

Sorbent	Q^0 (mg/g) V(III)	Q^0 (mg/g) V(IV)	Q^0 (mg/g) V(V)	Reference
PCF	12.22	6.50	2.58	Padilla et al., 2015a
Ca-Fe(III)-AB	-	6.77	0.79	Sánchez, 2013
Sludge	-	0.03	0.36	Sánchez, 2013
PONF-g-GMA	-	-	14.60	Yeom et al., 2009
$ZnCl_2$-activated carbon	-	-	24.90	Namasivayam and Sangeetha 2006
Metal sludge	-	-	24.80	Bhatnagar et al.,2008
Aluminum-pillared bentonite	-	24.16	-	Manohar et al., 2005

Adsorption Mechanism

The vanadium oxyanions are removed using adsorption due to electrostatic attraction interactions between the positive charge of the PCF and the negative charge of the adsorbate. This was confirmed by the study using the point of zero charge (pH_{pzc}), which obtained a value of 6.3 ± 0.05 (Figure 27). Therefore, the electrostatic attraction between the positively charged surface and negatively charged adsorbate ($H_2VO_4^-$) facilitate the adsorption of vanadium oxyanions. The possible mechanism for the removal of vanadium oxyanions using PCF is shown

in Figure 50. The mechanism showed the protonation of the amine functional group present in chitosan when in contact with hydrochloric acid. Once the sorbent is protonated, it attracts the vanadium oxyanions through electrostatic attraction between the protonated species and the negative charge of the $H_2VO_4^-$. To revert the process and recover the adsorbent, the PCF is exposed to acid or alkaline solutions to extract the oxyanions. The electrostatic mechanism is also supported by the FTIR spectra, which did not showed displacement in the characteristic IR band before and after the exposition to the vanadium oxyanions (Shown Figure 36), thus suggesting an electrostatic mechanism.

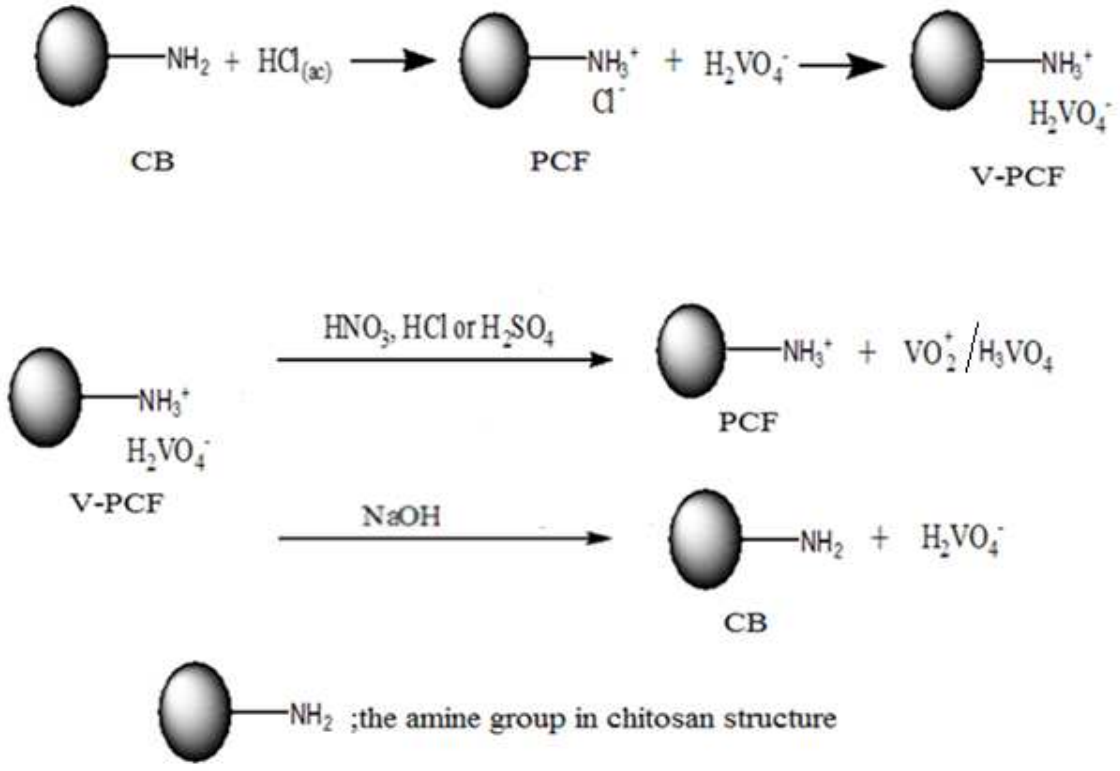

Figure 50: Possible mechanism for vanadium oxyanions adsorption onto PCF and its recovery.

4.2.3 Desorption Analysis

Figure 51 shows the various eluent used in the desorption studies. These were 0.1 and 1 M of hydrochloric, nitric and sulfuric acid, and sodium hydroxide. Hydrochloric acid 1 M was the best eluent for the recovery of the PCF with 100% for every vanadium oxyanions, which suggests the formation of a more stable product. Our results show that in acidic and alkaline medium takes place repulsion between the oxyanions and PCF, by destroying the electrostatic attractions between the protonated amine functional groups in the adsorbent (shown in Figure 50). However, the basic solutions using NaOH gives the most efficient desorption without dissolution of the PCF. The desorption process occurs because the amine is neutralized releasing the oxyanions. A possible desorption mechanism is showed in Figure 50.

The studies of adsorption/desorption were not performed with PCF because it is not feasible and cost-effective. This is due to damage to the flakes when using acids as eluents. Also, when alkaline eluents are used, requires the use of several rinses of the PCF to eliminate the hydroxide excess. These additional procedures for the removal of the oxyanions are not cost-effective.

It is important mentioning that the method of fixation or stabilization could be applied once these pollutants are desorbed of the adsorbent surface. The fixation process is standard procedures, which involves the aggregation of additives (ie. Portland cement) to reduce the hazardous nature of waste, its toxicity, or to minimize the rate of migration of the contaminant in the environment (Mohan and Pittman, 2007).

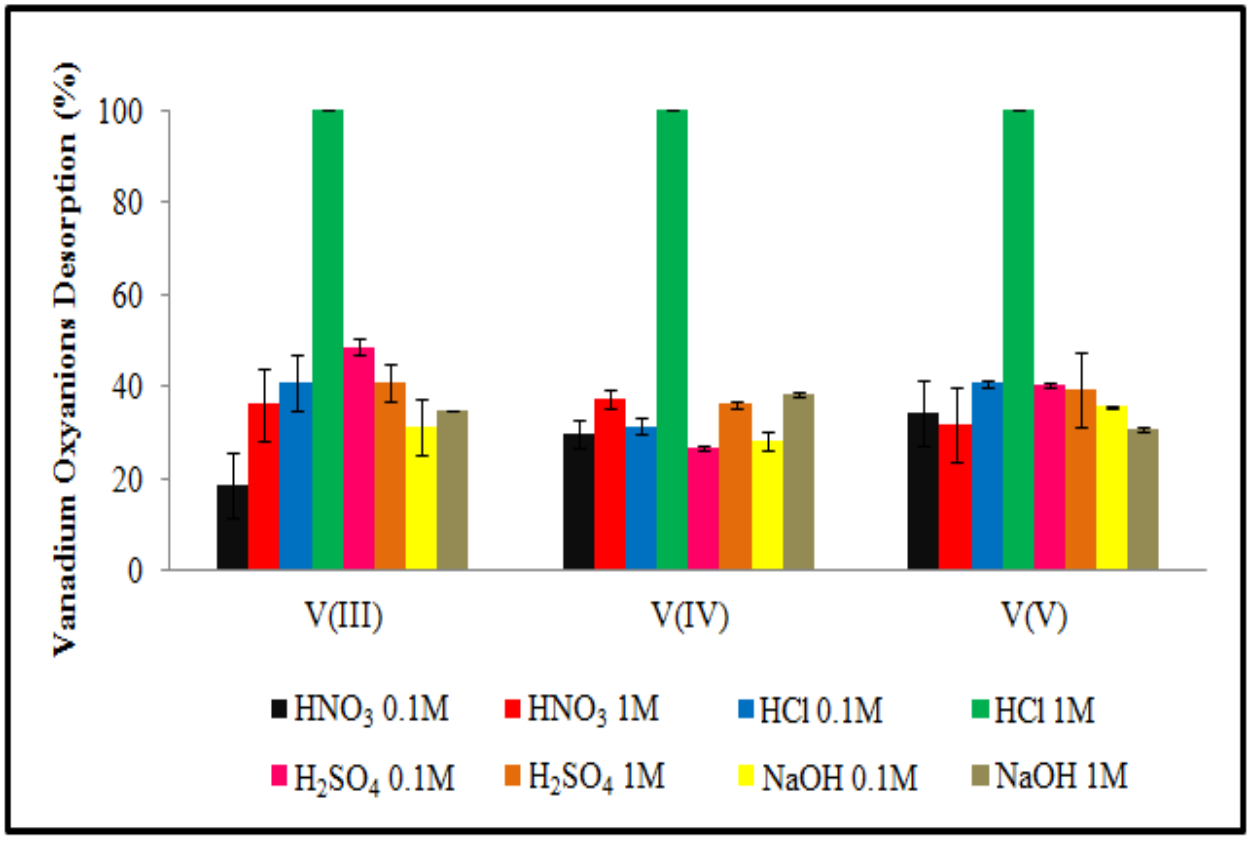

Figure 51: Desorption of vanadium oxyanions using 0.1 M and 1 M sodium hydroxide, nitric acid, hydrochloric and sulfuric acids from PCF.

4.3 Arsenic Adsorption using PCF Results

4.3.1 Synthesis and Characterization

4.3.1.1 Adsorbent Synthesis Optimization and Protonation Procedure

The maximum percent removal of As(V) using PCF as a function of pH adsorbent suspension solution is shown in Figure 52. The pHs evaluated were 4, 5, 6, 7, 8, 10 and 12 when 5 g/L of adsorbent were placed in contact with an initial arsenate concentration of 0.500 mg/L at room temperature and at 200 rpm. The adsorption of As(V) decreased when the pH for the conditioning of chitosan beads/flakes was increased. This is due to the lower concentration of H^+ for protonation of the NH_2 group and an increase in electrostatic repulsions as predicted by the pH_{pzc} (6.3). Instead, at acidic pH, the amine group is protonated and therefore the electrostatic attraction between the NH_3^+ and the arsenate oxyanion predominates, thus increasing the adsorption of As(V). The maximum adsorption was at pH 5.00 with 97%, below this pH, the beads/flakes will start dissolving and a decrease in adsorption capacity was observed.

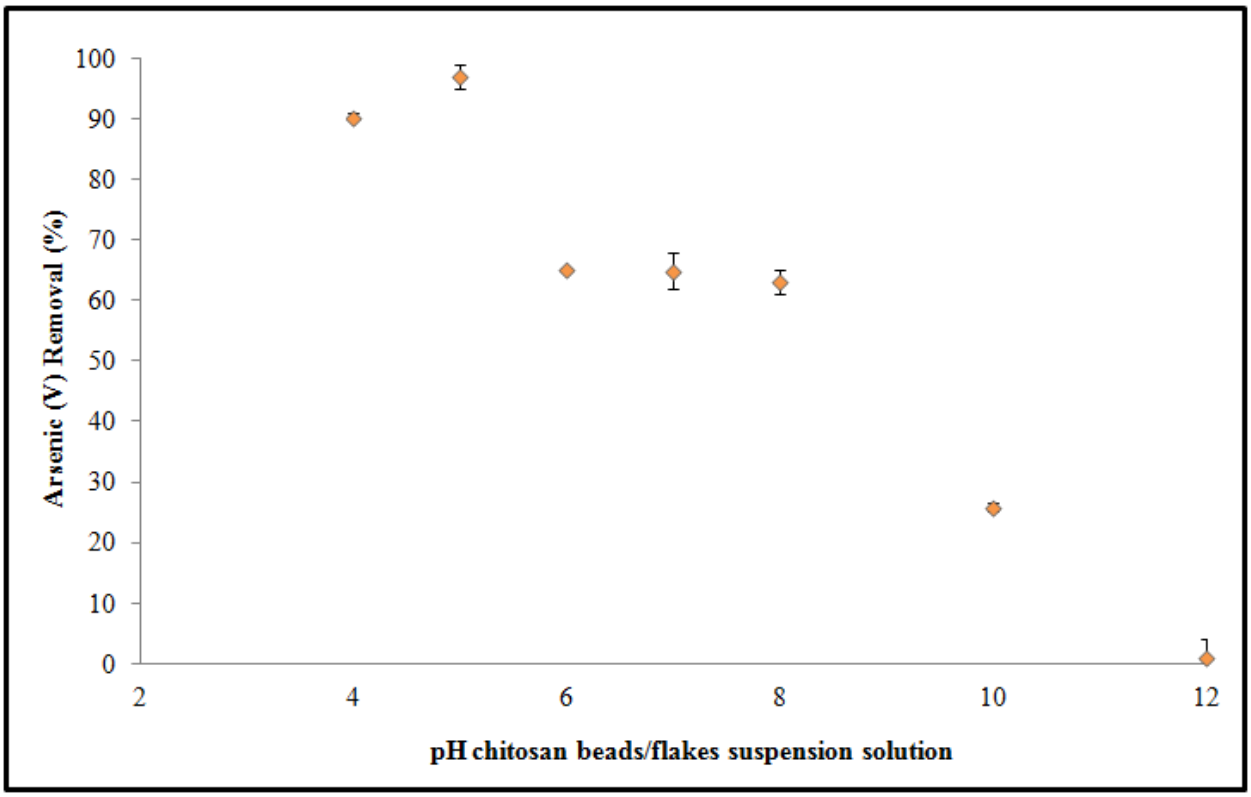

Figure 52: pH of chitosan beads/flakes suspension solutions on the As(V) oxyanion adsorption onto the chitosan. Experimental conditions: initial concentration of As(V) = 0.500 mg/L; adsorbent concentration = 5 g/L; contact time = 26 h; shaker speed = 200 rpm; and pH aqueous solution = 6.0 ± 0.1.

4.3.1.2 Scanning Electron Microscopy Analysis

SEM micrographs at A) 30X, B) 1500X, and C) 7000X magnifications of PCF, and PCF in contact with arsenate solution (Shown in Figures 53 and 54). The figures show that after the arsenate oxyanion adsorption; the surface does not show a significant difference when compared with PCF without the contaminant.

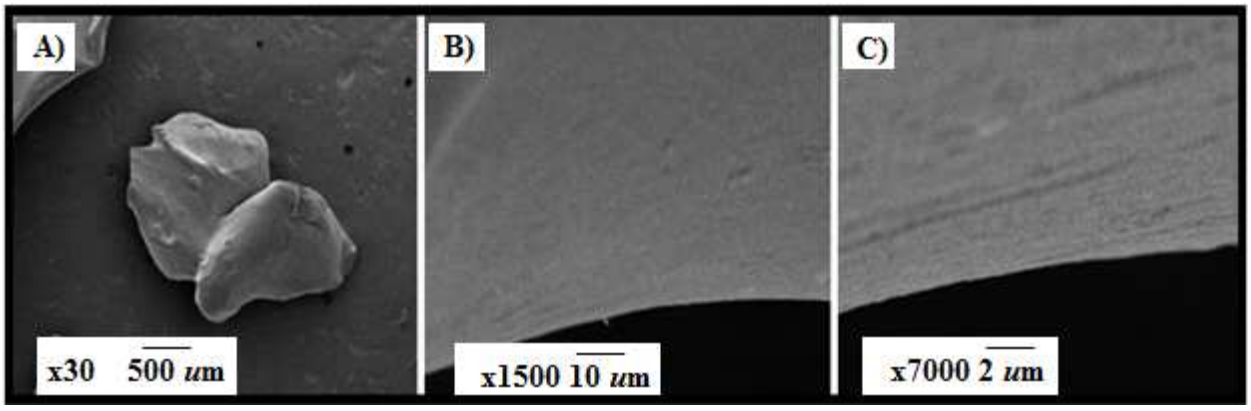

Figure 53: SEM micrographs of PCF at magnification A) 30X, B) 1500X and C) 7000X.

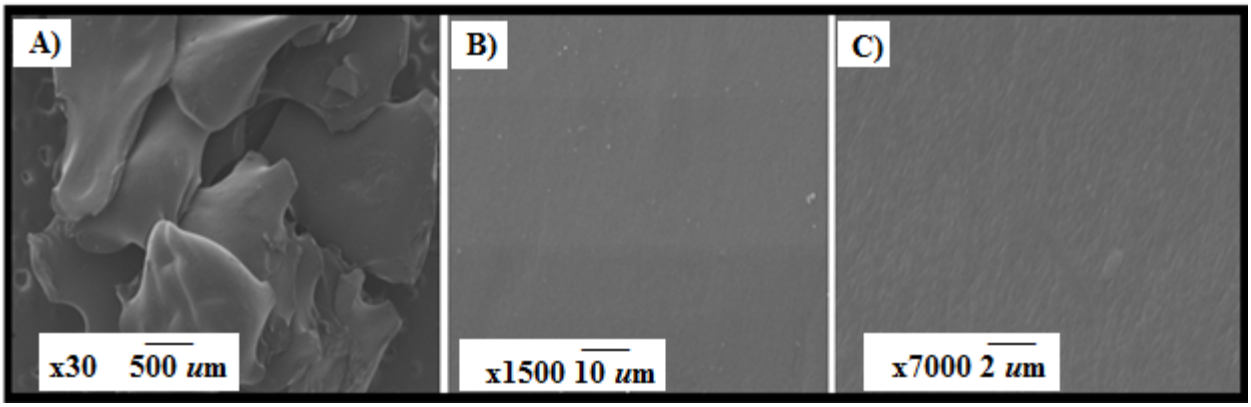

Figure 54: SEM micrographs of As(V) onto PCF at magnification A) 30X, B) 1500X and C) 7000X.

4.3.1.4 Infrared Spectroscopy Analysis

Figure 55 shows the FT-IR spectrum of PCF and the interactions of As(V) onto PCF. The functional groups of the PCF were discussed in section 4.1.1.3. Once the As(V) oxyanion is adsorbed by the PCF adsorbent, the different functional groups are similar to PCF bands. When the PCF was used for the removal of As(V) no displacement of the NH_2 stretching vibration is observed suggesting that the mechanism does not involve chelation with this functional group, thus supporting an electrostatic interaction.

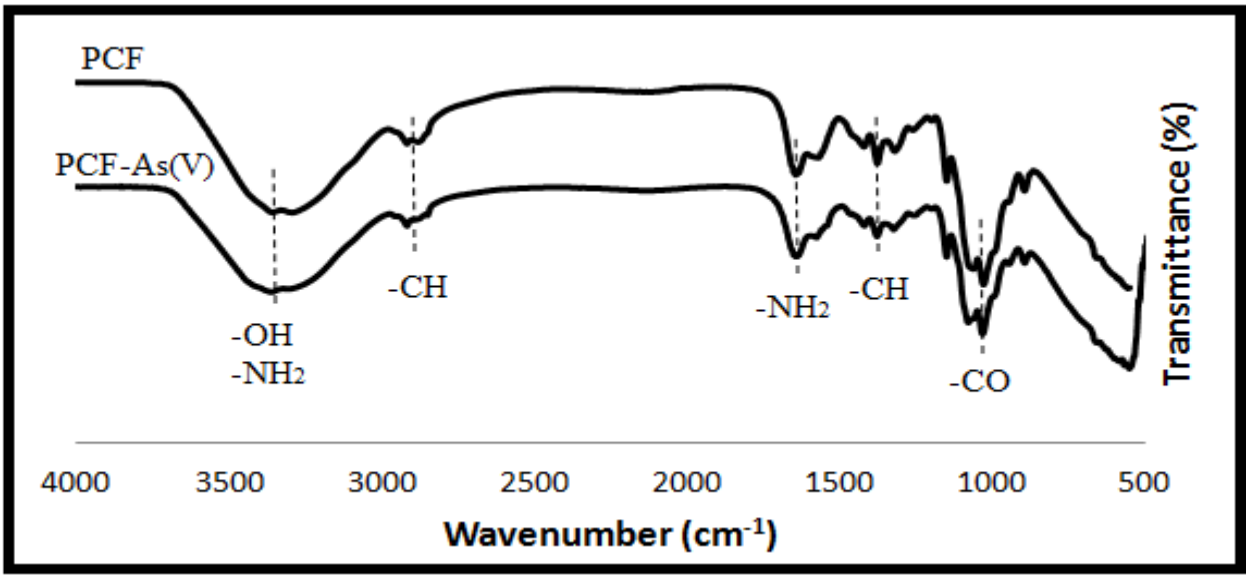

Figure 55: FT-IR spectra of PCF, and PCF in contact with As(V).

4.3.1.5 LA-ICP-MS Analysis

Figure 56 shows the presence of trace amounts of arsenate (blue line) onto PCF using a LA-ICP-MS. The surface of the PCF was directly analyzed by ablating with a pulsed laser beam where the intensity of the received signal is proportional to the concentration. A significant increase in the blue line intensity is observed when compared with the background line as a result of the laser ablation process due to the arsenic signal. The red signal is due to the carbon present in the chitosan matrix. The inserted image in the upper right shows the incident laser path during the ablation of the chitosan matrix. Carbon is used as an internal standard.

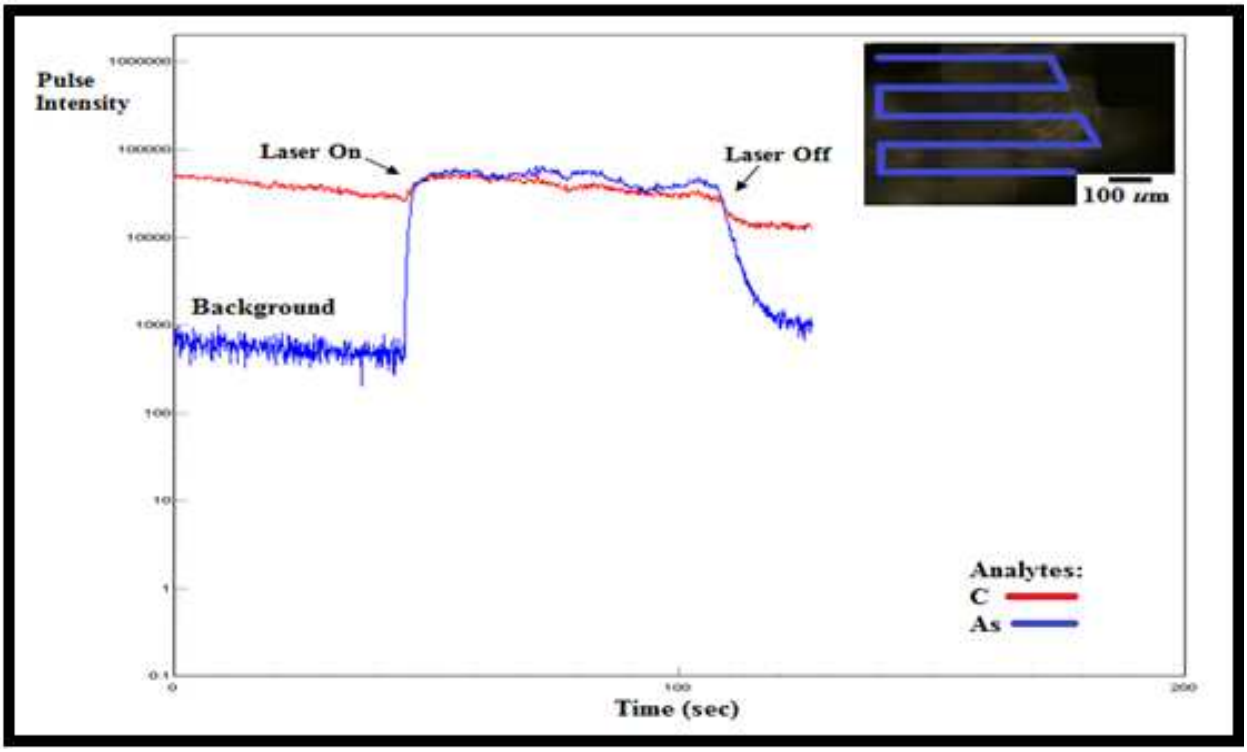

Figure 56: LA-ICP-MS spectra and image of As(V) interacting with PCF.

4.3.1.6 XRF Analysis

Figures 57 and 58 shows the comparison of the spectra XRF between traces of arsenate present onto PCF and PCF without arsenate. Also, the circle in the upper right of the inserted image shows the point of incidence of the X-ray. Figure 57 shows, with the dark blue color, where the characteristic Ka_1 (10.5 KeV), Kb_1 (11.7 KeV), La_1 (1.28 KeV) and Lb_1 (1.31 KeV) fluorescence lines from As are expected. The fluorescence lines corresponding to the arsenic signal onto the PCF are presents the distinctive As Ka_1, Kb_1 fluorescence peaks (Figure 57). Figure 58 shows other peaks that belong to the PCF control signal and the Ti base used as background to avoid interfere with the arsenic signal; the dark red line shows Ka_1 and Kb_1 from the Ti XRF stage.

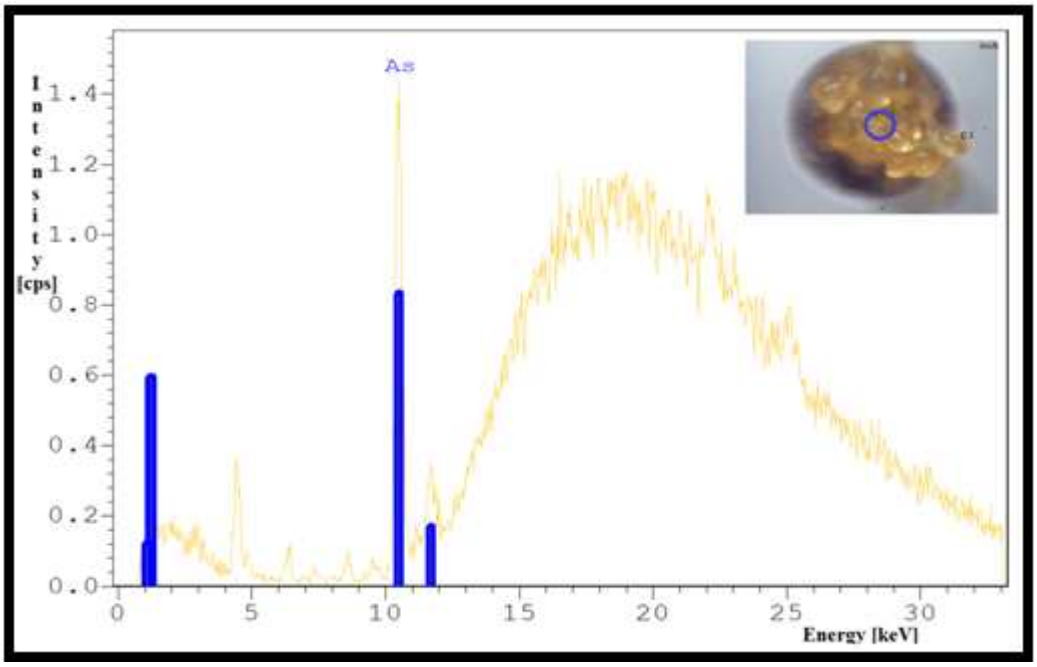

Figure 57: XRF spectra and image of As(V) onto PCF.

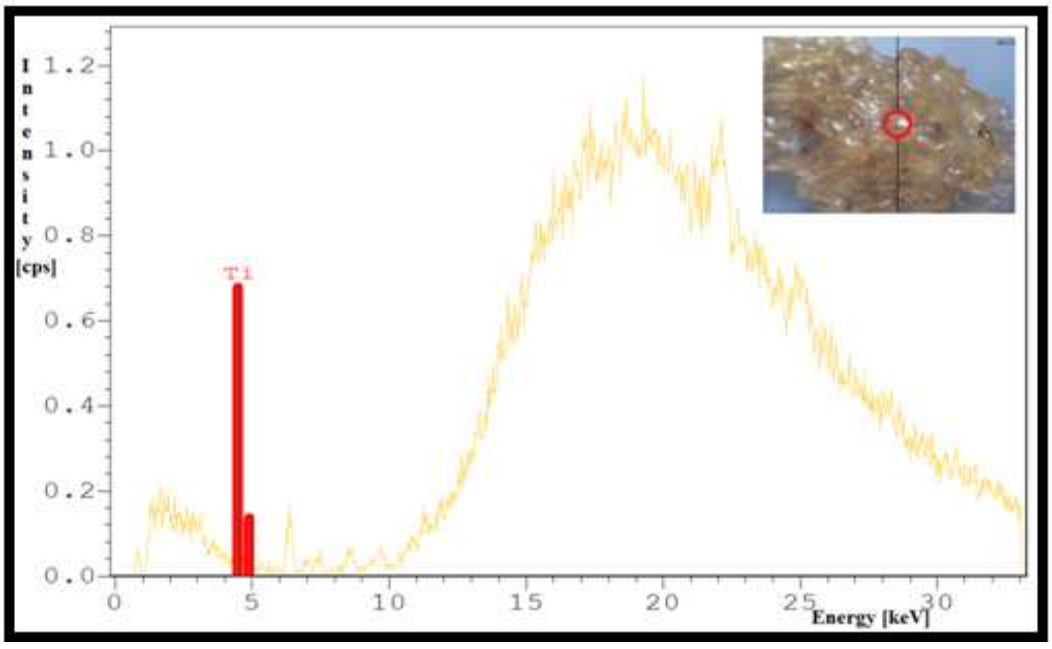

Figure 58: XRF spectra and image of PCF without As(V).

4.3.2 Adsorption Analysis

This section discusses the adsorption studies for the arsenate oxyanion removal, such as pH aqueous solution, concentration adsorbent, contact time, co-existing anions competence, and adsorption isotherms.

Effect of pH aqueous solution

The pH aqueous solution used in the adsorption process of As(V) (0.500 mg/L) by the PCF (5 g/L) was studied at pHs 2, 4, 6, 8 and 10 and were agitated at 200 rpm for 26 h. Figure 59 shows that the adsorption decreased in acidic and alkaline pH, showing the maximum adsorption at pH 6.0. These results are consistent with those obtained for the pH_{pzc} of 6.3 (Section 4.1.1.4). Above the pH_{pzc} decreasing the adsorption process because occurs repulsion between the negatively charge of beads/flakes surface and the negatively charged $HAsO_4^{-2}$ and AsO_4^{-3} species (shown in figure 59). At pH 6, generates electrostatics attractions due to the formation of $H_2AsO_4^-$ species which is attracted by the positively charged NH_3^+ thus increasing adsorption. Below pH 2 neutral species (H_3AsO_4) predominates and thus no interaction with the NH_3^+ groups and the PCF start to dissolve and the adsorption capacity significantly degrades. Also, a decrease in the adsorption is observed at high pHs because the formation of $HAsO_4^{-2}$ and AsO_4^{-3} species and the neutralization of the amines of chitosan structure leading to lack of electrostatic attractions (Langmuir et al., 2003). All the other studies were carried out in an aqueous solution at pH 6.00 ± 0.1. It is important to point out that the pH of natural and potable water is also near the optimum pH of the aqueous solution used for PCF and consequently it can be used for field applications.

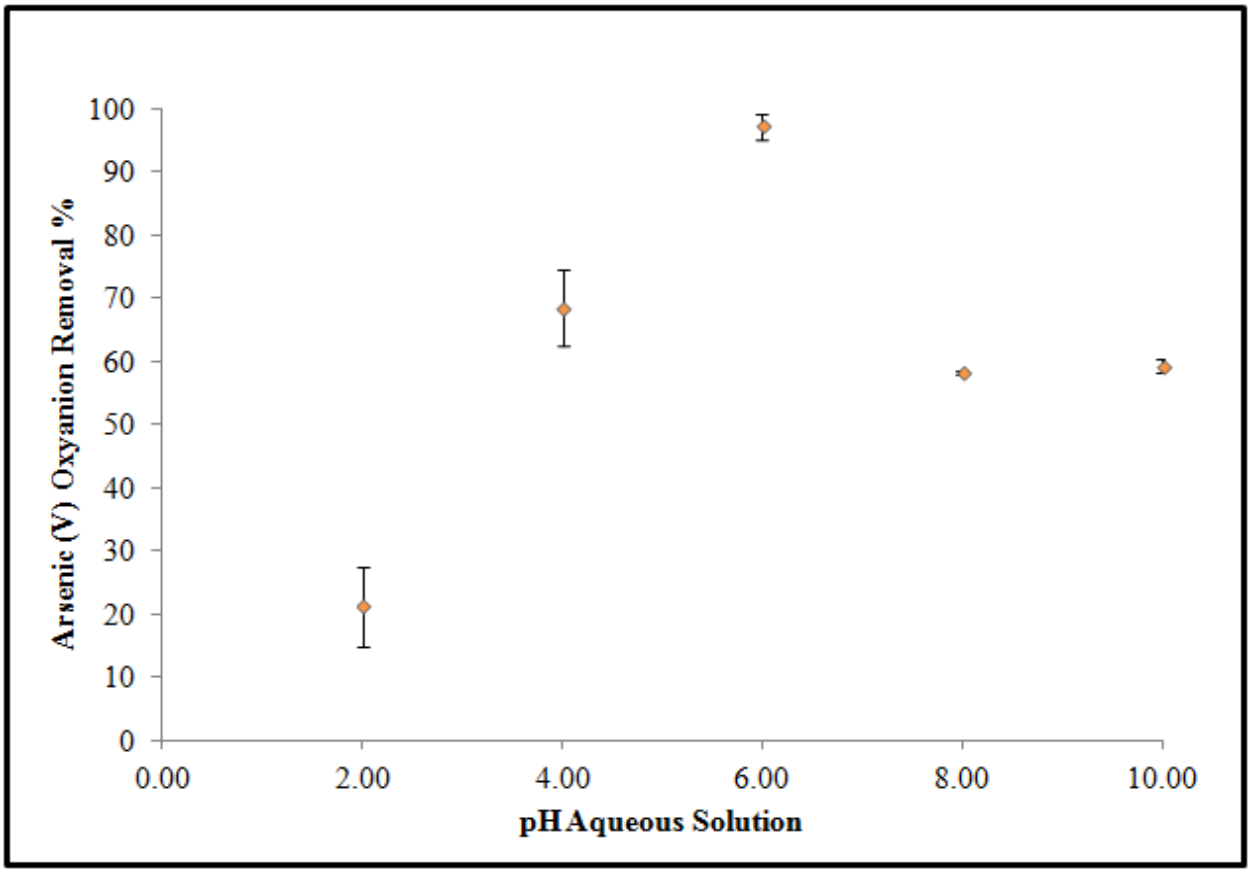

Figure 59: Effect of pH aqueous solutions on the As(V) oxyanion adsorption onto PCF. Experimental conditions: initial concentration of As(V) = 0.500 mg/L; adsorbent concentration = 5 g/L; contact time = 26 h; and shaker speed = 200 rpm.

Effect of adsorbent concentration

Studies on optimum adsorbent concentration were carried out by adding 1, 3, 5 and 10 g/L of PCF at initial arsenate concentration of 0.500 mg/L, at room temperature, and pH of the aqueous solution of 6.00 ± 0.1. These were studied to verify the maximum tolerance limit for arsenate oxyanion removal. Figure 60 shows the percentage removal of arsenate, which was 67% (1 g/L), 65% (3 g/L), 97% (5 g/L) and 96% (10 g/L). It is evident that a higher adsorbent amount will cause a greater removal of the oxyanion due to the increase of available active sites,

however 5 g/L of PCF showed approximately the same adsorption that 10 g/L and based on this, all the studies were performed using 5 g/L of PCF as the optimum adsorbent concentration.

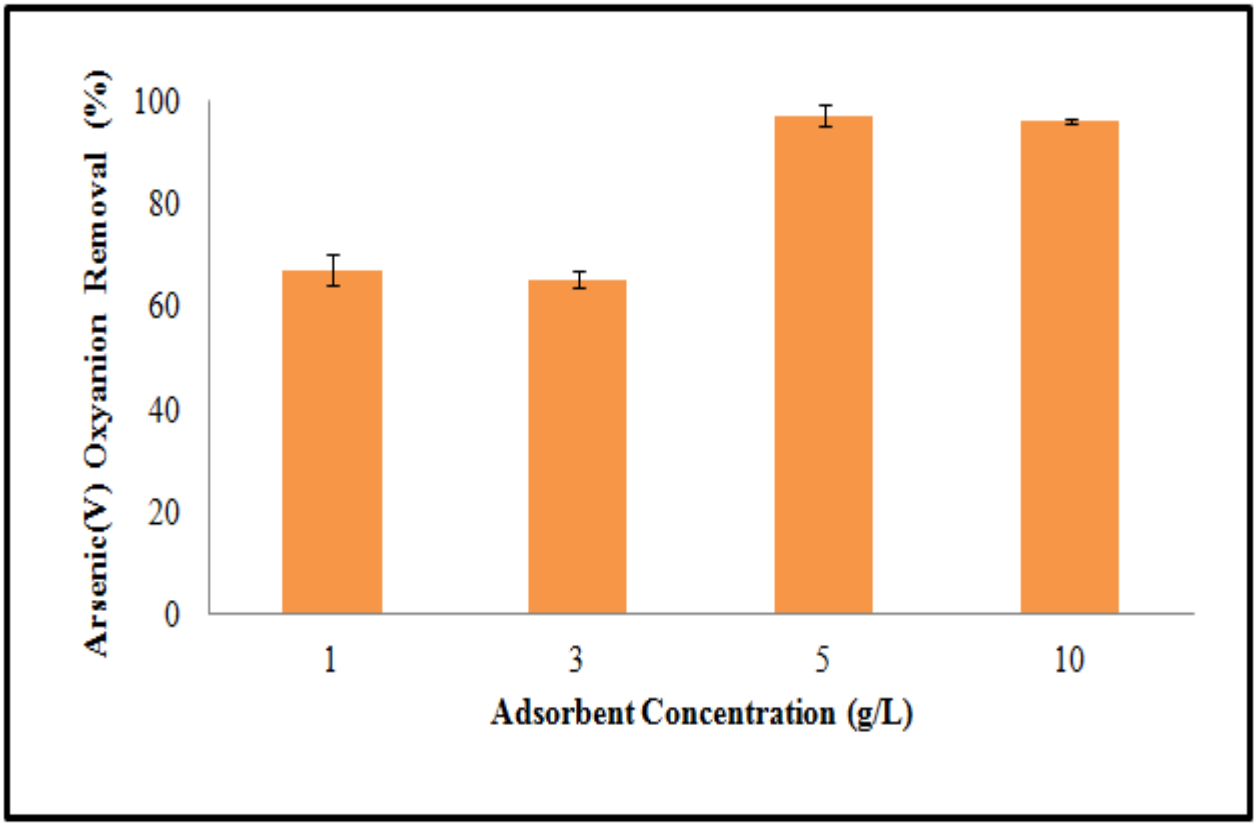

Figure 60: Effect of adsorbent concentration on the As(V) oxyanion adsorption onto PCF. Experimental conditions: initial concentration of vanadium species = 0.500 mg/L; contact time = 26 h; shaker speed = 200 rpm; and pH aqueous solutions = 6.0 ±0.1.

Effect of contact time

Figure 61 shows the variation of arsenate oxyanion onto PCF found by varying contact time between 0-26 hours. We can see that arsenate oxyanion reached equilibrium approximately

after 2 hours. The percentage of removal obtained was a 97% with a final concentration of 0.014 mg/L, which is very close of complying with the MCL (0.010 mg/L) of the EPA regulation. Concentrations As(V) lower than 0.500 mg/L obtained a final concentration of 0 mg/L, thus fully complying with EPA and WHO compliance. The ideal contact time was 26 hours in order to observe that it remained in constant equilibrium.

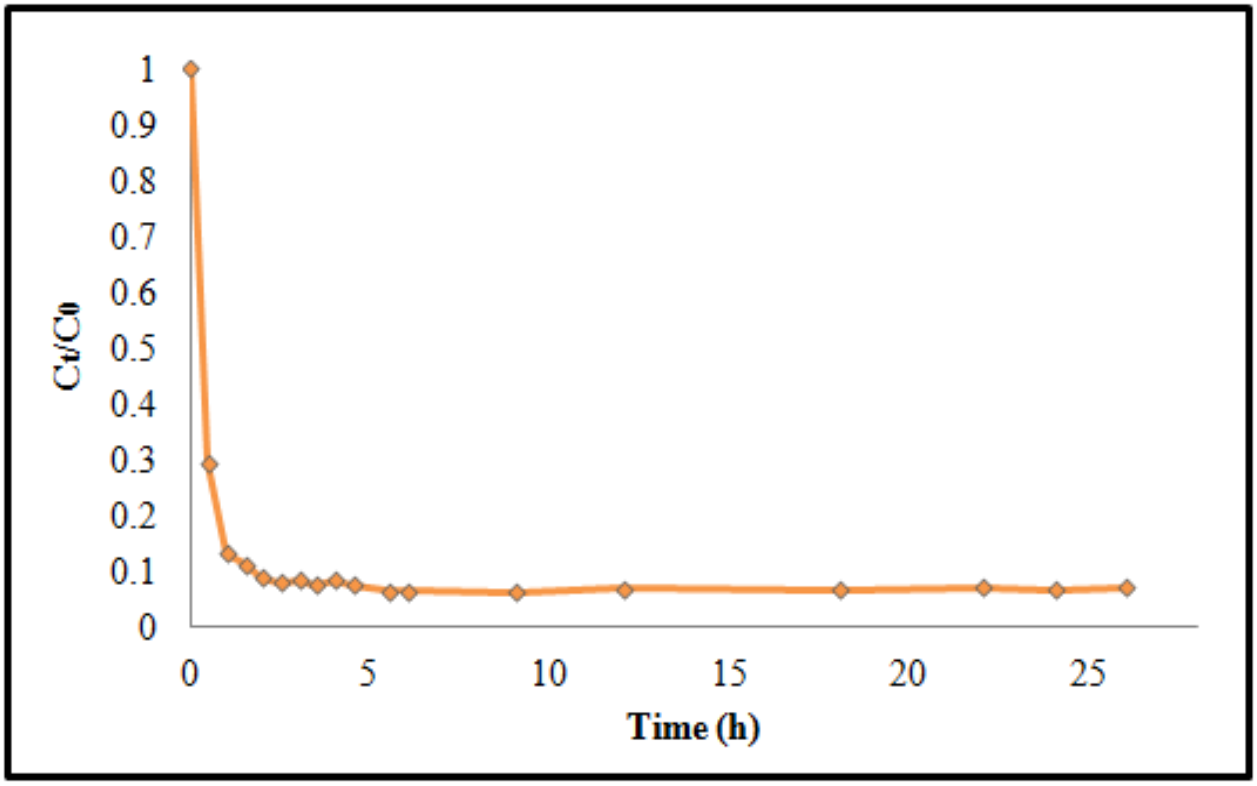

Figure 61: Effect of contact time on As(V) oxyanion onto PCF. Experimental conditions: initial concentration of arsenic(V) oxyanion = 0.500 mg/L; adsorbent concentration = 5 g/L; shaker speed = 200 rpm; and pH aqueous solutions = 6.0 ± 0.1.

Effect of Co-existing anions competence

The effects of co-existing anions were studied using carbonate, chloride, sulfate and phosphate as common anions. The initial concentrations of these competitive anions were 0.01 and 0.02 mmol at a proportion of 1:0, 1:20 and 1:30 (As:CA) by keeping 0.0007 mmol (0.5 mg/L) as the initial arsenate concentration at pH 6.0 ± 0.1 onto 5 g/L of PCF. Table 10 shows the percentage removal of arsenate with the addition of the co-existing anions. The orders of arsenate removal in the presence of common anions were 84-85% for carbonate, 81-82% for chloride, 68-72% for phosphate and 67-68% for sulfate. These results showed that the addition of common anions slightly affect the removal of arsenate when in competition with chloride and carbonate anions at both concentrations. Also, the percentage removal of arsenate showed a modest decrease in both proportion for sulfate and phosphate, this can be attributed to the competition for adsorption sites on the surface of PCF because they both have a similar chemical structure to arsenic oxyanions (Bhakat et al., 2006; Vitela and Rangel, 2013; Sahiner et al., 2011).

Table 10: Adsorption studies for As(V) oxyanions onto 5 g/L of PCF at diverse co-existing anions (CA).

		As(V)
	Ratio As:CA (mol:mol)	**% Removal ± SD**
	1:0	97.2 ± 2
Cl^-	1:20	81.6 ± 0.1
	1:30	80.5 ± 0.04
CO_3^{-2}	1:20	83.5 ± 0.1
	1:30	84.8 ± 2
SO_4^{-2}	1:20	66.8 ± 0.1
	1:30	67.8 ± 3
PO_4^{-3}	1:20	67.9 ± 2
	1:30	72.4 ± 2

Adsorption Isotherm

Table 11 shows examples of initial As(V) concentrations used for adsorption studies using 5 g/L of PCF at pH 6.0. The uptake capacity for As(V) oxyanion increased once the initial concentration increased, and the removal percentages decreased as As(V) concentration increased. Langmuir and Freundlich isotherm plots are shown in figures 62 and 63, respectively. Langmuir isotherm showed a better fit, which is demonstrated by the value of the linear

correlation coefficient (R^2), as shown in Table 12. The R^2 values were 0.9740 and 0.9250 for the Langmuir and Freundlich isotherm, respectively. The Langmuir Q^0 parameter for the arsenate was 5.43 mg/g and K_F 17.86 mg/g, indicating a good adsorption capacity. The results of the b constant of 0.15 L/mg show that the adsorption process is energetically favorable because it needs less energy. The dimensionless R_L parameter fluctuates between 0.98 - 0.51 for initial arsenate concentration between 0.100 – 5 mg/L, which demonstrated that it is a favorable adsorption process (shown in Table 13). Also, the results showed the n and 1/n values, which were 1.86 and 0.54, respectively. This indicates that the adsorption process is favorable at low concentrations and that the adsorbate has a good affinity for the adsorbent. Thus it was observed that the adsorption primarily occurred by electrostatic attraction between the As(V) oxyanion and the PCF. Table 14 compares the maximum capacity of adsorption (Q^0, Langmuir parameter) with other adsorbents reported in previous studies. These sorbents showed inferior adsorption capacity to our adsorbent (PCF), are expensive and present complex procedures for their synthesis. Therefore, PCF is cost-effective, easy to synthesis, and an environmentally friendly alternative to remove As(V) oxyanion from aqueous solutions.

Table 11: Adsorption Results for Arsenic(V) Oxyanion using 5 g/L of PCF at pH 6.0.

As(V)		
Initial concentration (mg/L)	% Removal	Uptake capacity (mg/g)
0.075	100	0.01
0.1	100	0.02
0.5	97.2	0.11
1.5	75.0	0.23
3	78.1	0.49
5	73.4	0.74

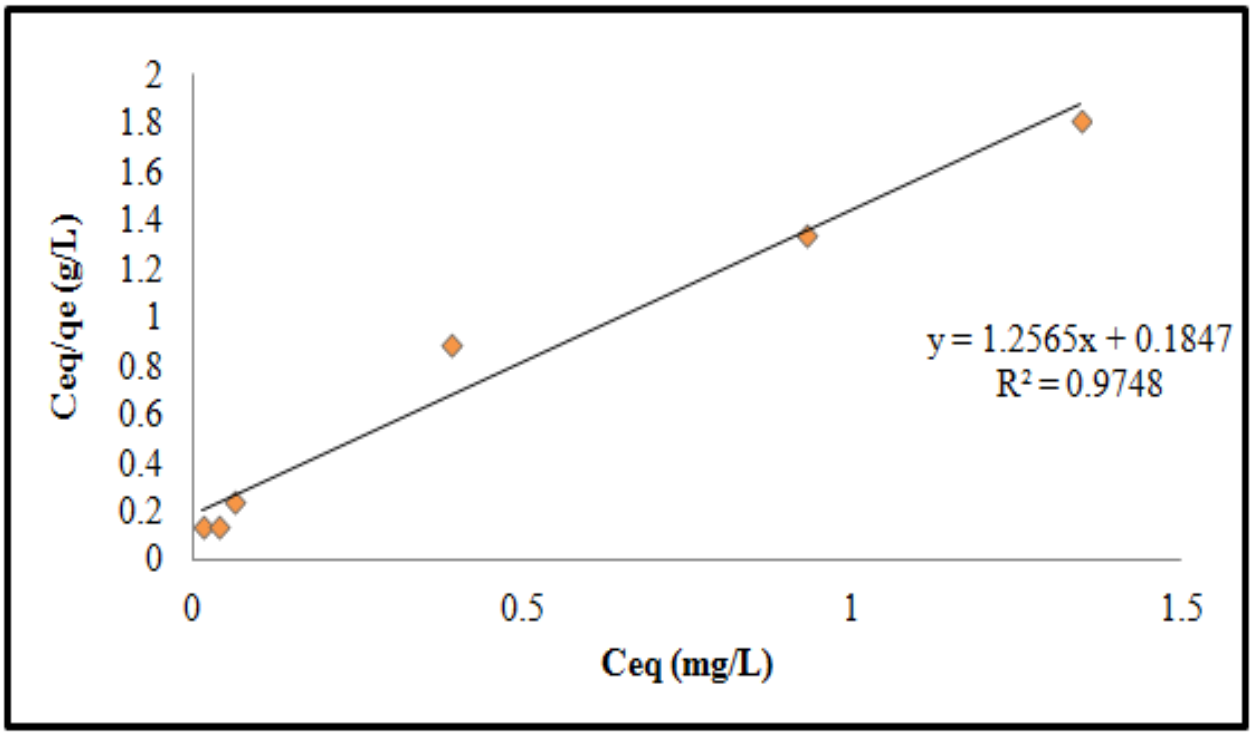

Figure 62: Langmuir isotherm model for As(V) oxyanion adsorption onto PCF.

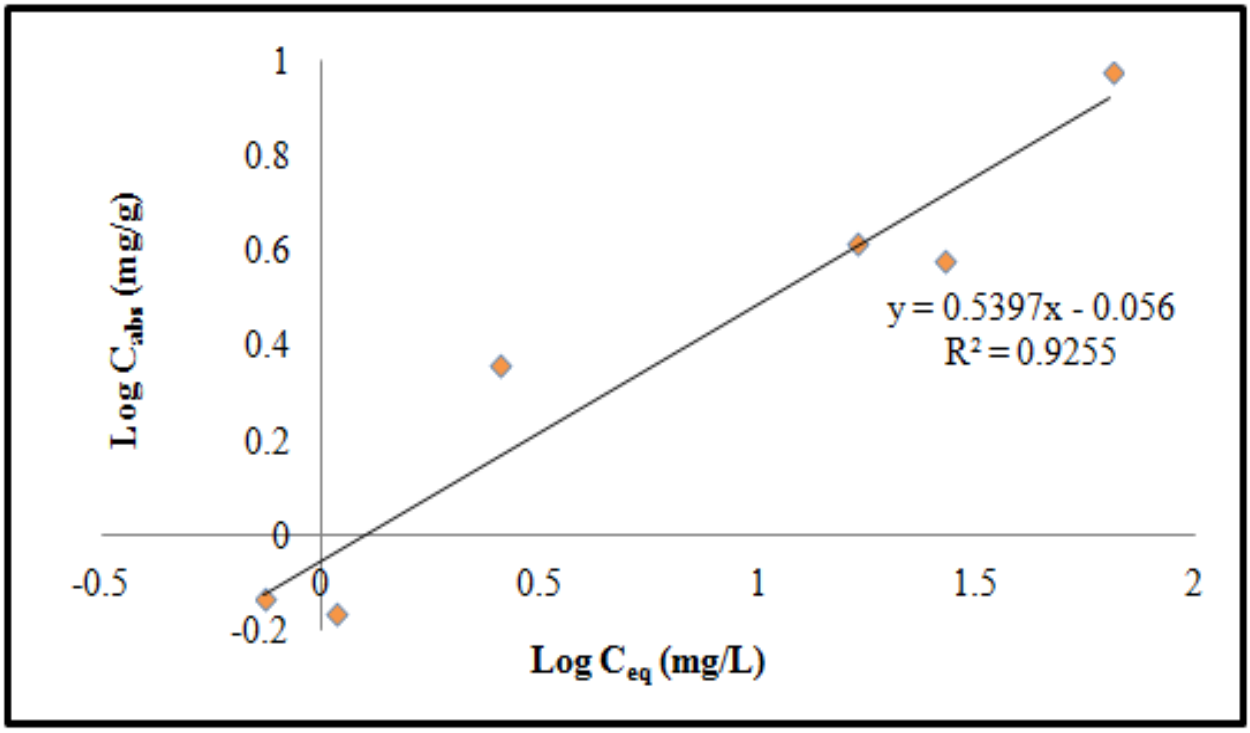

Figure 63: Freundlich isotherm model for As(V) oxyanion adsorption onto PCF.

Table 12: Langmuir and Freundlich parameter using 5 g/L of PCF at pH 6.0 for the removal of As(V).

		As(V)
Langmuir	R^2	0.974
	Q^0 (mg/g)	5.43
	b (L/mg)	0.15
Freundlich	R^2	0.925
	K_F ((mg/g)(L/mg)n)	17.86
	n	1.86
	1/n	0.54

Table 13: R_L parameter for As(V) oxyanion using 5 g/L of PCF at pH 6.0.

	R_L
Concentration (mg/L)	**As(V)**
0.1	0.98
0.5	0.91
1.0	0.83
1.5	0.78
2.0	0.72
1.5	0.68
3.0	0.63
3.5	0.58
4.0	0.55
5.0	0.51

Table 14: Comparison of Q^0 Langmuir parameters with other adsorbents reported in previous studies for the removal of As(V).

Sorbent	Q^0 (mg/g)	Reference
PCF	5.43	Padilla et al., 2015b
Activated carbon	1.22	Yürüm et al., 2014
F400-M[a]	0.847	Vitela and Rangel 2013
O-CAB[b]	1.9	Garlaschelli 2013
Dried sludge	0.133	Sánchez et al., 2013
Fe-AC	1.322	Asadullah et al., 2013
TICB[c]	2.540	Miller et al, 2011
Siderite and hematite	0.202	Guo et al., 2007
Iron oxide	0.66	Jeong et al. 2007
Aluminum oxide	0.17	Jeong et al. 2007
Zero-valent iron	2.47	Kanel et al., 2006

[a]Activated carbon with iron(hydroxide) nanoparticle.
[b] Industrial waste entrapped in alginate beads.
[c] TiO_2-impregnated chitosan bead.

Adsorption Mechanism

The removal of As(V) oxyanion in contact with PCF is attributed to the interaction with the positive charge of NH_3^+ present in the PCF and the negative charge of the arsenate ($H_2AsO_4^-$) which causes electrostatic attraction. The point of zero charge (pH_{pzc}) obtained in our study (pH_{pzc} = 6.3) confirmed that below this pH, the net charge surface of the PCF is positive and above this pH, it is negative. Figure 64 shows the possible mechanism of removal of As(V) oxyanion using PCF as an adsorbent (Padilla et al., 2015b). The amine group of chitosan is

protonated by adding diluted HCl. In this mechanism, PCF removed the As(V) oxyanion through coulombic forces. To recover the adsorbent, the PCF is exposed to an acid (HCl, HNO_3, H_2SO_4) or alkaline (NaOH) solution to extract the As(V) oxyanion. Figures 52 and 59 also support the proposed mechanism. In figure 52, it is observed that the maximum adsorption for As(V) is obtained when the adsorbent pH is below the pH_{pzc} and above this pH electrostatic repulsion decreases the adsorption. Also, it is worth pointing out that when the pH is decreased to a point when the $HAsO_4^{-2}$ and AsO_4^{-3} species are protonated a significant decrease in As(V) adsorption is also observed. Figure 59 also shows the same behavior and that the maximum adsorption is obtained when the aqueous solution pH is 6.0 and above this pH also electrostatic repulsion decreases the adsorption of As(V).

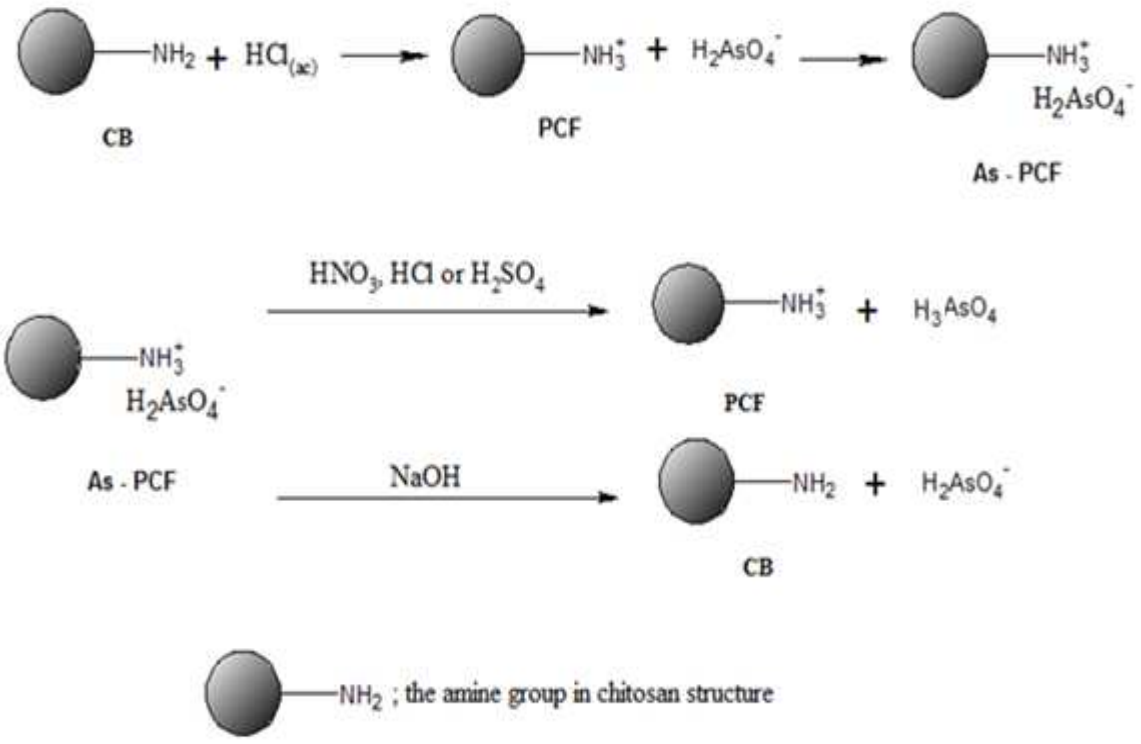

Figure 64: Possible mechanism for As(V) oxyanion adsorption onto PCF and its recovery.

4.3.3 Desorption Analysis

Figure 65 shows the desorption efficiency of PCF using acidic and alkaline eluents, such as hydrochloric acid (HCl), nitric acid (HNO_3), sulfuric acid (H_2SO_4) and sodium hydroxide (NaOH) at 0.1 M and 1 M. The results of the percentage of arsenate desorption were in the following order: HNO_3 1 M (91%), NaOH 0.1 M (86%), NaOH 1 M (78%), H_2SO_4 1 M (63%), HCl 1 M (59%), HNO_3 0.1 M (51%), H_2SO_4 O.1 M (47%) and HCl 0.1 M (40%). The maximum percentage of desorption was obtained when using 1 M HNO_3, which suggests the formation of a more stable product. Our results showed a good percent of arsenate desorption when using eluents with a concentration of 1 M because at a low pH, the As(V) species exists as a neutral form, which is more easily released from the adsorbent, due to lack of electrostatic attraction. However, the best desorption was achieved using NaOH solutions due to the neutralization of the protonated amine and a disruption of the electrostatic interactions between the oxyanions. The possible desorption mechanism is showed in Figure 64. As in section 4.2.3, the adsorption/desorption tests were not performed for the same reasons. The method of fixation or stabilization can be applied as explained in the section 4.2.3

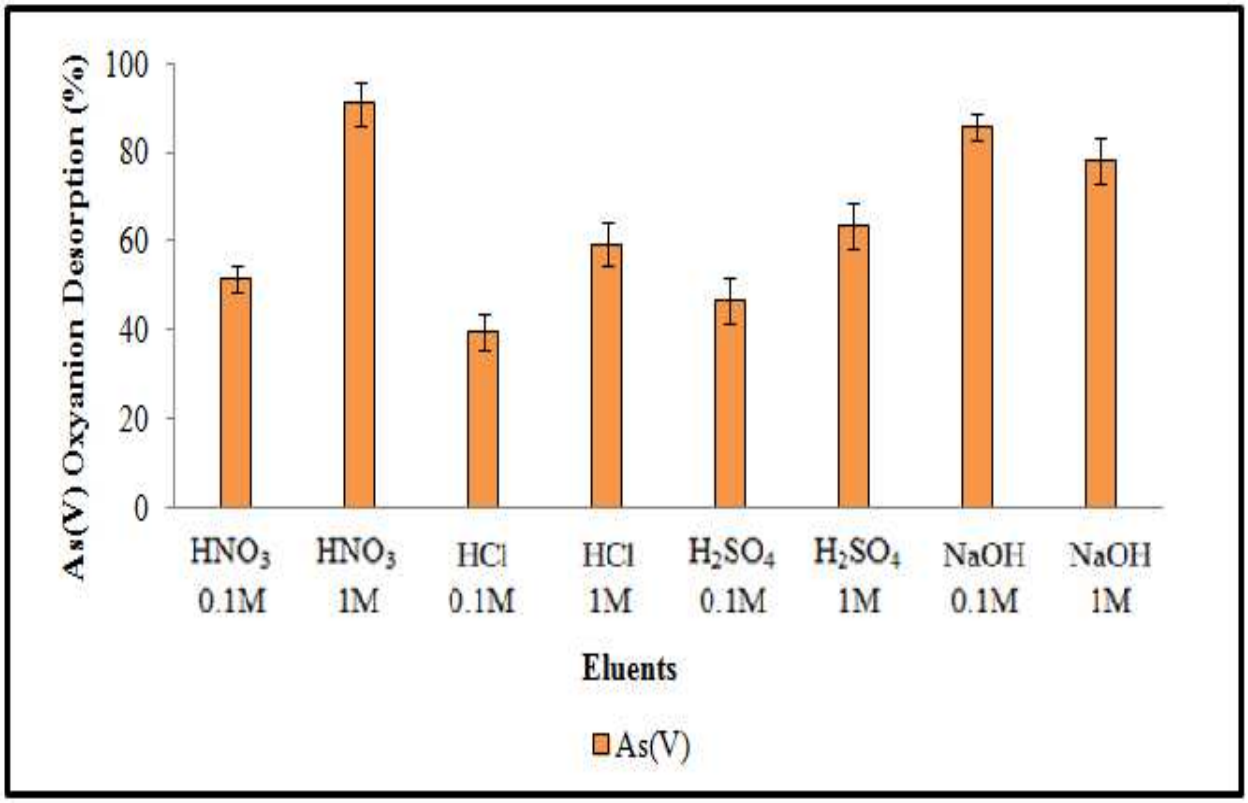

Figure 65: Desorption of As(V) oxyanion using 0.1 M and 1M sodium hydroxide, nitric acid, hydrochloric and sulfuric acids from PCF.

4.4 Arsenic Adsorption using Fe(III)-Chitosan Beads Results

4.4.1 Synthesis and Characterization

4.4.1.1 Adsorbent Synthesis Optimization

Figure 66 shows the arsenic oxyanions removal at diverse concentration of iron in the chitosan beads. The initial concentrations of iron(III) were 0.01, 0.05 and 0.1 M using an optimum pH of 8.0 for the formation of ferric hydroxide. The results showed a removal of a 90% (0.01 M), 95% (0.05 M), and 94% (0.1 M) for As(III) oxyanion. As(V) oxyanion showed a 86% (0.01 M), 99% (0.05 M), and 100% (0.1 M) of removal. Once the concentration increased, the percent removal of the As(III) and As(V) species increased, however 0.05 M showed approximately the same adsorption that 0.1 M. Also, table 15 shows the iron concentration onto the Fe(III)-CB after digestion process. The results were 2.7 ± 0.1 (0.3%) for 0.01 M, and 6.3 ± 0.3 mg/g (0.6%) for 0.05 and 0.1 M. These results showed the addition of more iron onto the chitosan beads synthesis did not show an increased in the arsenic oxyanions adsorption. This could be due to the saturation of iron on the chitosan beads surface. Therefore, the optimum concentration of iron(III) was 0.05 M (0.6%) which was capable of removing a 95% for As(III) and a 99% for As(V) oxyanions.

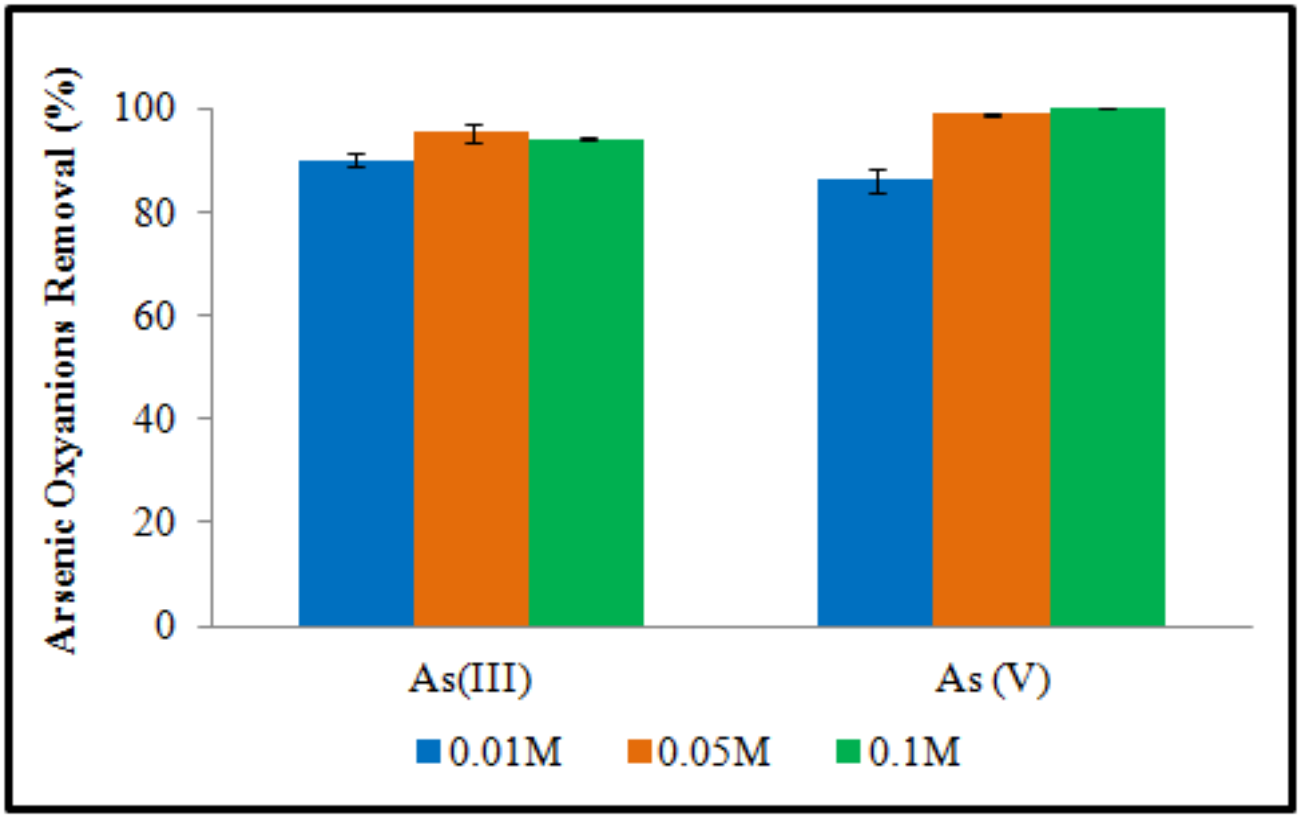

Figure 66: Percentage Removal Comparison of 0.500 mg/L at As(III) and As(V) Oxyanion using 5 g/L of the Fe(III)-CB (0.01, 0.05 and 0.1 M) at pH 6.0.

Table 15: Iron release from 0.01, 0.05 and 0.1 M Fe(III)-CB after digestion process.

Concentration (M)	Iron release (mg/g)
0.01	2.7 ± 0.1
0.05	6.3 ± 0.3
0.1	6.3 ± 0.3

Figure 67 shows the comparison of arsenic oxyanions removal using CB, pure $Fe(OH)_3$, and Fe(III)-CB. Our results showed that CB removes 0% and 26% for As(III) and As(V) oxyanions, respectively. Therefore, it's necessary to disperse iron onto the beads surface to increase the adsorption. The dispersed iron was evaluated in the form of ferric hydroxide at pH 8 to obtain a good adsorption of arsenic oxyanions. The pure $Fe(OH)_3$ showed a removal for As(III) of 99% and 96% for As(V). Finally, the Fe(III)-CB shows a 95% and 99% for As(III) and As(V) oxyanions, respectively. Therefore, these results suggest that the immobilization of ferric hydroxide on the chitosan beads surface is responsible for the adsorption of arsenic oxyanions. We did not use pure $Fe(OH)_3$ because it's a more complex process more due to its need to be filtered, centrifuged, sedimented, and not is practical for its recovery.

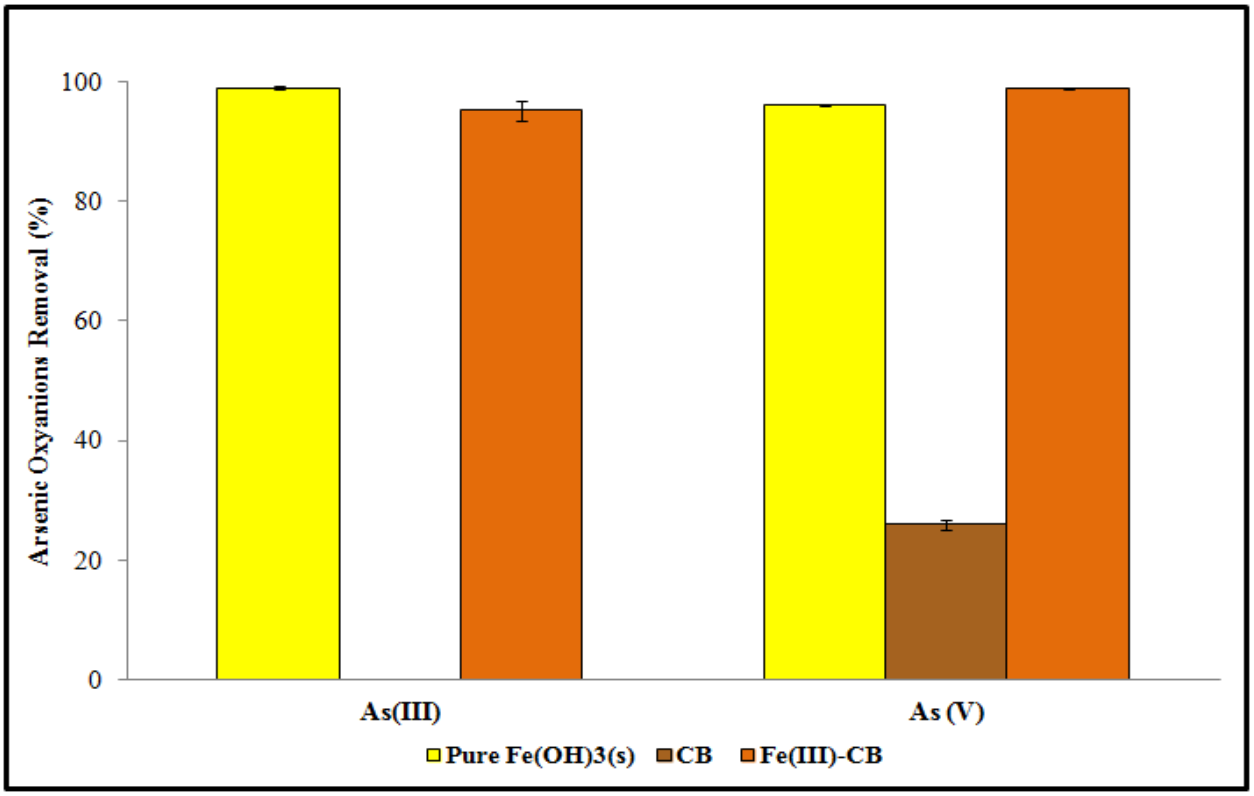

Figure 67: Percentage Removal Comparison of 0.500 mg/L at As(III) and As(V) Oxyanion using 5 g/L of the $Fe(OH)_3$, CB and Fe(III)-CB at pH 6.0.

4.4.1.2 Image Stacking Photography Analysis

Figure 68 shows the image stacking photography of A) $Fe(OH)_3$, B) CB washing, and C) Fe(III)-CB groups. The Fe(III)-CB showed a spherical shape and irregular edges, and an average size of 1.7 ± 0.3 mm (Refer section 4.1.1.1).

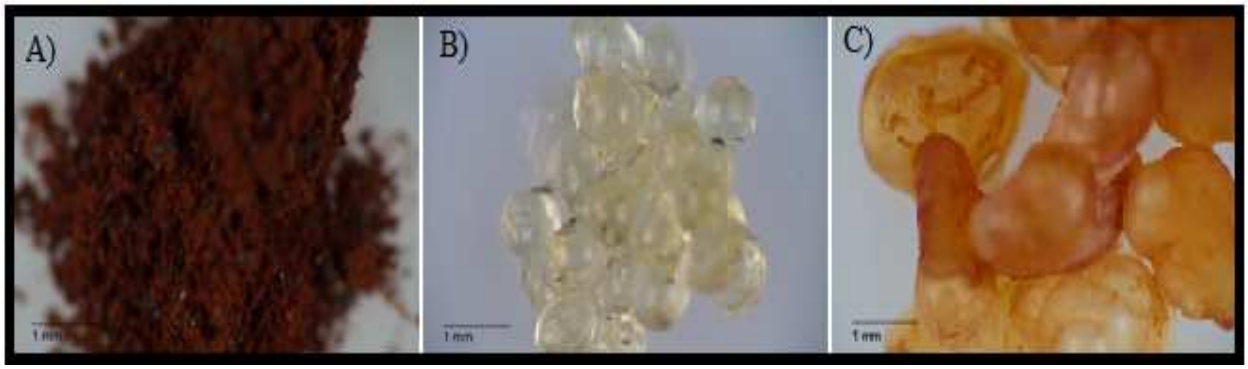

Figure 68: ISP images of (A) $Fe(OH)_3$; (B) CB; and (C) Fe(III)-CB.

4.4.1.3 Scanning Electron Microscopy Analysis

Figures 69-73 show SEM micrographs at A) 30X, B) 1500X and C)7000X magnification of $Fe(OH)_3$, CB washing, Fe(III)-CB, and Fe(III)-CB in contact with Arsenic(III and V) oxyanions solution. The Fe(III)-CB shows a rough surface. The images shown than after of the arsenic oxyanions adsorption, the surface does not show a significant difference compared with Fe(III)-CB without contaminant.

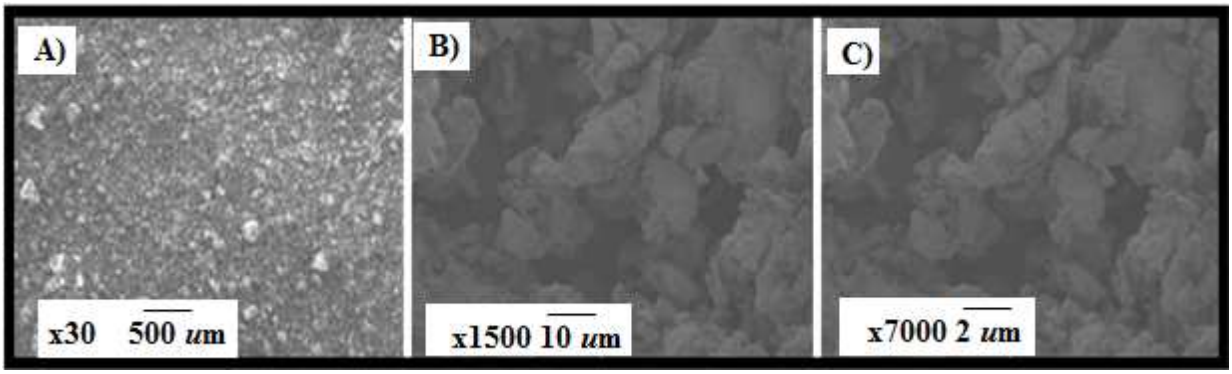

Figure 69: SEM micrograph of $Fe(OH)_3$ at magnification of A) 30X, B) 1500X, and C) 7000X.

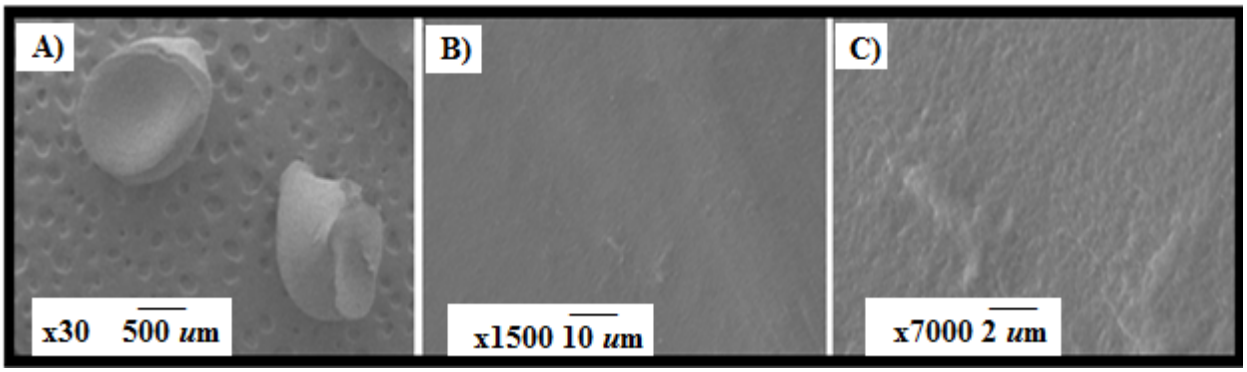

Figure 70: SEM micrograph of CB at magnification of A) 30X, B) 1500X, and C) 7000X.

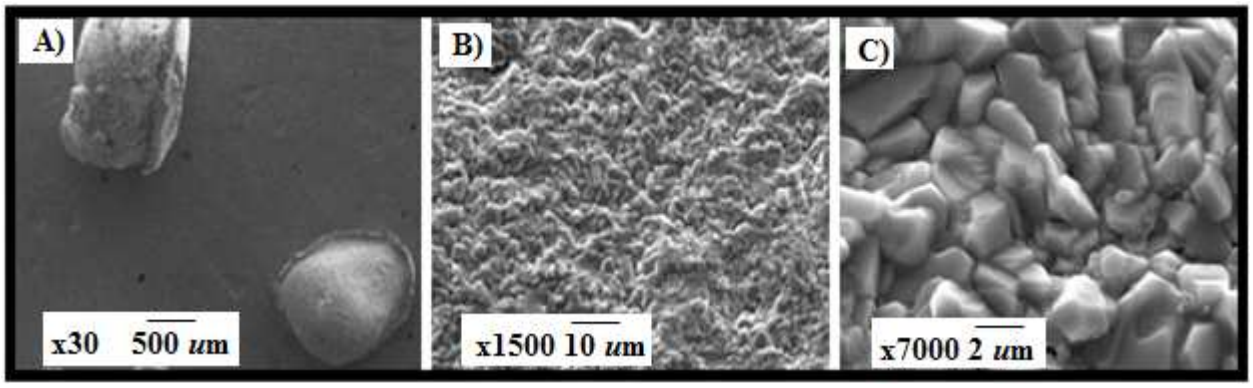

Figure 71: SEM micrograph of Fe(III)-CB at magnification of A) 30X, B) 1500X, and C) 7000X.

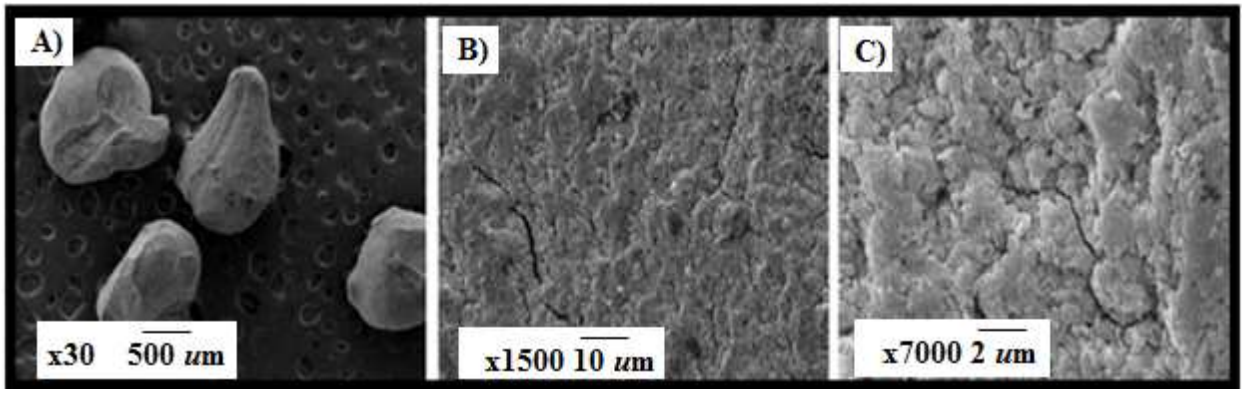

Figure 72: SEM micrograph of As(III) onto Fe(III)-CB at magnification of A) 30X, B) 1500X, and C) 7000X.

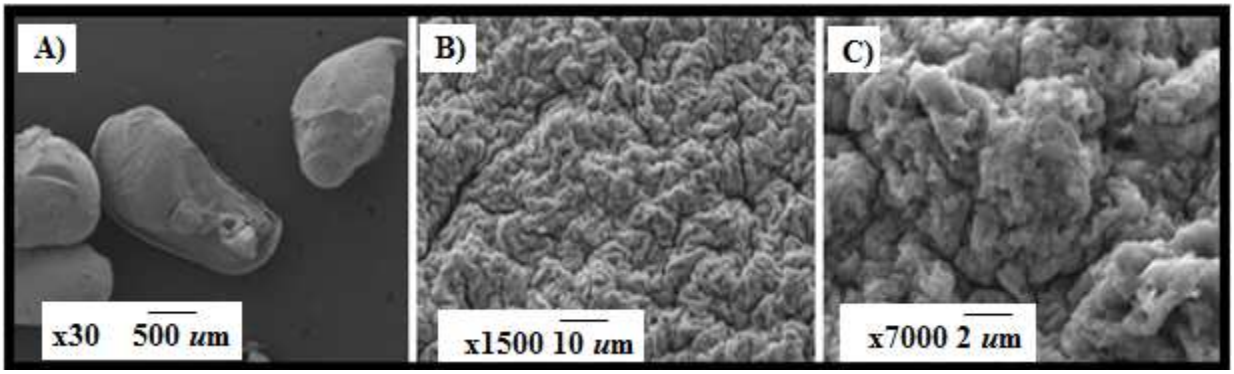

Figure 73: SEM micrograph of As(V) onto Fe(III)-CB at magnification of A) 30X, B) 1500X, and C) 7000X.

4.4.1.4 Infrared Spectroscopy Analysis

FT-IR spectrum of CB, Fe(III)-CB and the Fe(III)-CB in contact with As(III) and As(V) oxyanions is shown in figure 74. The identified functional groups in the spectrum were discussed in section 4.1.1.3. Figures 74C and 74D shows the bands of Fe(III)-CB once exposed to the As(III) and As(V) oxyanion solutions, which showed similar bands in Fe(III)-CB without As oxyanions. No significant differences are observed between the exposed and unexposed beads.

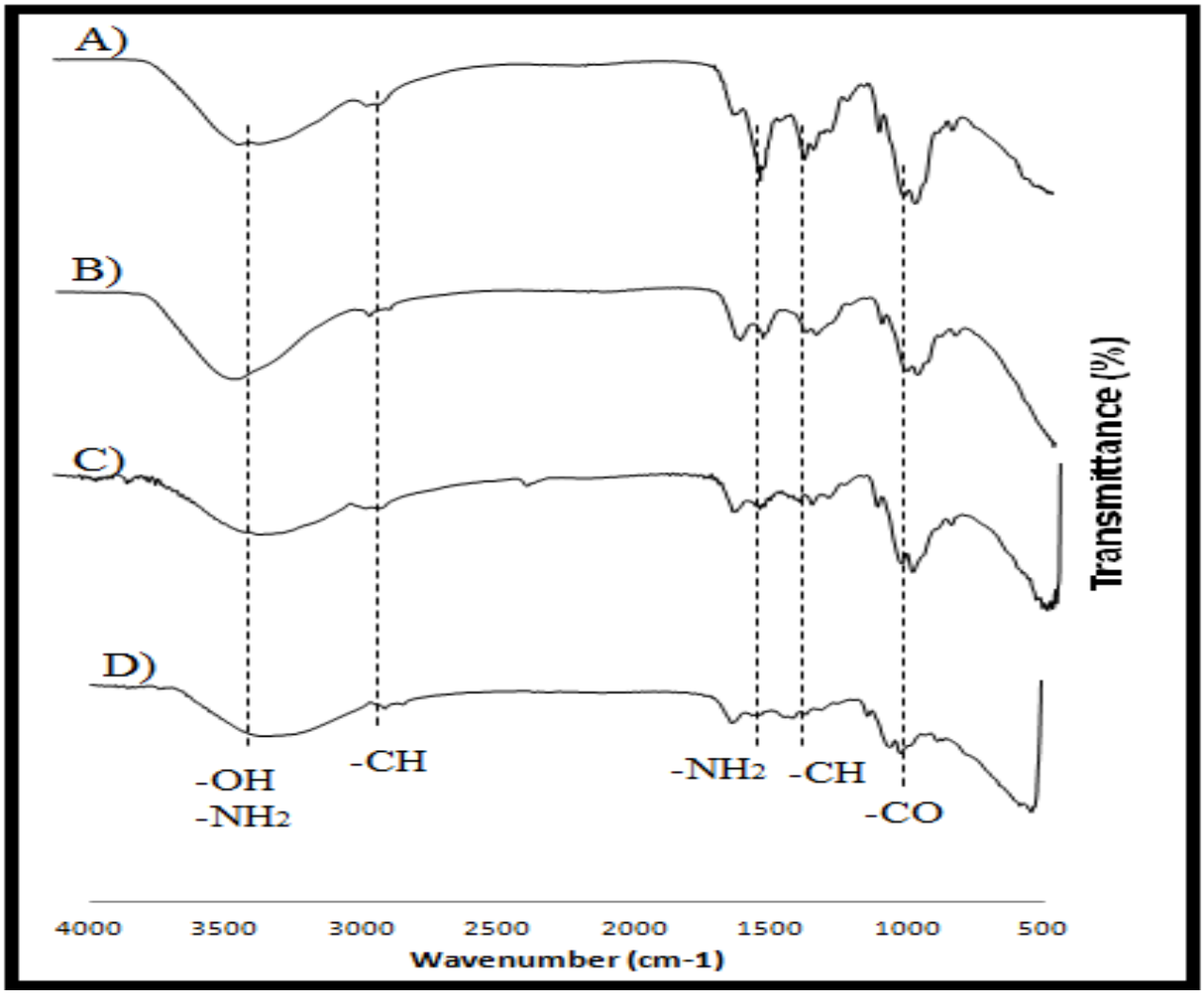

Figure 74: FT-IR images of (A) Chitosan beads, (B) Fe(III)-CB, and Fe(III)-CB in contact with (C) As(III) and (D) As(V).

4.4.1.5 ICP-MS Elemental Analysis

The iron concentration onto the 0.05 M Fe(III)-CB was of 6.3 ± 0.3 mg/g (0.6%) (Refer section 4.4.1.1). In the pH range of 4-10 in aqueous solution, the Fe(III)-CB did not show release of iron into the solution during the adsorption process (Shown in Table 16). Only at pH 2, the Fe(III)-CB showed small release of iron (1.67 mg/g) because it was exposed to a very acidic solution that caused dissolution of iron from the chitosan matrix. These results show that the

beads are stable at diverse pH conditions and are an effective adsorbent for the adsorption process.

Table 16: Elemental Analysis of Fe(III)-CB.

pH aqueous solution	Fe Concentration (mg/g)
2.00	1.67
4.00	0
6.00	0
8.00	0
10.00	0

4.4.2 Adsorption Analysis

Discussed in this section is the adsorption studies for the Arsenic(III and V) oxyanions removal, such as pH aqueous solution, concentration adsorbent, contact time, co-existing anions competence, and adsorption isotherms.

Effect of pH aqueous solution

Figure 75 shows the removal percentages of As(III) and As(V) species (0.5 mg/L) when using chitosan beads immobilized with 0.6% Fe as a function of pH. The removal varied from 85% to 95% for As(III) oxyanion, and from 89-99% for As(V) oxyanion in a pH range of 4 to 10. The obtained results can be attributed to the electrostatic attraction between the positively charged surface of Fe(III)-CB and the anionic As(V) species ($H_2AsO_4^-$ or $HAsO_4^{-2}$), and by ligand exchange. The negative character of the beads surface was confirmed by determining the point of zero charge (pH_{pzc}) of 8.4 for the Fe(III)-CB adsorbent (Refer section 4.1.1.4). Below the pH_{pzc} (8.4) the surface of the beads would be positively charged. The low removal (34%) of As(V) at pH 2 would be due to the formation of neutral species (H_3ASO_4), which do not electrostatically interact with the positively charged beads surface, and the dissolution of ferric hydroxide from the chitosan beads surface. These results suggest that As(III) removal in the pH range of 2-10 was due to the formation of an inner-sphere complex via a ligand exchange mechanism. As(III) exists as a neutral species (H_3AsO_3) at pH< 9.2 and $H_2AsO_3^-$ at pH> 9.2 (Langmuir et al., 2003; Couture and Capellen, 2011). The maximum adsorption for both species was obtained at pH 6.0 with a 95% removal for As(III) and a 99% for As(V), which is an approximate pH for applications in natural and potable water systems.

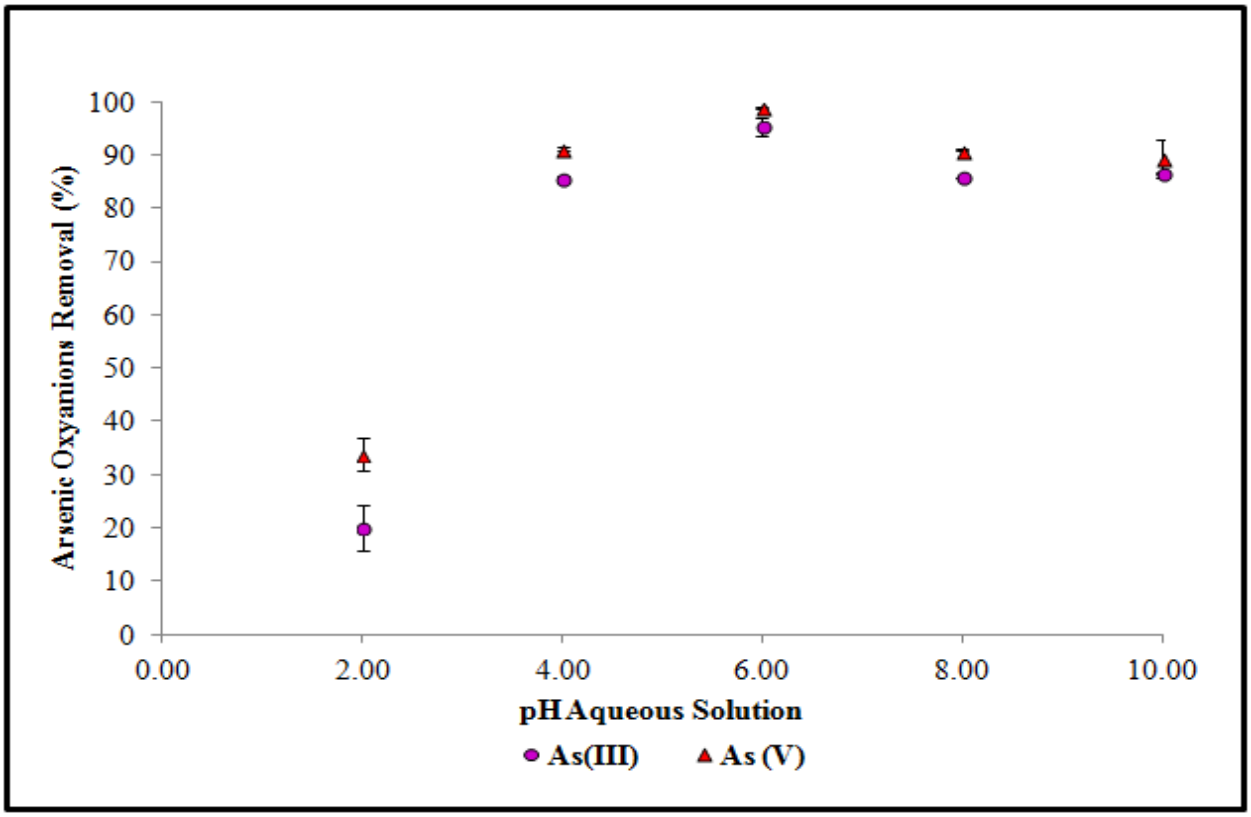

Figure 75: Effect of pH aqueous solutions on the As(III) and As(V) oxyanions adsorption onto Fe(III)-CB. Experimental conditions: initial concentration of arsenic species = 0.500 mg/L; adsorbent concentration = 5 g/L; contact time = 26 h; and shaker speed = 200 rpm.

Effect of adsorbent concentration

The optimum adsorbent concentration studies were carried out by adding 1, 3, 5 and 10 g/L of Fe(III)-CB to the As(III) and As(V) oxyanions solutions of 0.500 mg/L to verify the maximum tolerance limit. Figure 76 shows the removal percentages of As(III) and As(V) as a function of increased adsorbent concentration. For As(III), the results were 60% (1 g/L), 82% (3 g/L), 95% (5 g/L) and 100% (10 g/L). Also, the removal percentages of As(V) were 86% (1 g/L), 95% (3 g/L), 99% (5 g/L) and 100% (10 g/L) showing a similar pattern. As the

concentration of the adsorbent was increased, the percent removed of the As(III) and As(V) species increased showing a maximum removal at 5 g/L. The optimum adsorbent concentration was 5 g/L at pH 6 which was capable of removing 95% of As(III) and 99% for As(V) oxyanions. These results demonstrate that Fe(III)-CB represents an excellent alternative for the removal of As(III and V) species from contaminated aqueous effluents. Our method yielded superior removal percentages than those reported by Ansari and Sadegh (2007), which used a high dose (100 g/L) of activated carbon (the industry standard) at pH 3 and only achieved a removal of As species up to 60%, thus demonstrating that it is not an efficient and cost-effective method for arsenic removal.

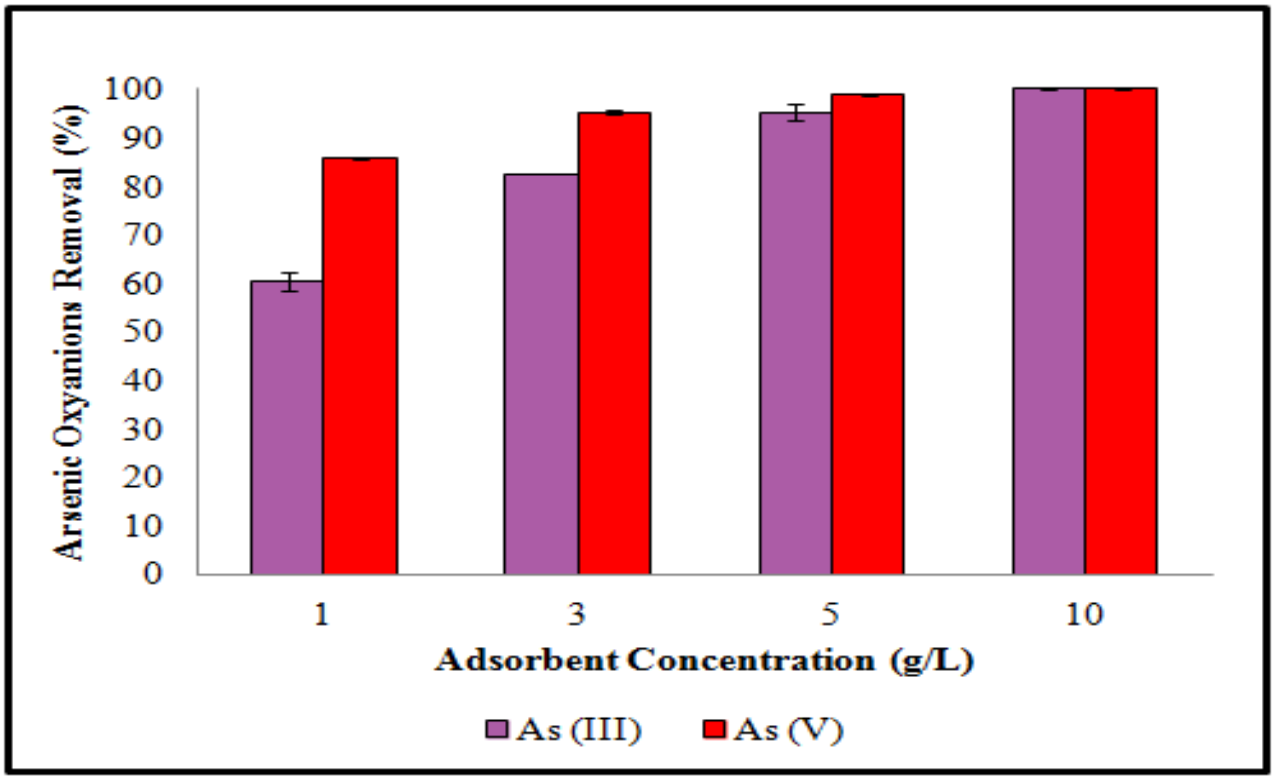

Figure 76: Effect of adsorbent concentration on the As(III) and As(V) oxyanions adsorption onto Fe(III)-CB. Experimental conditions: initial concentration of arsenic species = 0.500 mg/L; contact time = 26 h; shaker speed = 200 rpm; and pH aqueous solutions = 6.0 ± 0.1.

Effect of contact time

The variation of As(III) and As(V) oxyanions onto Fe(III)-CB found by varying contact time, between 0–26 hours, is shown in figure 77. The results show that arsenic oxyanions reached equilibrium approximately after 12 hours with 95% and 99% for As(III) and As(V) oxyanions, respectively. The final concentrations in equilibrium were 0.02 mg/L for As(III) and 0.005 mg/L for As(V). Lower concentrations obtained a final concentration of 0.00 mg/L complying with the regulations of the EPA and WHO. The higher sorption capacity is due to the immobilized iron onto the chitosan beads surface. To observe a constant equilibrium, the optimum contact time was of 26 hours.

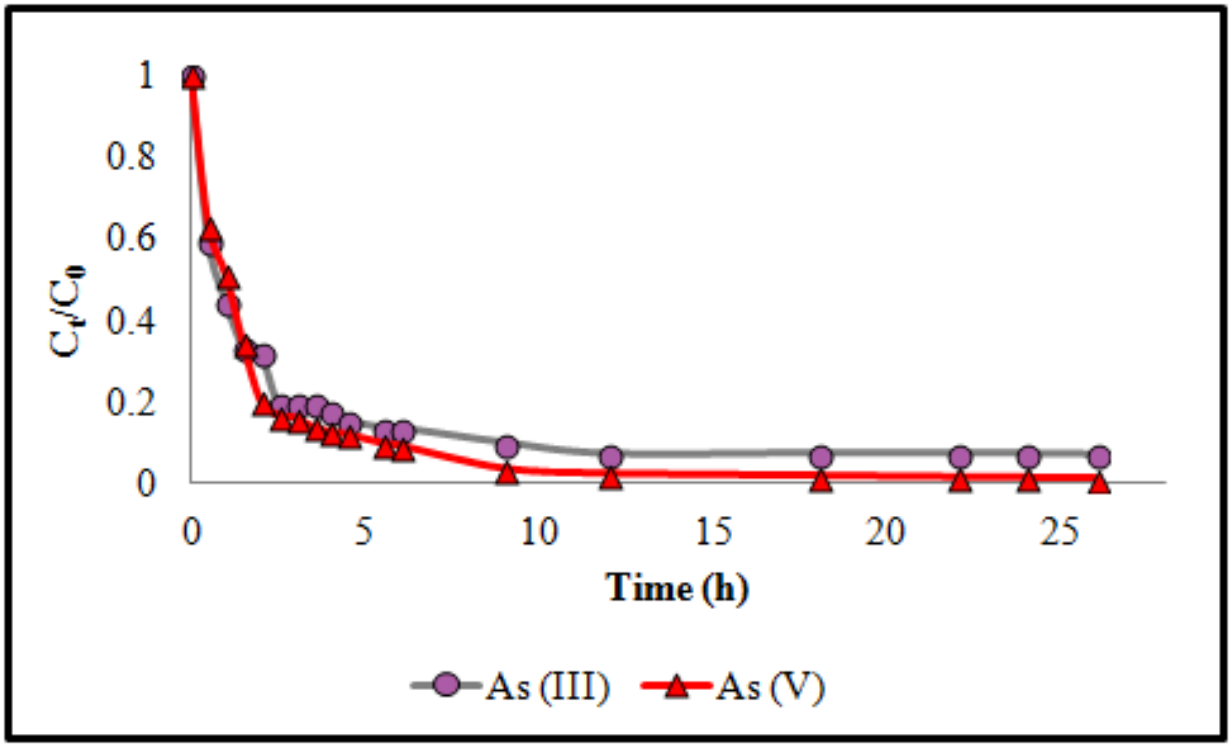

Figure 77: Effect of contact time on As(III) and As(V) oxyanions onto Fe(III)-CB. Experimental conditions: initial concentration of arsenic species = 0.500 mg/L; adsorbent concentration = 5 g/L; shaker speed = 200 rpm; and pH aqueous solutions = 6.0 ± 0.1.

Effect of co-existing anions competence

The effect in the removal of As(III) and As(V) oxyanions in the presence of co-existing anions that are commonly present in natural waters are shown in table 17. The common anions were carbonate, chloride, phosphate and sulfate. The removal percentages of As(III) in presence of chloride were 91%, 92-95% for carbonate, 86-88% for phosphate and 92-93% for sulfate at the evaluated As:CA ratios of 1:20 and 1:30, respectively. The removal efficiency for As(V) in the presence of all co-existing anionic species, at both evaluated As:CA ratios, was 100%. These results show that the co-existence of selected anionic species did not affect the removal of arsenic oxyanions; on the contrary, their presence increased the As removal efficiency from 98.8 to 100%. These results suggest that the adsorption process for As(III) and As(V) proceeded by different mechanisms as discussed above; the results showed that the removal efficiency improved to 100% for As(V) and on the other hand, it slightly decreased (95% to 86%) for the removal of As(III), thus suggesting a different mode of action. It also demonstrated that the Fe(III)-CB adsorbent can be applied to remove contaminants from natural waters containing similar anionic species.

Table 17: Adsorption studies for As(III) and As(V) oxyanions onto 5 g/L of Fe(III)-CB at diverse co-existing anions (CA).

		As(III)	As(V)
	Ratio As:CA (mol:mol)	**% Removal ± SD**	**% Removal ± SD**
	1:0	95.2 ± 2	98.8 ± 0.1
Cl^-	1:20	90.6 ± 0.6	100.0 ± 0
	1:30	90.9 ± 0.2	100.0 ± 0
CO_3^{-2}	1:20	94.5 ± 0.1	100.0 ± 0
	1:30	92.3 ± 1	100.0 ± 0
SO_4^{-2}	1:20	92.5 ± 0.1	100.0 ± 0
	1:30	91.8 ± 0.9	100.0 ± 0
PO_4^{-3}	1:20	88.4 ± 1	100.0 ± 0
	1:30	86.0 ± 1	100.0 ± 0

Adsorption Isotherms

Table 18 shows examples of initial arsenic concentrations used for the adsorption studies using 5 g/L of Fe(III)-CB at pH 6.0. The removal percentages were efficient for arsenic oxyanions, these decreased once the initial concentration increased. The uptake capacity for all arsenic oxyanions increased once the initial concentration increased.

Figure 78 and 79 show the Langmuir and Freundlich isotherm plot and Table 19 shows the results of the isotherm parameters. These show that the isotherm model that best fitted the

adsorption data was the Langmuir model. As it is shown in Table 19, the linear correlation coefficient (R^2) for the Langmuir isotherm was 0.9858 and 0.9637 for As(III) and As(V), respectively. The adsorption capacity (Q^0) for As(III) was 1.48 mg/g and for As(V) it was 2.72 mg/g, indicating a better adsorption capacity for arsenate. The Langmuir constant (b), which obtained a value of 0.36 and 0.23 L/mg for As(III) and As(V), respectively shows that the adsorption process is energetically favorable because it needs less energy to occur. Table 20 shows the dimensionless R_L parameter, which fluctuated between 0.98 - 0.54 for the initial concentration between 0.100 - 5 mg/L for both species, demonstrating that it is a favorable adsorption process. The removal of As(III) and As(V) oxyanions in contact with Fe(III)-CB is attributed to the interaction of the ferric hydroxide surface onto chitosan beads. Table 21 and Table 22 report the adsorption capacity of diverse adsorbents containing chitosan, and other adsorbents, respectively in comparison with our results. Our Fe(III)-CB showed superior adsorption capacity than the majority of published adsorbents including activated carbon based adsorbents. Only two of the 20 published studies shown in tables 21 and 22 are capable of removing As(III) and As(V) and have adsorption capacities that exceeded our Fe(III)-CB (Gupta et al., 2011; Martinson and Reddy, 2009). For example, copper oxide nanoparticles exhibited superior adsorption capacities, but due to their size and possible impact on the environment are not feasible for water treatment applications. In addition, these types of adsorbents are also very expensive, toxics and present complex procedures for their synthesis (Türk and Alp, 2014; Sankararamakrishnan et al., 2014; Martinson and Reddy, 2009; Raven et al., 1998). Fe(III)-CB is cost-effective, reusable, and an environmentally friendly alternative for removing arsenic oxyanions from aqueous solutions.

Table 18: Adsorption results of As(III) and As(V) oxyanions using 5 g/L of Fe(III)-CB at pH 6.0.

	As(III)		As(V)	
Initial concentration (mg/L)	% Removal	Uptake capacity (mg/g)	% Removal	Uptake capacity (mg/g)
0.075	100	0.015	100	0.015
0.1	100	0.02	100	0.01
0.5	95.2	0.10	98.8	0.10
1.5	81.8	0.36	81.2	0.23
3	92	0.52	66.4	0.40
5	52.5	0.53	48	0.45

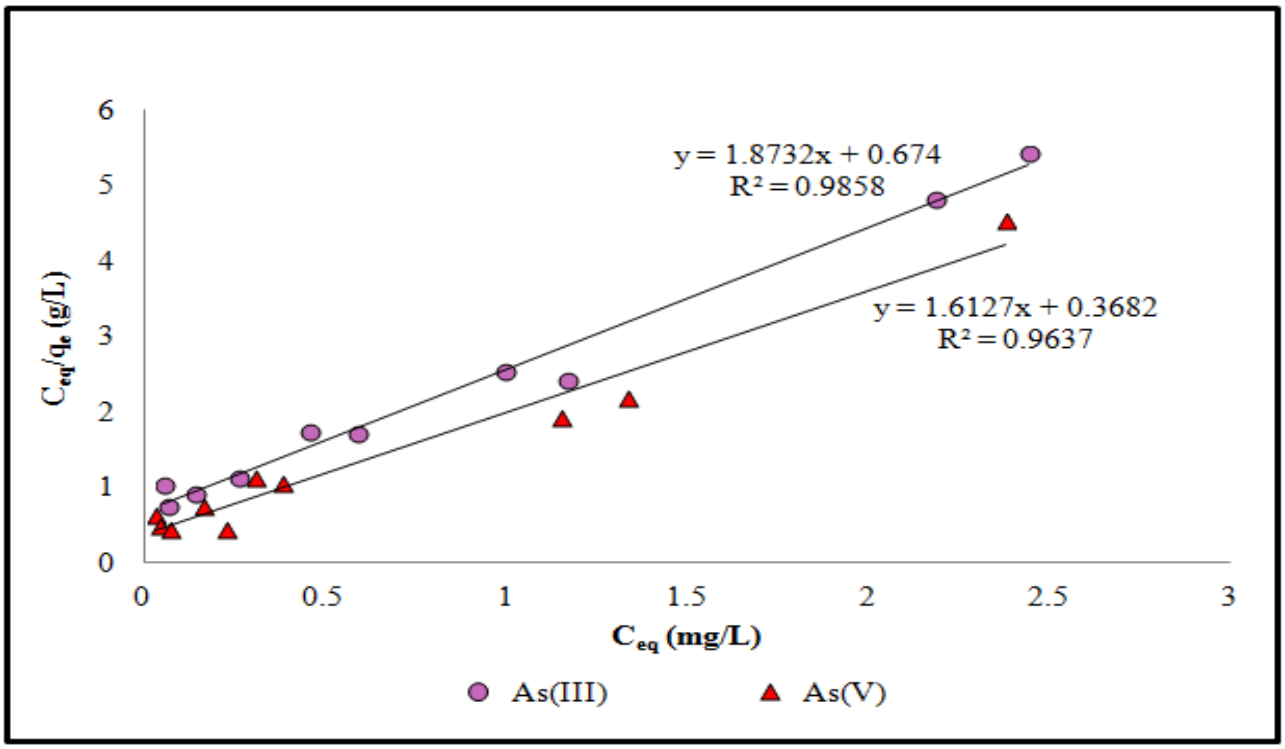

Figure 78: Langmuir isotherm model for As(III) and As(V) oxyanions adsorption onto Fe(III)-CB.

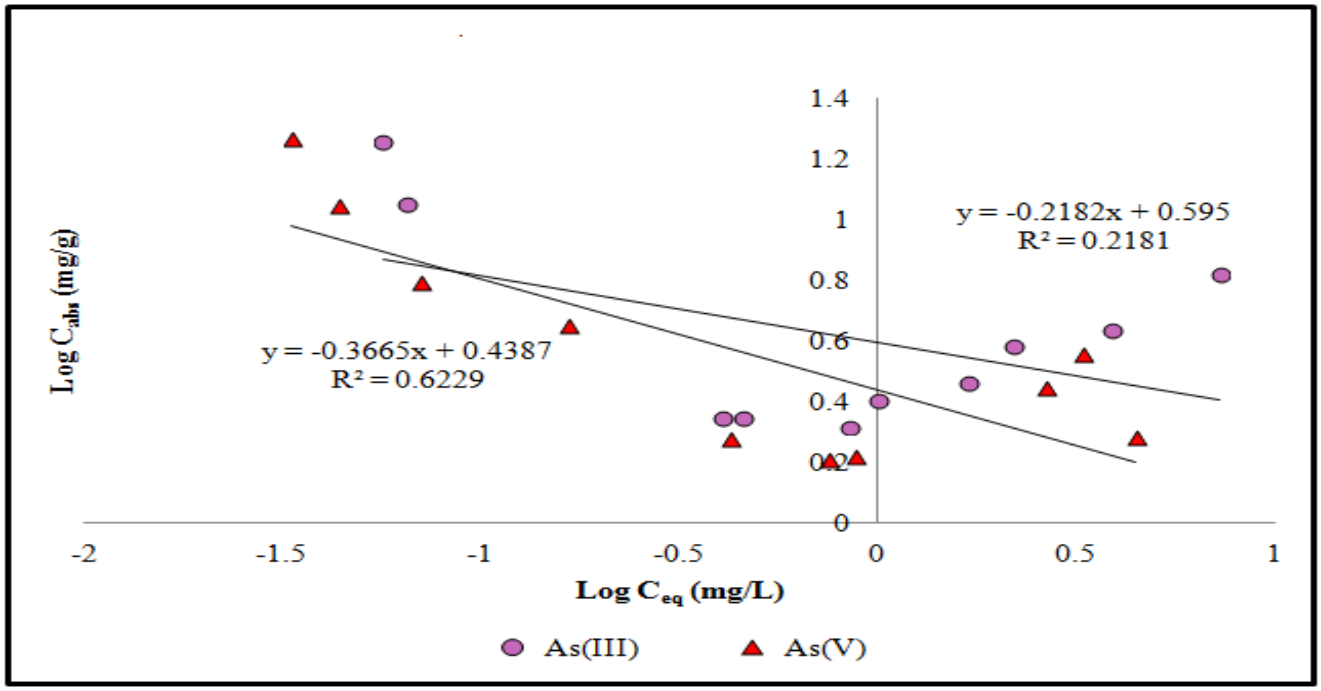

Figure 79: Freundlich isotherm model for As(III) and As(V) oxyanions adsorption onto Fe(III)-CB.

Table 19: Langmuir and Freundlich parameters using 5 g/L of Fe(III)-CB at pH 6.0 for the removal of As(III) and As(V).

		As(III)	As(V)
Langmuir	R^2	0.9858	0.9637
	Q^0 (mg/g)	1.48	2.72
	b (L/mg)	0.36	0.23
Freundlich	R^2	0.2181	0.6229
	K_F (mg/g)(L/mg)^n	1.68	2.28
	n	4.58	2.73
	1/n	0.22	0.37

Table 20: R_L parameter for As(III) and As(V) oxyanions using 5 g/L of PCF at pH 6.0.

	R_L	
Concentration (mg/L)	**As (III)**	**As(V)**
0.1	0.98	0.98
0.5	0.92	0.92
1.0	0.87	0.87
1.5	0.81	0.78
2.0	0.75	0.73
2.5	0.71	0.68
3.0	0.67	0.63
3.5	0.62	0.58
4.0	0.60	0.60
5.0	0.54	0.55

Table 21: Comparison of our results in Q^0 Langmuir parameters with diverse chitosan based sorbents.

Sorbent	Q^0 (mg/g) As (III)	Q^0 (mg/g) As (V)	Reference
Fe(III)-CB	1.48	2.72	Padilla et al., 2014
CTS Resins	3.70	-	Liu et al., 2012
Chitosan sand	17	23	Gupta et al., 2011
CH-Fe	2.78	-	Santos et al., 2011
Iron impregnated chitosan	2.0	-	Gang et al., 2010
Chitosan	-	0.730	Gérente et al., 2010
ICB*	2.32	2.24	Gupta et al, 2009

*ICB (Iron chitosan beads)

Table 22: Comparison of our results in Q^0 Langmuir parameters with other reported sorbents in previous studies.

Sorbent	Q^0 (mg/g) As (III)	Q^0 (mg/g) As (V)	Reference
Fe(III)-CB	1.48	2.72	Padilla et al., 2014
M-FeHT[a]	0.121	1.28	Türk and Alp 2014
MWCNT[b]	0.124	0.373	Sankararamakrishnan et al., 2014
F400-M[c]	-	0.847	Vitela and Rangel 2013
IAC-Fe(II)[d]	-	2.023	Tuna et al., 2013
IAC-Fe(III)[d]	-	3.009	Tuna et al., 2013
Fe(III)-CAB	0.117	0.364	Sánchez et al., 2012
Fe_3O_4 nanoparticle	-	0.400	Akin et al., 2012
p(4-VP)-HCl bulk hydrogel	-	23.26	Sahiner et al., 2011
Iron activated carbon	-	0.024	Ghanizadeh et al., 2010
Cupric oxide nanoparticle	26.9	22.6	Martinson and Reddy 2009
Granulated activated carbon	0.0811	0.2624	Mondal et al., 2008
Magnetite alginate beads	-	6.75	Lim and Chen 2007
Siderite and hematite	-	0.202	Guo et al., 2007
Activated carbon	0.21	-	Budinova et al., 2006
Ferrihydrite	0.58	0.16	Raven et al., 1998

[a]Fe-hydrotalcite-supported magnetite nanoparticles

[b]Multiwalled carbon nanotubes

[c]Activated carbon with iron(hydroxide) nanoparticle

[d]Loaded Activated carbon-Fe(II), LoadedActivated carbon-Fe(III)

Adsorption Mechanism

The results suggest that the main mechanism for As(III) and As(V) oxyanions is adsorption onto the ferric hydroxide surface of the chitosan beads (shown in Figure 80). Thus, the adsorption occurred with the formation of an outer-sphere complex which primarily involved the electrostatic attraction interactions of the As(V) oxyanion with the adsorbent and inner-sphere complex via ligand exchange. The adsorption for As(III) occurred by an inner-sphere complex which involved the ligand exchange mechanism. The outer-sphere complexes involve a water molecule between the metal ion and ligand or surface. Van der Waals forces and electrostatic interactions are including in outer-sphere complexes. On the other hand, an inner-sphere complex involves ligand exchange mechanism, covalent bonding and hydrogen bonding. These do not form a water molecule between the metal ion and ligand or surface. Both can occur simultaneously and various environmental factors (pH, ionic strenght, type of adsorbent, and another) can affect the system. Outer-sphere complexes are weaker and are a far more rapid process compared to inner-sphere complexes (Sparks, 2003). Figure 81 show an example of outer and inner-sphere complexes (Cheng et al., 2009).

$$3H_2AsO_4^-{}_{(ac)} + Fe(OH)_{3(s)} \longrightarrow Fe(H_2AsO_4)_{3(s)} + 3OH^-$$

$$3H_3AsO_{3(ac)} + Fe(OH)_{3(s)} \longrightarrow Fe(H_2AsO_3)_{3(s)} + 3H_2O$$

Figure 80: Mechanism of the interactions of Fe(III)-CB with arsenic oxyanions

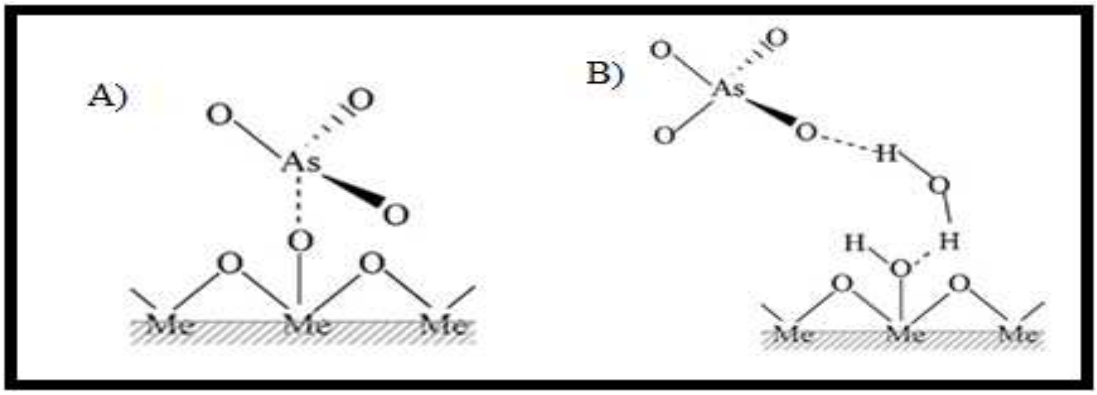

Figure 81: A) Inner-sphere and B) Outer-sphere complexes for arsenate.

(Cheng et al., 2009)

4.4.4 Desorption Analysis

Figure 82 shows the results for the desorption percentages of As(III) and As(V) in the Fe(III)-CB when using 0.1 and 1 M of HNO_3, HCl, H_2SO_4 and NaOH. The desorption results for As(III) were 52% for 0.1 M HNO_3,73% for 0.1 M HCl, and a 100% for 1 M HCl and 0.1 M and 1 M H_2SO_4 and NaOH. In addition, As(V) showed a desorption percentage of 60-75% for 0.1 M HNO_3 and a 100% for 0.1 M and 1 M HCl, H_2SO_4 and NaOH. The NaOH was the only eluent that maintained the integrity of the Fe(III)-CB. On the other hand, when acids were used for the desorption tests, 100% of the original acid was released in the solution leaving the surface of the chitosan beads free of iron and therefore not feasible for reuse. The method of fixation or stabilization could also be used once the contaminats are desorbed for the adsorbent as explained in the section 4.2.3.

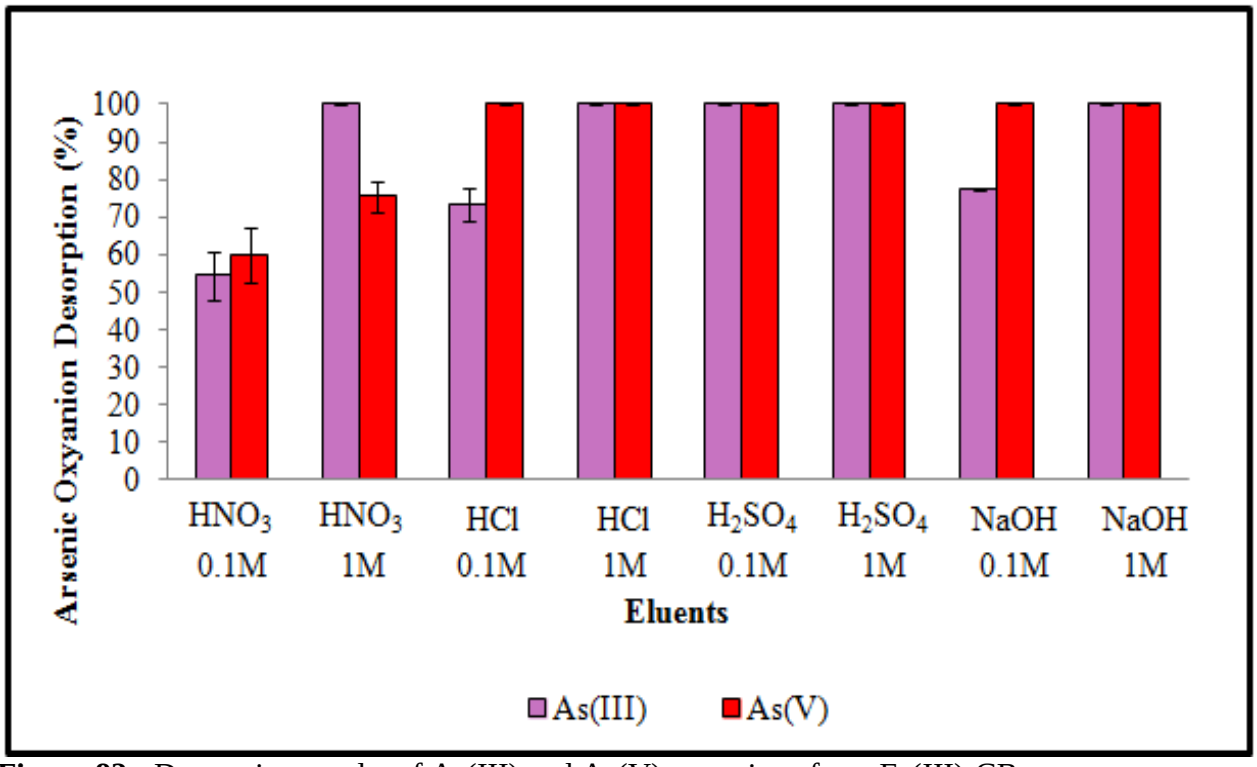

Figure 82: Desorption results of As(III) and As(V) oxyanions from Fe(III)-CB.

*Percentage determined on the total adsorption of the As species.

4.4.5 Adsorption/Desorption Cycles Analysis

Figures 83 to 86 show the adsorption and desorption percentages of As(III) and As(V) using sodium hydroxide (0.1 and 1M) as the eluent during five consecutive adsorption/desorption cycles. As(III) removal in cycle 1-3 was approximately 96% and decreased to 89% from cycle 4-5 when using 0.1M NaOH. In contrast, when using 1 M of NaOH, the As(III) removal percentage for cycle 1 was 96% and decreased during cycles 2-5 to approximately 80%. Desorption removal of As(III) was 100% for both concentrations of sodium hydroxide. As(V) removal in cycle 1 was 95%, but successively decreased approximately to 73% for 0.1 M NaOH and to 44% for 1 M NaOH. The desorption removal of As(V) was 100% for 1M NaOH in all cycles and it was 100% for 0.1 M NaOH in cycle 1-4 and decreased in cycle 5 to 82%. The decreased efficiency of adsorption of the Fe(III)-CB is attributed to the partial loss (0-0.1%) of Fe from the Fe(III)-CB matrix.

The desorption of As species from the Fe(III)-CB matrix is probably due to the displacement of As ions to form $Fe(OH)_3$ inside the bead matrix. When the pH of the solution is adjusted back to 6.0, the $Fe(OH)_3$ is dissolved and the Fe(III)-CB is regenerated. These results show that Fe(III)-CB is an effective reusable sorbent material to remove arsenic oxyanions from aqueous solutions at a trace levels especially when using 0.1M NaOH as the eluent (shown in figures 83 and 84).

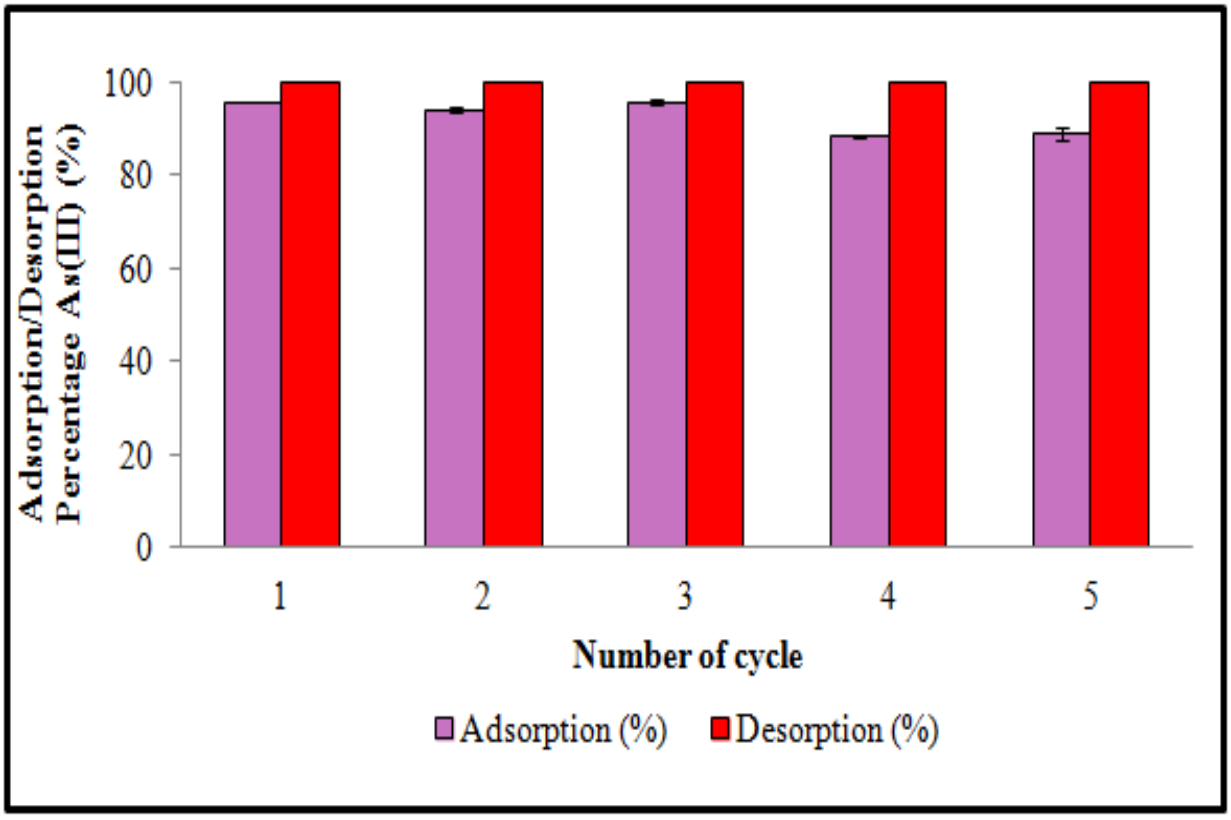

Figure 83: Adsorption/Desorption cycles of As(III) from Fe(III)-CB using NaOH 0.1 M as eluent for desorption.

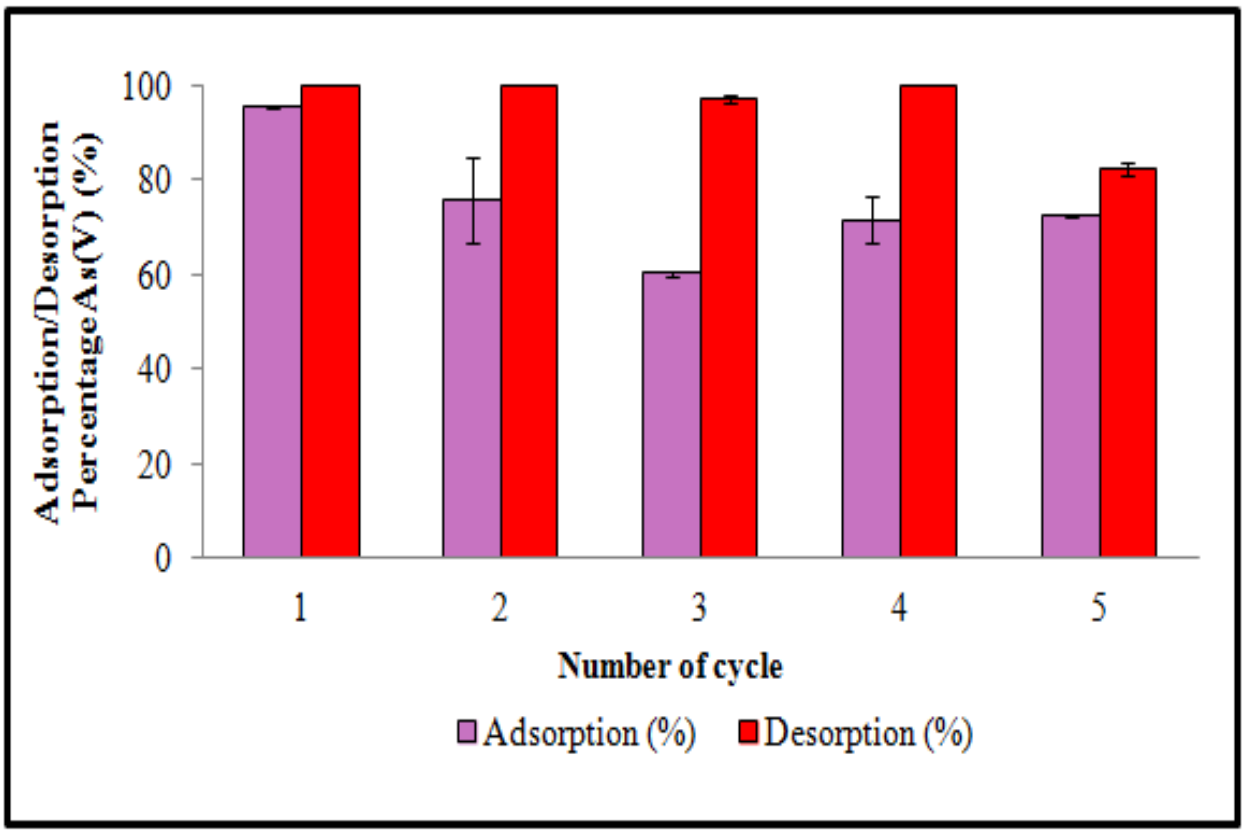

Figure 84: Adsorption/Desorption cycles of As(V) from Fe(III)-CB using NaOH 0.1 M as eluent for desorption.

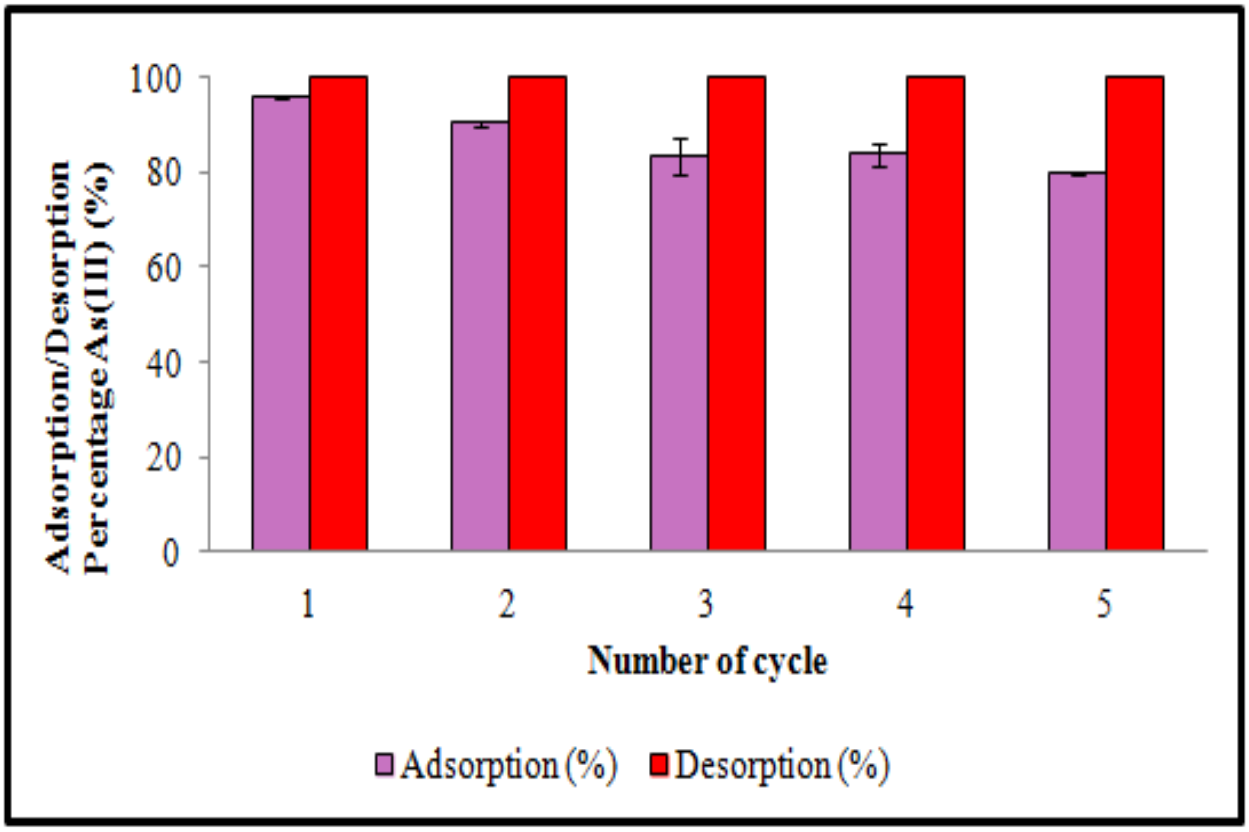

Figure 85: Adsorption/Desorption cycles of As(III) from Fe(III)-CB using NaOH 1 M as eluent for desorption.

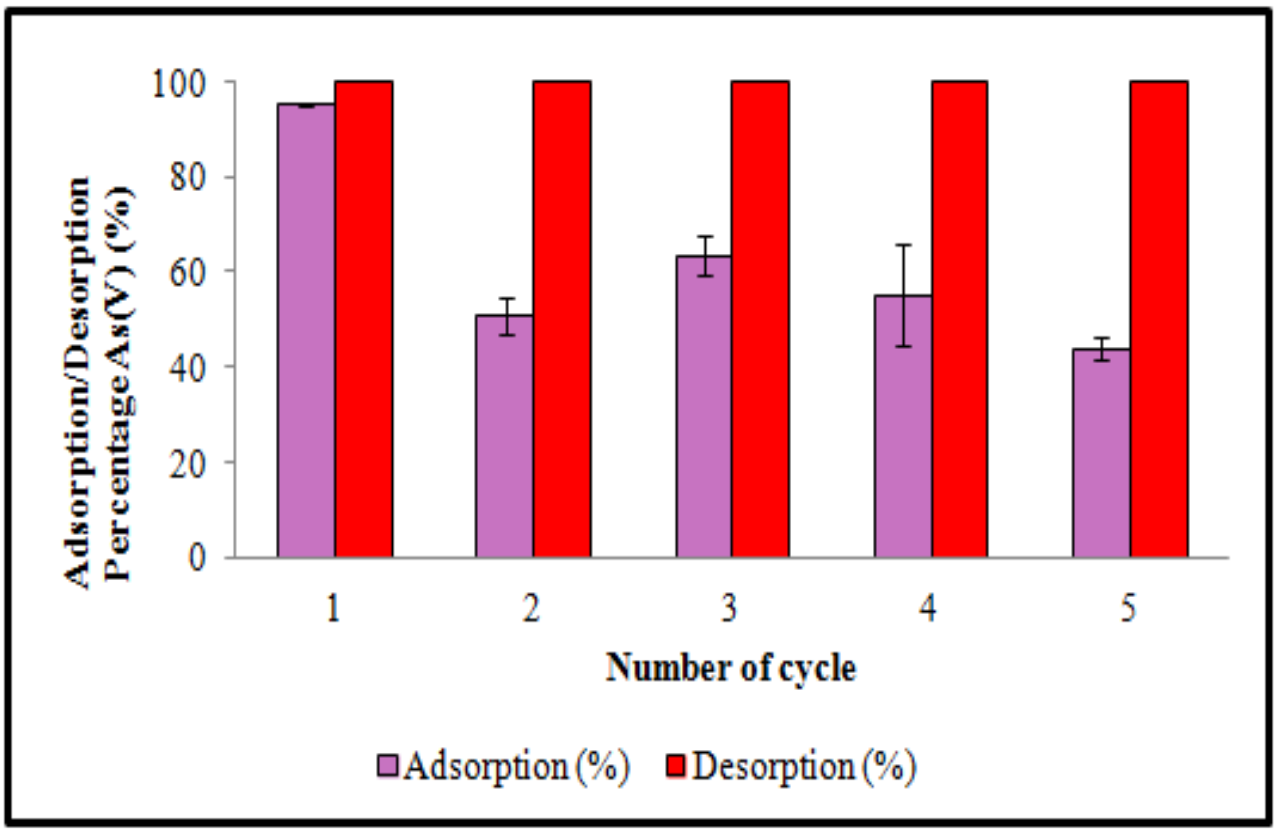

Figure 86: Adsorption/Desorption cycles of As(V) from Fe(III)-CB using NaOH 1 M as eluent for desorption.

5 CONCLUSIONS

The general conclusions of this study are described below:

The different adsorbent containing chitosan such as CB, CB-GLA, CB-DMSA, CF-NAC, PCF and Fe(III)-CB were synthesized successfully. ISP and SEM analysis confirmed that the PCF and CF-NAC morphology displays an irregular shape and are non-porous. CB, CB-DMSA, CB-GLA and Fe(III)-CB showed to be morphologically spherical and slightly roughened. FT-IR measurements confirmed the functional groups present in chitosan structure such as -OH, $-NH_2$, -CH, $-CH_2$ and -CO groups. TGA analysis showed that the beads or flakes are stable in high temperatures up to 300˚C. BET and Langmuir measurements showed that the beads or flakes have an average surface area of 0.27 to 2.99 m^2/g and 0.28 to 14.7 m^2/g, respectively. The swelling effect showed that the different chitosan beads/flakes are stable for the adsorption process.

PCF showed be an efficient adsorbent for the removal of V(III), V(IV), V(V) and As(V) oxyanions at trace levels from aqueous solutions due to the electrostatic attraction between the positively charged PCF and the negatively charged oxyanions. The optimum conditions for all the oxyanions were at pH 6.0 and 5 g/L adsorbent concentration reaching equilibrium at approximately 26 hours. LA-ICP-MS and XRF techniques qualitatively confirmed the presence of V(III), V(IV), V(V) and As(V) onto the PCF surface. The removal percentage of the vanadium oxyanions onto PCF was found to be 99-100% at optimum conditions, while the CB showed only 4-18% at initial concentration of 0.500 mg/L. Also, for As(V) oxyanion was a 97% using PCF, while with CB was only 1% of removal at initial concentration of 0.500 mg/L. PCF removed V(III), V(IV) and V(V) oxyanions selectively in

the presence of co-existing anions (chloride, carbonate, sulfate and phosphate) without a considerable effect in the percentage removal, however As(V) was slightly affected by the addition of co-existing anions. The Langmuir isotherm showed the best fit for V(III) (R^2= 0.99), V(IV) (R^2= 0.96), V(V) (R^2= 0.99), and As(V) (R^2= 0.97) oxyanions using PCF as adsorbent. The maximum adsorption capacity (Q^0) were 12.22, 6.50, 2.58 and 5.43 mg/g for V(III), V(IV), V(V) and As(V), respectively. Desorption studies have shown that the vanadium species are more easily recovered by the addition of hydrochloridic acid 1 M and for As(V) species using nitric acid 1 M due to the formation of neutral species. The best desorption for all oxyanions species (V(III), V(IV), V(V) and As(V)) was achieved using sodium hydroxide due to the neutralization of the amine, thus destroying the electrostatic interactions.

Fe(III)-CB was an excellent adsorbent for the removal of As(III) and As(V) oxyanions from aqueous solution with a 95% and 99%, respectively at initial arsenic concentration of 0.500 mg/L. The optimum conditions were at pH 6.0 and 5 g/L of adsorbent concentration by 26 hours. Fe(III)-CB removed arsenic oxyanions selectively in the presence of other common anions (chloride, carbonate, sulfate and phosphate) without a considerable effect in the percentage removal. The Langmuir isotherm was the best model for fitting the adsorption data for As(III) (R^2= 0.99) and As(V) (R^2= 0.96) using Fe(III)-CB as adsorbent. The maximum adsorption capacity (Q^0) were 1.48 and 2.72 mg/g for As(III) and As(V), respectively. The main mechanism of adsorption for As(V) were electrostatic attractions and ligand exchange with the adsorbent; and for the As(III) it was the complex formation in a ligand exchange between the As(III) and the Fe(III)-CB. The desorption studies showed that the arsenic oxyanions using Fe(III)-CB as an adsorbent are easily recovered by basic eluents

or acids and have the capability to be reused for several cycles if basic solutions are used as eluents.

In general, PCF and Fe(III)-CB are an effective, selective, inexpensive, stable, non-toxic and environmentally friendly material for V(III), V(IV), V(V), As(III) and As(V) oxyanions removal at trace levels from aqueous solutions and can be used to remove other anions with great potential to be used to remediate natural and drinking water.

6 REFERENCES

1. "Arsenic in Your Food | Consumer Reports Investigation". Consumerreports.org. 2012-11-01. Retrieved 2013-08-21.

2. Arsenic in drinking water, Office of ground water and drinking water, EPA **2007**, http://www.epa.gov//safewater/arsenic.html.

3. The drinking water contaminant candidate list. U.S. Environmental Protection Agency **2009**. Fed Regist 74:194. http://www.gpoaccess.gov/fr/index.html.

4. "Monographs Evaluating Carcinogenic Risks to Humans". International Agency for Research on Cancer, Lyon. (IARC) **2006**, *86*.

5. "Oral Exposure to Tetravalent and Pentavalent Vanadium Compounds. Supporting Nomination for Toxicological". Evaluation by the National Toxicology Programs. NTP **2008**, http://ntp.niehs.nih.gov/.

6. "Technologies and Costs for Removal of Arsenic from Drinking Water". EPA **2000**, www.epa.gov/safewater.

7. "Toxicological Profile for Vanadium". U.S. Department of Health and Human Services. Atlanta, Georgia. ATSDR **2012**, http://www.atsdr.cdc.gov.

8. AbdElhady, M., Preparation and characterization of chitosan/zinc oxide nanoparticles for imparting antimicrobial and UV protection to cotton fabric. *International Journal of Carbohydrate Chemistry* **2012**, Article ID 840591, 6 pages, doi:10.1155/2012/840591.

9. Adriano, W.; Veredas, V.; Santana, C.; Gonçalves, L., Adsorption of amoxicillin on chitosan beads: Kinetics, equilibrium and validation of finite bath models. *Biochemical Engineering Journal* **2005**, *27* (2), 132-137.

10. Akin, I.; Arslan, G.; Tor, A.; Ersoz, M.; Cengeloglu, Y., Arsenic (V) removal from underground water by magnetic nanoparticles synthesized from waste red mud. *Journal of Hazardous Materials* **2012**, *235*, 62-68.

11. Al Anbari, R. H.; Albaidani, J.; Alfatlawi, S. M.; Al-Hamdani, T. A., Removal of Heavy Metals from Industrial Water using Electro-Coagulation Technique. *Twelfth International Water Technology Conference, IWTC12* ***2008*** *Alexandria, Egypt.*

12. Alagumuthu, G.; Sumathi, T., Removal of As(V) in Drinking Water by using Moringa Oleifera, *International Journal of Research in Environmental Science and Technology* **2012**, *2* (4), 108-113.

13. Albarghouthi, M.; Fara, D. A.; Saleem, M.; El-Thaher, T.; Matalka, K.; Badwan, A., Immobilization of antibodies on alginate-chitosan beads. *International Journal of Pharmaceutics* **2000**, *206* (1), 23-34.

14. Amin, M. N.; Kaneco, S.; Kitagawa, T.; Begum, A.; Katsumata, H.; Suzuki, T.; Ohta, K., Removal of arsenic in aqueous solutions by adsorption onto waste rice husk. *Industrial & Engineering Chemistry Research* **2006**, *45* (24), 8105-8110.

15. An, B.; Liang, Q.; Zhao, D., Removal of arsenic (V) from spent ion exchange brine using a new class of starch-bridged magnetite nanoparticles. *Water Research* **2011**, *45* (5), 1961-1972.

16. Ansari, R.; Sadegh, M., Application of activated carbon for removal of arsenic ions from aqueous solutions. *Journal of Chemistry* **2007**, *4* (1), 103-108.

17. Appel, C.; Ma, L. Q.; Dean Rhue, R.; Kennelley, E., Point of zero charge determination in soils and minerals via traditional methods and detection of electroacoustic mobility. *Geoderma* **2003,** *113* (1), 77-93.

18. Aranaz, I.; Mengíbar, M.; Harris, R.; Paños, I.; Miralles, B.; Acosta, N.; Galed, G.; Heras, Á., Functional characterization of chitin and chitosan. *Current Chemical Biology* **2009**, *3* (2), 203-230.

19. Asadullah, M.; Jahan, I.; Ahmed, M. B.; Adawiyah, P.; Malek, N. H.; Rahman, M. S., Preparation of microporous activated carbon and its modification for arsenic removal from water. *Journal of Industrial and Engineering Chemistry* **2013**, *20* (3), 887-896.

20. Awual, M. R.; El-Safty, S. A.; Jyo, A., Removal of trace arsenic (V) and phosphate from water by a highly selective ligand exchange adsorbent. *Journal of Environmental Sciences* **2011**, *23* (12), 1947-1954.

21. Awual, M. R.; Shenashen, M.; Yaita, T.; Shiwaku, H.; Jyo, A., Efficient arsenic (V) removal from water by ligand exchange fibrous adsorbent. *Water Research* **2012**, *46* (17), 5541-5550.

22. Aydin, I.; Aydin, F.; Hamamci, C., Vanadium fractions determination in asphaltite combustion waste using sequential extraction with ICP-OES. *Microchemical Journal* **2013**, *108*, 64-67.

23. Azlan, K.; Wan Saime, W. N.; Lai Ken, L., Chitosan and chemically modified chitosan beads for acid dyes sorption. *Journal of Environmental Sciences* **2009**, *21* (3), 296-302.

24. Babiker, E. E. Effect of chitosan conjugation on the functional properties and bactericidal activity of gluten peptides. *Food Chemistry* **2002**, *79*, 367-372.

25. Balan, V.; Verestiuc, V., Strategies to improve chitosan hemocompatibility: A review. *European Polymer Journal* **2014**, *53*, 171-188.

26. Balasubramanian, N.; Kojima, T.; Basha, C. A.; Srinivasakannan, C., Removal of arsenic from aqueous solution using electrocoagulation. *Journal of Hazardous Materials* **2009**, *167* (1), 966-969.

27. Bhakat, P.; Gupta, A.; Ayoob, S.; Kundu, S., Investigations on arsenic (V) removal by modified calcined bauxite. *Colloids and Surfaces A: Physicochemical and Engineering Aspects* **2006**, *281* (1), 237-245.

28. Bhatnagar, A.; Sillanpää, M., Applications of chitin- and chitosan-derivatives for the detoxification of water and wastewater — A short review. *Advanced Colloid Interface Sciences* **2009**, *152*, 26-38.

29. Bhatnagar, A.; Minocha, A. K.; Pudasainee, D.; Chung, H.-K.; Kim, S.-H.; Kim, H.-S.; Lee, G.; Min, B.; Jeon, B.-H., Vanadium removal from water by waste metal sludge and cement immobilization. *Chemical Engineering Journal* **2008**, *144* (2), 197-204.

30. Blagg, A. Synthesis and Thermo-Mechanical Characterization of Bare and Composite Films. MS Thesis **2012**. University of Puerto Rico at Mayagüez.

31. Bocanegra, O. C.; Bocanegra, E. M.; Alvarez, A. A. In *Arsénico en aguas subterráneas: su impacto en la Salud*, XXXII IAH and VI ALHSUD CONGRESS "Aguas Subterráneas y Desarrollo Humano". Mar del Plata, **2002**, 21-27.

32. Boddu, V. M.; Abburi, K.; Talbott, J. L.; Smith, E. D.; Haasch, R., Removal of arsenic (III) and arsenic (V) from aqueous medium using chitosan-coated biosorbent. *Water Research* **2008**, *42* (3), 633-642.

33. Boyacı, E.; Eroğlu, A. E.; Shahwan, T., Sorption of As (V) from waters using chitosan and chitosan-immobilized sodium silicate prior to atomic spectrometric determination. *Talanta* **2010**, *80* (3), 1452-1460.

34. Budinova, T.; Petrov, N.; Razvigorova, M.; Parra, J.; Galiatsatou, P., Removal of arsenic (III) from aqueous solution by activated carbons prepared from solvent extracted olive pulp and olive stones. *Industrial & Engineering Chemistry Research* **2006**, *45* (6), 1896-1901.

35. Bundschuh, J.; Farias, B.; Martin, R.; Storniolo, A.; Bhattacharya, P.; Cortes, J.; Bonorino, G.; Albouy, R., Groundwater arsenic in the Chaco-Pampean plain, Argentina: case study from Robles county, Santiago del Estero province. *Applied Geochemistry* **2004**, *19* (2), 231-243.

36. Chatterjee, S.; Lee, D. S.; Lee, M. W.; Woo, S. H., Nitrate removal from aqueous solutions by cross-linked chitosan beads conditioned with sodium bisulfate. *Journal of Hazardous Materials* **2009**, *166* (1), 508-513.

37. Chen, C.-C.; Chung, Y.-C., Arsenic removal using a biopolymer chitosan sorbent. *Journal of Environmental Science and Health Part A* **2006**, *41* (4), 645-658.

38. Chen, C.-Y.; Chang, T.-H.; Kuo, J.-T.; Chen, Y.-F.; Chung, Y.-C., Characteristics of molybdate-impregnated chitosan beads (MICB) in terms of arsenic removal from water and the application of a MICB-packed column to remove arsenic from wastewater. *Bioresource Technology* **2008**, *99* (16), 7487-7494.

39. Chen, W.; Parette, R.; Zou, J.; Cannon, F.S.; Dempsey, B.A. Arsenic removal by iron-modified activated carbon. *Water Research* **2007**, *41*, 1851 – 1858.

40. Cheng, H.; Hu, Y.; Luo, J.; Xu, B.; Zhao, J., Geochemical processes controlling fate and transport of arsenic in acid mine drainage (AMD) and natural systems. *Journal of Hazardous Materials* **2009**, *165*, 13–26.

41. Chio, C.-P.; Yuan, T.-H.; Shie, R.-H.; Chan, C.-C., Assessing vanadium and arsenic exposure of people living near a petrochemical complex with two-stage dispersion models. *Journal of Hazardous Materials* **2014**, *271*, 98-107.

42. Codling, E.E., Effect of Flooding Lead Arsenate–Contaminated Orchard Soil on Growth and Arsenic and Lead Accumulation in Rice. *Communications Soil Sciences Plant* **2009**, *40*, 2800–2815.

43. Codling, E.E.; Chaney, R.L.; Green, C.E. Accumulation of Lead and Arsenic by Carrots Grown on Lead-arsenate Contaminated Orchard Soils. *Journal Plant Nutrition* In press, **2014**.

44. Codling, E.E.; Ritchie, J.C., Eastern Gamagrass Uptake Lead and Arsenic from Lead Arsenate Contaminated Soil Amended with Lime and Phosphorus. *Soil Sciences* **2005**, *170* (6), 413-424.

45. Colinet, I.; Dulong, V.; Mocanu, G.; Picton, L.; Le Cerf, D., Effect of chitosan coating on the swelling and controlled release of a poorly water-soluble drug from an amphiphilic and pH-sensitive hydrogel. *International Journal of Biological Macromolecules* **2010**, *47* (2), 120-125.

46. Couture, R.-M.; Van Cappellen, P., Reassessing the role of sulfur geochemistry on arsenic speciation in reducing environments. *Journal of Hazardous Materials* **2011**, *189* (3), 647-652.

47. Crini, G., Recent developments in polysaccharide-based materials used as adsorbents in wastewater treatment. *Progress in Polymer Science* **2005**, *30* (1), 38-70.

48. Cruz-Romero, M.; Murphy, T.; Morris, M.; Cummins, E.; Kerry, J., Antimicrobial activity of chitosan, organic acids and nano-sized solubilisates for potential use in smart antimicrobially-active packaging for potential food applications. *Food Control* **2013**, *34* (2), 393-397.

49. Cui, H.; Su, Y.; Li, Q.; Gao, S.; Shang, J. K., Exceptional arsenic (III, V) removal performance of highly porous, nanostructured ZrO_2 spheres for fixed bed reactors and the full-scale system modeling. *Water Research* **2013**, *47* (16), 6258-6268.

50. D'Oriano, C.; Da Pelo, S.; Podda, F.; Cioni, R., Laser-Ablation Inductively Coupled Plasma Mass Spectrometry (LA-ICP-MS): setting operating conditions and instrumental performance. *Periodico di Mineralogia* **2008**, *77*, 65-74.

51. Dambies, L.; Vincent, T.; Guibal, E., Treatment of arsenic-containing solutions using chitosan derivatives: uptake mechanism and sorption performances. *Water Research* **2002,** *36* (15), 3699-3710.

52. Dash, M.; Chiellini, F.; Ottenbrite, R.; Chiellini, E., Chitosan—A versatile semi-synthetic polymer in biomedical applications. *Progress in Polymer Science* **2011**, *36* (8), 981-1014.

53. Domingo, J. L.; Gomez, M.; Sanchez, D. J.; Llobet, J. M.; Keen, C. L., Toxicology of vanadium compounds in diabetic rats: the action of chelating agents on vanadium accumulation. *Molecular and Cellular Biochemistry* **1995**, *153* (1-2), 233-240.

54. Donmez, M.; Akbal, F., The Removal of As(V) from Drinking Waters by Coagulation Process using Iron Salts. *World Academy of Science, Engineering and Technology* **2011**, *5*, 384-386.

55. dos Santos, H. H.; Demarchi, C. A.; Rodrigues, C. A.; Greneche, J. M.; Nedelko, N.; Ślawska-Waniewska, A., Adsorption of As (III) on chitosan-Fe-crosslinked complex (Ch-Fe). *Chemosphere* **2011**, *82* (2), 278-283.

56. Du, J.; Jing, C.; Duan, J.; Zhang, Y.; Hu, S., Removal of arsenate with hydrous ferric oxide coprecipitation: Effect of humic acid. *Journal of Environmental Sciences* **2014**, *26*, 240-247.

57. Eisazadeh, H., Removal of arsenic in water using polypyrrole and its composites. *World Applied Sciences Journal* **2008**, *3*, 10-13.

58. Engi, M.; Cheburkin, A. K.; Köppel, V., Nondestructive chemical dating of young monazite using XRF: 1. Design of a mini-probe, age data for samples from the Central Alps, and comparison to U–Pb (TIMS) data. *Chemical Geology* **2002**, *191* (1), 225-241.

59. EPA Method 200.8. Determination of Trace Elements in Waters and Wastes by Inductively Coupled Plasma- Mass Spectrometry. Version 5.4. **1994**.

60. EPA Method 305. Microwave Assisted Acid Digestion of Sediments, Sludges, Soils, and Oils. Revision 0 September **1994**.

61. Erdem, A.; Shahwan, T.; Çağır, A.; Eroğlu, A. E., Synthesis of aminopropyl triethoxysilane-functionalized silica and its application in speciation studies of vanadium (IV) and vanadium (V). *Chemical Engineering Journal* **2011**, *174* (1), 76-85.

62. Ergican, E.; Gecol, H.; Fuchs, A., The effect of co-occurring inorganic solutes on the removal of arsenic (V) from water using cationic surfactant micelles and an ultrafiltration membrane. *Desalination* **2005**, *181* (1), 9-26.

63. Fan, H.-T.; Sun, T.; Xu, H.-B.; Yang, Y.-J.; Tang, Q.; Sun, Y., Removal of arsenic (V) from aqueous solutions using 3-[2-(2-aminoethylamino) ethylamino] propyl-trimethoxysilane functionalized silica gel adsorbent. *Desalination* **2011**, *278* (1), 238-243.

64. Fan, Z.; Hu, B.; Jiang, Z., Speciation analysis of vanadium in natural water samples by electrothermal vaporization inductively coupled plasma optical emission spectrometry after separation/preconcentration with thenoyltrifluoroacetone immobilized on microcrystalline naphthalene. *Spectrochimica Acta Part B: Atomic Spectroscopy* **2005**, *60* (1), 65-71.

65. Faria, P.; Orfao, J.; Pereira, M., Adsorption of anionic and cationic dyes on activated carbons with different surface chemistries. *Water Research* **2004**, *38* (8), 2043-2052.

66. Feng, H.; Li, J.; Wang, L., The removal of reactive red 228 Dye form aqueous solutions by Chitosan modified Flax Shive. *BioResources* **2012**, *7* (1), 624-639.

67. Ferreccio, C.; Sancha, A. M., Arsenic exposure and its impact on health in Chile. *Journal Health Popular Nutrition* **2006**, *24* (2), 164-75.

68. Filik, H.; Yanaz, Z., A sensitive method for determining total vanadium in water samples using colorimetric-solid-phase extraction-fiber optic reflectance spectroscopy. *Journal of Hazardous Materials* **2009**, *172.2*, 1297-1302.

69. Fortoul, T. I.; Rodriguez-Lara, V.; González-Villalva, A.; Rojas-Lemus, M.; Cano-Gutiérrez, G.; Ustarroz-Cano, M.; Colín-Barenque, L.; Bizarro-Nevares, P.; García-Pealez, I.;Montaño, L. F.; Jimenez-Martinez, R. S.; Lopez-Valdez, N.; Ruiz-Guerrero, M. L.; Meléndez-García, N. A.; García-Ibarra, F. A.; Martínez-Baez, V.; Zapata Alfaro, D.; Muñiz-Rivera-Cambas, A.; López-Zepeda, L. S.; Quezada-Maldonado, E. M.; Cervantes-Yépez, S.,*J*Inhalation of vanadium pentoxide and its toxic effects in a mouse model. *Inorganica Chimica Acta* **2014**, *In Press, Accepted Manuscript*.

70. Fu, F.; Wang, Q., Removal of heavy metal ions from wastewaters: a review. *Journal of Environmental Management* **2011**, *92* (3), 407-418.

71. Gang, D. D.; Deng, B.; Lin, L., As (III) removal using an iron-impregnated chitosan sorbent. *Journal of Hazardous Materials* **2010**, *182* (1), 156-161.

72. Gao, M.; Gawel, K.; Stokke, B. T., Polyelectrolyte and antipolyelectrolyte effects in swelling of polyampholyte and polyzwitterionic charge balanced and charge offset hydrogels. *European Polymer Journal* **2014**, 53, 65-74.

73. Garcia-Sanchez, R.; Bettmer, J.; Ebdon, L., Development of a new method for the separation of vanadium species and chloride interference removal using modified silica capillaries-DIN-ICP-MS. *Microchemical Journal* **2004**, *76*(1), 161-171.

74. Garlaschelli, F.; Alberti, G.; Fiol, N.; Villaescusa, I., Application of Anodic Stripping Voltammetry to assess sorption performance of an industrial waste entrapped in alginate beads to remove As (V). *Arabian Journal of Chemistry* **2013**, In press, Corrected proof.

75. Ge, F.; Li, M.-M.; Ye, H.; Zhao, B.-X., Effective removal of heavy metal ions Cd^{2+}, Zn^{2+}, Pb^{2+}, Cu^{2+} from aqueous solution by polymer-modified magnetic nanoparticles. *Journal of Hazardous Materials* **2012**, *211*, 366-372.

76. Gecol, H.; Ergican, E.; Fuchs, A., Molecular level separation of arsenic (V) from water using cationic surfactant micelles and ultrafiltration membrane. *Journal of Membrane Science* **2004**, *241* (1), 105-119.

77. Gerente, C.; Andres, Y.; McKay, G.; Le Cloirec, P., Removal of arsenic (V) onto chitosan: From sorption mechanism explanation to dynamic water treatment process. *Chemical Engineering Journal* **2010**, *158* (3), 593-598.

78. Ghanizadeh, G.; Ehrampoush, M.; Ghaneian, M., Application of iron impregnated activated carbon for removal of arsenic from water. *Iranian Journal of Environmental Health Science & Engineering* **2010**, *7* (2), 145-156.

79. Goh, K.-H.; Lim, T.-T.; Dong, Z., Application of layered double hydroxides for removal of oxyanions: a review. *Water Research* **2008**, *42* (6), 1343-1368.

80. Gorzsás, A., Vanadate and Peroxovanadate Complexes of Biomedical Relevance: A speciation approach with focus on diabetes. PhD thesis **2005**. Umeå University, Sweden.

81. Gotoh, T.; Matsushima, K.; Kikuchi, K.-I., Preparation of alginate–chitosan hybrid gel beads and adsorption of divalent metal ions. *Chemosphere* **2004**, *55* (1), 135-140.

82. Guibal, E., Interactions of metal ions with chitosan-based sorbents: a review. *Separation and Purification Technology* **2004**, *38* (1), 43-74.

83. Guibal, E.; Milot, C.; Tobin, J. M., Metal-anion sorption by chitosan beads: equilibrium and kinetic studies. *Industrial & Engineering Chemistry Research* **1998**, *37* (4), 1454-1463.

84. Guidroz, J. M.; Sneddon, J., Fate of vanadium determined by nitrous oxide–acetylene flame atomic absorption spectrometry in unburned and burned Venezuelan crude oil. *Microchemical Journal* **2002**, *73*(3), 363-366.

85. Guo, H.; Stüben, D.; Berner, Z., Removal of arsenic from aqueous solution by natural siderite and hematite. *Applied Geochemistry* **2007**, *22* (5), 1039-1051.

86. Gupta, A.; Chauhan, V. S.; Sankararamakrishnan, N., Preparation and evaluation of iron–chitosan composites for removal of As (III) and As (V) from arsenic contaminated real life groundwater. *Water Research* **2009**, *43* (15), 3862-3870.

87. Gupta, A.; Yunus, M.; Sankararamakishnan, N., Adsorption potential of As (III) & As (V) from water using low cost modified natural sand, *International Conference on Environment Science and Engineering* **2011**, *8*, 29-32.

88. Gupta, K.; Jabrail, F. H., Effects of degree of deacetylation and cross-linking on physical characteristics, swelling and release behavior of chitosan microspheres. *Carbohydrate Polymers* **2006**, *66* (1), 43-54.

89. Guzmán, J.; Saucedo, I.; Navarro, R.; Revilla, J.; Guibal, E., Vanadium interactions with chitosan: influence the polymer protonation and metal speciation. *Langmuir* **2002**, *18*, 1567-1573.

90. Haque, M. N.; Morrison, G. M.; Perrusquía, G.; Gutierréz, M.; Aguilera, A.F.; Cano-Aguilera, I.; Gardea-Torresdey, J. L., Characteristics of arsenic adsorption to sorghum biomass. *Journal of Hazardous Materials* **2007**, *145*, 30–35.

91. Hu, J.; Wang, X.; Xiao, L.; Song, S.; Zhang, B., Removal of vanadium from molybdate solution by ion exchange. *Hydrometallurgy* **2009**, *95*(3), 203-206.

92. Hu, G.; Chen, D.; Wang, L.; Liu, J. C.; Zhao, H.; Liu, Y.; Qi, T.; Zhang, C.; Yu, P., Extraction of vanadium from chloride solution with high concentration of iron by solvent extraction using D2EHPA. *Separation and Purification Technology* **2014**, *125*, 59–65.

93. Hu, Q.; Paudyal, H.; Zhao, J.; Huo, F.; Inoue, K.; Liu, H., Adsorptive recovery of vanadium (V) from chromium (VI)-containing effluent by Zr (IV)-loaded orange juice residue. *Chemical Engineering Journal* **2014**, *248*, 79-88.

94. Israt Jahan, M.; Abdul Motin, M.; Moniuzzaman, M.; Azadulah, M., Arsenic removal from water using activated carbon obtained from chemical activation of jute stick. Indian *Journal of Chemistry Technology* **2008**, *15*, 413-416.

95. Iqbal, J.; Wattoo, F. H.; Wattoo, M. H. S.; Malik, R.; Tirmizi, S. A.; Imran, M.; Ghangro, A. B., Adsorption of acid yellow dye on flakes of chitosan prepared from fishery wastes. *Arabian Journal of Chemistry* **2011**, *4* (4), 389-395.

96. Jackson, S. E., Calibration strategies for elemental analysis by LA-ICP-MS. *Laser-Ablation-ICP-MS in the Earth Sciences: Current Practices and Outstanding Issues, Mineralogical Association of Canada* **2008**, *40*, 169-188.

97. Jansson-Charrier, M.; Guibal, E.; Roussy, J.; Delanghe, B.; Le Cloirec, P., Vanadium (IV) sorption by chitosan: kinetics and equilibrium. *Water Research* **1996**, *30* (2), 465-475.

98. Jeong, Y.; Fan, M.; Singh, S.; Chuang, C.-L.; Saha, B.; Hans van Leeuwen, J., Evaluation of iron oxide and aluminum oxide as potential arsenic (V) adsorbents. *Chemical Engineering and Processing: Process Intensification.* **2007**, *46* (10), 1030-1039.

99. Kamari, A.; Ngah W. W. S.; Liew, S. K., Chitosan and chemically modified chitosan beads for acid dyes sorption. *Journal of Environmental Sciences* **2009**, *21*, 296–302.

100. Kanel, S. R.; Greneche, J.-M.; Choi, H., Arsenic (V) removal from groundwater using nano scale zero-valent iron as a colloidal reactive barrier material. *Environmental Science & Technology* **2006**, *40* (6), 2045-2050.

101. Kanel, S. R.; Manning, B.; Charlet, L.; Choi, H., Removal of arsenic (III) from groundwater by nanoscale zero-valent iron. *Environmental Science & Technology* **2005**, *39* (5), 1291-1298.

102. Kannan, A.; Singanan, M., Removal of cadmium from aqueous solution using carbon derived from palmyra palm fruit seed. *International Journal of Hazardous Materials* **2014**, *2* (1), 1-6.

103. Kartal, S. N.; Imamura, Y., Removal of copper, chromium, and arsenic from CCA-treated wood onto chitin and chitosan. *Bioresource Technology* **2005**, *96* (3), 389-392.

104. Katsoyiannis, I. A.; Zouboulis, A. I., Removal of arsenic from contaminated water sources by sorption onto iron-oxide-coated polymeric materials. *Water research* **2002**, *36* (20), 5141-5155.

105. Kiani, S.; Mousavi, S., Ultrasound assisted preparation of water in oil emulsions and their application in arsenic (V) removal from water in an emulsion liquid membrane process. *Ultrasonics Sonochemistry* **2013**, *20* (1), 373-377.

106. Kołodyńska, D., Adsorption characteristics of chitosan modified by chelating agents of a new generation. *Chemical Engineering Journal* **2012**, *179*, 33-43.

107. Kowalewska, M.; Szwedo, J., Examination of the Baltic amber inclusion surface using SEM techniques and X-ray microanalysis. *Palaeogeography, Palaeoclimatology, Palaeoecology* **2009**, *271* (3), 287-291.

108. Kumar, V.; Talreja, N.; Deva, D.; Sankararamakrishnan, N.; Sharma, A.; Verma, N., Development of bi-metal doped micro-and nano multi-functional polymeric adsorbents for the removal of fluoride and arsenic (V) from wastewater. *Desalination* **2011**, *282*, 27-38.

109. Kurita, K., Controlled functionalization of the polysaccharide chitin. *Progress in Polymer Science* **2001**, *26* (9), 1921-1971.

110. Lakshmipathiraj, P.; Prabhakar, S.; Raju, G. B., Studies on the electrochemical decontamination of wastewater containing arsenic. *Separation and Purification Technology* **2010**, *73* (2), 114-121.

111. Léonard, A.; Gerber, G., Mutagenicity, carcinogenicity and teratogenicity of vanadium compounds. *Mutation Research/Reviews in Genetic Toxicology* **1994**, *317* (1), 81-88.

112. Lertsutthiwong, P.; Boonpuak, D.; Pungrasmi, W.; Powtongsook, S., Immobilization of nitrite oxidizing bacteria using biopolymeric chitosan media. *Journal of Environmental Sciences* **2013**, *25* (2), 262-267.

113. Li, Y.; Zhang, F.-S.; Xiu, F.-R., Arsenic (V) removal from aqueous system using adsorbent developed from a high iron-containing fly ash. *Science of the Total Environment* **2009**, *407* (21), 5780-5786.

114. Lim, S.; Chen, J. P., Synthesis of an innovative calcium-alginate magnetic sorbent for removal of multiple contaminants. *Applied Surface Science* **2007**, *253* (13), 5772-5775.

115. Liu, B.; Lv, X.; Wang, D.; Xu, Y.; Zhang, L.; Li, Y., Adsorption behavior of As (III) onto chitosan resin with As (III) as template ions. *Journal of Applied Polymer Science* **2012**, *125* (1), 246-253.

116. Liu, Y.; Li, Y.; Yang, L., Histidine functionalized multi-walled carbon nanotubes as sorbent for flow injection-electrothermal atomic absorption spectrometric

ultrasensitive determination of trace vanadium (V) in biological and environmental samples. *Microchemical Journal* **2012**, *104*, 56-61.

117. Liu, S.; Zhang, F.; Chen, J.; Sun, G., Arsenic removal from contaminated soil via biovolatilization by genetically engineered bacteria under laboratory conditions. *Journal of Environmental Sciences* **2011**, *23* (9), 1544-1550.

118. Liu, T.; Zhao, L.; Sun, D.; Tan, X., Entrapment of nanoscale zero-valent iron in chitosan beads for hexavalent chromium removal from wastewater. *Journal of Hazardous Materials* **2010**, *184* (1), 724-730.

119. López-Morales, J.; Perales-Pérez, O.; Román-Velázquez, F., Sorption of Triclosan onto Tyre Crumb Rubber. *Adsorption Science & Technology* **2012**, *30* (10), 831-846.

120. López-Morales, J.; Sánchez-Rivera, D.; Luna-Pineda, T.; Perales-Pérez, O.; Román-Velázquez, F. (2013). Entrapment of Tyre Crumb Rubber in Calcium-Alginate Beads for Triclosan Removal. *Adsorption Science & Technology* **2013**, *31* (10), 931-942.

121. Lu, G.; Yao, X.; Wu, X.; Zhan, T., Determination of the total iron by chitosan-modified glassy carbon electrode. *Microchemical Journal* **2001**, *69*(1), 81-87.

122. Lv, L.; Xie, Y.; Liu, G.; Liu, G.; Yu, J., Removal of perchlorate from aqueous solution by cross-linked Fe (III)-chitosan complex. *Journal of Environmental Sciences* **2014**, *26* (4), 792-800.

123. Mahmudov, R.; Huang, C. P., Selective adsorption of oxyanions on activated carbon exemplified by Filtrasorb 400 (F400). *Separation and Purification Technology* **2011**, *77* (3), 294-300.

124. Mak, M. S.; Rao, P.; Lo, I., Effects of hardness and alkalinity on the removal of arsenic (V) from humic acid-deficient and humic acid-rich groundwater by zero-valent iron. *Water Research* **2009**, *43* (17), 4296-4304.

125. Makris, K. C.; Sarkar, D.; Parsons, J. G.; Datta, R.; Gardea-Torresdey, J. L., X-ray absorption spectroscopy as a tool investigating arsenic (III) and arsenic (V) sorption by an aluminum-based drinking-water treatment residual. *Journal of Hazardous Materials* **2009**, *171* (1), 980-986.

126. Manahan, S. E., *Environmental Chemistry*. CRC press: **2000**, 7th ed.

127. Manahan, S. E., *Toxicological Chemistry and Biochemistry*. CRC Press: **2003**, 3rd ed.

128. Manohar, D.; Noeline, B.; Anirudhan, T., Removal of vanadium (IV) from aqueous solutions by adsorption process with aluminum-pillared bentonite. *Industrial & Engineering Chemistry Research* **2005**, *44* (17), 6676-6684.

129. Martinson, C. A.; Reddy, K., Adsorption of arsenic (III) and arsenic (V) by cupric oxide nanoparticles. *Journal of Colloid and Interface Science* **2009**, *336* (2), 406-411.

130. Meng, Y.; Wang, J. N.; Cheng, C.; Yang, X.; Li, A. M., Preparation of new base-aluminum-chloride-loaded fiber as adsorbent for fast removal of arsenic (V) from water. *Chinese Chemical Letters* **2012**, *23* (7), 863-866.

131. Merrifield, J.D.; Davids, W.G.; MacRae, J.D.; Amirbahman A., Uptake of mercury by thiol-graftedchitosan gel beads. *Water Research* **2004**, *38*, 3132-3138..

132. Miller, S. M.; Spaulding, M. L. and Zimmerman, J. B., Optimization of capacity and kinetics for a novel bio-based arsenic sorbent, TiO_2-impregnated chitosan bead. *Water Research* **2011**, *45*, 5745-5754.

133. Miyazaki, Y.; Matsuoka, S.; Miura, Y.; Sakashita, H.; Yoshimura, K., Complexation of vanadium (V) oxoanion with ethanolamine derivatives in solution and in a cross-linked polymer. *Polyhedron* **2005**, *24* (9), 985-994.

134. Mnyusiwalla, A.; Daar, A. S.; Singer, P. A., 'Mind the gap': science and ethics in nanotechnology. *Nanotechnology* **2003**, *14* (3), R9.

135. Mohan, D.; Pittman Jr, C. U., Arsenic removal from water/wastewater using adsorbents—a critical review. *Journal of Hazardous Materials* **2007**, *142* (1), 1-53.

136. Mokgalaka, N.; Gardea-Torresdey, J., Laser ablation inductively coupled plasma mass spectrometry: Principles and applications. *Applied Spectroscopy Reviews* **2006**, *41* (2), 131-150.

137. Mondal, P.; Bhowmick, S.; Chatterjee, D.; Figoli, A.; Van der Bruggen, B., Remediation of inorganic arsenic in groundwater for safe water supply: A critical assessment of technological solutions. *Chemosphere* **2013,** *92* (2), 157-170.

138. Mondal, P.; Majumder, C.; Mohanty, B., Treatment of arsenic contaminated water in a batch reactor by using Ralstonia eutropha MTCC 2487 and granular activated carbon. *Journal of Hazardous Materials* **2008**, *153* (1), 588-599.

139. Morristown, N., Human Health Risk Assessment, Dundalk Marine Terminal, Baltimore, Maryland. **2009**.

140. Mukherjee, B.; Patra, B.; Mahapatra, S.; Banerjee, P.; Tiwari, A.; Chatterjee, M., Vanadium—an element of atypical biological significance. *Toxicology letters* **2004**, *150*(2), 135-143.

141. Murugan, T.; Ganapathy, A., Langmuir Isotherm and column studies on to Removal of Grey BL dye from waste water by Biomass adsorbent. *International Journal of Hazardous Materials* **2012**, *1* (1), 1-5.

142. Naeem, A.; Westerhoff, P.; Mustafa, S., Vanadium removal by metal (hydr) oxide adsorbents. *Water Research* **2007**, *41* (7), 1596-1602.

143. Namasivayam, C.; Sangeetha, D., Removal and recovery of vanadium (V) by adsorption onto ZnCl2 activated carbon: Kinetics and isotherms. *Adsorption* **2006**, *12* (2), 103-117.

144. Ngah, W. S.; Fatinathan, S., Pb (II) biosorption using chitosan and chitosan derivatives beads: Equilibrium, ion exchange and mechanism studies. *Journal of Environmental Sciences* **2010**, *22* (3), 338-346.

145. Ngah, W.; Fatinathan, S., Adsorption of Cu (II) ions in aqueous solution using chitosan beads, chitosan–GLA beads and chitosan–alginate beads. *Chemical Engineering Journal* **2008**, *143* (1), 62-72.

146. Nguyen, V.; Vigneswaran, S.; Ngo, H.; Shon, H.; Kandasamy, J., Arsenic removal by a membrane hybrid filtration system. *Desalination* **2009**, *236* (1), 363-369.

147. Nicolli, H. B.; Bundschuh, J.; Blanco, M. d. C.; Tujchneider, O. C.; Panarello, H. O.; Dapena, C.; Rusansky, J. E., Arsenic and associated trace-elements in groundwater from the Chaco-Pampean plain, Argentina: Results from 100years of research. *Science of the Total Environment* **2012**, *429*, 36-56.

148. Ning, R. Y., Arsenic removal by reverse osmosis. *Desalination* **2002**, *143* (3), 237-241.

149. Ninni, L.; Ermatchkov, V.; Hasse, H.; Maurer, G., Swelling behavior of chemically cross-linked poly (N-IPAAm-allylglycine) hydrogels: Effects of NaCl and pH. *Fluid Phase Equilibria* **2014**, *361*, 257-265.

150. Oehmen, A.; Viegas, R.; Velizarov, S.; Reis, M. A.; Crespo, J. G., Removal of heavy metals from drinking water supplies through the ion exchange membrane bioreactor. *Desalination* **2006**, *199* (1), 405-407.

151. Padilla-Rodríguez, A.; Perales-Pérez, O.; Román-Velázquez, F. R., Removal of As(III) and As(V) Oxyanions from aqueous solutions by using Chitosan Beads with immobilized Iron(III). *International Journal of Hazardous Materials* **2014**, *2* (1) ,7-17.

152. Padilla-Rodríguez, A.; Hernández-Viezcas, J.A.; Peralta-Videa, J.R.; Gardea-Torresday, J.L.; Perales-Pérez, O.; Román-Velázquez, F.R., Synthesis of Protonated

Chitosan Flakes for the removal of Vanadium(III, IV and V) Oxyanions from Aqueous Solutions. *Microchemical Journal* **2015a**, 118, 1-11.

153. Padilla-Rodríguez, A.; Hernández-Viezcas, J.A.; Peralta-Videa, J.R.; Gardea-Torresday, J.L.; Perales-Pérez, O.; Román-Velázquez, F.R., Adsorption of Arsenic(V) Oxyanion from Aqueous Solutions by Using Protonated Chitosan Flakes. Accepted manuscript in *Separation Science and Technology* **2015b**.

154. Pan, B.; Li, Z.; Zhang, Y.; Xu, J.; Chen, L.; Dong, H.; Zhang, W., Acid and Organic Resistant Nano-Hydrated Zirconium Oxide (HZO)/Polystyrene Hybrid Adsorbent for Arsenic Removal from Water. *Chemical Engineering Journal* **2014**, *248*, 290-296.

155. Park, Y. Y.; Tran, T.; Lee, Y. H.; Nam, Y. I.; Senanayake, G.; Kim, M. J., Selective removal of arsenic (V) from a molybdate plant liquor by precipitation of magnesium arsenate. *Hydrometallurgy* **2010**, *104* (2), 290-297.

156. Parks, J. L.; Edwards, M., Precipitative removal of As, Ba, B, Cr, Sr, and V using sodium carbonate. *Journal of Environmental Engineering* **2006**, *132* (5), 489-496.

157. Pennesi, C.; Totti, C.; Beolchini, F., Removal of Vanadium (III) and Molybdenum (V) from Wastewater Using Posidonia oceanica (Tracheophyta) Biomass. *Plos one* **2013**, *8* (10), e76870.

158. Pokhrel, D.; Viraraghavan, T., Arsenic removal from an aqueous solution by a modified fungal biomass. *Water research* **2006**, *40* (3), 549-552.

159. Pontoni, L.; Fabbricino, M., Use of chitosan and chitosan-derivatives to remove arsenic from aqueous solutions—a mini review. *Carbohydrate Research* **2012**, *356*, 86-92.

160. Pourret, O.; Dia, A.; Gruau, G.; Davranche, M.; Bouhnik-Le Coz, M., Assessment of vanadium distribution in shallow groundwaters. *Chemical Geology* **2012**, *294*, 89-102.

161. Prathap, K; Namasivayam, C., Recycling Fe (III)/Cr (III) hydroxide, an industrial solid waste for the removal of phosphate from water. *Journal of Hazardous Materials* **2005**, *123* (1), 127-134.

162. Qian, S.; Wang, H.; Huang, G.; Mo, S.; Wei, W., Studies of adsorption properties of crosslinked chitosan for vanadium (V), tungsten (VI). *Journal of Applied Polymer Science* **2004**, *92* (3), 1584-1588.

163. Rahmani, A.; Ghaffari, H.; Samadi, M., A comparative study on arsenic (III) removal from aqueous solution using nano and micro sized zero-valent iron. *Iranian Journal of Environmental Health Science & Engineering* **2011**, *8* (2), 157-166.

164. Rana, M. S.; Halsim, M. A.; Waliul Hoque, S. A. M.; Hasan, K.; Hossain, M. K., Bioadsorption of Arsenic by Prepared and Commercial Crab Shell Chitosan. *Biotechnology* **2009**, *8* (1), 160-165.

165. Rao, R. A. K.; Kham, M. A.; Rehman, F., Batch and Column Studies for the Removal of Lead(II) Ions from Aqueous Solution onto Lignite. *Adsorption Science and Technology* **2009**, *29* (1), 83-98.

166. Raven, K. P.; Jain, A.; Loeppert, R. H., Arsenite and arsenate adsorption on ferrihydrite: kinetics, equilibrium, and adsorption envelopes, *Environmental Science & Technology* **1998**, *32*, 344–349.

167. Reddy, K. R.; Xie, T.; Dastgheibi, S., Removal of heavy metals from urban stormwater runoff using different filter materials. *Journal of Environmental Chemical Engineering* **2014**, *2* (1), 282-292.

168. Richmond, W. R.; Loan, M.; Morton, J.; Parkinson, G. M., Arsenic removal from aqueous solution via ferrihydrite crystallization control. *Environmental Science & Technology* **2004**, *38* (8), 2368-2372.

169. Rintala, E.-M.; Ekholm, P.; Koivisto, P.; Peltonen, K.; Venäläinen, E.-R., The intake of inorganic arsenic from long grain rice and rice-based baby food in Finland–Low safety margin warrants follow up. *Food chemistry* **2014**, *150*, 199-205.

170. Richert, J. C.; Hardaway, C. J.; Sneddon, J., Laboratory controlled study of the uptake and release of vanadium by oysters (Crassostrea virginica). *Microchemical Journal* **2014**, *113*, 1-3.

171. Rodríguez-Lado, L.; Sun, G.; Berg, M.; Zhang, Q.; Xue, H.; Zheng, Q.; Johnson, C. A., Groundwater arsenic contamination throughout China. *Science* **2013**, *341* (6148), 866-868.

172. Rout, P. C.; Sarangi, K., Separation of vanadium using both hollow fiber membrane and solvent extraction technique–A comparative study. *Separation and Purification Technology* **2014**, *122*, 270-277.

173. Roy, R.; Sah, M.; Mazumdar, A.; Ray, S. S., Recent advancement in arsenic adsorbents: A mini review. *International Journal of Research in Environmental Science and Technology* **2014**, *4* (1), 10-15.

174. Sahiner, N.; Ozay, O.; Aktas, N.; Blake, D. A.; John, V. T., Arsenic (V) removal with modifiable bulk and nano p (4-vinylpyridine)-based hydrogels: The effect of hydrogel sizes and quarternization agents. *Desalination* **2011**, *279* (1), 344-352.

175. Saitúa, H.; Campderrós, M.; Cerutti, S.; Padilla, A. P., Effect of operating conditions in removal of arsenic from water by nanofiltration membrane. *Desalination* **2005**, *172* (2), 173-180.

176. Sánchez, D., Removal and Speciation of Oxyanions from Aqueous Solutions using Ca-Fe(III) Alginate Beads and Dried Sludge as Adsorbents. PhD Thesis **2013**. University of Puerto Rico at Mayagüez.

177. Sánchez-Rivera, D.; Perales-Pérez, O.; Román, F. R., LC-ICPMS speciation of arsenite and arsenate oxyanion mixtures during their adsorption with dried sludge. *Analytical Methods* **2013,** *5* (6), 1583-1589.

178. Sánchez-Rivera, D.; Perales-Pérez, O.; Román, F. R., Removal of inorganic arsenic oxyanions using Ca–Fe(III) alginate beads, *Desalination Water Treaments* **2012**, *51 (10-12)*, 2162-2169.

179. Sankararamakrishnan, N.; Gupta, A.; Rai Vidyarthi, S., Enhanced arsenic removal at neutral pH using functionalized multiwalled carbon nanotubes. *Journal of Environmental Chemical Engineering* **2014**, *2*, 802–810.

180. Santos, A.; de Oliveira, F. W. F.; Silva, F. H. A.; Maria, D. A.; Ardisson, J. D.; Macêdo, W. A. d. A.; Palmieri, H. E. L.; Franco, M. B., Synthesis and characterization of iron-PVA hydrogel microspheres and their use in the arsenic (V) removal from aqueous solution. *Chemical Engineering Journal* **2012**, *210*, 432-443.

181. Saravanan, D.; Gomathi, T.; Sudha, P., Sorption studies on heavy metal removal using chitin/bentonite biocomposite. *International Journal of Biological Macromolecules* **2013**, *53*, 67-71.

182. Sasaki, K.; Nakano, H.; Wilopo, W.; Miura, Y.; Hirajima, T., Sorption and speciation of arsenic by zero-valent iron. *Colloids and Surfaces A: Physicochemical and Engineering Aspects* **2009**, *347* (1), 8-17.

183. Senanayake, N.; Mukherji, A., Irrigating with arsenic contaminated groundwater in West Bengal and Bangladesh: A review of interventions for mitigating adverse health and crop outcomes. *Agricultural Water Management* **2014**, *135*, 90-99.

184. Shang, G.; Zhang, G.; Gao, C.; Fu, W.; Zeng, L., A novel nanofiltration process for the recovery of vanadium from acid leach solution. *Hydrometallurgy* **2014**, *142*, 94-97.

185. Sharma, V.K.; Sohn, M., Aquatic arsenic: toxicity, speciation, transformations, and remediation. *Environment International* **2009**, *35*, 743-759.

186. Shevade, S.; Ford, R. G., Use of synthetic zeolites for arsenate removal from pollutant water. *Water Research* **2004**, *38* (14), 3197-3204.

187. Shinde, R. N.; Pandey, A.; Acharya, R.; Guin, R.; Das, S.; Rajurkar, N.; Pujari, P., Chitosan-transition metal ions complexes for selective arsenic (V) preconcentration. *Water Research* **2013**, *47* (10), 3497-3506.

188. Shraim, A. M., Rice is a potential dietary source of not only arsenic but also other toxic elements like lead and chromium. *Arabian Journal of Chemistry* **2014**, In press, corrected proof.

189. Silva, C. M.; Ribeiro, A. J.; Figueiredo, M.; Ferreira, D.; Veiga, F., Microencapsulation of hemoglobin in chitosan-coated alginate microspheres prepared by emulsification/internal gelation. *The AAPS Journal* **2005**, *7* (4), E903-E913.

190. Sivaraman, D., Synthesis and Characterization of Thiol-Functionalized Chitosan Based Adsorbents for Arsenic Removal From water. Ms Thesis **2004**. University of Florida.

191. Smara, A.; Delimi, R.; Chainet, E.; Sandeaux, J., Removal of heavy metals from diluted mixtures by a hybrid ion-exchange/electrodialysis process. *Separation and Purification Technology* **2007**, *57* (1), 103-110.

192. Sparks, D. L., *Environmental Soil Chemistry*. Academic press: **2003**.

193. Tanboonchuy, V.; Hsu, J. C.; Grisdanurak, N.; Liao, C.H., Gas-bubbled nano zero-valent iron process for high concentration arsenate removal. *Journal of Hazardous Materials* **2011**, *186* (2), 2123-2128.

194. Tang, W.; Su, Y.; Li, Q.; Gao, S.; Shang, J. K., Superparamagnetic magnesium ferrite nanoadsorbent for effective arsenic (III, V) removal and easy magnetic separation. *Water research* **2013**, *47* (11), 3624-3634.

195. Tian, L.; Yang, J.; Alewell, C.; Huang, J. H., Speciation of vanadium in Chinese cabbage (Brassica rapa L.) and soils in response to different levels of vanadium in soils and cabbage growth. *Chemosphere* **2014**, *111*, 89-95.

196. Tikhonov, V. E.; Stepnova, E. A.; Babak, V. G.; Yamskov, I. A.; Palma-Guerrero, J.; Jansson, H.-B.; Lopez-Llorca, L. V.; Salinas, J.; Gerasimenko, D. V.; Avdienko, I. D., Bactericidal and antifungal activities of a low molecular weight chitosan and its *N*-/2(3)-(dodec-2-enyl)succinoyl/-derivatives. *Carbohydrate polymers* 2006, *64* (1), 66-72.

197. Trejos, T.; Montero, S.; Almirall, J. R., Analysis and comparison of glass fragments by laser ablation inductively coupled plasma mass spectrometry (LA-ICP-MS) and ICP-MS. *Analytical and Bioanalytical Chemistry* **2003,** *376* (8), 1255-1264.

198. Tuna, A. Ö. A.; Özdemir, E.; Şimşek, E. B.; Beker, U., Removal of As (V) from aqueous solution by activated carbon-based hybrid adsorbents: Impact of experimental conditions. *Chemical Engineering Journal* **2013**, *223*, 116-128.

199. Türk, T.; Alp, İ., Arsenic removal from aqueous solutions with Fe-hydrotalcite supported magnetite nanoparticle. *Journal of Industrial and Engineering Chemistry* **2014**, *20* (2), 732-738.

200. Vasireddy, D., Arsenic adsorption onto iron-chitosan composite from drinking water. MS Thesis **2006**. University of Missouri, Columbia.

201. Vicentini, F. C.; Silva, T. A.; Pellatieri, A.; Janegitz, B. C.; Fatibello-Filho, O.; Faria, R. C., Pb (II) determination in natural water using a carbon nanotubes paste electrode modified with crosslinked chitosan. *Microchemical Journal* **2014**, *116*, 191-196.

202. Vega, E.; Pedregosa, J.; Narda, G.; Morando, P., Removal of oxovanadium (IV) from aqueous solutions by using commercial crystalline calcium hydroxyapatite. *Water Research* **2003**, *37* (8), 1776-1782.

203. Viswanathan, N.; Sundaram, C. S.; Meenakshi, S., Removal of fluoride from aqueous solution using protonated chitosan beads. *Journal of Hazardous Materials* **2009**, 161 (1), 423-430.

204. Vitela-Rodriguez, A.V.; Rangel-Mendez, J. R., Arsenic removal by modified activated carbons with iron hydro (oxide) nanoparticles. *Journal of Environmental Management* **2013**, *114*, 225-231.

205. Wällstedt, T.; Björkvald, L.; Gustafsson, J. P., Increasing concentrations of arsenic and vanadium in (southern) Swedish streams. *Applied Geochemistry* **2010**, *25* (8), 1162-1175.

206. Wang, S.; Xu, X.; Yang, J.; Gao, J., Effect of the carboxymethyl chitosan on removal of nickel and vanadium from crude oil in the presence of microwave irradiation. *Fuel Processing Technology* **2011**, *92* (3), 486-492.

207. Wang, Y.; Tsang, D. C., Effects of solution chemistry on arsenic (V) removal by low-cost adsorbents. *Journal of Environmental Sciences* **2013**, *25* (11), 2291-2298.

208. WHO **2001**. *https://apps.who.int/inf-fs/en/fact210.html*.

209. Xia, S.; Shen, S.; Xu, X.; Liang, J.; Zhou, L., 2014. Arsenic removal from groundwater by acclimated sludge under autohydrogenotrophic condition. *Journal of Environmental Sciences* **2014**, *26*, 248-255.

210. Xie, Y.; Li, S.; Wang, F.; Liu, G., Removal of perchlorate from aqueous solution using protonated cross-linked chitosan. *Chemical Engineering Journal* **2010,** *156* (1), 56-63.

211. Xie, M.; Chen, D.; Zhang, F.; Willsky, G. R.; Crans, D. C.; Ding, W., Effects of Vanadium (III, IV, V)-chlorodipicolinate on Glycolysis and Antioxidant Status in the Liver of STZ-induced Diabetic Rats. *Journal of Inorganic Biochemistry* **2014**, *136*, 47-56.

212. Xu, Y.-h.; Nakajima, T.; Ohki, A., Adsorption and removal of arsenic (V) from drinking water by aluminum-loaded Shirasu-zeolite. *Journal of Hazardous Materials* **2002,** *92* (3), 275-287.

213. Yang, H. C.; Hon, M. H., The effect of the molecular weight of chitosan nanoparticles and its application on drug delivery. *Microchemical Journal* **2009**, *92* (1), 87-91.

214. Yeom, B.-Y.; Lee, C.-S.; Hwang, T.-S., A new hybrid ion exchanger: effect of system parameters on the adsorption of vanadium (V). *Journal of Hazardous Materials* **2009**, *166* (1), 415-420.

215. Yu, Y.; Zhao, C.; Wang, Y.; Fan, W.; Luan, Z., Effects of ion concentration and natural organic matter on arsenic (V) removal by nanofiltration under different transmembrane pressures. *Journal of Environmental Sciences* **2013**, *25* (2), 302-307.

216. Yürüm, A.; Kocabaş-Ataklı, Z. Ö.; Sezen, M.; Semiat, R.; Yürüm, Y., Fast Deposition of Porous Iron Oxide on Activated Carbon by Microwave Heating and Arsenic (V) Removal from Water. *Chemical Engineering Journal* **2014**, *242*, 321-332.

217. Zeng, L.; Li, Q.; Xiao, L., Extraction of vanadium from the leach solution of stone coal using ion exchange resin. *Hydrometallurgy* **2009**, *97* (3), 194-197.

218. Zhang, H., Zhu, G., Jia, X., Ding, Y., Zhang, M., Gao, Q.; Xu, S. Removal of microcystin-LR from drinking water using a bamboo-based charcoal adsorbent modified with chitosan. *Journal of Environmental Sciences* **2011**, *23* (12), 1983-1988.

219. Zhao, Y.; Huang, M.; Wu, W.; Jin, W., Synthesis of the cotton cellulose based Fe (III)-loaded adsorbent for arsenic (V) removal from drinking water. *Desalination* **2009**, *249* (3), 1006-1011.

220. Zouboulis, A. I.; Katsoyiannis, I. A., Arsenic removal using iron oxide loaded alginate beads. *Industrial & Engineering Chemistry Research* **2002**, *41* (24), 6149-6155.

7 APPENDIX: Related Results Internship Summary

Effect of turbidity of wastewater in Sewage/Wastewater at the Treatment Plant located in Aguada, Puerto Rico

By Abigail Padilla Rodríguez

University of Puerto Rico at Mayagüez

Abstract

Chitosan is a natural polymer that serves as an adsorbent of contaminants from water, which can also be used as an agent coagulant for the reduction of turbidity in wastewater. In this study, chitosan was used for the reduction of affluent and effluentt turbidity in a wastewater treatment plant at sewage/wastewater plants located in Aguada, Puerto Rico. Turbidity removal was evaluated utilizing diverse adsorbents containing chitosan, such as chitosan powder, protonated chitosan flakes, chitosan with immobilized iron, chitosan solution, column packed with chitosan, chitosan with the AF-501 polymer, and compared with the traditional AF-501 polymer. Chitosan solution was the best in reducing the turbidity of affluent wastewater with 99% removal achieved. Also, using columns packed with chitosan powder was effective, showing a 96% and 92% for affluent and effluent wastewater, respectively. The chitosan outperformed the AF-501 polymer at all concentrations, which was especially noticeable at low concentrations in the jar test for affluent wastewater. The results showed that chitosan is an excellent, non-toxic and inexpensive coagulant for turbidity removal from wastewater, with great potential to be applied for the reduction of turbidity of affluent in wastewater treatment plants.

1. Introduction

The quality of the water from wastewater treatment plants that is to be discharged into the sea/ocean or into rivers is of great importance environmentally. Several parameters should be monitored to maintain good levels in water quailty, these are: total solids suspended (TSS), chemical oxygen demand (COD), turbidity and pH. TSS is a measure of the combination of inorganic and organic solids substances contained in wastewater. COD is a measure of the amount of oxygen required to oxidize the organic and inorganic compounds in water; it's typically measured in mg/L, which indicates mass of oxygen consumed per liter of solution. The turbidity is caused by individual particles, suspended solids, organic and inorganic matter and other organisms which present cloudiness or are sometimes invisible to the naked eye. Finally, the pH is a measure of the basicity or acidity in aqueous solutions. The pH value indicates the relative amount of hydrogen ions (H^+) and hydroxyl ions (OH^-) present in water, which are essential to the health of ecosystems.

A method used for the removal of turbidity is coagulation then flocculation, followed by sedimentation. In coagulation, the particles are destabilized and agglomerated; in flocculation the formation of larger flocs occurs. Finally, in sedimentation, the flocs are completely separated from the liquid, thereby forming two layers in the solution which can be easily separated. Most common coagulants used are ferric sulfate, ferric chloride, aluminum sulfate. The disadvantages of these coagulants are that they generate secondary products which can be dangerous to the environment and humans. Therefore, it is recommended to use a non-toxic, inexpensive and environmentally friendly coagulant for the reduction of particles and turbidity in water.

Chitosan is a natural poly-N-acetylglucosamine extracted from the exoskeleton of crustaceans' shells, algae, fungal biomass, insects, lobsters and marine arthropod. It is obtained by the deacetylation of chitin, which is the second natural biopolymer after cellulose. Chitosan is a polymer cationic and partially soluble in dilute acidic solutions. Chitosan has excellent properties, such as, non-toxic, biodegradable, biocompatible, availability, antibacterial, affinity for heavy metals and proteins, and inexpensive. It has been used for the removal of organic and inorganic contaminants from water. Chitosan has been applied in the areas of biomedical, biotechnology, pharmaceutical, dietetic, food industry, biocompatible, agriculture and residual waters.

In the present work, chitosan is used as coagulant for the effect of the turbidity and pH of wastewater at a Sewage Plants located in Aguada, Puerto Rico, which belong to the Puerto Rican Aqueduct and Sewer Authority (PRASA). An environmentally friendly, inexpensive and simple procedure for the preparation of the chitosan beads/flakes and chitosan solution was developed. These achieved a 99% removal of turbidity from wastewater at an initial NTU which ranged from 326 to 841 without the need of wastewater pretreatment, thus resulting in simple and efficient process. On this basis, the work presented here represents a viable option for using a simple and non-toxic coagulant based on chitosan for the removal of turbidity in wastewater, thus resulting in a solution to an environmental problem faced in many parts of the world.

2. Objectives

The internship at the sewage plants (PAS) took place from September 2013 to February 2014 in Aguada, Puerto Rico. The main objectives were:

(1) Training in process control in a wastewater treatment plant (WWTP) for monitoring total solids suspended (TSS), chemical oxygen demand (COD), turbidity and pH.

(2) Evaluate the effect in the turbidity and pH once the chitosan polymer is added to the wastewater.

3. Experimental Procedure

3.1 Water Sample Collection

Water samples were taken at discharges of affluent and effluent sampling points. The wastewater that reaches the treatment plant are where the affluent samples were taken and the effluent samples were the ones that were treated by different processes to then be discharge in the sea or rivers, ie the affluent is the raw water and the effluent is treated water. The turbidity and pH were measured in all samples.

.

3.2 Turbidity and pH

The turbidity and pH were measured in every affluent and effluent sample. Studies were conducted simulating the jars tests. The turbidity and pH were measured in every affluent and effluent sample. The chitosan or AF-501 solutions were added to water, volume of 100 mL (affluent or effluent), in a 250 mL beaker and agitated. The initial velocity for agitation was 100 rpm for 1 min, then was decreased to 35 rpm for 10 min to

promote coagulation and flocculation, and finally 10 rpm for 10 min for sedimentation. At the beginning and at the end of the process, the pH (pH meter, Hach, USA) and turbidity (Turbidimeter, Hach, USA) levels were measured.

The polymers added to the samples were chitosan in diverse forms: chitosan powder (CP), protonated chitosan flakes (PCF), chitosan with immobilized iron (Fe(III)-CB), chitosan solutions and columns packed with chitosan. These were compared with the traditional AF-501 polymer used in PAS Aguada; and also in conjunction with chitosan/AF-501 polymer.

Various procedures were performed with each of the different adsorbents consisting chitosan. First, the adding of 12, 14, 16 and 18 ppm of AF-501 polymer individually Second, the adding of 5 g/L of CP, PCF or Fe(III)-CB in contact with wastewater. Third, CP, PCF or Fe(III)-CB in conjunction with AF-501 polymer in contact with wastewater. Fourth, a column packed with chitosan powder, PCF or Fe(III)-CB. Fifth, chitosan solution (1 and 2 % w/v diluted in 1% and 5% acetic acid) added to affluent wastewater. Some samples were filtered before and after the process. Others were filtered at only the start or at the end of the process. All experiments were performed in duplicate.

4. Results and Discussions

4.1 AF-501 polymer

The AF-501 is the industrial polymer used in the Sewage/Wastewater Treatment Plant in Aguada, Puerto Rico, the location under evaluation. AF-501 is a cationic polymer that permits the coagulation and flocculation of affluent wastewater to decrease the turbidity and

consisted of polyaluminum chloride and polydimethyldiallylammonium chloride. The polymer concentrations used to determine the effective dosage to decrease the turbidity were 12, 14, 16 and 18 ppm. Table 1 shows the initial and final turbidity of affluent; the optimum concentration used, was 14 ppm, which reached a final NTU of 13.1 from an initial 538.0 NTU. For effluent samples, the best concentration used was 12 ppm with a final value of 4.1 NTU (Shown in Table 1) from an initial concentration of 286.5 NTU. Also, the percentages of turbidity removal, which ranged between 77 to 98% for affluent samples and from 50 to 92% for the effluent samples were shown. The optimum concentration of AF-501 that worked best for the removal of turbidity in both wastewater types was 12 ppm with a 93 and 92% removal for affluent and effluent, respectively.

Table 1 shows the pH values for affluent and effluent samples, which obtained a final pH between 6.5 to 7.7 units. These pH readings are in the range allowed (pH 6-9) for the wastewater treatment plants. Internal documents from the treatment plant (not published) indicate that the particles causing the turbidity are negatively charged, thus it is suggested that the removals of turbidity from these wastewater samples were due to electrostatic attraction between the negatively charged particles in the wastewater and the positive charge of the polymer.

Table 1: Turbidity values from affluent and effluent samples in contact with AF-501 polymer.

Polymer	Type	Initial		Final		% Removal Avg		pH	
		NTU	stdv	NTU	stdv	%NTU	stdv	Initial	Final
AF-501 12 ppm	Affluent	286.5	0.7	21.7	0.3	92.4	0.1	7.0	7.4
	Effluent	54.3	0.9	4.1	0.1	92.4	0.2	7.0	7.6
AF-501 14 ppm	Affluent	538.0	2.8	13.1	0.3	97.6	0.1	6.9	7.3
	Effluent	41.5	0.3	10.8	0.1	73.8	0.3	7.1	7.3
AF-501 16 ppm	Affluent	538.0	2.8	22.3	0.3	95.9	0.1	6.5	7.3
	Effluent	41.5	0.3	20.7	0.6	50.0	1.8	7.2	7.4
AF-501 18 ppm	Affluent	277.0	4.2	63.7	0.8	77.0	0.1	6.5	7.7
	Effluent	49.9	0.5	9.7	0.5	80.5	0.9	7.2	7.5

4.2 AF-501 polymer in conjunction with chitosan

Tables 2 to 5 show turbidity values from affluent and effluent samples in contact with AF-501 (12 to 18 ppm) mixed with chitosan polymers (5 g/L of CP, PCF or Fe(III)-CB), individually. AF-501 12ppm showed a decrease of 92% to 82% for affluent wastewater and 92% to 28% for effluent wastewater (shown in table 2). Table 3 shows a decrease of 98% to 58% and 74% to 37% for affluent and effluent wastewater, respectively, using AF-501 14ppm. AF-501 16 and 18 ppm show a decrease of 97% to 80% and 83% to 28% for affluent and effluent wastewater using AF-501 16ppm, and 89% to 77% for affluent wastewater using AF-501 18 ppm. On the other hand, effluent wastewater increase from 66% to 80% and 66% to 70% using AF-501 18ppm when combined with Fe(III)-CB and CP, respectively.

AF-501 mixed with chitosan polymer showed a decrease in removal of turbidity in all the concentrations (12 – 18 ppm). This could be to the competition of the sites actives of both polymer for removal the turbidity of wastewater. During the study, the pH of the wastewater weas between 6 and 9, complying with the discharge regulations (pH 6-9).

Table 2: Values of turbidity from affluent and effluent samples in contact with AF-501 12ppm mixed with CP, PCF or Fe(III)-CB individually.

	AF-501 12ppm	stdv	AF-501 12ppm + CP	stdv	AF-501 12ppm + PCF	stdv	AF-501 12ppm + Fe(III)-CB	stdv
Affluent Initial	287.0	1.4	289.5	2.1	279.0	1.4	304.0	8.5
Affluent Final	21.9	0.6	46.8	0.5	30.1	6.8	55.6	0.2
% Removal Affluent	**92.4**	0.2	**83.9**	0.1	**89.2**	2.5	**81.7**	0.6
Effluent Initial	54.5	1.2	57.3	0.3	51.7	0.2	50.6	0.5
Effluent Final	4.2	0.0	6.1	0.1	21.6	0.6	36.7	0.2
% Removal Effluent	**92.2**	0.1	**89.3**	0.1	**58.3**	1.1	**27.5**	0.3

Table 3: Values of turbidity from affluent and effluent samples in contact with AF-501 14ppm mixed with CP, PCF or Fe(III)-CB individually.

	AF-501 14ppm	stdv	AF-501 14ppm + CP	stdv	AF-501 14ppm + PCF	stdv	AF-501 14ppm + Fe(III)-CB	stdv
Affluent Initial	538.0	2.8	282.5	13.4	282.5	13.4	282.5	13.4
Affluent Final	13.1	0.4	4.8	0.2	23.2	0.4	119.5	0.7
% Removal Affluent	**97.6**	0.1	**98.3**	0.2	**91.8**	0.5	**57.7**	1.8
Effluent Initial	41.5	0.3	22.0	3.0	22.0	3.0	22.0	3.0
Effluent Final	10.9	0.1	18.5	0.4	8.0	0.0	13.7	0.4
% Removal Effluent	**73.9**	0.3	**15.0**	13.4	**63.1**	5.1	**37.1**	10.3

Table 4: Values of turbidity from affluent and effluent samples in contact with AF-501 16ppm mixed with CP, PCF or Fe(III)-CB individually.

	AF-501 16ppm	stdv	AF-501 16ppm + CP	stdv	AF-501 16ppm + PCF	stdv	AF-501 16ppm + Fe(III)-CB	stdv
Affluent Initial	216.0	1.4	216.0	1.4	216.0	1.4	216.0	1.4
Affluent Final	6.5	0.1	22.9	0.9	23.0	0.3	42.7	4.2
% Removal Affluent	**96.9**	0.1	**89.4**	0.5	**89.4**	0.2	**80.2**	1.8
Effluent Initial	33.8	0.1	33.8	0.1	33.8	0.1	33.8	0.1
Effluent Final	5.6	0.04	5.6	0.04	8.7	0.7	24.2	0.3
% Removal Effluent	**83.3**	0.1	**83.3**	0.1	**74.3**	2.3	**28.3**	1.3

Table 5: Values of turbidity from affluent and effluent samples in contact with AF-501 18ppm mixed with CP, PCF or Fe(III)-CB individually.

	AF-501 18ppm	std	AF-501 18ppm + CP	std	AF-501 18ppm + PCF	std	AF-501 18ppm + Fe(III)-CB	stdv
Affluent Initial	362.5	3.5	274.5	0.7	279.5	0.7	274.5	0.7
Affluent Final	40.8	0.6	51.0	1.4	48.0	1.1	63.9	0.9
% Removal Affluent	**88.8**	0.1	**81.4**	0.5	**82.8**	0.3	**76.7**	0.3
Effluent Initial	65.9	0.1	40.8	0.3	41.9	0.3	49.8	0.4
Effluent Final	22.6	0.4	12.2	0.5	21.2	0.2	10.0	1.0
% Removal Effluent	**65.7**	0.7	**70.2**	1.4	**49.5**	0.2	**79.9**	1.8

4.3 Chitosan polymer

Figure 1 shows the unfiltered affluent and effluent turbidity using 5 g/L of CP, PCF and Fe(III)-CB. The results show a 57% (CP), 57% (PCF) and 54% (Fe(III)-CB) for affluent turbidity. For the effluent turbidity the results presented a 18%, 20% and a 52% using CP, PCF and Fe(III)-CB, respectively. These results indicate that the best polymer for affluent tests were CP and PCF, and for effluent, Fe(III)-CB. This removal occurs because chitosan is a cationic polymer that removes negative charges from wastewater. Once exposed, the chitosan polymers to wastewater, the pH values were between 6-8.

Figures 2 to 4 present the turbidity of wastewater filtered at the beginning, filtered at the end, and filtered at the beginning and at the end. The best results were when the wastewater was filtered at the beginning and at the end, it showed a 94% removal using PCF for affluent and a 78% removal using CP for effluent. The high surface area of PCF could be responsible for the turbidity removal of wastewater.

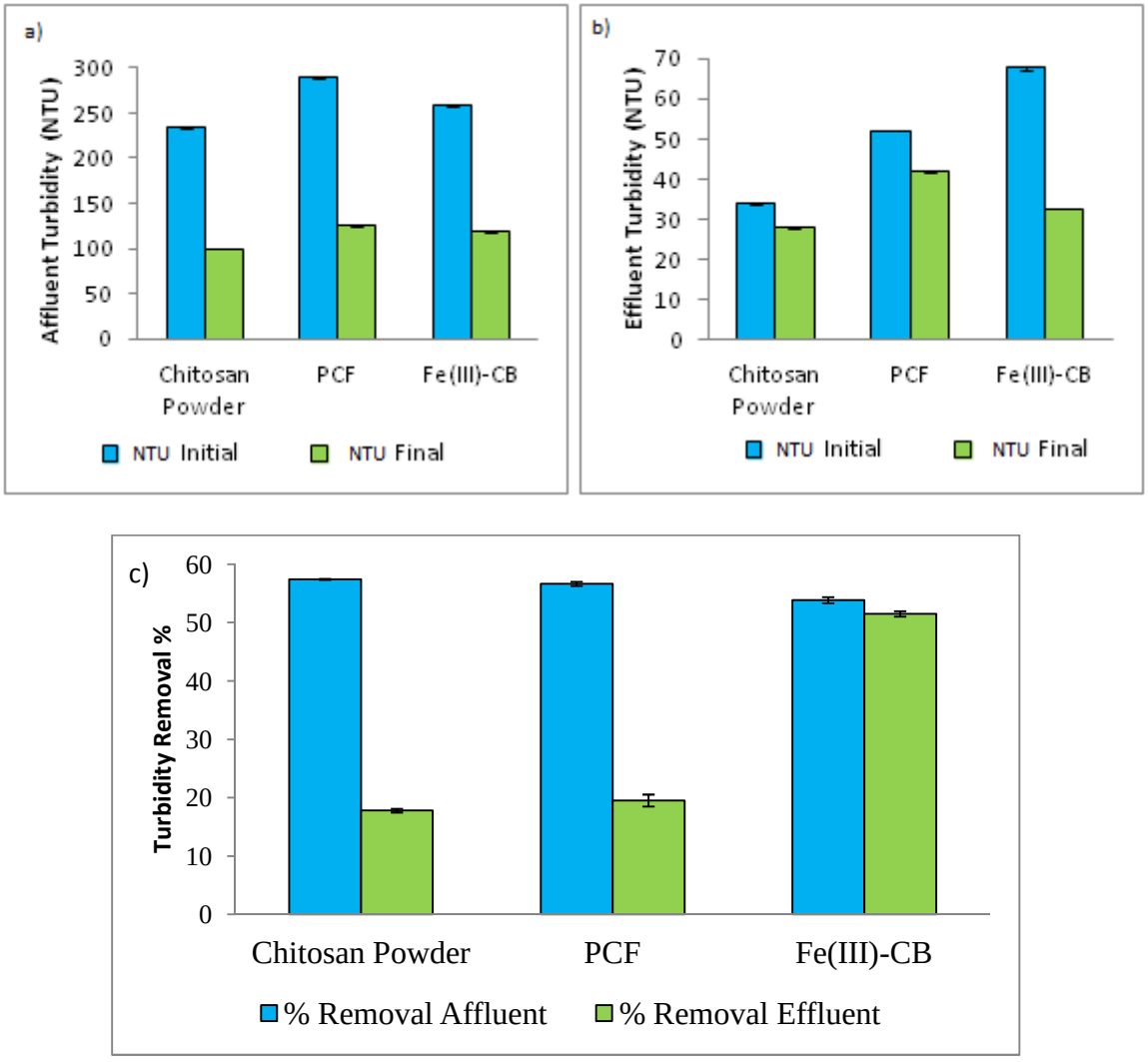

Figure 1: Initial and final turbidity from affluent (a) and effluent (b) samples, and turbidity removal (c) from affluent and effluent samples using Chitosan powder, PCF and Fe(III)-CB individually.

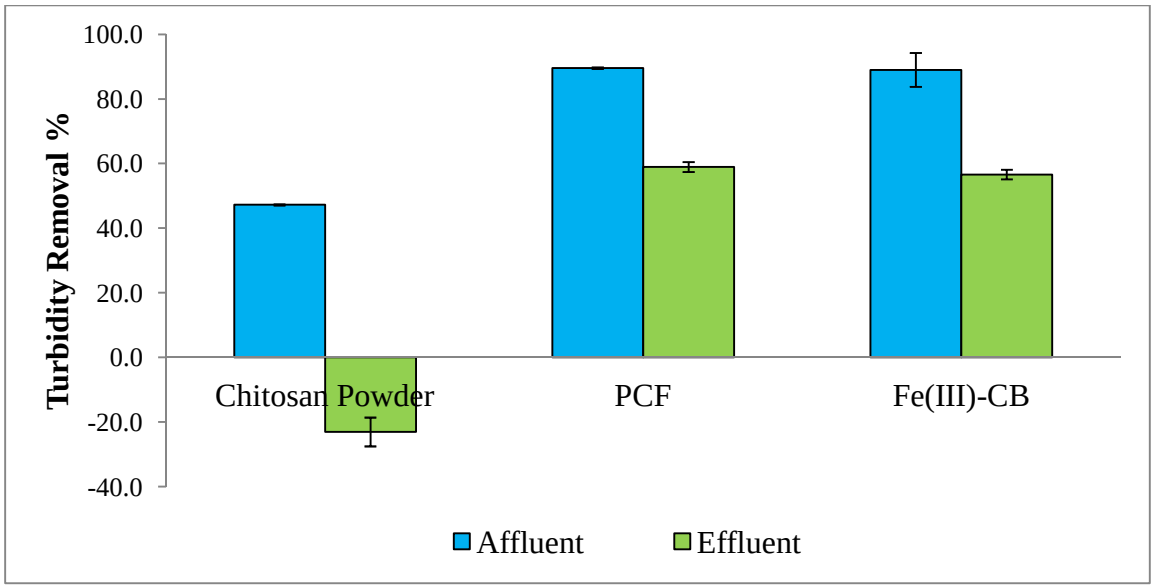

Figure 2: Removal of turbidity from affluent and effluent samples filtered at the beginning using CP, PCF and Fe(III)-CB individually.

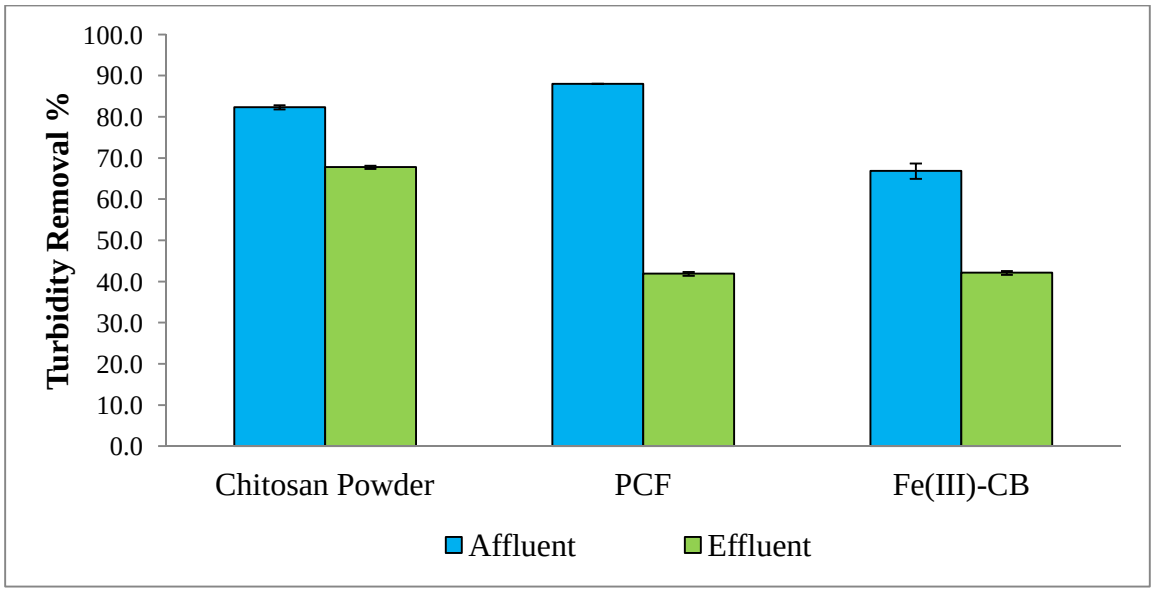

Figure 3: Removal of turbidity from affluent and effluent samples filtered at the end using CP, PCF and Fe(III)-CB individually.

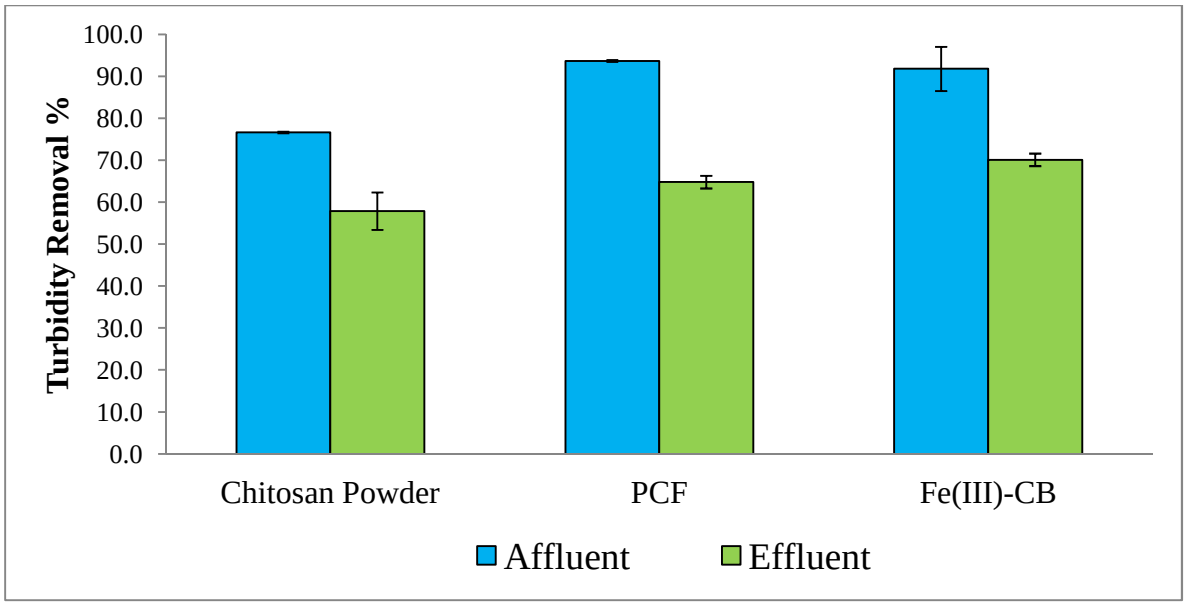

Figure 4: Removal of turbidity from affluent and effluent samples filtered at the beginning and end using CP, PCF and Fe(III)-CB individually.

4.4 Chitosan solution polymer

Figure 5 shows the affluent and effluent turbidity in wastewater using 2% chitosan solution diluted in 5% acetic acid. The wastewater was unfiltered, filtered at the beginning, and filtered at the beginning and at the end. The best results were found when filtered at the beginning and at the end for affluent samples, and filtered at the beginning for effluent samples, with a 99.2% and 80% of turbidity removal, respectively. The results were excellent due to the fact that chitosan solution permits the coagulation/flocculation and sedimentation of affluent wastewater, as showed in figure 6. The pHs of both ranged between 6.0 to 7.5, complying with the regulations of the treatment plant.

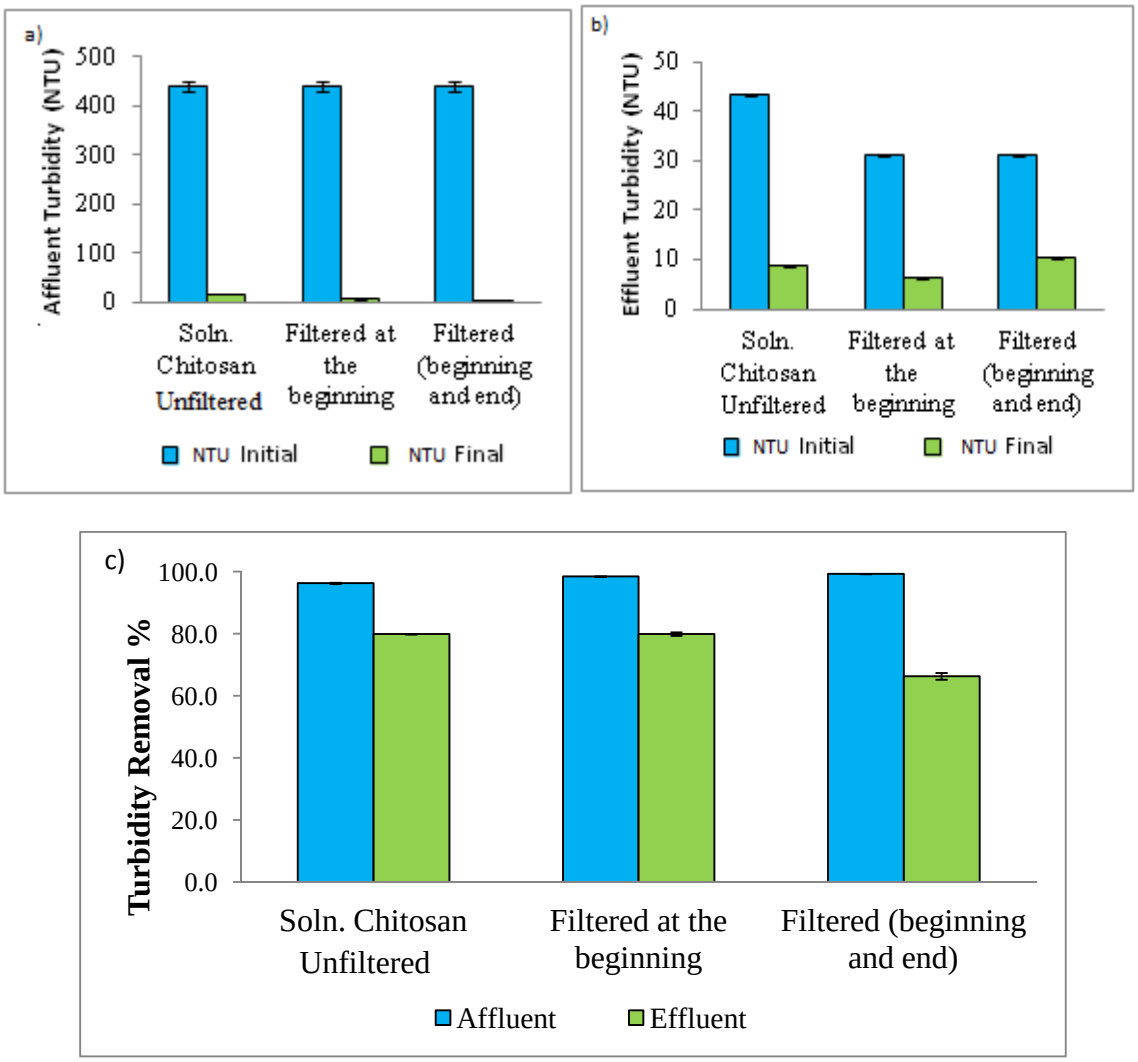

Figure 5: Initial and final turbidity of affluent (a), effluent (b) samples, and turbidity removal (c) from affluent and effluent samples using chitosan solution unfiltered, chitosan solution filtered at the beginning or chitosan solution filtered at the beginning and end.

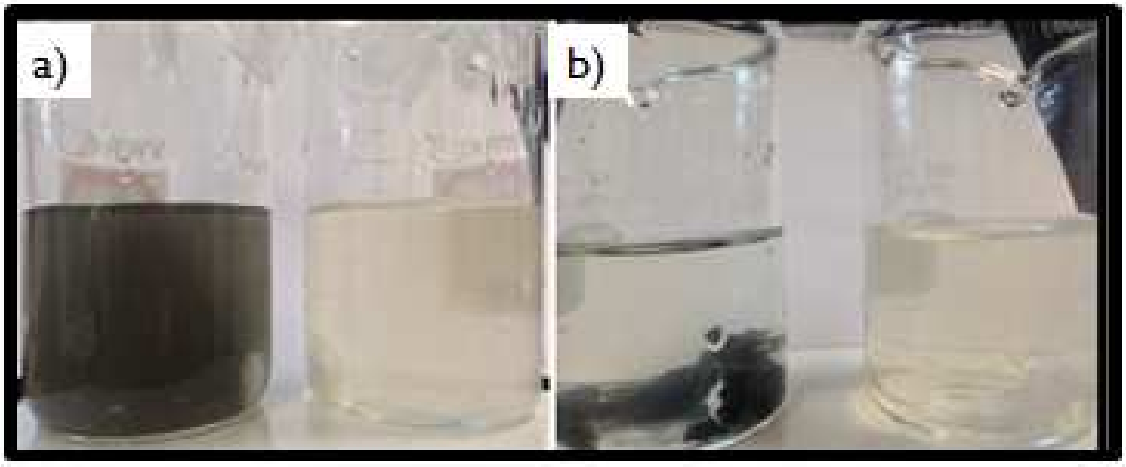

Figure 6: Affluent and effluent samples of wastewater PAS Aguada a) before and b) after contact with chitosan solution.

Table 6 represents the removed turbidity from affluent wastewater using diverse volumes (between 100 – 1000 µL) of chitosan solution in agitation for six hours. The results showed excellent values of final turbidity, with an 11.4 (800 µL), 14.5 (250 µl) and 16.5 (120 µl) NTU. However, the best removal of turbidity was using 120 µl of chitosan solution, with a 96.3% result. All the diverse volumes of chitosan solutions removed the turbidity below the parameter of PAS Aguada (84 NTU). The pH values did not show significant change. The results were excellent due to the fact that chitosan solutions permit the coagulation/flocculation and sedimentation of affluent wastewater.

Table 6: Removed turbidity from affluent wastewater using diverse volumes of chitosan solution.

	Initial		Final		% Removal		pH	
Sol. (uL)	NTU	STDV	NTU	STDV	% NTU	STDV	Initial	Final
100	129.5	10.6	38.3	4.7	**70.5**	1.2	7.0	7.0
120	441.0	21.2	16.5	0.0	**96.3**	0.2	7.0	7.0
150	129.5	10.6	33.6	1.3	**74.1**	3.2	7.0	7.5
250	129.5	10.6	14.5	0.2	**88.8**	0.8	7.0	6.7
500	129.5	10.6	28.9	1.3	**77.7**	2.8	7.0	7.1
800	144.0	15.6	11.4	1.3	**92.1**	0.0	7.0	7.0
1000	144.0	15.6	81.1	1.5	**43.7**	7.2	7.0	7.1

4.5 Column packed with chitosan

Chitosan polymers (1g) were added to the column, then 10 mL of affluent or effluent unfiltered water were added to the column. The average turbidity was measured at the beginning and at the end of process. Figure 7 shows the column packed with chitosan powder, PCF and Fe(III)-CB. The results show a best removal of turbidity using CP with a 96% and 92% for affluent and effluent wastewater, respectively. This is because the water has a longer retention in the chitosan powder, and this allows it to adsorb more suspended particles from the wastewater. The pH values of the wastewater after the process were between 6-8.

Table 7: Values and removed turbidity from affluent and effluent wastewater using CP, PCF and Fe(III)-CB packed onto column.

Polymer	Type	Initial		Final		% Removal		pH	
		NTU	stdv	NTU	stdv	%NTU	stdv	Initial	Final
Chitosan Powder	Affluent	105.5	0.3	4.3	1.0	**95.9**	0.1	6.9	7.9
	Effluent	47.8	0.1	3.8	0.01	**92.0**	0.1	6.8	7.5
PCF	Affluent	105.5	0.3	47.2	5.2	**55.2**	5.1	6.9	6.7
	Effluent	47.8	0.1	20.2	1.7	**57.8**	3.3	6.8	6.9
Fe(III)-CB	Affluent	105.5	0.3	70.0	5.8	**33.6**	5.9	6.9	7.0
	Effluent	47.8	0.1	28.5	1.3	**40.3**	2.5	6.8	6.9

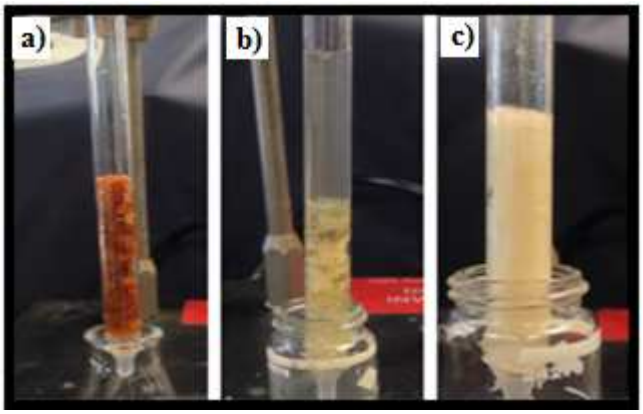

Figure 7: Column packed with a) Fe(III)-CB, b) PCF and c) Chitosan powder.

4.6 Jar Test

The jar test was used to simulate when the polymer is applied to the affluent from the wastewater treatment plant in order to determine the optimum dosage to reduce the turbidity of wastewater. In this case, 2L of wastewater was added to a jar and then agitated for 1 min to a maximum 100 rpm, then for 10 min down to 35 rpm to promote coagulation and flocculation, and finally 10 min at 10 rpm for sedimentation. Figure 8 shows the turbidity removal percentage from wastewater using diverse percentages of chitosan solutions in acetic

acid (2% w/v diluted in 5% acetic acid, 2% w/v diluted in 1% acetic acid, 1% w/v diluted in 1% acetic acid) and AF-501. The results showed that all concentrations in the range of 0.5 to 36 ppm were effective for the turbidity removal of the affluent samples. The initials turbidity values ranged between 275 to 841 NTU for all experiments, and the finals turbidity obtained ranged between 8.4 to 115 NTU. The percentages of removal obtained were between 81 to 98%, 81 to 99%, 86 to 99% and 57 to 93% using chitosan, 2% diluted in 5% acetic acid, chitosan, 2% diluted in 1% acetic acid, chitosan, 1% diluted in 1% acetic acid and AF-501, respectively. The most effective concentration for the removal of turbidity using a 2% chitosan solution diluted in 5% acetic acid were 16 and 18 ppm, which achieved a 97% removal (18 NTU final from an initial of 516.0 NTU) and 98% (14 NTU final from an initial of 841.0 NTU). For the chitosan 2% solution diluted in 1% acetic acid, 14 and 16 ppm were most effective concentrations with 99% (9-10 NTU final from an initial of 841.0 NTU) for both concentrations. The most effective concentrations, using a 1% chitosan solution diluted in 1% acetic acid, were 12-16 ppm with 99% (8-9 NTU final turbidity from an initial of 705.5 NTU) removal. On the other hand, using AF-501, the best concentration found was 18 ppm with a final NTU of 32 from an initial 427.5 NTU. Most effective for the removal of turbidity was the Chitosan solution (1% w/v diluted in 1% acetic acid) of the affluent samples with a maximum removal of 99% and a final turbidity which ranged between 8 and 9 NTU from an initial 705.5 NTU.

Table 8 shows the pH final values of the affluent samples using chitosan solution and AF-501 polymers. The initials pHs of the wastewater ranged between 6 to 7, which did not show a significant difference with the final pH, which also ranged between 6 and 7. The pH prior to discharge must be near neutral due to the fact that acidic or alkaline pHs' are harmful

to the environment, our health and are corrosive to equipment used in the treatment plants. The results showed pH values between 6 and 7. These values are neutrals and will not have environmental implications.

Finally, the results showed that both polymers are excellent for the removal of turbidity from wastewater because both are cationic polymers and are viable alternatives for removing the negatives charges present in particulates causing the turbidity in wastewater. The coagulant used in Sewage/Wastewater Treatment Plant in Aguada (AF-501) can be toxic to marine arthropods due to the fact that it contains aluminum salts. These aluminum particles generate products that are toxic to humans and the environment, and at high concentration in water might be carcinogenic and or have been related with Alzheimer disease. In comparison with AF-501, chitosan is non-toxic, inexpensive and a natural polymer. Chitosan removes the turbidity of the affluent samples under 84 NTU, while maintaining the pH between 6 to 9, as required by the treatment plant and regulatory agencies.

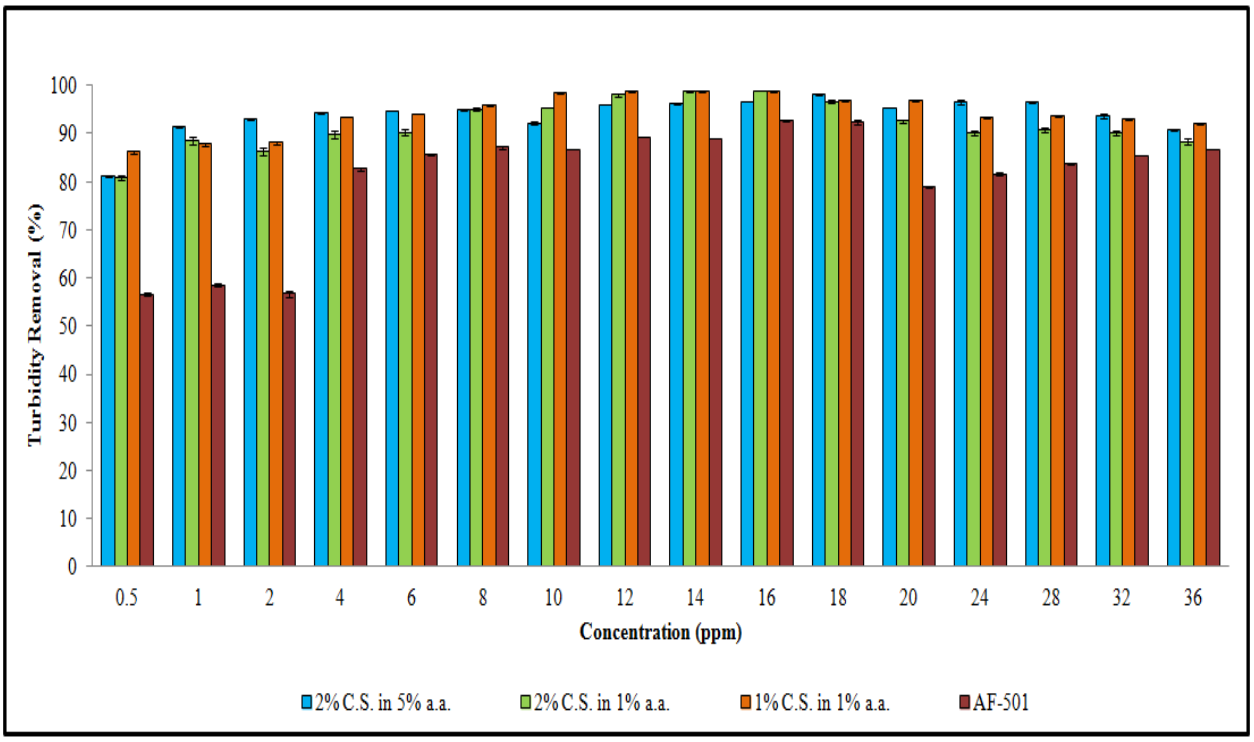

Figure 8: Effects of chitosan solutions (x % diluted in x% acetic acid) and AF-501 solutions on turbidity removal of affluent samples during jar test experiments using concentrations between 0.5 to 36 ppm.

Table 8. Final pH values of affluent samples using chitosan and AF-501 solutions.

	pH final			
Concentration	**Chitosan Solution (x % w/v diluted in x % acetic acid)**			
(ppm)	2% in 5%	2% in 1%	1% in 1%	AF-501
0.5	7.16	7.34	7.03	7.29
1	7.14	7.15	7.08	7.31
2	7.24	7.20	7.12	7.32
4	7.22	7.20	7.12	7.18
6	7.20	7.17	7.11	7.21
8	7.19	7.18	7.12	7.23
10	7.17	7.35	7.01	7.25
12	7.00	7.10	7.01	7.25
14	7.02	7.10	7.01	7.26
16	6.99	7.04	6.96	7.28
18	7.00	7.03	7.02	7.20
20	6.99	7.00	7.15	7.20
24	6.86	6.96	7.18	7.23
28	6.87	6.99	7.21	7.33
32	6.98	7.00	7.22	7.37
36	6.97	6.98	7.22	7.30

5. Conclusions

Chitosan is an excellent coagulant for the removal of turbidity from wastewater in treatment plants. Experiments were conducted utilizing diverse forms of chitosan, such as chitosan powder, protonated chitosan flakes, chitosan immobilized with iron, column packed with chitosan and chitosan solution, and compared with AF-501 polymers, which is commonly used in PAS Aguada. The results show an excellent turbidity removal capacity from wastewater when utilizing chitosan as coagulant. The polymer most effective for the turbidity removal of affluent samples was chitosan solution in concentration between 12-18ppm with a 97-99% of turbidity removal. Also, chitosan achieved lower turbidity

parameters required by the Sewage/Wastewater Treatment Plant in Aguada (84 NTU) and the pH was neutral as required by the regulating agencies. Finally, chitosan showed to best performance in reducing turbidity, when compared with the coagulant used actually in use in wastewater treatment plant (AF-501).

6. Acknowledgements

This work had financial support from the United States Department of Agriculture (Award # USDA/NIFA: 2011-38422-30835 and USDAGRANT: PRE2011-02986. The author would like to acknowledge the Eng. Joel Lugo Rosa, from the Puerto Rico Aqueduct and Sewer Authority (PRASA). Thanks to PAS Aguada plant manager Agustín Collazo, plant operators supervisor Gino Giovanetti, and operators and to every personnel